A Spectroscopic Investigation of the Thermal Decomposition of Cellulose and Alginic Acid

Dissertation submitted as a partial fulfilment of the requirements of the University of Greenwich for the Degree of Doctor of Philosophy

by

Steven Coburn

University of Greenwich

June 2006

ACKNOWLEDGMENTS

I would like to thank Dr John Tetteh for his supervision, advice and enthusiasm throughout this study. Many thanks also go to Dr Chuan Liu for his help, guidance and dedication in helping me to the end of this project.

Thanks are also due to Prof. Ed Metcalfe and Dr Kevin McAdam who gave me the opportunity to undertake this study and helped to start the project rolling. I am grateful to all of my friends and colleagues at GR&D who have provided me with opportunity to discuss ideas, receive advice and opinion on my work.

My friends and family also deserve thanks for their support and understanding throughout this long process, particularly Michelle Dowle who let me disappear into my studies for months at a time.

Finally thanks to British American Tobacco for allowing me the time and resource to complete this work.

ABBREVIATIONS

CrI	Crystallinity Index
DP	Degree of polymerisation
DSC	Differential scanning calorimeter
DTA	Differential thermal analyser
EGA-FTIR	Evolved gas analyser - Fourier Transform infrared
ESR	Electron spin resonance
FTIR	Fourier Transform infrared
GC-IR	Gas chromatography - Infrared
GC-MS	Gas chromatography - mass spectrometry
HTT	Heat treatment temperature
IR	Infrared
NMR	Nuclear magnetic resonance
PAH	Polynuclear aromatic hydrocarbons
PCA	Principal component analysis
Py-GC-MS	pyrolysis - gas chromatography - mass spectrometry
SVD	Singular value decomposition
TFA	Target factor analysis
TGA	Thermogravimetric analyser
T_g	Glass transition temperature

ABSTRACT

A spectroscopic investigation of the thermal decomposition of cellulose and alginic acid

The combustion and pyrolysis of biomass impacts directly on a number of areas such as, energy production, public health, environmental protection and feedstock for chemical production. This study investigated the thermal decomposition of two structurally similar polysaccharides – cellulose and alginic acid, arguably being the two largest sources of biomass on land and from the sea respectively. Despite the similarity in the two materials and applications, reviewing literature of the combustion and pyrolysis mechanisms of the two materials showed a relatively well-established framework of knowledge for cellulose, although there is still some lack of agreement in some areas. This contrasted with the almost total absence of any information on the thermal behaviour of alginic acid. The aim of the work reported in this thesis was to use the structural similarities and the mechanistic framework for cellulose to conduct a comparative investigation of the two materials.

Taking advantage of high throughput multivariate algorithms to process complex spectroscopic data produced by TGA-FTIR, a method was developed to identify infrared active volatile species generated above a detectable threshold during the thermal degradation process. The ability to plot an evolution profile of a selected compound in time- and/or temperature domain significantly enhanced the capabilities of a standard TGA-FTIR system for mechanistic investigations. With the technique established, the two materials were analysed under different heating rates (5, 10, 30, 60°C/min) under nitrogen and again under 10% oxygen in nitrogen. A reconstruction of the cellulose decomposition pathway was carried out using the data obtained from this work. Compared to the methods available in the scientific literature, the current method was a simpler and more efficient technique for providing information related to the thermal degradation behaviours of the sample materials. The application of the method to alginic acid revealed for the first time that this material responded differently and more sensitively to the presence of oxygen than did cellulose. Its decomposition pathway has a number of distinctive steps, in contrast to cellulose.

To complement the analysis of the volatiles, the surface of charred residues of the two materials were also analysed by using attenuated total reflectance (ATR) infrared spectroscopy. This information was also used to deduce the combustion chemistry for the two materials.

Steven Coburn [BSc(Hons) Applied Chemistry]

Publications

S. Coburn, R.R. Baker, C. Liu and J. Tetteh

"Pyrolysis of saccharide tobacco ingredients: a TGA–FTIR investigation"

J. Analytical and Applied Pyrolysis, 74 (2005) 171-180

Richard R. Baker, Steven Coburn, Chuan Liu

"The pyrolytic formation of formaldehyde from sugars and tobacco"

J. Analytical and Applied Pyrolysis, In Press

Conferences

R.R. Baker, S. Coburn, C. Liu, J. Tetteh

"Pyrolysis of saccharide tobacco ingredients: a TGA-FTIR investigation" (Poster)

16th International Symposium of Analytical and Applied Pyrolysis – Alicante, Spain, 23-27th June 2004

S. Coburn and J. Tetteh

"Use of chemometrics in the spectral analysis of tobacco ingredients"

International Informatics and Data Visualisation Conference – Intech Centre, Winchester, 21-22nd October 2004

S. Coburn, R.R. Baker and C. Liu

"The effect of nitrogenous compounds on the generation of formaldehyde from pyrolysis of sugars",

Coresta – Joint Study Groups Meeting, Stratford-upon-Avon, UK, 2005

TABLE OF CONTENTS

CHAPTER 1 INTRODUCTION AND SCOPE OF THE STUDY 10

1.1 CELLULOSE 11

1.1.1 General 11

1.1.2 Structure and Properties 12

1.2 PYROLYSIS AND COMBUSTION OF CELLULOSE 14

1.2.1 General Introduction 14

1.2.2 Physical effects 16

1.2.3 Mechanism of thermal degradation 18

1.2.4 Levoglucosan 23

1.2.5 Char Formation 25

1.3 KINETICS OF CELLULOSE PYROLYSIS 30

1.4 REACTION PATHWAYS FOR CELLULOSE THERMAL DECOMPOSITION 38

1.4.1 Fire research and flame retardants 39

1.4.2 Treatment of biomass 50

1.4.3 Other 55

1.4.4 Summary of reaction pathways 57

1.5 ALGINIC ACID AND ALGINATES 59

1.5.1 General 59

1.5.2 Structure 60

1.5.3 Thermal properties of alginic acid 61

1.6 EXPERIMENTAL METHODS 62

1.6.1 Thermogravimetric analysis (TGA) 62

1.6.2 Other thermal analysis techniques 64

1.6.3 Calorimetry 65

1.6.4 Fourier Transform Infrared Spectroscopy (FTIR) 65

1.6.5 Nuclear Magnetic Resonance Spectroscopy (NMR) 66

1.6.6 Pyrolysis Gas Chromatography-Mass Spectrometry (py-GC-MS) 66

1.7 SUMMARY 67

1.8 AIMS 67

CHAPTER 2 EXPERIMENTAL PROCEDURES 69

2.1 MEASUREMENT TECHNIQUES 69

2.1.1 Thermogravimetry 69

2.1.2 Infra-Red Spectroscopy 70

2.1.3 Fourier Transform Infrared (FTIR) 73

2.2 MULTIVARIATE ANALYSIS 74

2.2.1 The InSight™ Software *78*
2.2.2 Quantitative Analysis *84*
2.3 TESTING THE PARAMETERS OF THE TGA-FTIR 86
2.3.1 Scanning Parameters *87*
2.3.2 Flow rate *88*
2.3.3 Sample Weight *90*
2.3.4 Isothermal Temperature *91*
2.4 CALIBRATION PROCEDURE 91
2.4.1 Calibration of Solid and Liquid Compounds *92*
2.4.2 Calibration of Gas Phase Compounds *93*
2.4.3 Testing the Calibrations *94*
2.5 MATERIALS 96
2.6 EXPERIMENTAL CONDITIONS 97
2.6.1 Thermal Decomposition using TGA-FTIR *97*
2.6.2 Char Analysis *99*

CHAPTER 3 RESULTS 103

3.1 THERMOGRAVIMETRIC ANALYSIS 103
3.1.1 Effect of sample weight *103*
3.1.2 Effect of temperature ramp rate *105*
3.1.3 Effect of TGA furnace purge gas *113*
3.1.4 Summary of TGA data *117*
3.2 MULTIVARIATE ANALYSIS OF THE SPECTRAL DATA 118
3.2.1 Qualitative identification of compounds *120*
3.2.2 Quantitative analysis of selected compounds *123*
3.2.3 Summary of FTIR data *137*
3.3 CHAR ANALYSIS 139
3.3.1 Elemental analysis of the char samples *140*
3.3.2 ATR spectroscopy of the char samples *143*
3.3.3 Summary of the char analysis *148*

CHAPTER 4 DISCUSSION 150

4.1 USING MULTIVARIATE ANALYSIS TO TREAT TGA-FTIR SPECTRA 150
4.1.1 Multivariate Analysis by InSight™ *151*
4.2 THERMAL DEGRADATION PATHWAY FOR CELLULOSE 151
4.2.1 Analysis of Cellulose Char *152*
4.2.2 Spectroscopic Analysis of Volatiles from Cellulose *157*
4.2.3 Cellulose summary *162*
4.3 THERMAL DEGRADATION PATHWAY FOR ALGINIC ACID 164

4.3.1 Analysis of Alginic Acid Residue *164*
4.3.2 Spectroscopic Analysis of Volatiles Evolved from Alginic Acid *170*
4.3.3 Alginic acid summary *174*
4.3.4 Effects of Mixing Alginic Acid with Cellulose *177*

CHAPTER 5 CONCLUSIONS 179

5.1 REVIEW OF THE AIMS OF THIS STUDY 179
5.2 FURTHER WORK 182

CHAPTER 6 REFERENCES 184

APPENDIX A. ASH AND METAL ANALYSIS OF THE CELLULOSE AND ALGINIC ACID USED IN THIS STUDY 197

APPENDIX B. CALIBRATION RANGE FOR FACTORS USED WITH INSIGHT™ 198

CHAPTER 1 INTRODUCTION AND SCOPE OF THE STUDY

The pyrolysis and combustion of cellulose has been studied by a large number of researchers over the years and as a result is relatively well understood. Part of this interest is due to the use of cellulosic biomass as a renewable energy source, in the light of depleting fossil fuel deposits. Alginates are the marine equivalent of cellulose, found in the cellular structure of various seaweeds. They are, structurally, similar molecules to cellulose and although alginates are used in food and pharmaceutical applications, their use as a potential renewable fuel source has not been explored.

Within the tobacco industry reconstituted materials may use a number of different substances as binders to allow the formation of a usable sheet material. These may be cellulose, a cellulosic derivative or other natural polymeric materials such as alginic acid, pectins and various gums such as xanthan. These reconstituted sheet materials are to be included into a cigarette or other tobacco products, so the pyrolysis and combustion behaviour is essential knowledge. In tobacco products cellulose is subject to both pyrolysis and combustion processes in the form of the paper wrapping, and also as approximately 10% of the tobacco leaf structure [1]. The cellulosic structure of the tobacco leaf is also exploited in the formation of reconstituted tobacco materials, which may be added to many commercial tobacco products, as a method of utilising otherwise waste tobacco that is unable to pass through the manufacturing process.

In light of the aforementioned, a literature survey has been conducted to assess the current state of knowledge regarding both cellulose and alginic acid with respect to their thermal behaviour. Cellulose is well characterised and a wealth of literature is available. However, the scientific literature surrounding alginic acid, and in particular its thermal decomposition, is sparse. There is literature that details the gelling process and factors that affect this property of alginates. However, the lack of literature detailing the thermal behaviour is perhaps surprising as alginic acid and its substituted derivatives are commonly used in the food industry, including applications that involve exposure to heat, e.g. baking, roasting or frying. Table 1-1 shows some typical applications of various forms of alginate.

It is therefore of interest to discover more about the thermal degradation process of alginic acid in comparison to cellulose. The rationale for this is two-fold; firstly, cellulose is very similar structurally to alginic acid, and secondly, the thermal degradation mechanism of cellulose is

fairly well established. Therefore, it may be possible to draw parallels between the thermal decomposition of the two materials.

Table 1-1. Some typical applications of alginic acids and alginates used in the food industry, extracted from ISPAlginates UK Ltd product guide [2].

Alginate Type	Primary Function	Comments	Typical Applications
Sodium Alginate	Thickening, gelling, film-forming, coating, suspending, stabilisation.	High viscosity, coarse mesh, low Ca^{++}	Soft reversible gels, thickening, bakery fillings, low fat spreads, onion rings.
		High viscosity, fine mesh, low Ca^{++}	
		High Viscosity, fine mesh	Batters, burrito glue.
Propylene Glycol Alginate	Stabilisation, emulsification.	Low viscosity, 50-59% esterified, not clarified.	Fruit and chocolate syrups, mustards, batters, barbeque sauces, dressing, dry mix meringues, pulp suspension.
Alginic Acid	-	-	Noodles, binding.
Alginic Acid Blend	Gelling.	Produce sodium alginate in-situ to achieve hydration in dairy systems	Ice-cream.

1.1 Cellulose

1.1.1 General

In 1838 Anselme Payen suggested that the cell walls of plants were all made from the same material, which he named cellulose [3]. Cellulose is the major structural component of many higher plants, though it is usually mixed with other polysaccharides, lignin, resins,

hemicelluloses, fats and other inorganic materials [4, 5]. It is the most abundant naturally occurring organic raw material available, and is naturally regenerable. As a raw material cellulose has many uses; firstly it has been used for centuries as a source of heat, for cooking, as a construction material in the form of timber, as textile fibres such as cotton or flax, and as the base pulp for paper making. Cellulose and its derivatives are used in the food and pharmaceutical industries as thickeners [6]. Wood and other cellulosic materials are used as fuel materials, but this use diminished towards the start of the 20th century for much of the developed world, replaced by the use of fossil fuels [7]. As fossil fuels are becoming depleted and environmental concerns more important, using renewable biomass is becoming a key area of interest once more in research. Biomass is a generic term for organic non-fossil material of biological origin, and is taken from many sources – woods, grasses, agricultural waste, manure, municipal waste, and even sewage sludge [8, 9]. Most biomass materials have a high cellulose content (about 50%), the exact levels are dependent on source [10].

Interest in studying the combustion of cellulose has been generally related to one of two issues; flame retardance of textiles and soft furnishings, or to its use as a regenerable fuel source. In these studies of biomass, and indeed wood research, it is believed that the cellulose is the more important factor in combustion, whereas lignin, another major component of such materials, has less importance [11]. As an easily obtainable and renewable material, biomass is also being investigated as starting material for other industrial chemicals (such as acetol, acetic acid, glucose for fermentation to ethanol [12]), modified cellulose fibres and other cellulosic materials for domestic and industrial use [13].

1.1.2 Structure and Properties

Cellulose is a simple straight chain monopolymer of anhydroglucose molecules linked by a 1-4, β-glucosidic bond [10, 14]. This initially forms a disaccharide, cellobiose, shown in Figure 1-1. These units then link together on a screw axis with each monomer unit being at 90° to the previous in chains of up to 5000 degrees of polymerisation (DP). There is no free rotation, in the solid state, about the C-O-C bond due to steric hindrance [15]. Each of the anhydroglucose units contains three hydroxyl groups, which may be esterified or substituted with other adducts to form the various cellulose derivatives which are used commercially such as cellulose acetate, carboxymethyl cellulose (CMC), and ethylcellulose [14].

Cellulose contains a mixture of highly ordered crystalline regions, and non-crystalline amorphous regions. These are roughly in the ratio of 70:30 crystalline to amorphous. Little

experimental knowledge has been obtained that describe the structure of the amorphous regions [16]. The structure of the crystalline region of cellulose is complex and a number of different forms have been identified, labelled cellulose Iβ, II, II_I, IV_I and IV_2 [17]. These designations describe different conformations and packing of the cellulose structure but generally all of them retain a ribbon like shape, and these ribbons are arranged in flat layers which form the crystalline structure [17]. The linear polymer chains are held together by hydrogen bonds [5] in three-dimensional microfibrillar structures of average molecular weight of about 10^6 though the exact structure of the hydrogen-bonded network is still not clear [13]. However, it is thought to involve the hydroxyl groups and the hemiacetal (ring) oxygen of the crystalline regions (Figure 1-2). This makes these bonds relatively unreactive compared to the amorphous regions [18]. This extensive hydrogen bonding is the reason why cellulose is insoluble in water, despite the fact that the monomer D-glucose is extremely soluble [6]. This is the naturally occurring structure of cellulose in plant materials, in particular cotton species which are almost pure cellulose (98%), as well as flax (80-90%) and ramie (~80%)[3].

The principal functional group of cellulose is the hydroxyl (-OH) group; therefore cellulose behaves as a polyalcohol under oxidation conditions. On oxidation other functional groups are formed that influence the chemistry of the molecule, including carbonyl, keto, and carboxyl [19].

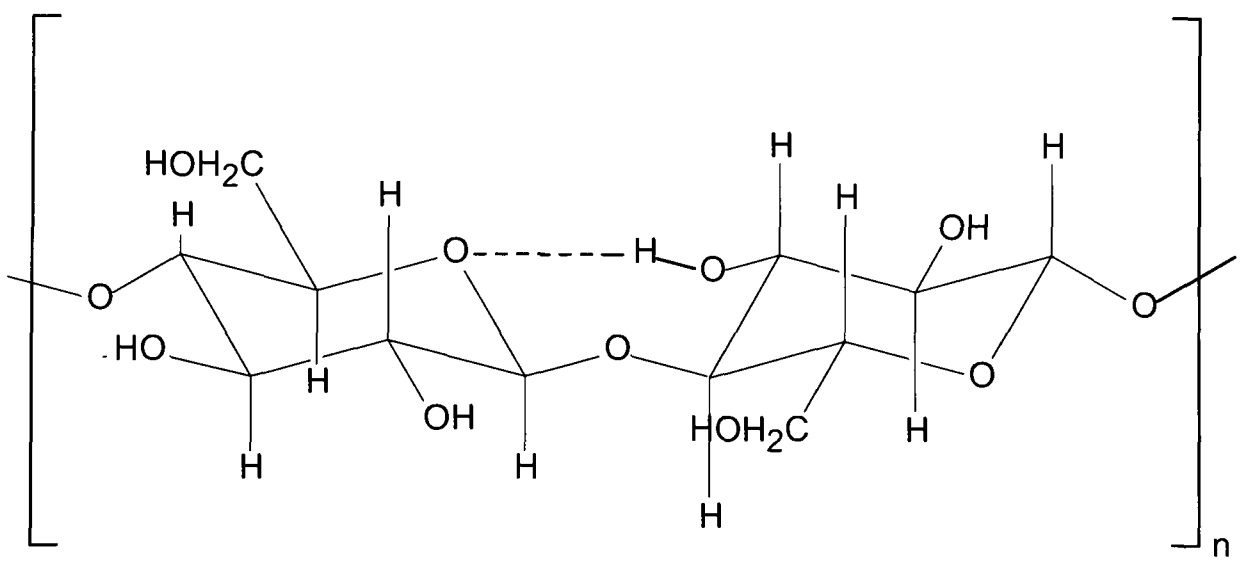

n = 1500 to >6000

Figure 1-1. Structure of cellulose showing the repeat unit of the polymer, β-cellobiose residue [20].

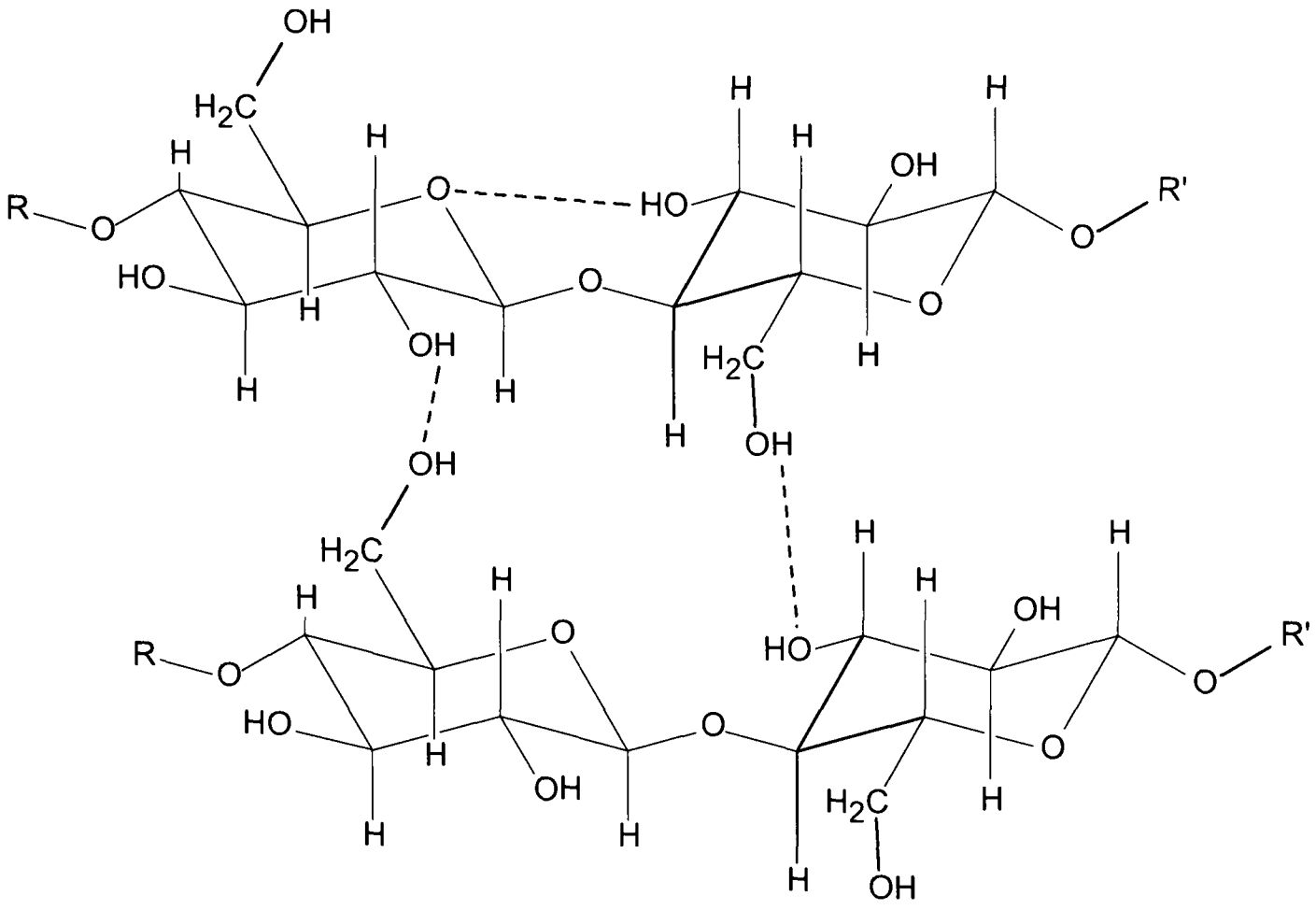

Figure 1-2. Proposed structure of hydrogen bonding in the crystalline regions of cellulose [18].

α-cellulose refers to cellulose extracted from wood using specific techniques. There are two processes, sulphite and sulphate. Both involve cooking wood in either acid (sulphite process) or alkali (sulphate or Kraft process) at 120 – 170°C to remove the lignins and other non-cellulose components [3]. About 50% of the weight of most wood is α-cellulose [10]. Pure (microcrystalline) cellulose is obtained by hydrolysis of natural cellulose leaving the acid resistant crystalline sections of the polymer. This is readily obtained as a commercial material, under a number of trade names [5, 21].

1.2 Pyrolysis and Combustion of Cellulose

1.2.1 General Introduction

In one of the earliest books on the subject of pyrolysis, Charles DeWitt Hurd wrote that, 'pyrolysis is the transformation of a compound into another substance or substances by heat alone' [22]. That is to say pyrolysis is primarily concerned with decompositions and elimination reactions induced by heat, generally resulting in the formation of products that are smaller molecules than the starting material. Pyrolysis usually occurs between 500 – 800°C, but may begin at 250°C, dependent on the material. Normally reactions occurring below this

temperature would be described as thermal degradation not pyrolysis. Although pyrolysis is often just a thermal decomposition, it is a less definitive term than thermal decomposition as other reactions may occur, such as rearrangements, formation of larger molecules from smaller fragments as well as decompositions [22]. Pyrolysis temperatures for cellulose are placed around 325 – 375°C [19], however, external factors such as the heating rate may cause an increase in onset and final decomposition temperatures [23].

Combustion is described as a rapid oxidation generating heat, or both heat and light. It may also be a slow oxidation process that produces little heat and no light [24]. Flaming combustion involves gas phase oxidation of volatile products and smouldering combustion involves solid phase oxidation of the chars remaining after evaporation of the volatile products. Smouldering can also be described as a suppressed exothermic combustion, which generally occurs below the surface in a limited oxygen supply [25]. Both of these involves complex interactions between chemical reactions and heat, and mass transport [26].

Much literature has been generated studying the pyrolysis and combustion of cellulose, including several comprehensive reviews of the subject [7, 10, 27-30]. The thermal decomposition, pyrolysis and combustion of cellulose provide a complex mixture of chemical and physical changes. It involves heat and mass transfer, both competing and concurrent reactions of various types, such as decomposition, fragmentation, depolymerisation, transglycosylation, oxidation and elimination [14]. Evolved compounds may also contribute via secondary reactions which cause further complexity to the overall process. Such is this complexity, that after over 60 years of study of cellulose pyrolysis, by a large number of different researchers, it is generally acknowledged that the mechanism of cellulose pyrolysis is still uncertain.

Some of the earliest work on the thermal behaviour of cellulose was carried out, by pyrolysing the material under a nitrogen flow, and capturing various fractions of pyrolysates generated. Mass and infrared spectrometry were used to identify the product fractions, but this identification was limited describing only 'tar', water, carbon monoxide, carbon dioxide and carbonaceous residue [31]. It was postulated that cellulosic materials such as wood, paper and related fibrous materials did not pyrolyse directly, but under the influence of heating they decompose. The gases and volatiles formed will subsequently produce flaming combustion when oxygen is added to the system. The heat generated by the flame continues the process of

decomposing the starting cellulosic material [32, 33]. This process can be summarised schematically as shown in Figure 1-3.

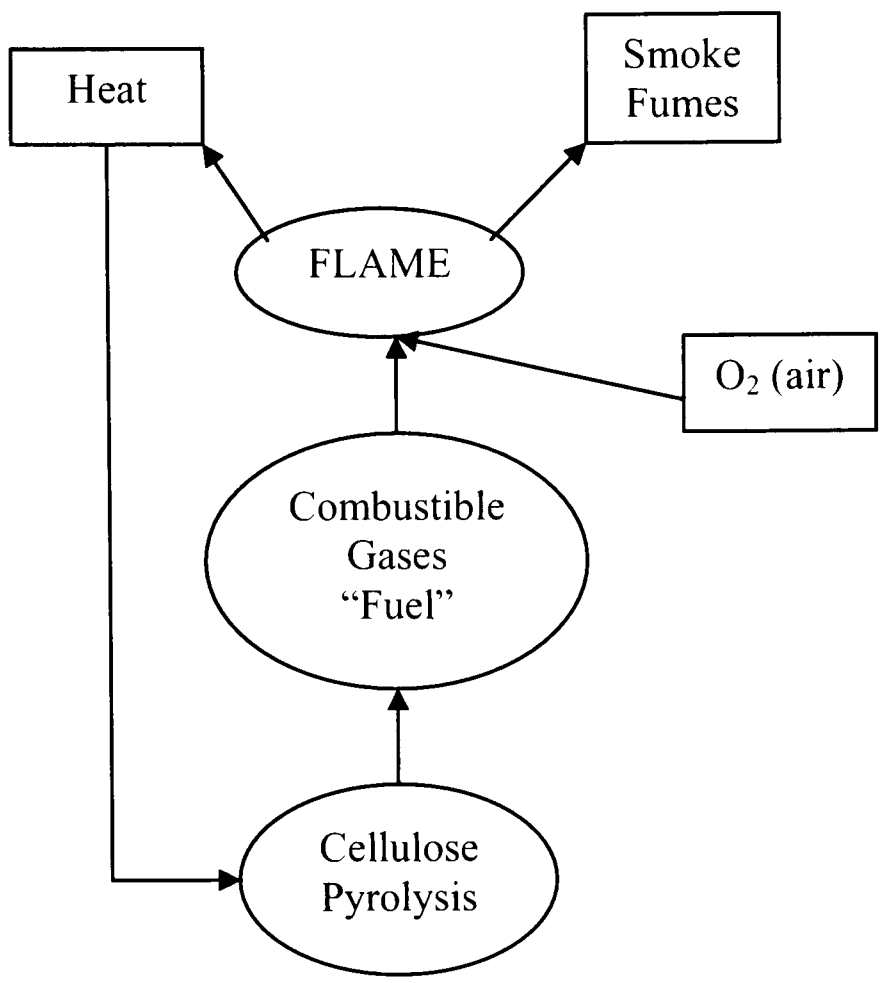

Figure 1-3. General schematic of the cycle of self-sustaining combustion of a polymeric material such as cellulose.

Since those pioneering studies, the pyrolysis of cellulose and cellulosic materials has been investigated under a variety of conditions and from a number of different views. These interests include fire and fire safety of cellulosic materials used in fabrics and furnishings, chemical utilisation and other technical subjects [34].

1.2.2 Physical effects

Interest has also been shown in the physical changes occurring in the cellulose substrate during pyrolysis. In particular, the degree of polymerisation (DP) and the crystalline fraction have both been studied with respect to changes on heating. Naturally occurring cellulose has a normal DP in the range of 1200 – 5000, depending on source. Under heating there is a lowering of the DP, particularly under slow heating rates and low temperatures. This has been noted as a key step in the decomposition of the molecule. Under these conditions degree of polymerisation was

observed to be greatly reduced from around 1400 to a value of approximately 200 – 400 [35, 36].

The crystallinity of the polymer has been shown to increase on heating, implying that thermal degradation occurs in the amorphous regions first [37]. This principle of the amorphous region being more reactive than the crystalline region is exploited for the formation of microcrystalline cellulose. It has been observed that the amorphous region is attacked first by solvents and chemical reagents [5]. From observations of inorganic salts added to the cellulose it was suggested that they act as catalysts in the amorphous region, and not penetrate the crystalline regions. A differential scanning calorimetry (DSC) study concluded that any thermal degradation below 200°C was likely to occur in the amorphous region [38]. After ~50% weight loss the pyrolysed cellulose samples had very similar crystallinity index (CrI) values. Therefore further depolymerisation reactions must occur along the polymer chains through both regions [39]. Thermogravimetric analysis (TGA) studies show cellulose with high degrees of crystallinity are more thermally stable, with the major weight loss occurring from 280-380°C. A DSC study concluded that the rapid weight loss region (300 - 380°C) occurred mostly in the crystalline region [38]. Cotton cellulose with low degrees of crystallinity shows slow, steady weight loss starting at 100°C and continuing until around 500°C [36].

Contrary to these studies, Weinstein and Broido[39], using data from their x-ray diffraction study, postulated that the initial decomposition reactions in cellulose occur via cross-linking reactions primarily in crystalline regions of the cellulose leading to a lowering of the CrI. Back [40] confirmed that there are cross-linking reactions occurring as cellulose is heated by making measurements of Young's modulus. The Young's modulus value for the cellulose sample was observed to decrease rapidly between 220°C and 230°C on heating, indicating a loss of rigidity. Increasing the temperature further showed a rise in the modulus value, reaching a maximum in the range 230°C - 320°C, which was interpreted as increase in cross-linking between the polymer chains. Above this temperature the modulus value decreases rapidly as the polymer begins to decompose.

The change in the physical character of cellulose has been studied via a number of different techniques. The lowering of the DP shows that the polymer beaks down through some depolymerisation mechanism [41, 42], and the corresponding increases in CrI seem to confirm that this occurs in the amorphous regions initially. The cross-linking mechanism reason for the

increase in CrI is less well defined. The proposal for cross-linking would include formation of ether bonds [43, 44], but these types of bonds were not observed in other work [36].

1.2.3 Mechanism of thermal degradation

Cellulose is widely believed to decompose via an initial activation stage and then via one of two competing reactions, normally referred to as the Broido-Shafizadeh mechanism (Figure 1-4). The first is a dehydration reaction leading to yield a carbonaceous char, water, CO and CO_2 and the second a depolymerisation reaction to yield a tar consisting mainly of levoglucosan and other anhydrosaccharides which may also be released into the particulate phase. Simultaneously a number of small volatile compounds are also formed that are released into the gaseous phase [45]. Subsequently the primary volatile products may then pass through secondary gas phase pyrolysis to form a large variety of compounds [10].

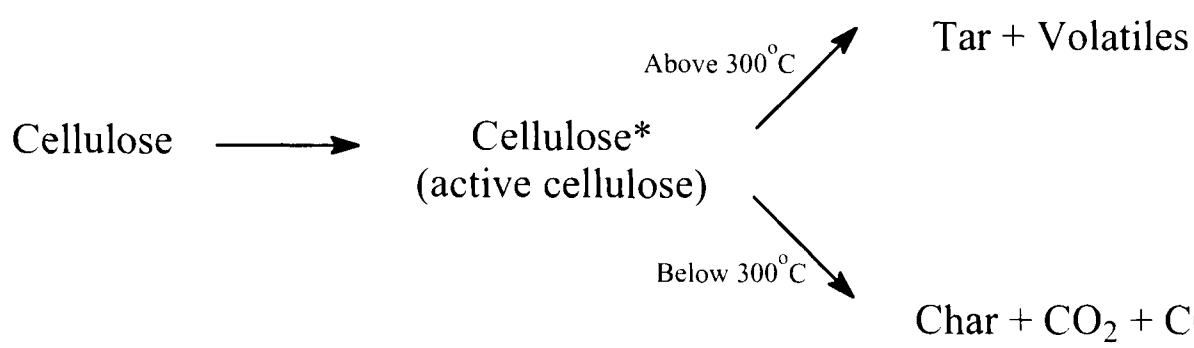

Figure 1-4. Broido-Shafizadeh mechanism for cellulose pyrolysis.

The first step in this general mechanism, which is not always associated with weight loss, is the formation of an 'active' cellulose (denoted cellulose*). Other mechanisms also have a similar step with a lower DP cellulose [12], or in the case of Kilzer and Broido, dehydrocellulose [43].
It is generally believed in the two competing step mechanism (Figure 1-4) the char forming reactions are dominant under low temperatures (below 300°C) and slow heating rates, while the volatile forming reactions become more important at higher temperatures. Pyrolysis conducted using short heating times and high heating rates also favour the volatiles route [34, 46]. Pastorova proposed that these cellulose pyrolysis routes may proceed through three competing reactions types [36]–

- Transglycosylation leading to levoglucosan and oligomers having a 1,6-anhydroglucose unit at the reducing end.

- Retro-aldolisation, yielding 2-hydroxyacetaldehyde and oligomers containing ring-cleavage fragments
- Elimination reactions leading to anhydrohexoses and pyranones.

Other concurrent and consecutive reactions may include depolymerisation, dehydration, rearrangement, formation of carbonyl and carboxyl groups and evolution of CO and CO_2 leaving a residual char [47].

Though the Broido-Shafizadeh mechanism is widely accepted and provides foundation for many more complex pathways some dispute this mechanism for two main reasons. The first point of disagreement is the activated cellulose step. One author [48] concluded that they could not find a fit for the cellulose – active cellulose step in the Broido-Shafizadeh model kinetically. They surmised that either it did not exist, or was a low temperature reaction (below 370°C). Varhegyi [48, 49] and co-workers reviewed the Broido-Shafizadeh mechanism for cellulose critically, and considered it an oversimplification of a complex system. They stated that a model such as the Broido-Shafizadeh mechanism is too simplistic to describe the complex events that occur if primary pyrolysis products are hindered from escaping the sample, leading to secondary reactions. They favour a pair of competing reactions directly from cellulose (Figure 1-5), followed by a higher temperature decomposition step (370°C) [48].

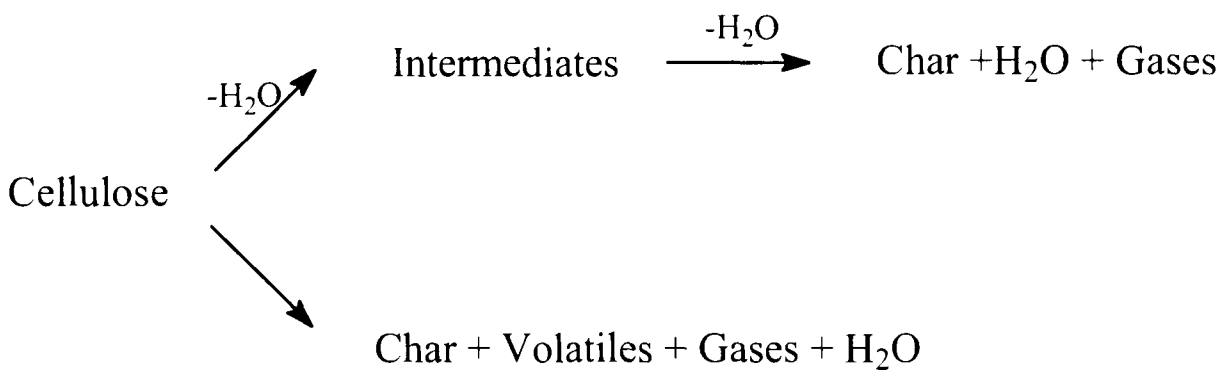

Figure 1-5. Mechanism for the thermal decomposition by Varhegyi et al [48].

The lower temperature reactions favour the formation of char, water, and CO_2, as will the addition inorganics and moisture [9, 50, 51]. Lowering the heating rate with an identical sample of cellulose (same initial mass and bulk density) increases the yield of char formed [52]. It is accepted that high temperatures and heating rates tend to promote the volatile tar route. Fast pyrolysis is used to give high yields of liquid product; fluidised beds are commonly used for this to gain a commercially viable process of extracting useful products from biomass, which is predominantly cellulose based. Rapid heating of cellulose to temperatures above 300°C may

start a more complex chain of thermally induced reactions – transglycosylation, elimination, fission and disproportionation. These reactions provide complex mixtures of low molecular weight compounds that escape from the heated zone as tar and gaseous fractions [19, 36].

At 500°C and above, using fast heating rates the route of depolymerisation is favoured, leading to a mixture of anhydrosugars, primarily levoglucosan. One proposal is that the levoglucosan then is hydrolysed and decomposes into smaller molecules [53]. Another may be that it undergoes cleavage into smaller molecules [46]. The presence of the ether linkages, carboxyl and carbonyl functional groups increase the complexity of the formed products [19]. The degree of polymerisation is seen to be greatly reduced from around 1400 to a value of approximately 200 – 400 on heating. This supports a general depolymerisation route of thermal degradation for cellulose [35].

Instantaneous heating (flash pyrolysis) of cellulose to high temperatures above 500°C, may involve similar reactions to give a mixture of volatiles and gaseous products. It may be possible that direct fission of cellulose to low weight products occurs by the addition of such high amounts of heat energy [44].

The effects of changing the atmosphere in which the thermal degradation of the cellulose occurs have been examined; vacuum pyrolysis shows an increase in the amount of liquid products formed [44], whereas, elevated pressures during biomass pyrolysis yield higher levels of char (the solid residue remaining after pyrolysis) [49]. This may be indicative of secondary reactions being the main cause for the formation of char. Under vacuum the pyrolysis products are removed rapidly, whereas in a pressured system the primary pyrolysis products remain and may react to form other compounds, promoting the formation of char.

Thermogravimetric experiments showed the same weight loss for cellulose, in both air and nitrogen (~89%). The maximum rate of weight loss occurs at a slightly lower temperature in air (330°C vs. 385°C). The charred residue is completely combusted under air only. This indicates that the mechanism for this weight loss of the residue is an oxidative process [54].

The level of impurities or additives can have a large effect on the pyrolysis of cellulose. Addition of compounds to cellulose is used as a method of fireproofing cellulosic fibres, textiles, and soft furnishings. Inorganic additives as flame retardants enhance the char forming reaction rather than the volatile forming reaction in the competing reactions model of Broido-Shafizadeh. The additives conduct heat more evenly through the material, avoiding hotspots or form a solid layer in the polymer blocking the migration of degradation products to the surface,

reducing the amount of fuel available and thus the flammability [6, 26]. Vapour phase flame retardants work by enhancing the formation of volatile phase compounds. The retardant material, which generally has a halide moiety (usually bromine) is also released into the vapour phase and will react with other materials, replacing oxygen in volatile molecules, lowering vapour phase oxidation in the combustion [6, 55].

Depending upon the conditions, discussed above, cellulose decomposition passes through a number of mechanisms to form a huge range of breakdown products. These reactions include conversion of glycosyl units to levoglucosan and evaporation of the other volatile products. In 1976 Shafizadeh published a list of pyrolysates from cellulose heated to 550°C (Table 1-2), since then a large number of compounds have been identified from pyrolysis studies of cellulose.

Table 1-2. The main pyrolysis products of cellulose at 550°C in nitrogen [56].

Product	Yield Wt %
Acetaldehyde	1.5
Furan	0.7
Propenal	0.8
Methanol	1.1
2-Methyl furan	Trace
2,3-Butanedione	2.0
1-Hydroxy-2-propanone; glyoxal	2.8
Acetic acid	1.0
2-Furaldehyde	1.3
5-Methyl-2-furaldehyde	0.5
Carbon dioxide	6
Water	11
Char	5
Tar	66

More detailed studies of cellulose pyrolysis using pyrolysis gas chromatography-mass spectrometry (py-GC-MS) show a large number of evolved products. The amount of material

converted to volatiles was seen to peak at around 600°C, with the most complex region of evolved compounds in the temperature range of 400 - 600°C. In this particular study, by Faroq et al [57], cotton fabric was used as the cellulose source. They did not provide absolute quantification on their data, but used arbitrary units of intensity for groups of compounds. They arranged their compounds by functional groups to give an overview of the range of compounds that are formed on pyrolysis:

- furans – peaked at 500°C (which may be a dehydration reaction of the carbohydrates)
- aldehydes – mainly formed from 300 - 560°C (from decomposition of levoglucosan)
- ketones – less abundant than the aldehydes, possibly formed from fragment recombination reactions of primary pyrolysis products. Peak evolution at 500°C
- aromatic hydrocarbons – rise to a maximum at 500°C then rapidly decreases to a low level.
- CO – more abundant than the volatiles, peaking at 500°C then decreasing to a minimum at about 700°C before slowly rising again with a smaller maximum at 900°C.

They used this relative ranking of the groups of compounds to compare their textile samples to study the effects of burn retardants [57]. Pouwels and Moldoveanu, have both published much more extensive lists of cellulose decomposition products under different pyrolysis conditions [21, 34].

Generally, however, it is agreed that pyrolysis or thermal degradation of cellulose or cellulosic materials are a mixture of complex concurrent and consecutive reactions that are strongly influenced by a number of parameters [35]:

- composition of the material – different types of plant fibres or textiles or pure compound.
- time-temperature profile – slow gradual heating rates at low temperatures or rapid high temperature rates, or extreme conditions such as flash pyrolysis.
- conditions – oxidising or inert atmosphere. Atmospheric pressure or vacuum. Water and CO_2 in the pyrolysis atmosphere may also affect the process.
- inorganic impurities – such as ash or added catalysts or additives.
- particle size and sample mass are important factors to consider in kinetic studies, as a heat transfer limitation is considerable at high temperatures, thus must be taken into account in designing the experiment [12, 52].

1.2.4 Levoglucosan

Thermal decomposition of cellulose in a vacuum was first performed in 1918 by Picter and Sarasin, who discovered that levoglucosan (1,6 anhydro-β-D-glucopyranose. IUPAC; 6,8-dioxabicyclo [3.2.1.] octane-2,3,4-triol) was a major pyrolysis product of cellulose [58], therefore the study of its formation provides information on the mechanism of cellulose pyrolysis. The mechanism of formation for levoglucosan is still unclear though two main mechanisms are proposed, either a homolytic or heterolytic cleavage of the glycosidic bond (Figure 1-6) or a free radical mechanism.

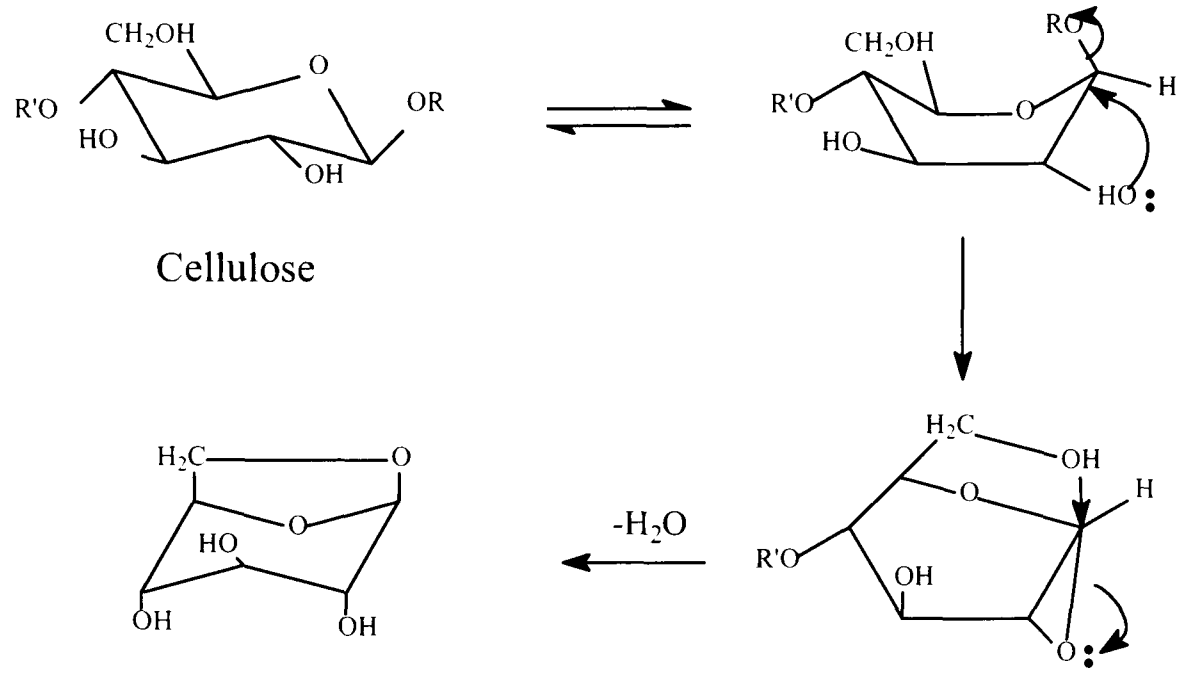

Levoglucosan

Figure 1-6. Formation of levoglucosan via dehydration and homolytic cleavage of the glucosidic bonds (Where R and R' are the continuing cellulose chains).

Evidence for a heterolytic route was proposed by a study that blocked the formation of levoglucosan by converting the primary alcohol to an ester. Madorsky concluded that the reduced levoglucosan levels were due to steric hindrance between carbons 1 and 6 [31]. There is also some evidence to suggest that the levoglucosan formation may also be related to the degree of polymerisation (DP), with high DP samples giving higher yields of levoglucosan. Crystallinity of the cellulose also has an effect, with the low ordered regions of cellulose having faster rates of thermal decomposition [35].

Other studies have shown that decomposition of the primary products of cellulose is the route of formation of many of the smaller molecules. Levoglucosan is thought to further degrade to

form most of the flammable gases observed from the combustion of cellulosic materials [34, 53, 59]. This was shown by comparison of the pyrolysis products of cellulose and levoglucosan, which contain similar gases, semi-volatiles and volatile compounds [29]. Decomposition of levoglucosan occurs at moderate temperatures, implying low activation energies. Radio labelled levoglucosan showed that the thermal decomposition of the levoglucosan yielded formaldehyde from the C_1-C_5 fragment. It was also seen that production of the 3,6 anhydro-ring leads to the formation of furyl methyl ketone that decomposes to form furaldehyde from the C_2-C_6 fragment of the monomer unit [42]. Nimlos and his team identified some simple reactions for further decomposition of levoglucosan that include elimination of water and formaldehyde as shown in Figure 1-7 [60].

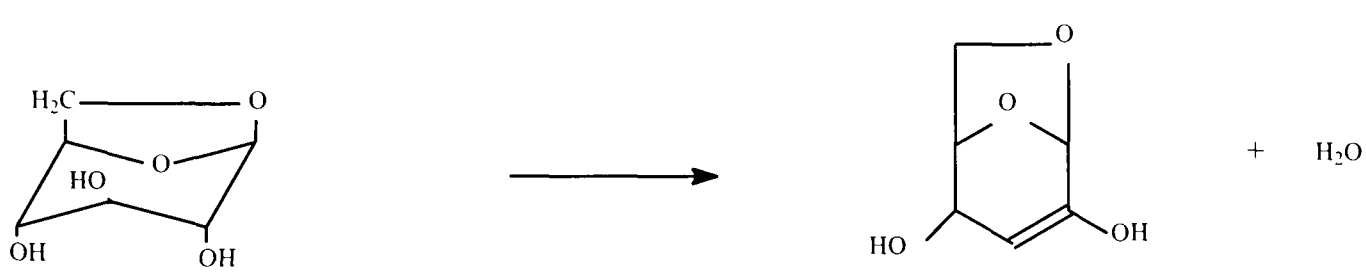

Figure 1-7. Suggested decomposition routes for levoglucosan pyrolysis [60].

More detailed mechanisms for the formation of levoglucosan and its subsequent decomposition are given in Figure 1-12 and Figure 1-17.

1.2.5 Char Formation

Cellulose pyrolysis yields a carbonaceous char that breaks down further under oxidising conditions. The definition of char used by Broido and Nelson was "the solid residue collected at 370°C", more recent studies define it more as the solid residue remaining after much higher temperatures are reached (above 500°C). In the present study char refers to the solid residue remaining after subjecting the sample material to a defined heat treatment temperature (HTT). HTT is defined as the temperature at which the initial cellulose material was heated to prepare the char sample.

Cellulose chars have been characterised as having large surface areas, and may be a source of large numbers of free-radicals. The char may also be chemically active as high rates of oxygen chemisorption have been measured, with the rate of chemisorption dependant on the HTT. The peak rate observed was at a HTT of 550°C [61]. The precise chemical nature of the char is believed to be dependant upon the temperature at which it is formed. The higher the temperature of formation, the higher the aromatic content; a lower temperature leads to higher amount of aliphatic content in the char. Chars formed at 350°C still contain nearly 50% of the original cellulose structure. By 400°C all of the glycosidic structure has decomposed leaving a mainly aromatic char with some paraffinic character. Between 400°C and 500°C the paraffinic groups are preferentially decomposed leading to an increased aromatic 'stable' char [62]. A DSC study of cellulosic chars confirm the presence of two char types by the presence of two exotherms - the first exotherm due to oxidation of the aliphatic carbons and the second exotherm due to the oxidation of the aromatic carbons [47]. Comparison of NMR and FTIR studies confirm earlier work on cellulose chars that used permanganate oxidation as a method of elucidating the structure of the char. The glycosidic structure is completely broken down on heating cellulose at 400°C under nitrogen for 5 minutes. The formation of new structures of carbonyl and carboxyl groups is apparent and also increasing aromaticity of the carbon content of the char is observed. Heating from 400 - 500°C produces little additional change [26]; the carboxyl and carbonyl groups are diminished and the aromatic groups are increased in the NMR. The FTIR investigation revealed similar trends with loss of the hydroxyl and glycosidic bonds observed at 3500cm^{-1} and 900-1200cm^{-1}, respectively, and the emergence of more C=C

absorption bands at 1600cm^{-1} and carbonyl absorption bands at 1700cm^{-1}. At higher temperatures the absorption band at 1600cm^{-1} is further enhanced [62, 63].

Shafizadeh and Sekiguchi showed that by changing the HTT of the cellulose (in forming the char) the aromaticity of the char increases as shown in Table 1-3. In this study cellulose powder (Whatman CF-11) was acid washed, then pyrolysed in a pre-heated oven for 5 minutes under 60ml.min^{-1} nitrogen flow [47]. At a HTT of 500°C for 5 minutes the char's empirical formula had changed from cellulose ($C_6H_{10}O_5$) to $C_6H_{3.2}O_{0.9}$. This reduction in H/C ratio is confirmed by IR and X-ray diffraction studies which show a lack of oxygen molecules in the structure of the char [61]. Antal [64], however, found in his study that thermal pre-treatment had no significant effect on cellulose pyrolysis. He indicated that earlier studies had used much larger sample masses. This was confirmed by Mok who noted that increased sample mass (increased mass in the constant volume of the reactor) in a sealed reactor observed increased char yields [63]. The resultant increased transport resistance would lead to increased secondary reactions, which would explain the increased char levels at higher temperatures [27].

Table 1-3. Elemental composition of the chars prepared at different temperatures under nitrogen [47].

Condition	Char Yield	Carbon Functionalities										
		Composition			Paraffinic			Aromatic		Oxygenated groups		
°C	%	C	H	O	CH3	Others	Glycosylic	ϕ-H	ϕ-O	-COOH	C=O,-CHO	Total
Untreated	-	42.8	6.5	50.7	-	-	100	-	-	-	-	100
325	63.3	47.9	6.0	46.1	4		85	3		8		100
340	50.1	51.8	5.4	42.8								
350	33.1	61.3	4.8	33.9	9	15	30	23	13	5	5	100
400	16.7	73.5	4.6	21.9	14	13	<1	56	13	1	2	100
450	10.5	78.8	4.3	16.9	10	11	~0	66	11	1	1	100
500	8.7	80.4	3.6	16.1	6	6	-	79	9	-	<1	101
600	5.3	88.3	2.9	8.8								

Volker [49] concurred that a lower heating rate gave more char; he observed that changing the heating rate from 3 to 0.14°C.min^{-1} with an identical sample of cellulose (same initial mass and bulk density) doubled the yield of char formed. It has also been noted that a higher sample load lowered the temperature at which charring occurs and increased the char yield.

The effect of additives is shown to increase the yield of char formed in the pyrolysis process, in particular Lewis acids ($MgCl_2$, NaCl, $FeSO_4$ and $ZnCl_2$) have a strong effect [64]. For example, treatment with inorganic additives increases the char yield (from 15.3% for untreated cellulose, to 17.5% from NaCl treated and 28.9% for diammonium phosphate treated cellulose). The char yields measured by TGA in one study also varied 7-10%, indicating that there were other factors involved in char formation other than ash (inorganic impurities) content [28]. Increased aromaticity was seen in these increased yields compared to the untreated sample. The sodium chloride additive enhances the smouldering combustion, but the diammonium phosphate suppresses it. Both, however, suppress flaming combustion [61]. Inorganic species may have the effect of lowering the temperature of ignition in cellulosic material, but have no effect on the rate of chemisorption of oxygen onto the carbonised char. However, they do seem to increase the rate of gasification from the char [65].

The composition of the intermediate chars can also be affected by inorganic species [26]. DeGroot [66] illustrated this in a study in which acid washed wood samples were shown to reduce the char yield by 2-3% compared to untreated samples. This shows that the natural, inorganic 'ash' content of the wood has a significant effect on the thermal decomposition of the material. This effect on cellulose has been seen with all alkali metal ions, particularly sodium. However, contrary to other studies it was found that char yields were unaffected. Conversely, calcium ion treatment of the wood increases the decomposition temperature.

Elevated pressures increases the yield of char formed [63] and rapid removal of the primary pyrolysis gases also has the effect of reducing the char yield [67]. Therefore char formation can be linked to the vapour-solid phase reactions. By controlling these interactions the Antal and Varhegyi showed that it was possible to achieve char yields from 0% to 40% [27]. It was also seen that addition of water also increased the char yield, implying that the char forming reaction is autocatalysed by water, a major pyrolysis product [63].

Antal also similarly noted that char formation in Avicel (a commercial powdered form of α-cellulose), under identical conditions but in a covered pan, changes from 7% to 19%. It was concluded that it must be due to volatile-solid reactions, and therefore did not relate to char forming mechanisms proposed by the models of Broido-Shafizadeh or Arseneau-Várhegyi [28]. At higher heating rates they also found that heat transport effects were more important with increasing sample masses. This was observed by differential thermal analysis (DTA) as an increase in the temperature of the maximum decomposition rate from 361°C to 378°C. This

increase in transport resistance leads to an increase in secondary reactions due to the inability of primary products to leave the bulk sample, allowing secondary cracking of the gases and volatiles [52].

The ratio of aliphatic to aromatic carbon groups affects the subsequent combustion temperature of the char in air, the higher the aromatic content the higher the combustion temperature [47]. The combustion process involves chemisorption of oxygen on the reactive sites of the char. This reaction is highly exothermic and occurs at relatively low temperatures forming surface oxides, which in turn sustains the process in the absence of any major sources of heat loss. Gann et al [33] found that, assuming zero-order kinetics, the energy absorbed by cellulose pyrolysis in air was $850J.g^{-1}$ (in the temperature range 300 – 650°K). Under nitrogen they obtained a value of $\sim 1400J.g^{-1}$ in the range of 300 - 500°K, which shows the role of oxygen in the combustion process.

The net heat of combustion of cellulose char has been shown to be related to the carbon content of the reacting substrate [47] –

$$\mathbf{H_{comb}\ (J/g) = 94.45 \times \%C - 685.3} \qquad \textbf{Equation 1-1}$$

Consequently the high temperature chars, which are more aromatic in character and have a higher %C, oxidise and also give out more heat for a given weight [47]. Therefore once the char has begun to form, a low heat rate is sufficient to continue the spread of the char through the substrate. Another study found that using a reaction temperature of 470°C, the reaction order for cellulose char = 0.83 ± 0.06 [68]. They also calculated activation energy of 112.9kJ/mol for cellulose char. Subsequent formation of CO and CO_2 is believed to promote the formation of new active sites on the surface of the char. The rate of propagation of the charring process is dependant on the rate of formation of CO and CO_2. The carbon-oxygen mechanism involved consists of the following mechanisms with the formation of the new stable oxide at an active site (C*) with subsequent high temperature desorption.

$$C^* + O_2 \longrightarrow \underset{\text{Stable surface oxide}}{C(O)_s} \xrightarrow{\text{Slow}} CO + CO_2$$

This is followed by the rapid gasification of CO and CO_2, via a short lived transitory oxide.

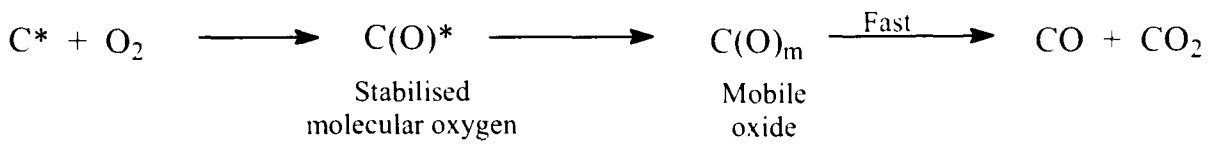

This latter process is thought to be responsible for the majority of the CO and CO_2 formed during combustion [65, 69].

Oxidation of the char is highly exothermic and is then thought to be the driving force for the continued thermal decomposition of the cellulose molecule. This process has been examined by DSC which showed oxidation of the residual char occurs at two different temperatures, with observed exotherms at 360°C and 520°C. The first corresponds to the oxidation of aliphatic components and the second with oxidation of the aromatic components. Oxidation of the aliphatic components of the char occurs almost at the same temperature as the pyrolysis of the glycosyl units. The aromatic components of the char oxidise at a higher temperature and also release more heat, indicating that the rate of the aromatic char oxidation is likely to be the driving force of the combustion process [26]. The addition of acidic additives lowered the temperatures of oxidation and also slowed the rate of oxidation, witnessed by the shifting and broadening, respectively, of the DSC exotherms.

Chemisorption of oxygen onto the char is a controlling factor in the solid phase combustion of cellulosic materials [61, 70]. Additives, such as NaCl, appear to increase the initial rate of chemisorption, which increases the solid phase combustion of the cellulose. Burn inhibitors such as diammonium phosphate, suppress the chemisorption rate. This may be due to the additives either increasing or decreasing formation of 'active' sites, during carbonisation of cellulose, for the chemisorption to occur.

A different study also showed that additives may enhance or retard the gasification rates, but have little effect on the adsorption of oxygen. The rate of adsorption reaches a maximum in chars prepared at 550°C, which corresponds to the usual temperature at a smouldering front in a cellulosic material [69].

Electron spin resonance (ESR) studies have shown that the oxygen chemisorbed onto the char inhibits the production of free radicals [70]. It was seen that the amount of oxygen that chemisorbed onto cellulose chars was ten times higher than that expected from the free-radical counts. Though a depolymerisation type free-radical generation is possible by peroxy radicals pulling more H atoms from C-H bonds, another possibility is formation of reactive peroxide

intermediates being formed via 1:4 addition to unsaturated diene type groups through a Diels-Alder process. This is a thermally activated process, and therefore potentially more likely at the temperatures that occur during pyrolysis and combustion [69].

From the above review it is clear that there are two stages of char formation in the decomposition of cellulose, an aliphatic char and an aromatic char. Studies using various techniques (NMR, IR and DSC) have all agreed on the presence of two char types. The mechanism of formation of these chars is less clear, although a number of parameters that effect the formation (pressure, additives/impurities, heat rates, etc.) have been demonstrated, and proposals made regarding how these effects occur. However, it is apparent that gas-solid reactions at the char surface play a major role.

1.3 Kinetics of Cellulose Pyrolysis

The kinetics of cellulose pyrolysis has been studied extensively. This is mainly due to the need for accurate kinetic parameters for design of reactors for processing biomass, as a fuel or source material for other commercially viable products. Modelling combustion behaviour of cellulose and similar materials is extremely complex [29]. It involves consideration of heat transfer, mass transfer and chemical reaction processes in the solid and vapour phases [71]. For example, Baker suggests that to describe the process as a simple one step kinetic mechanism seems unlikely due to the complexity of the decomposition process [72]. The complexity of "cellulose pyrolysis kinetics' is described in one study as, 'the attempt to produce a mathematical description of the thermal decomposition of a small, homogeneous sample of pure cellulose that is free from contaminants, with a well defined DP and crystallinity. The temperature is uniform through out the sample during the process and mass transfer is such that it permits the immediate escape of volatile products without incurring any secondary reactions. Further to this the assumption is also made that the sample holder has no influence on the pyrolysis chemistry' [27]. Disagreements are, however, commonplace in the literature when describing the reaction rates and apparent activation energy of cellulose pyrolysis. It is possible to describe the global reaction rates and activation energy using a number of models [73] but commonly first order reaction kinetics are assumed for simplicity [14, 29]. As the process for cellulose combustion is described as two competing reactions the kinetics may be described as a coupled set of competing first order reactions [74]. However, some authors have described part or all of the

process as zero order [71, 75, 76], whereas others have used expressions other than first or zero order [37, 77, 78] to fit their proposed models.

Early work on thermal degradation rates of cellulose were performed under vacuum and gave results that showed deviation from linearity in the logarithm of initial reaction rate vs. time plots. It was postulated that the reaction was complex and could not be described fully by assuming first order [31]. The logarithms of apparent initial rates were plotted against the reciprocal of absolute temperature to give a straight line plots (the so-called Arrhenius plot). From these plots the activation energy for the process was calculated – the authors obtained a figure of ~188 kJ/mole [31]. Since this early work a wide variety of values for activation energy have been produced, using different techniques (most commonly TGA) covering different temperature ranges and source materials (cellulose mostly, some cotton and wood).

For example, Nada et al used TGA data to study cellulose pyrolysis [79]. They analysed the weight loss data differentially and found that the slope of the plot (rate of weight loss vs. time) is the rate constant for the thermal decomposition. In this study the result gave a two-stage line. The first shallow part was ascribed to water loss, the steeper part was said to be due to the decomposition. The authors assumed a first order reaction and calculated the activation energy from an Arrhenius plot, using the main decomposition temperature region 260 – 450°C. They obtained an activation energy of 182.4 $kJ.mol^{-1}$ [79]. However, a considerable range of values from 109 to 251 $kJ.mol^{-1}$ was previously reported in the literature [35].

Pyrolysis of cellulose under isothermal conditions (in inert atmosphere) shows an initial fast weight loss until a maximum rate is reached. After this the rate decreases asymptotically until a final char residue is reached [80]. Studies have described this observation with two phases as an initial zero order reaction followed by a first order reaction within the unreacted cellulose, in order to describe the kinetics [71, 75, 76]. Others have argued for a pair of competing endothermic reactions [74]. Braun and Burnham produced a method for quantifying the limitations of global kinetics for describing complex systems [81]. They showed that using a pseudo-nth-order gives better fits and slightly higher effective activation energies than a first order model. The pseudo-nth-order reaction can also be used for parallel, competing first order reactions.

Generally, however, most treatments of TGA data used to measure the rates of decomposition take an Arrhenius form, such as:

$$-\frac{dW}{dt} = A\exp\left(-\frac{\Delta E}{RT}\right)W^n \qquad \textbf{Equation 1-2}$$

where:

W = the fractional residual weight of the sample

T = the absolute temperature

R = gas constant

t = time of reaction

A = the pre-exponential factor

ΔE = activation energy

n = the order of the reaction.

These equations are treated in one of two ways; first, the equation is written as a differential equation and the fractional weight determined by integration as a function of the temperature. The other method is to plot logarithms of the terms of the equation and from them obtain the kinetic constants [82].

In Figure 1-8 Bradbury et al. describe a kinetic model for cellulose pyrolysis under inert conditions as two competing first order reactions [80] which was extended by Radlein [12].

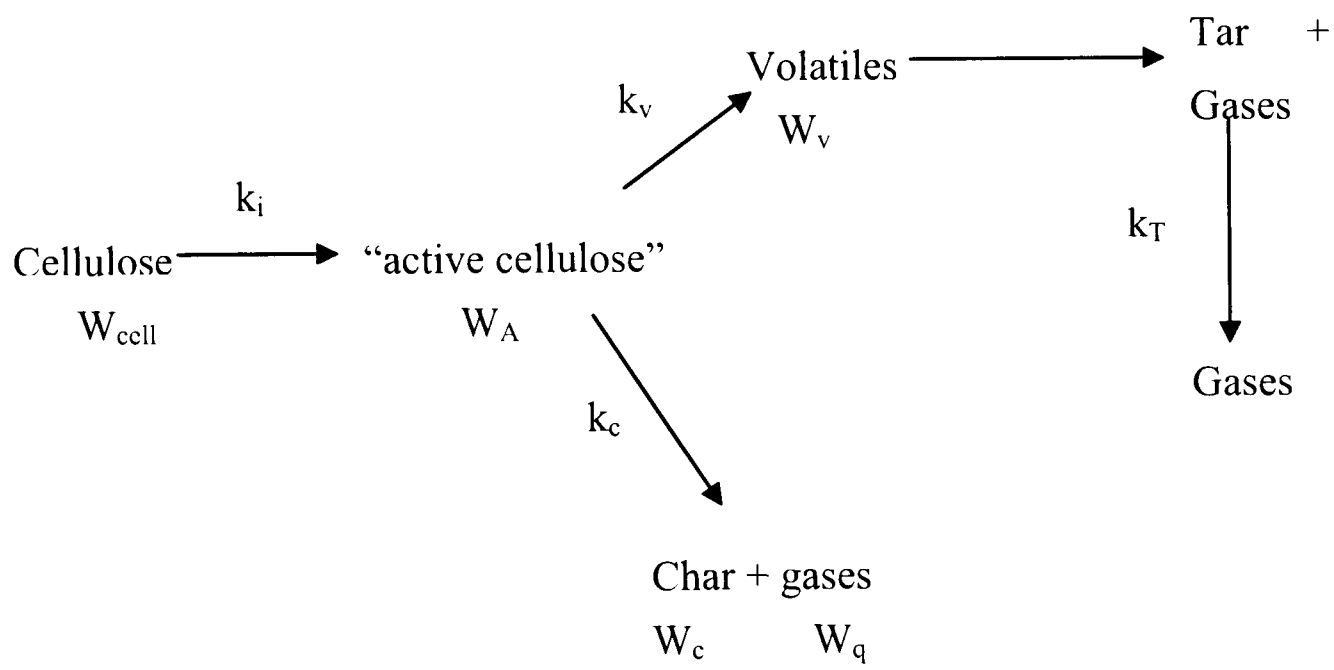

Figure 1-8. Kinetic model for cellulose pyrolysis in inert atmosphere [12].

where:

$$\frac{-d(W_{cell})}{dt} = k_i[W_{cell}] \qquad \textbf{Equation 1-3}$$

$$\frac{d(W_A)}{dt} = k_i[W_{cell}] - (k_v + k_c)[W_A] \qquad \textbf{Equation 1-4}$$

$$\frac{d(W_c)}{dt} = 0.35k_c[W_A] \qquad \textbf{Equation 1-5}$$

$k_i = 1.7 \times 10^{21}\ e^{-(58{,}000/RT)}\ min^{-1}$

$k_v = 1.9 \times 10^{16}\ e^{-(47{,}300/RT)}\ min^{-1}$

$k_c = 7.9 \times 10^{11}\ e^{-(36{,}000/RT)}\ min^{-1}$

$k_T = 3.4 \times 10^{0}\ e^{-(25{,}000/RT)}\ min^{-1}$

However, the use of single first order reaction rate models to describe overall volatile formation can lead to activation energies being calculated that may not be realistic for real chemical processes [83]. Antal and Varhegyi [27] showed a high activation energy ~238kJ/mol by minimizing the secondary vapour-solid char-forming interactions. They suggested that under these conditions decomposition of cellulose fits an irreversible, first order reaction equation. The experiments were performed such that secondary reactions were almost completely eliminated by rapid removal of primary products, and that the cellulose sample was pure and ash-free.

It is thought that perhaps the large sample sizes used in early work by Broido, etc. may have encountered secondary reactions occurring due to the large sample sizes used in those studies. Primary pyrolysis products could then be trapped in the substrate long enough to undergo vapour-solid phase reactions, which then complicate the kinetics of the system [48].

Choosing the correct method for analysis of thermogravimetric data is a complex task in its own right and much research has been done to show how TGA data may be used to derive kinetic parameters for a reaction [82, 84-86].

Activation energy for the thermal decomposition of cellulose was calculated from a technique developed by Ozawa [82]. For fractions of decomposition (α) between 0.1 and 0.9 the log of heating rate was plotted against reciprocal of absolute temperature. This is known as an isoconversional method of evaluating Arrhenius parameters. Overall Faroq et al suggest that the decomposition of the untreated cotton fabric fits a second order reaction [87].

An improved model was proposed that included some of the secondary reactions that may occur during the pyrolysis of cellulose, the Diebold model (Figure 1-9).

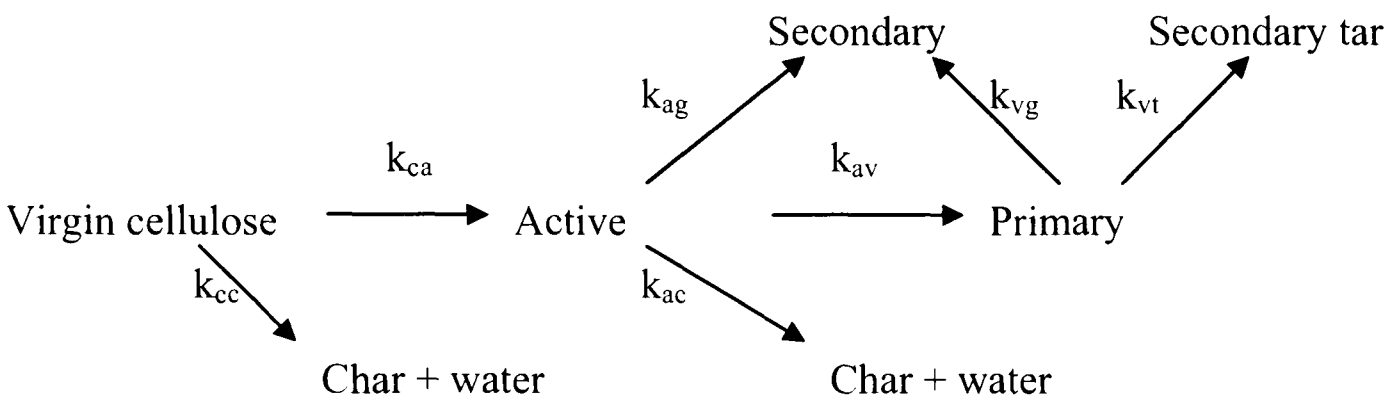

Figure 1-9. The Diebold model for cellulose pyrolysis [88].

The different models used to describe the global kinetics of the thermal degradation of cellulose, assuming the Arrhenius form of data treatment (Equation 1-5), seem to show little difference in the constants derived from them (Table 1-4).

Table 1-4. Activation energies (E) and pre-exponential (logA) terms from various pyrolysis models [89].

Rate/Model	Virgin to 'active' step		'active' to volatiles step	
	log(A)	E	Log(A)	E
	[log(s^{-1})]	[kJ/mol]	[log(s^{-1})]	[kJ/mol]
Multistep models				
Classic	19.45	242.4	14.5	196.5
Diebold	19.45	242.4	9.83	140
1-step models				
Antal-Varhegyi	18	238	NA	NA
Reynolds-Burnham	12.94	180.45	NA	NA

Note: One step models should be considered as virgin to product, but are placed in the virgin to active columns for comparison.

To examine cellulose using global kinetic studies it is important to define exactly what the char is. In most TGA traces the asymptotic char yield is evidence of temperature gradients within the sample. As noted previously, Milosavljevic and Suuberg observed that in normal, non-isothermal TGA experiments there was a potential for serious heat transfer limitations and associated temperature measurement problems that had to be considered [71]. Also heating rates did have a significant effect on the data determined from the experiments. As a result of these observations, Milosavljevic and Suuberg, in their TGA studies made sure that the samples were placed in a mono-layer rather than a pile in the sample pan [71]. Another consideration, particularly in non-oxidising atmospheres, is that the reaction may seem to be complete but there may be higher temperature pathways still open to the remaining material [71]. Antal also noted that the catalytic effect of the 'ash' (inorganic impurities) content of the cellulose needs to be included in the model of the process, although there is no simple technique capable of performing such a task [28]. It was the conclusion of one reviewer that many studies are rendered uncertain by these problems – especially those performed using TGA [12].

Despite the debate as to whether TGA is a suitable technique for kinetics studies, the majority of kinetic models are based upon weight loss information. Ozawa presented one of the earliest techniques for drawing kinetic information from TGA data [82]. He stated that thermogravimetry has advantages over isothermal data collection, as particularly with higher

polymers, initial structural change in the sample complicates the isothermal data. Ozawa's method for data treatment has been drawn on and refined over the years by other researchers. Flynn and Wall [90] described an alternative technique where simple thermogravimetric data can be used to produce a more accurate measurement of activation energy. The activation energy can be calculated from reading the temperature at a point of constant weight loss from a series of integral thermograms collected at different heating rates. They describe C as the rate of conversion, where 1-C (the residual fraction) is equals the weight of material loss divided by the total weight loss as T or t $\rightarrow \infty$. So the thermogravimetric rate is given by

$$dC/dT = (A/\beta)\,\mathrm{f}(C)e^{-E/RT} \qquad \textbf{Equation 1-6}$$

where:

T = absolute temperature, K

β = constant heating rate

A = pre-exponential factor of the Arrhenius equation

E = activation energy

R = ideal gas constant

f(C) = a function of degree of conversion (weight loss)

The variable parameters can be separated and then integrated assuming that A, f(C) and E are independent of temperature, and that A and E are independent from C. At the lower limit, T_0, the integral is negligible, thus as a logarithm the equation transforms to:

$$\log \mathrm{f(C)} = \log (\mathrm{AE/R}) - \log \beta + \log \mathrm{p(E/RT)} \qquad \textbf{Equation 1-7}$$

where p is the integral function of the exponential temperature. For E/RT > 20, log p(E/RT) can be approximated to

$$\log p(E/RT_i) \cong -2.315 - 0.457E/RT_i \qquad \textbf{Equation 1-8}$$

substituting this into the equation and differentiating at a constant degree of conversion gives the following equation

$$d\log\beta / d1/T \cong (0.457/R)E \qquad \textbf{Equation 1-9}$$

And for R = 8.643 $J.mol^{-1}.K^{-1}$

$$E \cong -4.35\, d\log\beta / d\,1/T \qquad \textbf{Equation 1-10}$$

Therefore activation energy (E) can be determined as the slope of a plot of log β vs. 1/T. Further values of E can be obtained by inserting different values of 1-C into the equation. From the approximate E/RT value the constant, -4.35, can be improved to obtain more accurate values of E through an iterative process. The independence of E from C and T can be tested by determining E for different values of constant weight loss. This expands the work of Friedman [85], by producing models that show less deviation from experimental results.

Friedman plots are used to describe complex solid phase pyrolysis reactions mathematically. For example, a simple single step model governing weight loss is assumed then the rate law:

$$dV/dt = k\left(V^* - V\right)^n; k = Ae^{-E/RT} \qquad \textbf{Equation 1-11}$$

is often used to fit experimental data.

Taking natural logarithm of both sides, the following equation is obtained:

$$\ln(dV/dt) = \ln A - E/RT + n\ln\left(V^* - V\right) \qquad \textbf{Equation 1-12}$$

If values of ln(dV/dt) obtained at different heating rates are plotted against T^{-1} for constant values of weight fraction (V*-V) the slope of the resulting line is –E/RT.

Where:

V = $(w_i-w)/w_i$

V* = $(w_i-w_f)/w_i$

k = rate constant

A = pre-exponential constant (apparent frequency factor)

E = apparent activation energy (kJ/gmol)

t = time of reaction (s)

n = apparent order

T = temperature (K)

$w(t)$ = time dependant sample weight (g)

w_i = initial sample weight (g)

w_f = final sample weight (g)

By plotting a number of these lines for different constant heating rates, a curve may be drawn through the points of same weight fraction that is unique to the active pathways during pyrolysis. Therefore it is a powerful way of interpreting complex solid phase pyrolysis information [73].

It is easy to conclude that processes measured in thermal experiments involve complex interactions that change over time. It is little wonder that simple kinetic models do not provide adequate descriptions of such systems in terms of mechanistic description [91].

With this in mind when designing an experiment with the goal of determining the kinetics of a complex pyrolysis system like cellulose, a number of parameters must be clearly defined [12]:

- the sample must be clearly defined, though it is not always clear which parameters are important in terms of the kinetics (e.g. crystalline index, purity, additive type and level)
- temperature range and pressure of the reaction system
- pyrolysis atmosphere – oxidising or non-oxidising
- internal and external heat transfer rates, and the relationship with particle size (particle size is an important factor to consider in kinetic studies, as a heat transfer limitation is considerable at high temperatures, thus must be taken into account in designing the experiment)
- pyrolysis temperature and also rate of heating

With these factors in mind the information surrounding the kinetics of cellulose is still an area of much research, with no clear agreement on the reaction order, whether or not to treat the system as concurrent or consecutive processes [78]. The range of proposed activation energy values (109 – 251kJ.mol^{-1}) also reflect this general disagreement of cellulose kinetics, and the wide variety of experimental conditions used in these studies.

1.4 Reaction pathways for cellulose thermal decomposition

A number of chemical reaction pathways have been produced that attempt to describe an overview of the process involved in cellulose combustion. These give a general picture of the

chemistry occurring during the pyrolysis or combustion processes, some have been built purely using kinetic information. As indicated previously the kinetics are still subject to some debate, so these mechanisms are formed by using global kinetic information based on weight loss data, combined in some cases with evolved pyrolysis product identification. Early mechanisms are based more around the identification of pyrolysis products using various different experimental conditions, so the associated mechanisms are postulated from these observations.

The pathways presented here are grouped into fields of study, the earliest being more concerned with fire research and the actions of flame retardant additives. Later papers start to show interest in the effective use of biomass, reflecting the attempts define kinetic parameters for design of biomass processing plants. Other models are derived form the interest of using biomass as a source for other industrial chemicals.

1.4.1 Fire research and flame retardants

One of the earliest models for cellulose pyrolysis was by Kilzer and Broido [43]. Published in 1965, their model for combustion of cellulose still forms the basis of many subsequent studies particularly by Shafizadeh and his co-workers [7, 44, 56, 92, 93]. Today these form a starting point for more recent studies and reviews of cellulose combustion. Though some more recent studies dispute some of the findings and kinetics proposed this initial work still forms much of the basis of later models. Kilzer and Broido began with a view to providing a greater understanding of the process of thermal decomposition of cellulose. The intention was that greater understanding would help in the development of flame retardants, and as such they were the first to note the effects of addition of salts on the mechanism. They proposed thermal decomposition of cellulose was a combination of two competing endothermic reactions (Figure 1-10) [43].

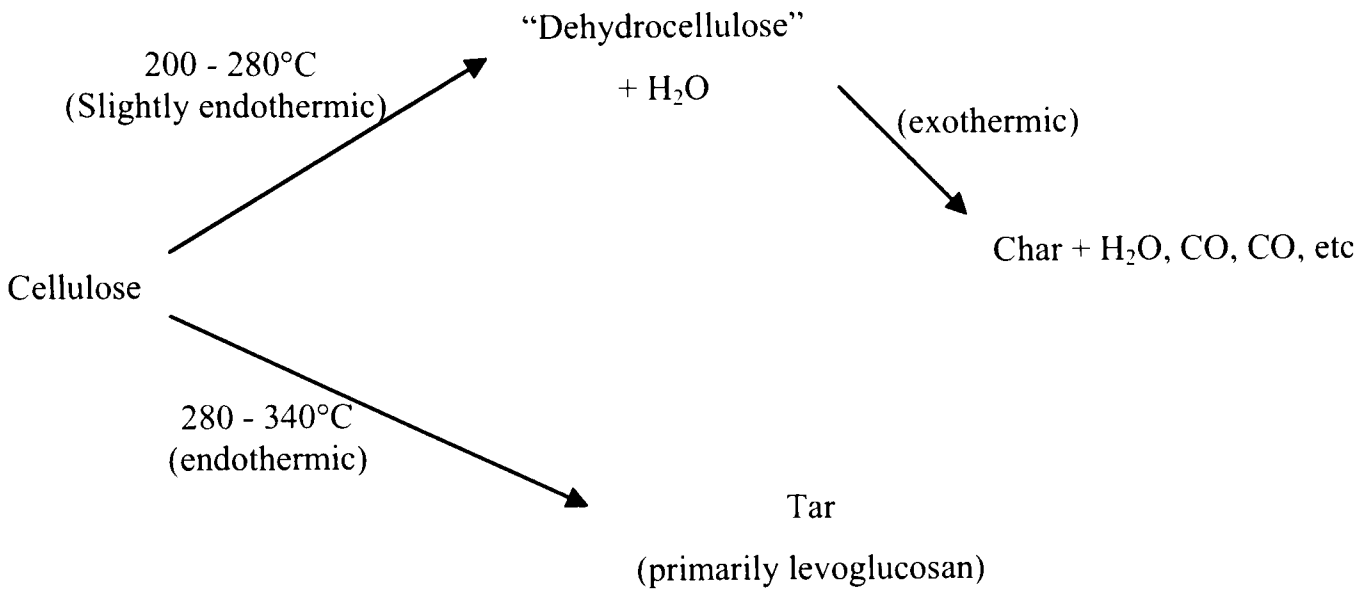

Figure 1-10. Kilzer and Broido reaction model for the combustion of cellulose [43].

The model has three distinct processes; the first a slightly endothermic reaction with the loss of water to give 'dehydrocellulose', as described in Figure 1-11. It is an intermolecular reaction, with a hydroxyl group from an adjacent chain (Figure 1-11-a) reacting at the glycosidic bond (Figure 1-11-b), resulting the elimination of water and the formation of a furanose end group (Figure 1-11-c) on the cellulose chain.

Finally the exothermic reactions of the 'dehydrocellulose' produce char with a number of gaseous products and volatile carbonyls. This competes with the other endothermic reaction which is postulated to be an unzipping of the polymer to give levoglucosan, via 1, 4 anhydro-α-glucopyranose (Figure 1-12).

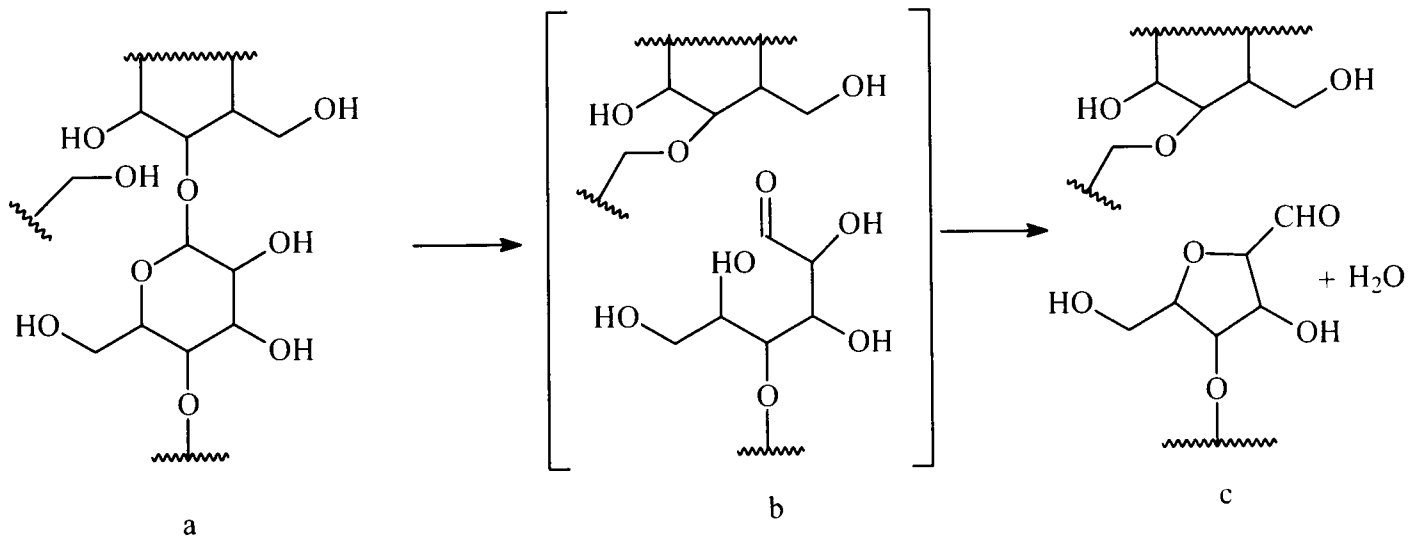

Figure 1-11. Proposed mechanism for intermolecular dehydration of cellulose – a. cellulose b. reaction intermediate c. 'dehydrocellulose'.

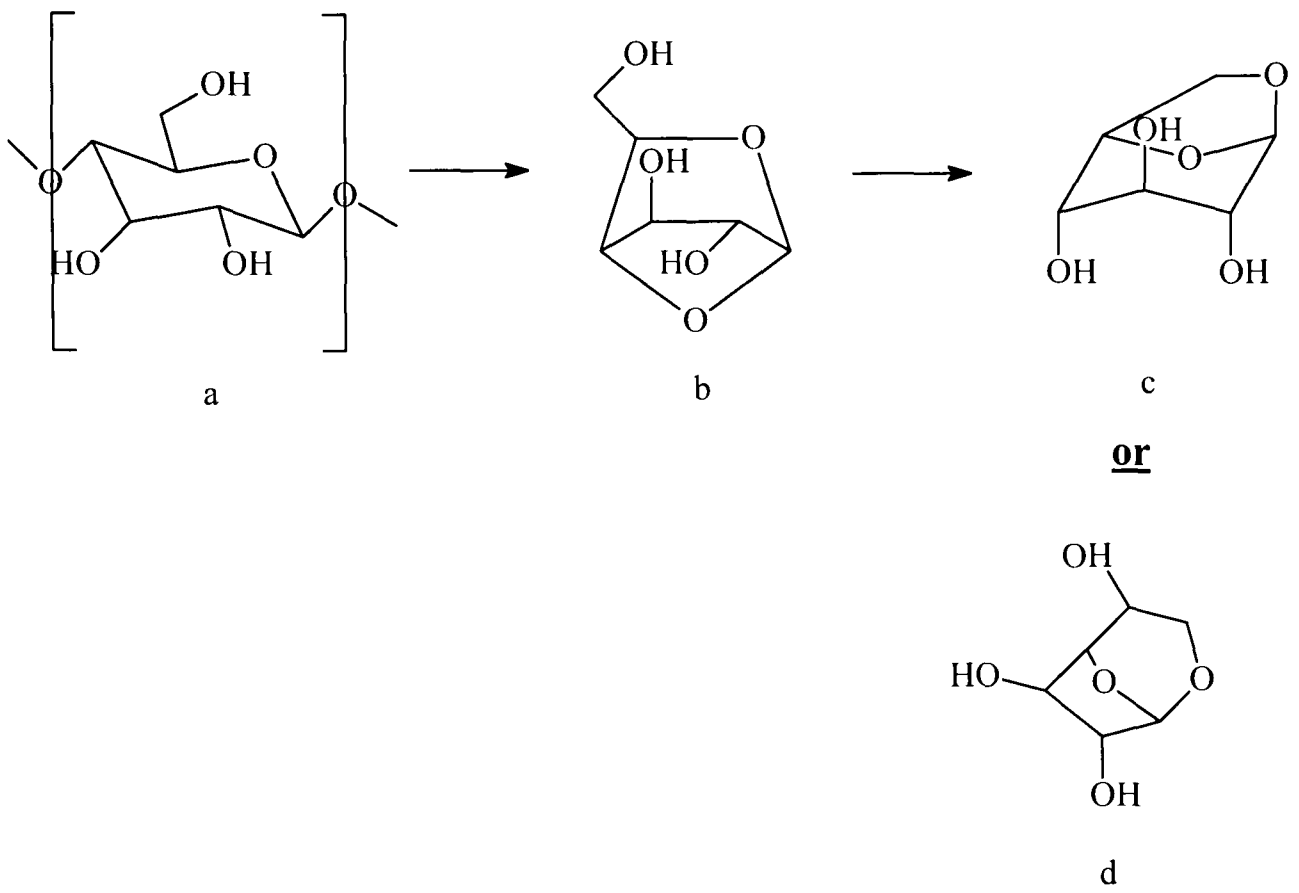

Figure 1-12. Proposed mechanism for depolymerisation of cellulose. a. Glucopyranose monomer, b. 1, 4 anhydro–α-glucopyranose, c. levoglucosan, d. 1, 6 anhydro –β-glucofuranose.

This mechanism is based mostly on kinetics from weight loss information and the assignment of compounds is disputed by Banyasz et al as an arbitrary assignment of compounds. Banyasz performed a similar kinetic study based upon product formation by evolved gas analysis (EGA), also allowing identification of the pyrolysis gases. However, in terms of predicted weight loss the kinetics from both models gave similar results, indicating overlap between the models, particularly at temperatures below 400°C [94]. Milosavljevic and Suuberg found that with large sample sizes tar may be formed under either slow heating or rapid heating. This was due to temperature gradients across the sample such that the heating displayed high rates occurring at the surface and slower rates in the centre [71].

Drews and Barker [95] studied the combustion of cellulosic fabrics but from a different angle. Their work was to examine the effect of phosphorus based burn additives on the chemical nature of the char formed on pyrolysis of cellulose. Cellulose fabrics were treated with phosphorus-containing burn retardants. The samples were charred by burning the samples in air using a paper match. Samples that extinguished were relit until fully charred. Calorimetric analysis was carried out on the samples to determine the heat of combustion. TGA analysis was also

used, and from it, concluding that the phosphorus flame retardants reacted directly with the cellulose rather than any of the intermediates. This was deduced from the change in activation energy of the treated cellulose (-33.4 to -41.8 kJ/mol) compared to the untreated cellulose (-188 kJ/mol) [95].

They used a slightly different model (Figure 1-13) that did not include the 'dehydrocellulose' step in the reaction proposed by Kilzer and Broido. Their kinetic model was not taken any further, though later models acknowledged that the ultimate end point of both of the reaction pathways was the formation of carbon dioxide and water.

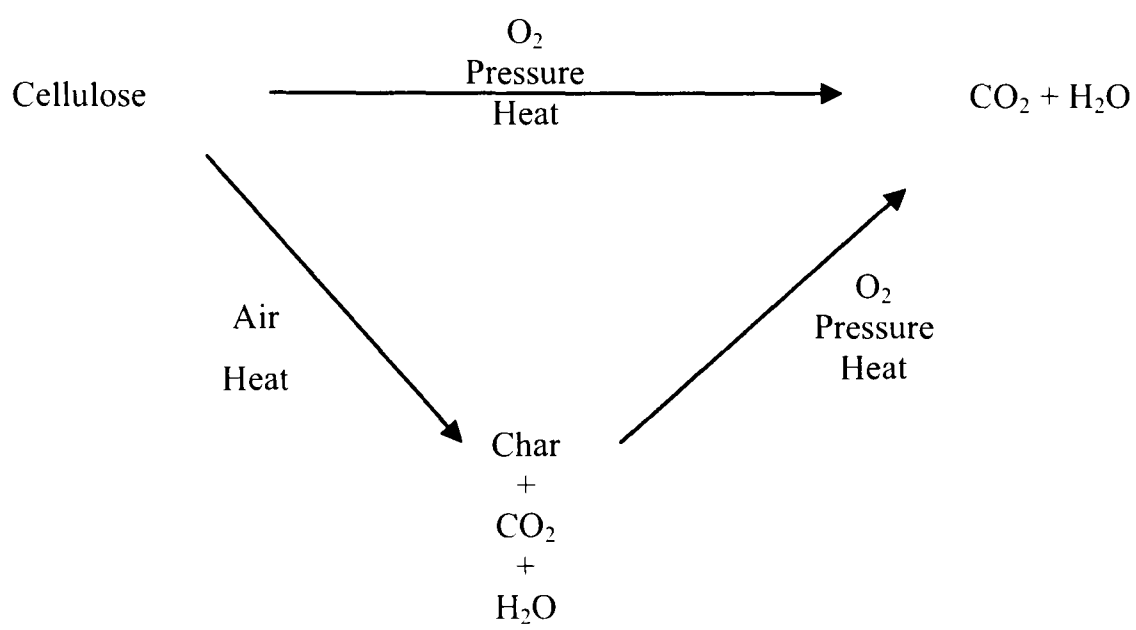

Figure 1-13. Mechanism for the pyrolysis of cellulose proposed by Drews and Barker [95].

Other researchers have also produced work expressing their doubts over the 'dehydrocellulose' or 'active cellulose' step that was used by Broido and Shafizadeh respectively [27, 48].

Shafizadeh and his various co-workers produced extensive work on combustion of cellulose over nearly 20 years at the Wood Chemistry Laboratory at the University of Montana. A great deal of their work was funded by fire research institutes, so the main focus was in the fundamentals of the process and the effects of flame retardants. His meticulous research along with his co-workers, have produced a number of findings that have become an essential part of the general understanding of cellulose combustion. Many research groups have quoted his work and built around his work in their studies of cellulose pyrolysis.

Shafizadeh summarised in one of his published discussions that pyrolysis or thermal degradation of cellulose or cellulosic materials are a mixture of complex concurrent and consecutive reactions that are strongly influenced by a number of parameters [35]:

- composition of the material – different types of plant fibres or textiles or pure compound.
- time-temperature profile – slow gradual heating rates at low temperatures or fast high temperature rates such as flash pyrolysis.
- atmospheric conditions – oxidising or inert. Atmospheric pressure or vacuum. Water and CO_2 in the pyrolysis atmosphere may also affect the process.
- inorganic impurities – such as ash or added catalysts or additives.

These parameters have been subjected to many studies by other authors and have been verified almost as many times.

In 1979 Shafizadeh and Bradbury produced the schematic model for cellulose combustion shown in Figure 1-14 [51]. They, however, noted that the proposed reaction lines are not distinct or clearly defined. The pathways often overlap and therefore may produce different proportions of the final products based on the experimental conditions [35].

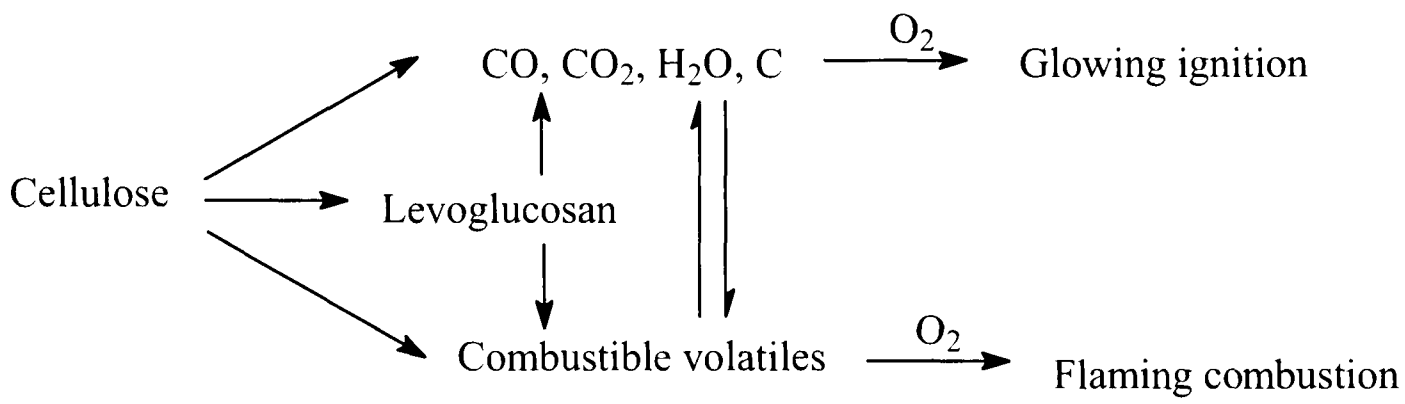

Figure 1-14. A schematic model of cellulose combustion by Shafizadeh and Bradbury [51].

They identified two main reaction paths; one reaction is the fragmentation of the molecule to form volatile compounds that feed the flaming combustion. The other is the dehydration of the cellulose and formation of a carbonaceous char leading to glowing ignition of the material. Heating at lower temperatures favours the latter route, whilst at higher temperatures, generally above 300°C, the formation of a tar which contains a large amount of levoglucosan (up to 60% of the tar) is seen along with other carboxyl and carbonyl decomposition products [29, 51, 92]. At higher temperatures a number of concurrent reactions occur including dehydration, rearrangement reactions and fission of the glucose units to form a variety of carbonyl compounds. These higher temperature reactions, generally above 500°C, produce the volatile

tars and residues that in air may lead to flaming combustion. Smaller particle sizes, fast heating rates will favour the formation of the volatile tars and gases [9, 50].

At temperatures below 300°C the reactions that occur in the pyrolysis of cellulose, in air or inert atmospheres include, free-radical initiation, elimination of water, depolymerisation reactions producing a carbonaceous char with carbonyl, carboxyl groups and evolution of CO and CO_2. The initiators in these reactions include thermal action on trace impurities in the cellulose, the action of oxygen on a substance other than the substrate (a very slow reaction unless heat is added), or direct hydrogen abstraction by oxygen – a highly endothermic reaction so quite unlikely. These initiators then can interact leading to auto-oxidative reaction common to polymers [96]. In a similar fashion to synthetic polymers, Shafizadeh observed the formation of hydroperoxide groups in cellulose at 170°C in air, and the subsequent decay in nitrogen. A mechanism for formation and decomposition of cellulose hydroperoxide is postulated (Figure 1-15).

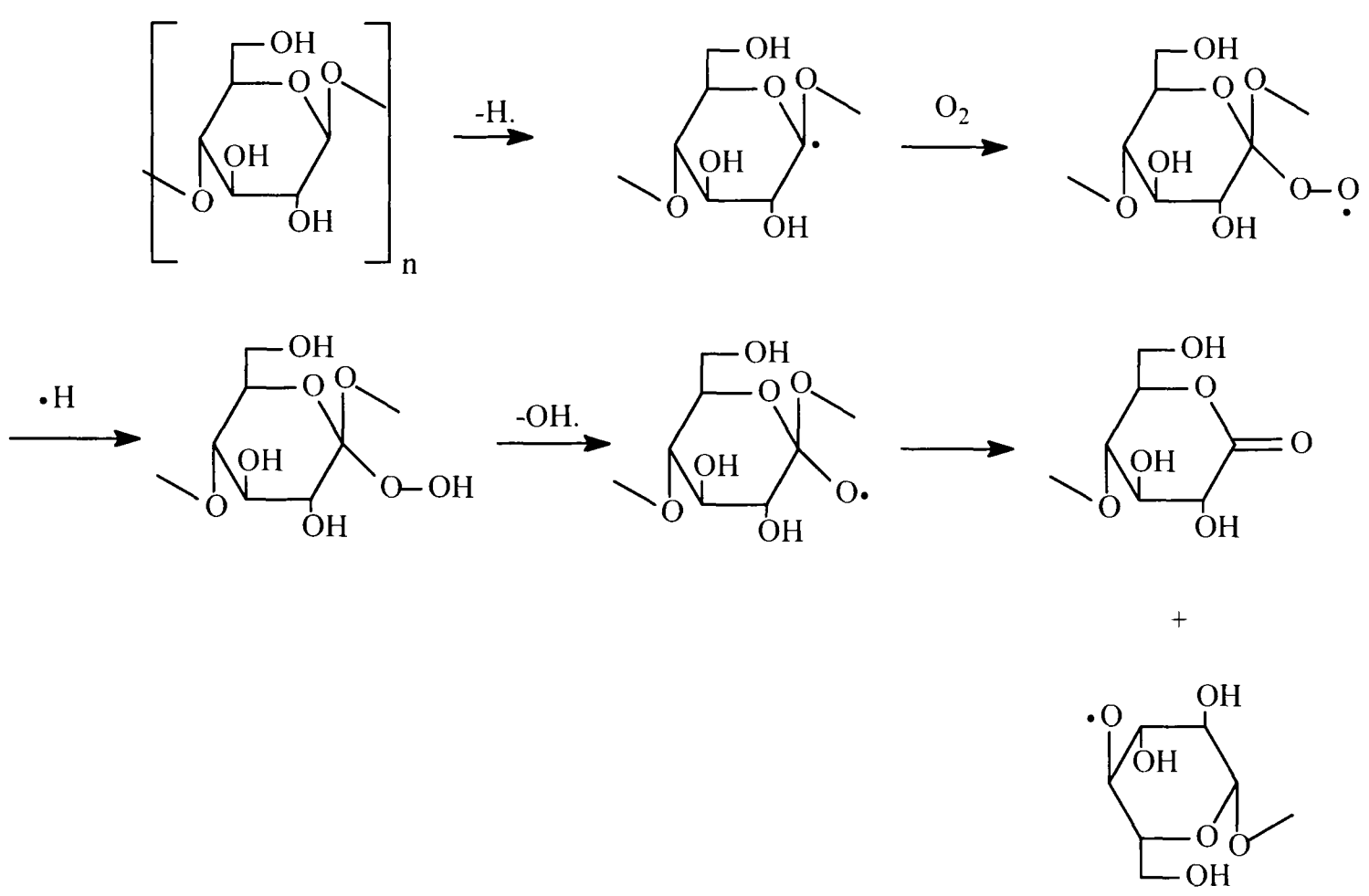

Figure 1-15. Possible mechanism of formation and decomposition of cellulose hydroperoxide formed thermally in air [44].

However, another study [36] did not find any evidence of ether linkages in pyrolysis of cellulose and pre-charred celluloses, as was also suggested by Kilzer and Broido in their proposed mechanism for the formation of 'dehydrocellulose' [43].

In the range of 300 - 450°C transglycosylation reactions occur, which is the cleavage of the glycosidic bond by substitution involving a free hydroxyl group [97]. Figure 1-16 describes the reaction. This reaction leads to levoglucosan (1, 6 anhydro-β-D-glucopyranose – centre second row) but also the 1, 2 and 1, 4 anhydro-β-D-pyranoses may be formed (left and right molecules respectively, second row). These compounds may then further decompose to form a mixture of other glucose derivatives and oligosaccharides. This reaction is believed to occur in the amorphous region of the cellulose polymer.

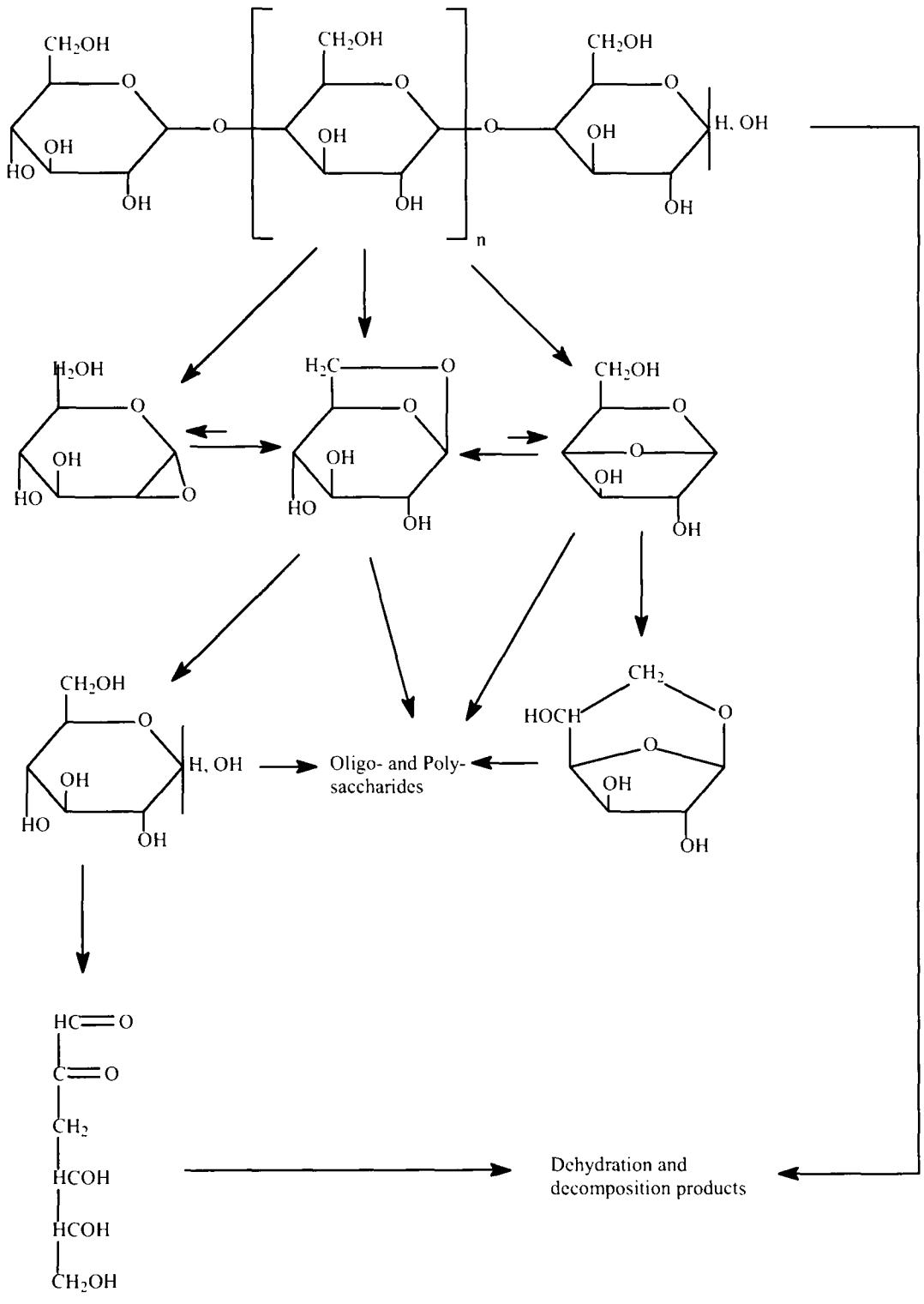

Figure 1-16. Mechanism for the transglycosylation reaction in cellulose heated above 300°C [97].

Lomax et al proposed a mechanism for the formation of free reducing end groups from cleavage of the glycosidic bonds. They dispute Shafizadeh's proposal that oligomers are formed by resynthesis from levoglucosan. Their GC-MS data of permethylated cellulose pyrolysate indicates the presence of oligomers, and some anhydrosugars. The amount of anhydrosugars present seemed to be dependant on sample size. It was concluded that there was some resynthesis but on the whole the oligomers are formed as primary pyrolysis products from cellulose [98]. Despite this, in a later treatise on biomass combustion Shafizadeh published an updated mechanism (Figure 1-17) from the transglycosylation reactions for cellulose pyrolysis, reiterating the formation of oligomers via resynthesis from anhydrosugars.

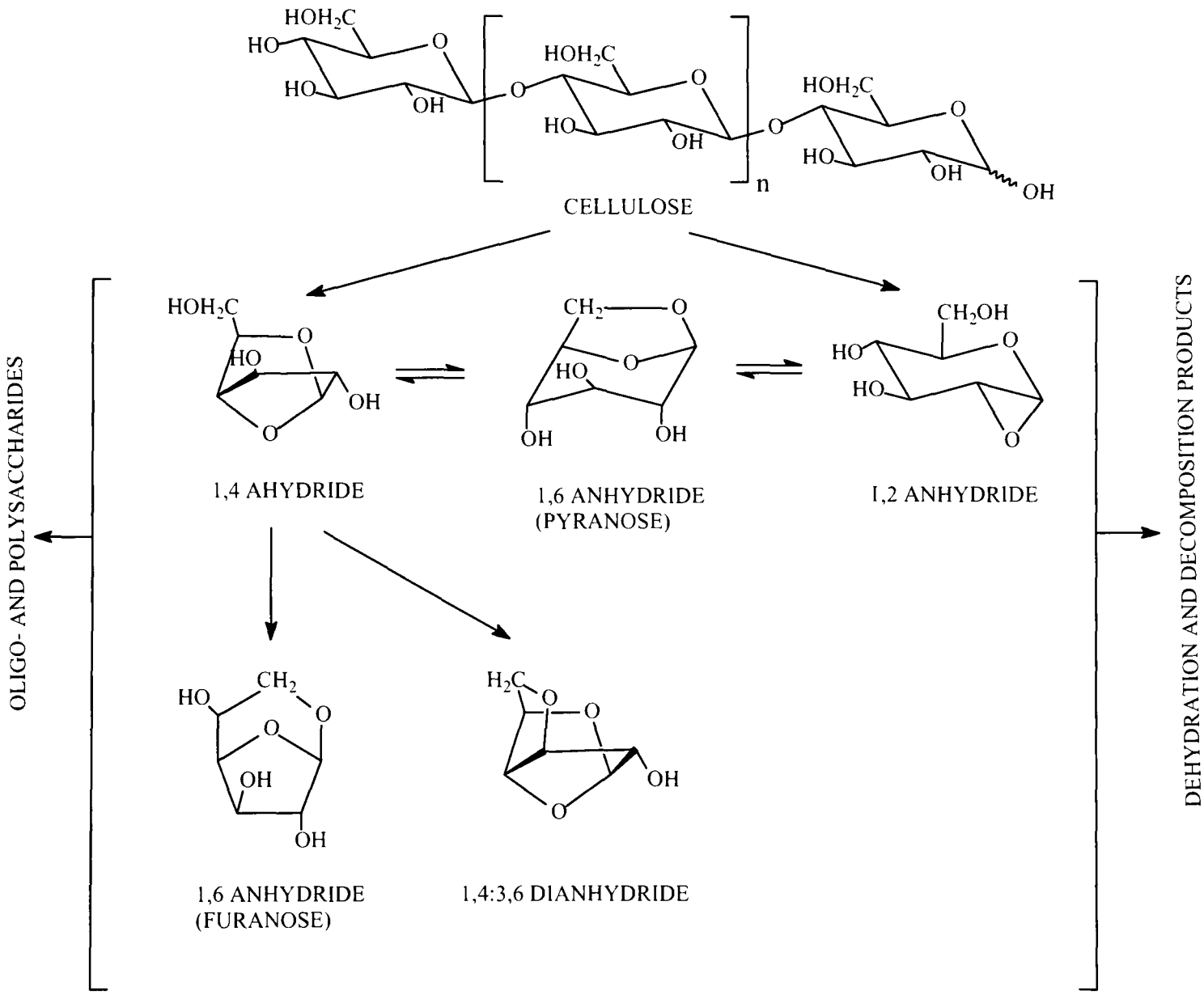

Figure 1-17. Updated mechanism for pyrolysis of cellulose to anhydrosugars and other compounds by transglycosylation reaction [44].

The higher temperature mechanism involves cleavage of glycosidic bonds to form anhydrosugars, notably levoglucosan. Higher temperatures still may involve free radical reactions as the solid residues char further [44].

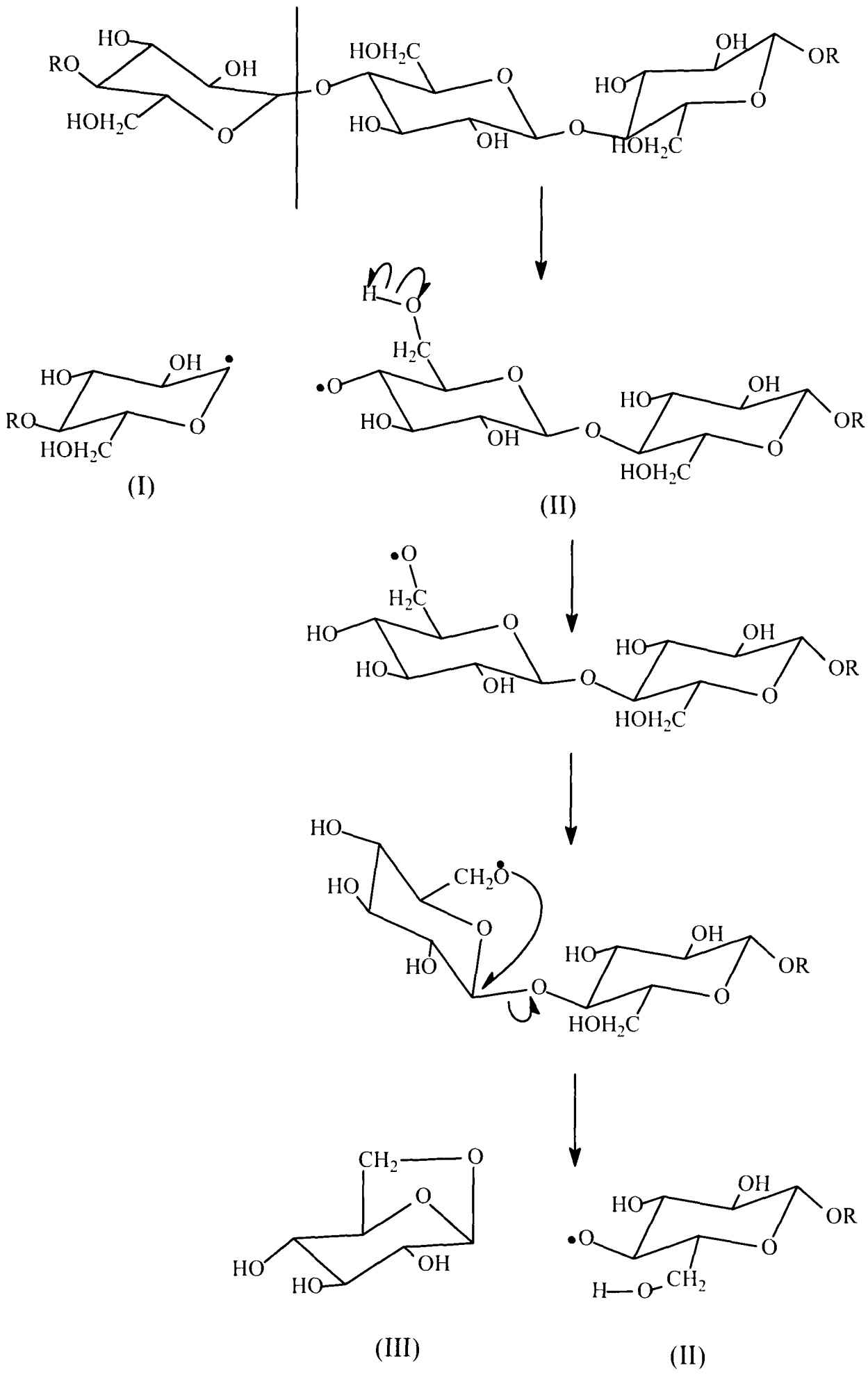

Figure 1-18. Free-radical depolymerisation of cellulose, in which (I) and (II) are radicals, Golova [42].

Golova produced a reaction scheme for a free-radical depolymerisation of cellulose (Figure 1-18). The mechanism begins with the cleavage of a glycosidic bond to initiate the reaction. The reaction continues, with the cellulose breaking down at the initiated end of the chain with one anhydroglucose unit detaching one after another. The initiated chain end (II) can then form levoglucosan, denoted (III), via a conformational shift continuing the depolymerisation [42]. However, Hirata in his review [29] suggests that the mobility of free-radicals in cellulose is likely to be limited. In contrast with synthetic linear polymers which may fuse before pyrolysing, cellulose thermal decomposition is primarily in the solid state.

More recently, Price and Horrocks et al made an extensive study on the mechanism of a number of specific flame retardants on cellulose textiles [15, 25, 57, 87, 99-103]. From their observations they created a more detailed pathway for cellulose pyrolysis [101].

They divided their model into three main stages:

- in the region 300-400°C, cellulose breaks down via an activated form of cellulose (cellulose*) to give a mix of aliphatic char and levoglucosan. DTA experiments show a low temperature transition peak (~330°C) which may support this theory [103].
- between 400-600°C the aliphatic char is oxidised in the presence of O_2 gas to give an oxidised char. At the same time the volatiles are oxidised to CO, CO_2, H_2O and various organic compounds. At higher temperatures (600-800°C) the aromatic char degrades to give low molecular weight compounds such as acetylene.
- above 800°C oxidation and combustion dominates.

The model that they proposed included a more comprehensive scheme for the formation of a number of classes of compounds. They used a number of different techniques to study the effects of the burn additives, including TGA, DSC and py-GC-MS to name but three [15, 25, 57, 87, 99-103]. The pathway they proposed is shown in Figure 1-19.

In support of the general Broido-Shafizadeh model, Price and his co-workers included a step of cellulose transforming into the active form of cellulose on heating (cellulose → cellulose*). They based this on data obtained from DTA coupled with Evolved Gas Analysis (DTA-EGA). They determined a low temperature transition (denoted T_2) that had no corresponding weight loss. This transition was confirmed by the more sensitive technique DSC. They noted that that the peak was reproducible but not reversible and also required the presence of an external source

of oxygen. The T_2 peak only occurred in samples pyrolysed in air, implying that the 'active cellulose' may be the result of an oxidation reaction.

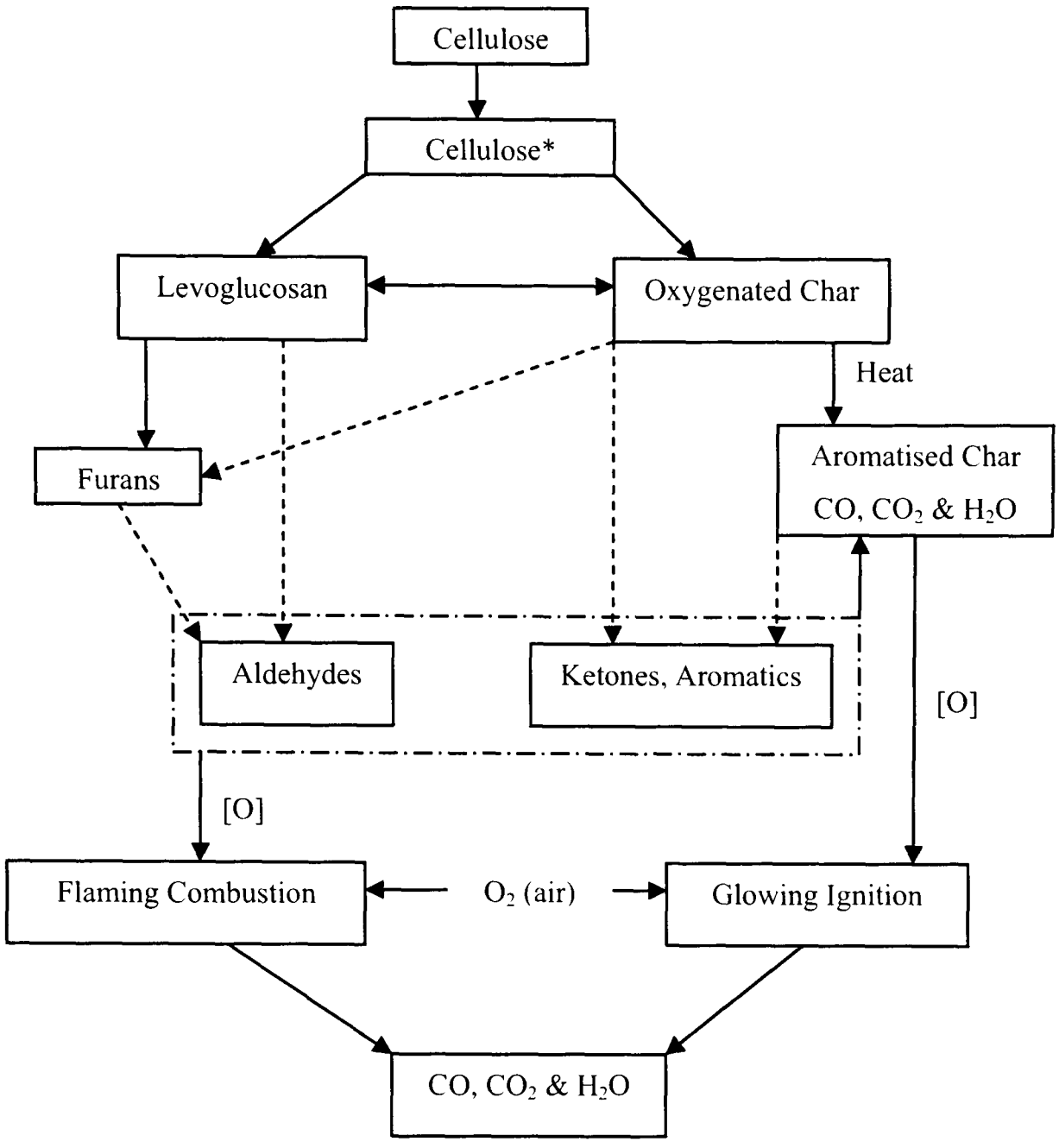

Figure 1-19. Model for cellulose pyrolysis by Price, Horrocks et al. where |O| represents oxygen available from the cellulose molecule [101].

During pyrolysis of the cotton fabric (cellulose) CO and CO_2 formation occurs from primary and secondary pyrolysis reactions and char oxidation [100]. Hajaligol at al also found that ethane, ethane and propane formation increases above 650-750°C, suggesting that a significant contribution is from secondary decomposition of the tar rather than the parent cellulose. To support their claim they also noted that the tar yield began to decrease in the same temperature region [104].

Pastorova agreed from her work that the char exists in two phases; she described them as a residual crystalline cellulose phase and a thermostable phase that was more aromatic in character. The chars prepared at lower temperatures (190 – 250°C) contained mostly residual crystalline cellulosic char, while the higher temperature chars (270 – 310°C) contained more aromatic character. Intermediate temperatures contained some of both types of char [36].

1.4.2 Treatment of biomass

Mok and Antal, in particular, have been very active in biomass research over the years; these references representing a selection of their papers [10, 30, 63, 64, 67, 73]. As a result of cellulose making up 50% of most biomass sources they and their various co-workers have contributed a huge amount of work in the field of cellulose pyrolysis. In particular they have produced a large amount of work on the kinetics of the pyrolysis process, for cellulose as well as other biomass [27, 28, 49, 77]. However, they also produced a mechanism for cellulose degradation after studying the effects of pressure on the pyrolysis of cellulose [53].

They verified this model for cellulose pyrolysis by also looking at the pyrolysis of levoglucosan, and anhydrocellulose under the same conditions of cellulose. They found that similar pyrolysis products were formed, particularly under low flow rates and high pressures. As a result they concluded that the secondary reaction between the pyrolysis products and also the remaining substrate were important factors in the pyrolysis process. Reactions 1 and 4 (Figure 1-20) are promoted under higher pressure and low flow rates leading to the maximum char formation. High pressure with high flow still produces more char; including a secondary char formed via reaction 6 which is visually different to the primary char, being less rigid and more 'soft and fluffy' in appearance. Under high flow rates and normal pressures the volatiles are allowed to escape more easily which promotes the reactions 2 and 5.

Repeating the study with cellulose it was discovered that there was no effect on the primary competitive reaction (1 & 2), form either the changing the pressure or flow rate. However, a later study by Essig and Richards [105], showed that this reaction may be influenced by the addition of low levels of salts (NaCl, $MgCl_2$ and Na_2CO_3). Small amounts (less than 1%) of these salts were added to cellulose that has been pre-treated to remove any naturally occurring metal ions. This has the effect of lowering the level of levoglucosan and raising the level of glycoaldehyde.

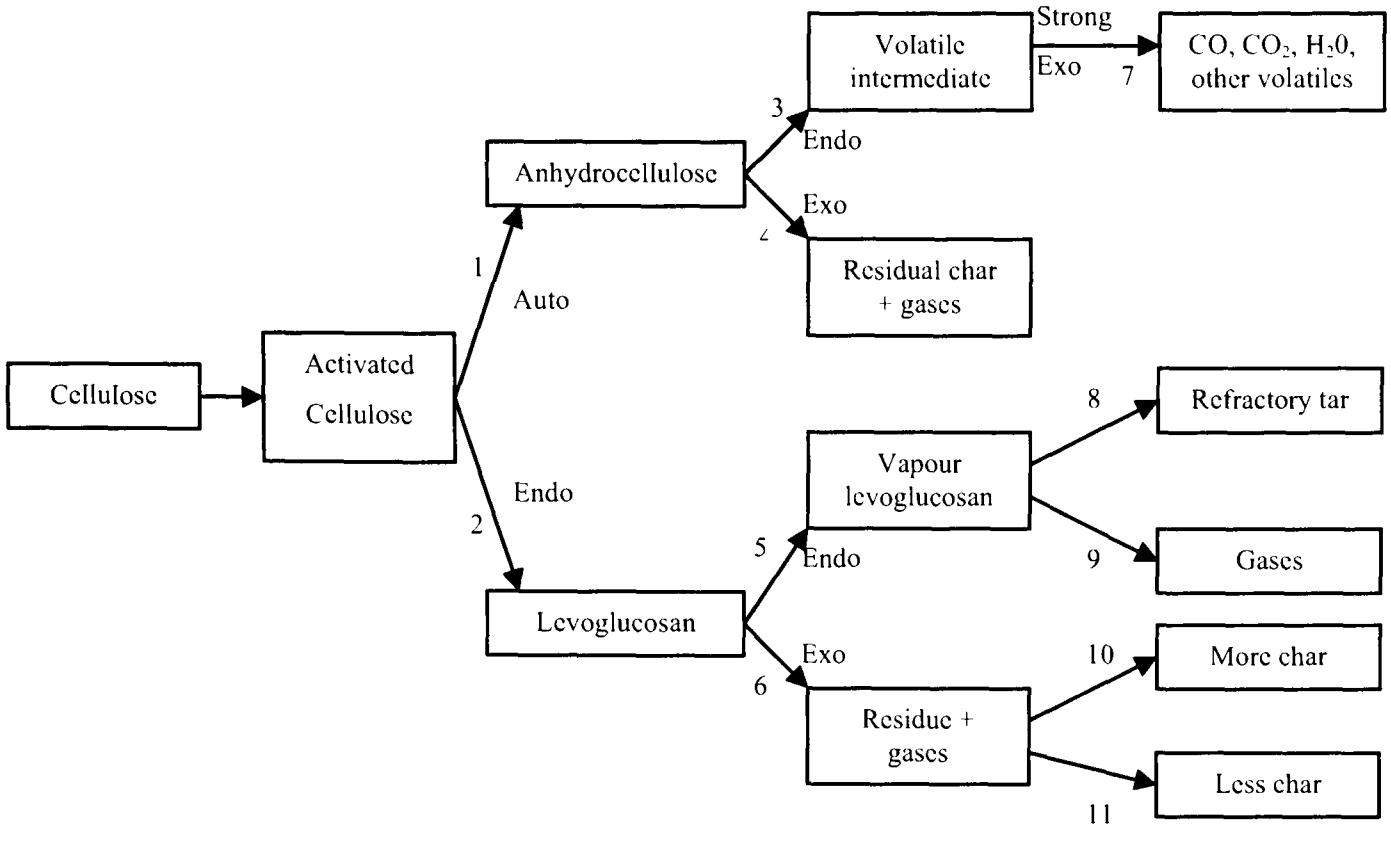

Figure 1-20. Detailed model of cellulose pyrolysis (Mok and Antal) [53].

Scheirs et al [41] studied the evolution of water during the combustion of cellulose. Primarily the interest was in the biomass field and in particular the auto-acceleration effect water has on the process of combustion. Although their reaction pathway is based around the evolution of water by various processes during cellulose combustion, it is possible to see links to some of the more complex models by Radlein [12], and Price and Horrocks [101]. In general water evolution had been noted previously as occurring in three different temperature regions during the pyrolysis process of cellulose:

- loss of water below 220°C. Physically absorbed water is lost from 25 – 100°C, and above this chemically adsorbed water and water of crystallinity is lost.
- chemical loss of water (220 – 550°C). Mostly from dehydration reactions of the molecule.
- chemical loss of water in pyrolysis (above 600°C).

However, Scheirs and his colleagues [41] only noted two evolution temperatures for water as their experiments had a maximum temperature of 400°C. They used these evolution temperatures (approximately 110°C and 300°C) to devise a more detailed mechanistic pathway for the evolution of water from cellulose pyrolysis, shown below in Figure 1-21 [41].

Using TGA-FTIR, Pan and Richards [106] found that at approximately 360°C a water peak is found, formed most likely via elimination reactions (probably from glycol groups, resulting in increasingly unsaturated residues and ultimately chars). This agrees with Scheirs theory of water formation from elimination reactions occurring from primary pyrolysis products.

Radlein and his group [12] studied the potential of biomass as a source for producing industrial chemicals. One part of the work was looking to shift the process of decomposition to favour one or more products, in particular levoglucosan and hydroxyacetaldehyde. Through this work they produced a pathway for cellulose combustion that differed to the traditional Broido-Shafizadeh mechanism [51] and, also to that of Mok and Antal [53]. In this mechanism there is no active cellulose stage, and the low temperature char formation route is direct from the virgin cellulose. They suggested that the high temperature route passed through a stage where the degree of polymerisation (DP) decreased considerably to around 200. This low DP cellulose could then pass through two different routes, or a mixture of the two. One is fragmentation of the polymer chain via dehydration and decarbonylation reactions, and the second a depolymerisation, unzipping, of the chain (Figure 1-22). The ring fragmentation route has the higher activation energy. Below 300°C the evolution of carbonyl, carboxyl, lactone and aldehyde groups in the pyrolysing residue increases linearly over a period of several hours. The formation of the char is an indication of cross-linking reactions in the region of 220°C [12].

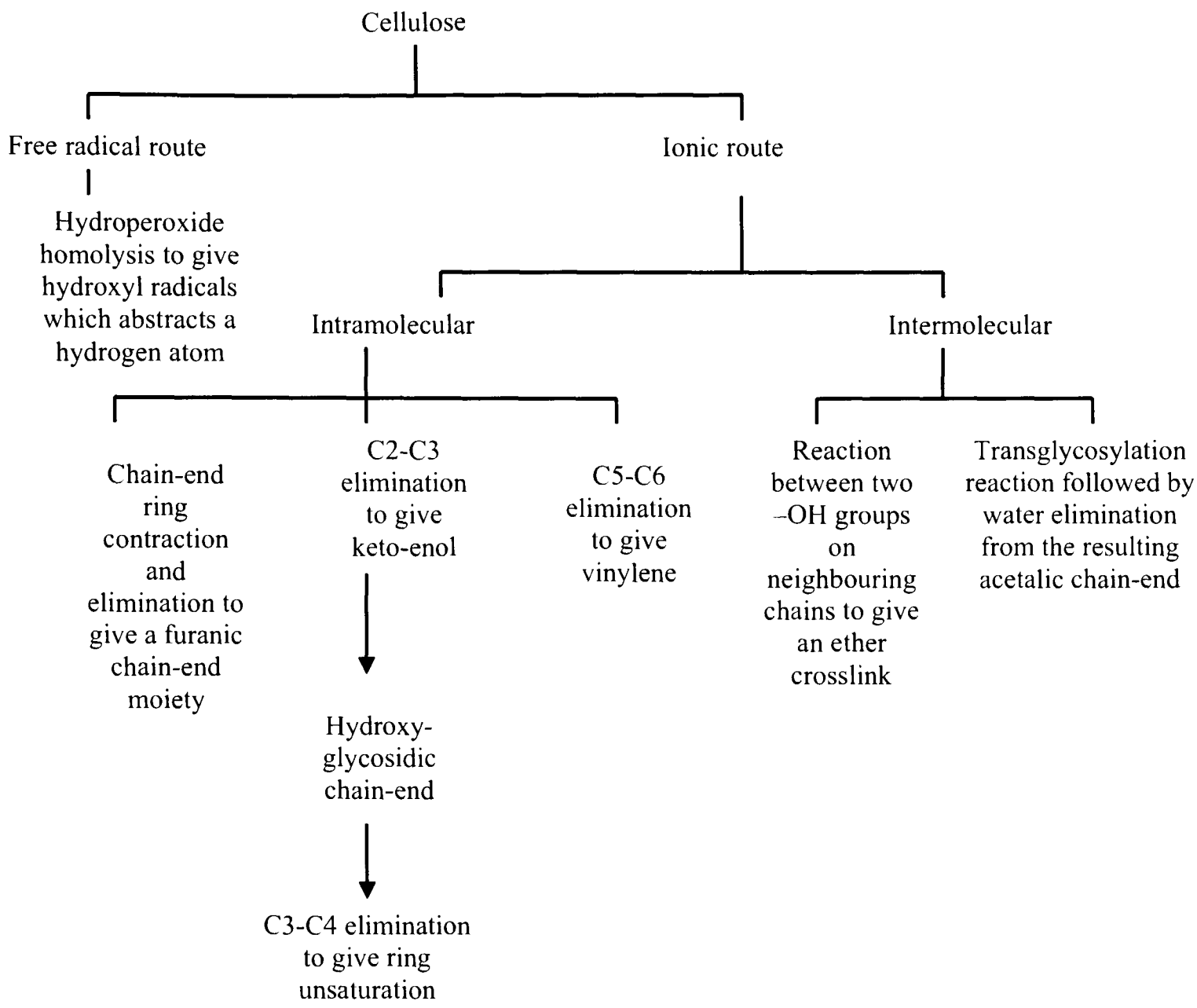

Figure 1-21. A schematic pathway for the different reactions that contribute to water during cellulose pyrolysis [41].

Lomax also presented an additional possibility or route of fragmentation, a reverse aldolisation (Figure 1-23) of the sugar fragments as a method of formation of hydroxyacetaldehyde [98]. They considered this as an alternative pathway to the formation of levoglucosan and cellobiosan, which agrees with Radlein's mechanism[12].

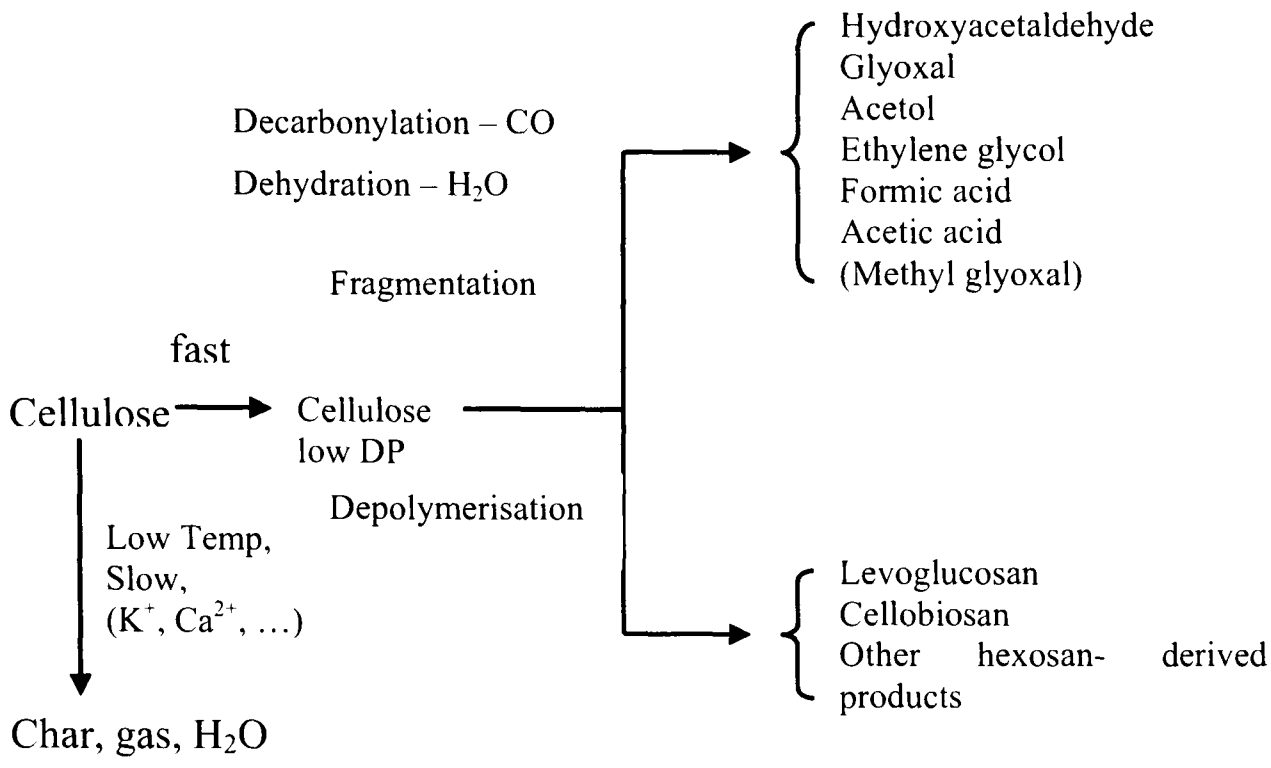

Figure 1-22. Mechanistic pathway for cellulose pyrolysis proposed by Radlein et al [12].

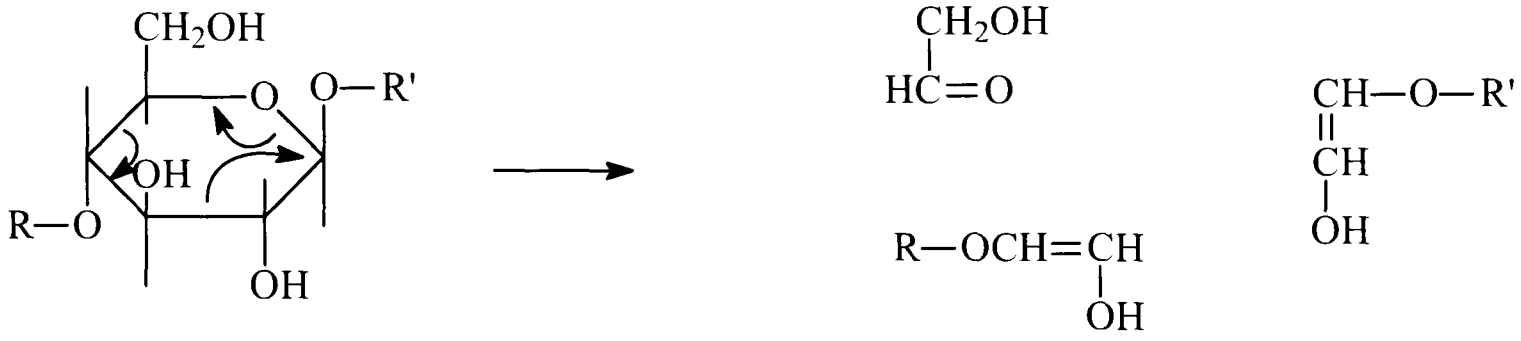

Figure 1-23. Reverse aldolisation fragmentation of a sugar residue, where R represents an adjacent saccharide residue [98].

Radlein noted that, under moderate heating rates and temperatures, levoglucosan (up to 40% from pure cellulose) and hydroxyacetaldehyde (~10%) are the highest yield products from cellulose, though the latter dehydrates readily at temperatures above 200°C to give ketene. This can be rehydrated to form acetic acid, which may be a route of formation for acetic acid. Acetic acid, formic acid and acetol are also compounds formed by pyrolysis of cellulose in relatively large yields (5-10%) [12]. Piskorz also reported acetol (1-hydroxy-2-propanone) and hydroxyacetaldehyde (glycolaldehyde) in their pyrolysis studies whilst noting that both had only reported in a couple of earlier studies [46]. Possibly elimination and retro-aldolisation predominate in amorphous cellulose regions, whilst crystalline centres are the main source of transglycosylation reactions to form levoglucosan.

As was proposed by Shafizadeh [35], Radlein et al found that the pyrolysis products from the high temperature reaction routes could be markedly different depending on the level, and nature of impurities within the cellulose. The mechanisms for this are not well understood [12].

1.4.3 Other

Banyasz, et al [94] produced a study that was primarily looking at the volatile production from cellulose pyrolysis. This originated from a study of formaldehyde production from tobacco (cellulose makes up approximately 10% wt of tobacco leaf [1]). Their work gave evolution kinetics that mapped onto the secondary reactions of cellulose evolution products. They only looked at this part of the mechanism, starting at the low DP cellulose, so the rest of the displayed mechanism (marked with dashed lines) was not studied as part of their investigation (Figure 1-24).

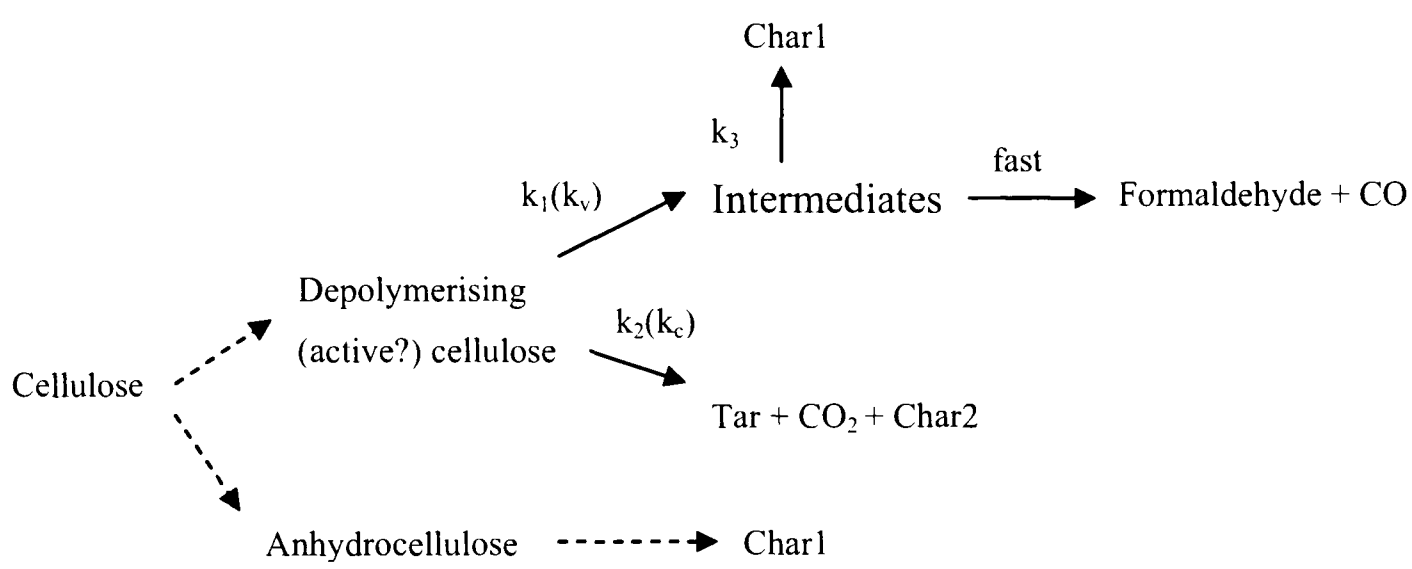

Figure 1-24. Proposed pathway for cellulose decomposition (Banyasz et al) [94]. Dotted arrows and italics refer to reactions not observed in their study.

The nature of the change from cellulose to active cellulose is not well understood. In the study they however, accept that the cellulose depolymerises but do not describe it as a separate species, as in Kilzer and Broido's 'dehydrocellulose' [43]. The study seems to support the Radlein mechanism of cellulose pyrolysis in which the activated form of cellulose (low DP cellulose) is only observed with fast heating rates. Banyasz et al [74] study of hydroxyacetaldehyde showed that it was a decomposition product of cellulose but not levoglucosan, indicating that they were separate pathways [74].

Sanders et al [107], compared the pyrolysis products of mono- and di-saccharide pyrolysis products with that of cellulose. They showed that there were different pyrolysis product distributions for D-glucose and cellulose (Table 1-5).

Table 1-5. Qualitative yields of three types of pyrolysis product from pure D-glucose and cellulose [107].

Compound	Levoglucosan	Furans	Low MW oxygenated compounds
D-Glucose	Less	More	Less
Cellulose	More	Less	More

They concluded that these differences were due to the reducing sugars reacting via their acyclic form that promoted formation of furans. As cellulose only has reducing groups at the ends of the chain this was a less important route for the pyrolysis behaviour.

From their work they produced a reaction pathway for cellulose as shown in Figure 1-25. The reaction pathway shows; (a) the formation of anhydrosugars such as levoglucosan and 1,6-anhydroglucofuranose, that break down further to low molecular weight oxygenated compounds; and (b) low molecular weight products such as hydroxyacetaldehyde and acetaldehyde. They also noted that at very high temperatures polynuclear aromatic hydrocarbons (PAHs) may be formed as well as other aromatics, CO, CO_2 and water.

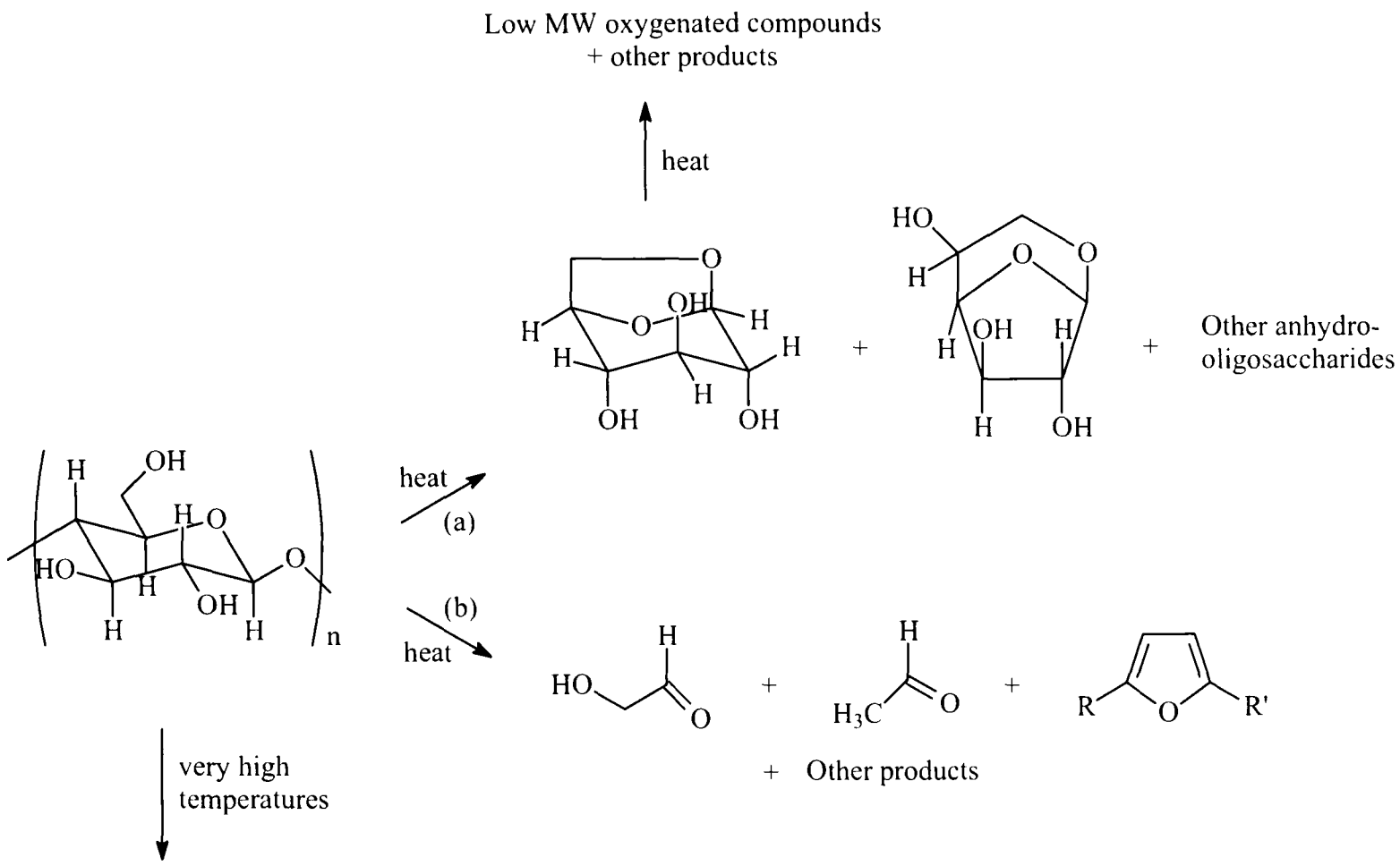

Figure 1-25. Illustration of the major reaction types observed during the pyrolysis of cellulose [107].

1.4.4 Summary of reaction pathways

It is clear from this review that the pyrolysis of cellulose is complex. There is difficulty in determining the number of steps or intermediates in the numerous pathways by which the evolved products are formed. Additionally how these steps are affected by changes in conditions and the presence of additives or impurities is unclear [107]. However, the mechanistic pathways that are proposed by the various researchers all have common features that may be described graphically by Figure 1-26.

Broadly speaking there is a great deal of agreement over the general mechanism of thermal decomposition for cellulose. That cellulose decomposes through a pair of concurrent reactions that form either a char residue that has a high degree of aliphatic character (Char 1) or a mixture of liquid tars and volatile compounds. However, there are variations on this theme (shown in blue in Figure 1-26) regarding whether there are secondary reactions involving the volatiles and if char forms directly from virgin cellulose.

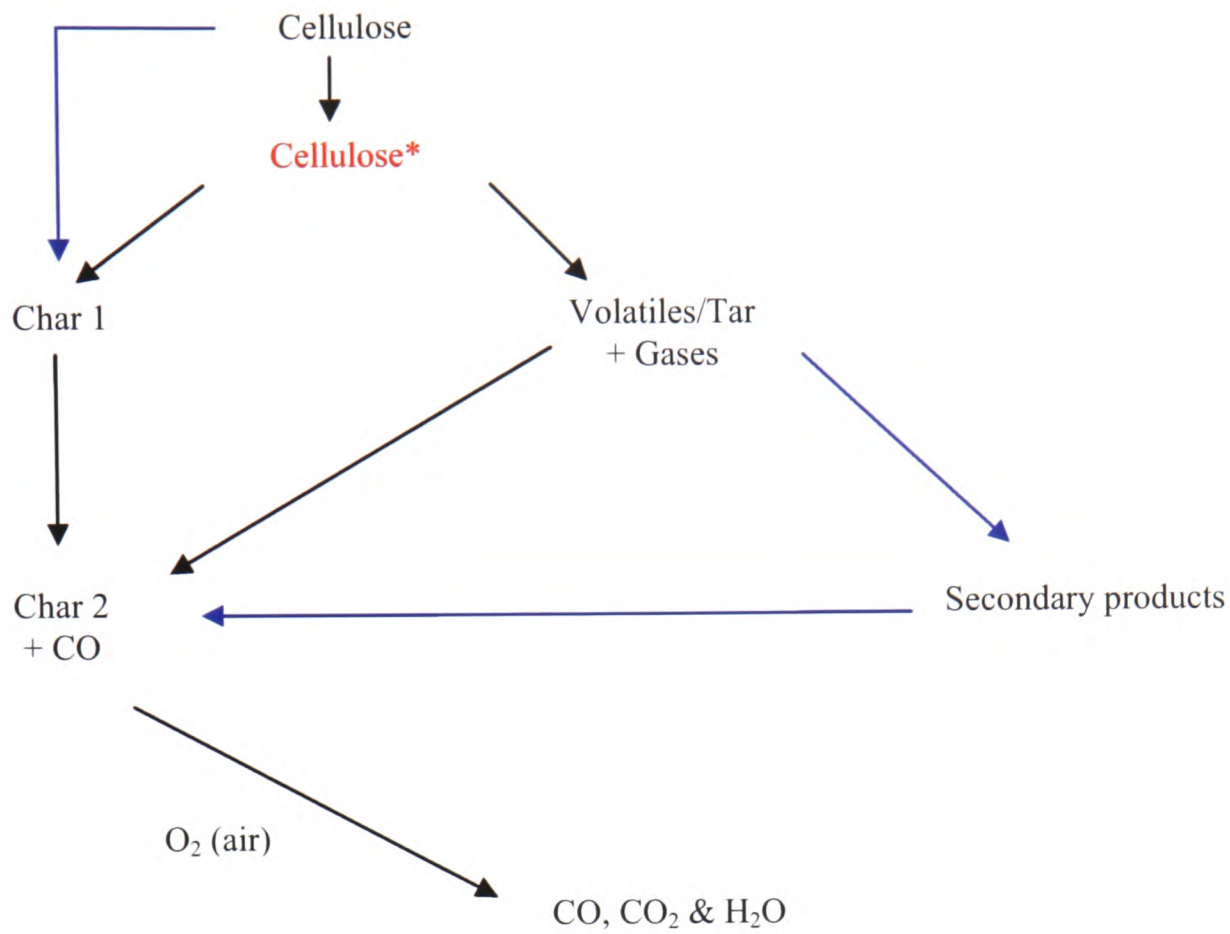

Figure 1-26. Summary diagram representing the key features of the mechanistic pathways presented in section 1.4. Items drawn in blue are proposed by studies, and items in red are still not clearly understood.

There is no precise definition of what active cellulose (cellulose*) is and even its presence is still debated. Price and Horrocks show DSC information to show its existence [103], whereas Antal concluded that they could not find a fit for the cellulose – active cellulose step in the Broido-Shafizadeh model kinetically [48]. However, the lack of a kinetic fit does not disprove the presence of active cellulose; though equally a kinetic fit also would not prove its existence. The active cellulose is also described as dehydrocellulose [43] and low DP cellulose [12].

The Price and Horrocks [101] model is probably the most detailed mechanism of cellulose thermal decomposition, and is therefore the best model to base any comparison upon. Their work also suggests three temperature ranges (section 1.4.1) that the reactions fall into, which may be possible to refine using the time and temperature resolved experiments of this study.

1.5 Alginic Acid and Alginates

1.5.1 General

Alginic acid is a natural polysaccharide, a common constituent of cell wall in all species of the brown seaweeds (*Phaeophyceae*). It performs a similar function in marine plants as cellulose does in land plants. It was discovered in 1881 by an English chemist, E. C. C. Standford, who obtained a viscous material by extracting *Laminaria stenophylla* (*Laminariaceae*) with alkali. He called the product "algin". He further found that, if a mineral acid was added, a gelatinous precipitate was obtained, which dried to a hard substance. He identified this as a new acid which he named "alginic acid" [108].

The seaweed industry has grown to producing 15,000 tonnes of polysaccharide every year from 400,000 tonnes of seaweed (figures quoted for 1981) [109]. The seaweed industry provides a wide variety of products that have an estimated total annual value of US$ 5.5-6 billion. Food products contribute about US$ 5 billion of this. Substances that are extracted from seaweeds, such as hydrocolloids (agar, alginate and carrageenan) account for a large part of the remaining billion dollars, while the remainder is made up of other miscellaneous uses, such as fertilizers and animal feed additives [110].

Seaweeds as a source of these hydrocolloids dates back to 1658, when the gelling properties of agar, extracted with hot water from red seaweed, were first discovered in Japan. Extracts of Irish Moss, another red seaweed, contain carrageenan and were popular as thickening agents in the nineteenth century. However, it was not until the 1930s that extracts of brown seaweeds, containing alginate, were produced commercially and sold as thickening and gelling agents. Figures listed in 2003 state that approximately 1 million tonnes of wet seaweed are extracted to produce these three hydrocolloids – agar, alginate and carrageenan. Total hydrocolloid production is about 55 000 tonnes, with a value of US$ 585 million [110]. The alginic acid is normally used commercially in its two most common forms, sodium alginate (the sodium salt) and propylene glycol alginate (propylene glycol substituted alginate). Alginate production is by extraction from brown seaweeds, all of which are harvested from the sea; cultivation of brown seaweeds is too expensive to provide raw material for industrial uses. Micro algal and bacterial sources of alginates have been discovered.

The main use for alginates is for gelling, viscofying and stabilising. The polymer's gelling properties are dependent upon interaction with multivalent cations, such as Ca^{2+} which in the

presence of polyguluronate (G-blocks) forms a rigid gel [111]. Unlike other polysaccharides the sol/gel transition is not particularly influenced by temperature. As a result of this alginates have found a great number of uses, with applications from the food industry through to biomedicine. It is used in the textile industry as a thickening agent for print dyes, in medicine in the form of wound dressings and as a stabiliser or thickener in medicinal preparations. In the food industry the gels are used extensively in restructuring, dried or flaked foodstuffs, and probably its best known use – the stabilisation of ice-cream (Table 1-1).

1.5.2 Structure

Originally it was thought to be a homopolysaccharide made up of mannuronic acid units. In 1955 Fischer and Dorfel obtained both D-mannuronic and its C5 epimer L-guluronic acid in varying proportions from different sources of alginic acid [3].

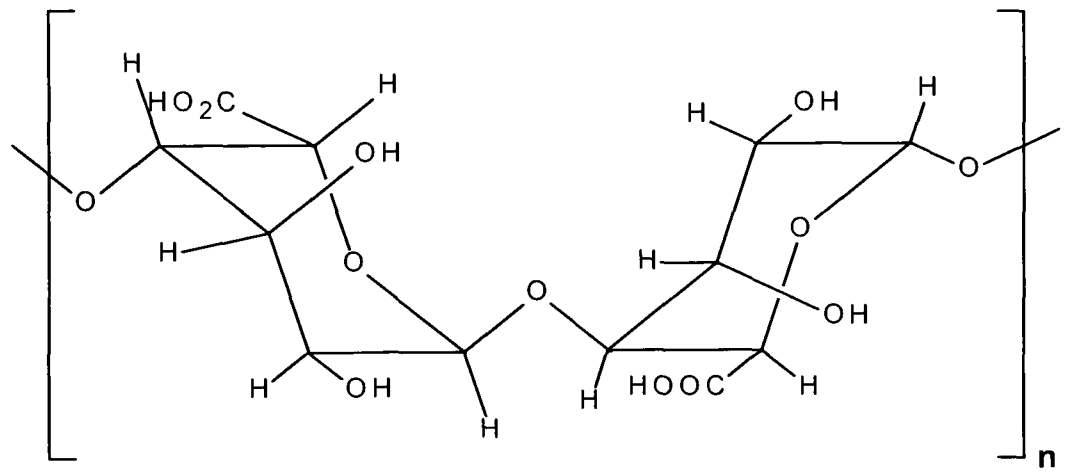

G-block unit of α-L-guluronic units

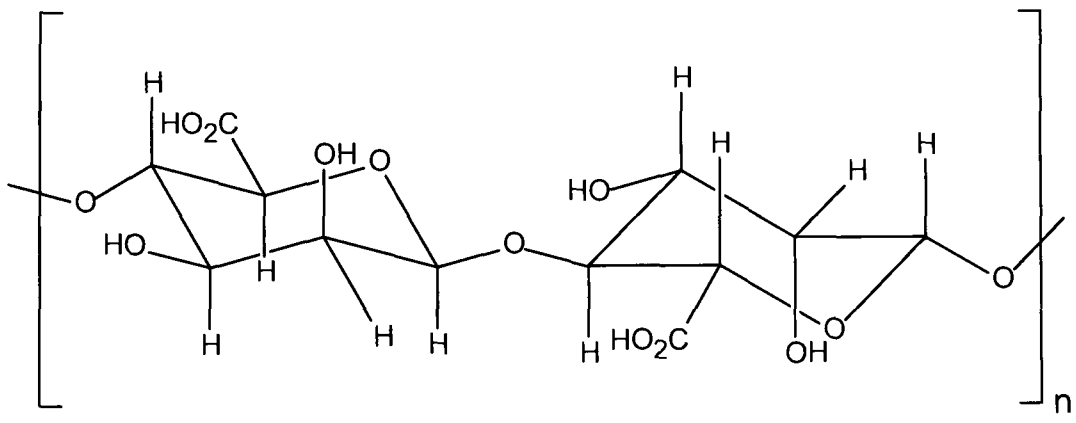

M-block of β-D-mannuronic units

Figure 1-27. Structure of G and M groups of alginate polymers

However, alginates are not simply two physical mixtures of the two polymers; they are unbranched copolymers consisting of β-D-mannuronic acid (M) and α-L-guluronic acid (G) groups that are 1-4 linked. The structures of these different units are shown in Figure 1-27. The mannuronic blocks are structurally similar to cellulose, but the functional group in alginic acid is a carboxylic acid group (–COOH), rather than a hydroxyl group (-OH) (cf cellobiose units - Figure 1-1). These M and G units are linked in linear blocks of pure G monomers and blocks of pure M monomers interspersed with alternating MG blocks, an example is given in Figure 1-28 [112].

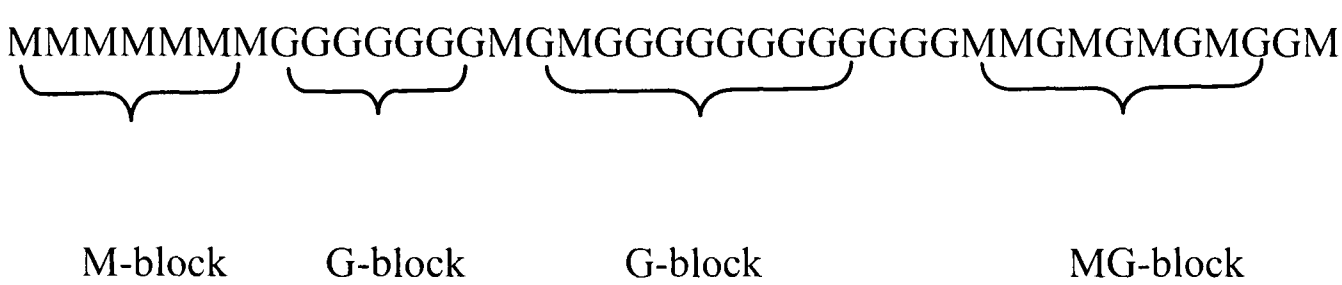

Figure 1-28. A hypothetical alginate polymer to illustrate the distribution of the G and M structural units.

This distribution of the M and G blocks within the main polymer chain determines the properties of the polymer, thus it is important to be able to determine the M:G ratio for alginates. Alginates which have a high proportion of G units will form strong but brittle gels, while those with high proportions of M units will form weaker gels that are more flexible.

1.5.3 Thermal properties of alginic acid

Unlike cellulose, there is little literature on the thermal properties of alginic acid, or its alginate derivatives, despite its use in various food applications, including barbeque marinades where the alginate would normally be placed in a high temperature environment. It is the main objective of this work to fill in this gap in knowledge.

Of the thermal studies that have been performed, the normal interest is in obtaining the calorific value for the material when used in food-stuffs for human consumption, or pet-food. Kienzle et al [113] measured values of 16.8 – 17.9 kJ/g for alginates, depending upon source. Similarly they obtained values of 17.0 -17.5 kJ/g for cellulose, again depending upon source. This is, perhaps, to be expected as the two compounds, alginate and cellulose are similar molecules, requiring a similar amount of kinetic energy to break down completely.

1.6 Experimental Methods

A large number of techniques have been used to study different aspects of the pyrolysis process, whether it be the primary steps [114] or examining the char [47], as mentioned in the previous mechanistic reviews.

1.6.1 Thermogravimetric analysis (TGA)

One of the most common techniques used is thermogravimetric analysis (TGA) [28, 38, 52, 54, 58, 77, 84]. Thermogravimetry is a relatively simple technique in which the mass of a sample is continuously monitored and recorded while subjected to a temperature programme. This procedure is carried out in a designated atmosphere, normally a choice of oxidising or non-oxidising, and the mass of the sample is plotted against time or temperature [79, 115, 116].

One limitation of TGA is that it cannot identify any evolved pyrolysis products. As a result, TGA is commonly hyphenated with other techniques, such as mass-spectroscopy (MS), evolved gas analysis (EGA) or Fourier Transform Infrared spectroscopy (FTIR) to monitor the evolved products.

Most TGA studies have used linear heating rates to observe changes in the cellulose as the temperature increases [54, 79, 87, 114]. The data gained is used to calculate the kinetic parameters, using weight loss information from a range of temperatures or temperature ramps [95]. TGA data may also be presented as both TG (α vs. T – where α is fraction of original material decomposed) and DTG (dw/dt vs. T) [87].

Other than the requirement of a hyphenated technique for product identification, TGA has other limitations as a tool for studying pyrolysis experiments. Over time it has been shown that there is a need to calibrate the TGA with Curie point standards regularly. Thermal lag (the difference between the thermocouple temperature and the sample temperature) is shown to be increasingly significant with increasing temperature ramp rate [28] and even on modern instruments that utilise small sample sizes (~2mg) to reduce this, it is still an important factor as the thermocouple is placed near the sample not in contact with it [67]. In a TGA experiment performed on wood and cellulose samples, DeGroot and Shafizadeh claim temperature variations between the sample and thermocouple temperature of 5-10°C could be observed [66]. Therefore, accurate measurements of temperature suitable for kinetic experiments can be difficult to obtain from TGA alone. Due to the thermocouple being placed near to the sample

pan it measures the heat from the furnace walls, and the evolved gases. Flynn proposed that heating rates that are still useful for discerning kinetic information from standard thermal analytical experiments have a maximum of about 6°C/min. Above this the flow of heat into the sample and sensors may be too slow for accurate measurements [91]. This criticism is also made about wire mesh heaters that are most commonly used in coal studies, which heat a small sample in the folds of a resistive wire mesh. Others argue that the sample is in such intimate contact with the heat source that heat transfer is less of an issue. Wire mesh heaters can achieve very high heating rates; up to 1000s of degrees per second, though there is some debate as to whether or not there are additional errors involved in measuring temperature accurately in such rapid heating systems [71].

To avoid inaccuracies during kinetic measurements Milosavljevic and co-workers placed a second thermocouple in contact with the sample to improve correlation with DSC experiments [50]. By measuring the actual temperature of the sample it was seen that the formation of the tars was highly endothermic. The sample temperature only matches the oven temperature when the rapid evaporation of the tars is complete. Large sample mass and high heating rates aggravate the situation and can delay apparent onset temperatures up to 40°C [28]. This shows that the heat transfer is more important than chemical reaction kinetics. Heating the sample in a vacuum oven shows that the yield of char decreases and the tar increases, therefore mass transport is also an important factor [44]. Várhegyi and co-workers used TGA samples sizes that were kept to 2-3mg for low heating rates (<10°C/min) and 0.5-0.6mg for high heating rates (50-80°C/min) to avoid heat- and mass-transfer problems occurring [48]. Magnaterra's study placed their samples as a monolayer in the TGA pan, but they determined that sample weight was not a controlling factor in the combustion process below 6mg [68]. However a different TGA-FTIR study found that on heating cellulose below 250°C there was weight loss, but the FTIR was not sensitive enough to measure the compounds evolved. They also found that almost 50% of the weight loss was not detected in the FTIR, indicating a large amount of evolved species condensating out prior to measurement [114].

It is easy to see that experimental design for pyrolysis studies requires a careful balance; a suitably small sample is required to avoid temperature gradients in the sample, but at the same time the sample must be large enough to allow quantitative measurements [91]. However, a large number of researchers use the technique, trying to minimise all of these effects where possible. A huge amount of data has been produced and equally large numbers of researchers

have produced ways of treating the TGA data. Ozawa concluded that thermogravimetry has advantages over isothermal data collection, particularly with larger polymers as the initial structural change in the sample can complicate isothermal data [82].

1.6.2 Other thermal analysis techniques

Differential thermal analysis (DTA) and Differential Scanning Calorimetry (DSC) are two other common techniques used [38, 54, 58, 63, 102, 103]. They are similar in nature; DTA uses a single heat source to heat the sample and a reference material. The heat difference is measured against time or heater temperature. This difference is proportional to enthalpy change, heat flow resistance and heat capacities of the sample material. DSC uses separate heat sources for the sample and reference. Therefore differences in temperature between the sample and reference are compensated for by changing the energy to the heaters. This allows the change in energy over changing time to be plotted against temperature or time [117]. As a result DSC is a more sensitive technique than DTA, though in both cases the thermocouple is placed near to the sample pan, as is the case in TGA, and may also measure heat from the furnace walls, and any evolved gases rather than the sample itself. Both of these techniques allow observation of endotherms, exotherms and other chemical transitions, such as glass transition (T_g) in polymers, during heating or cooling. TG and DTA experiments showed that the main weight loss in air coincides with a small endotherm. This is followed immediately by a large exotherm, which is due to the flaming combustion of the volatile products formed [54]. A exothermic process at 200°C was noted that coincided with water and CO_2 evolution, but not CO [103]. However, Aggarwal [118] suggested that both initial processes are exothermic. Although the degradation of cellulose via the gaseous combustion route is endothermic, the combustion process of the gaseous products is so exothermic that it overwhelms the endothermic character. This was confirmed by heating a sample of cellulose partially decomposed by heating until past the major weight loss then cooling in nitrogen. On reheating the sample in air there was no first exotherm. There are three observed exotherms, the second at 458°C and, third, at 478°C, which are also postulated to be due oxidation reactions, possibly in the char [54].

DSC in cellulose pyrolysis studies carried out by Price et al using cotton fabrics in static air and nitrogen with 500ml.min^{-1} flow rate. They used a lower temperature range (up to 360°C) to examine the cellulose to activated cellulose (cellulose*) transition, which they designated T_2. They noted that in untreated cellulose fabrics the peak occurred at 330°C, but only in air.

Experiments in nitrogen did not show the T_2 peak [102]. This is notable as the cellulose to 'active cellulose' step has been the subject of some debate [48].

1.6.3 Calorimetry

Standard oxygen bomb calorimetry has also been used to measure heat capacities of flame retarded cellulose samples in a study [95]. Colbert et al determined the enthalpy of combustion (ΔH_c) of microcrystalline cellulose as -2812.401 +/-1.725 kJ/mol [119]. Conventionally a negative energy value is quoted as it implies an exothermic reaction in calorimetric studies.

1.6.4 Fourier Transform Infrared Spectroscopy (FTIR)

FTIR is a technique that is used frequently for measurement of combustion products, evolved gases, pollutant gases and many other areas that require continuous monitoring of a reaction or process [120-127]. It has been used as part of evolved gas analysis (EGA-FTIR) where a furnace is coupled to the FTIR to monitor the gases. Usually some form of filtration is put into the line to prevent particulate matter entering the FTIR gas cell [94]. Other researchers have used it to analyse the volatiles or specific analytes, using a specific wavenumber for the purpose. For example, Banyasz [74] reported the following analytes:

- formaldehyde 2780.9 cm^{-1}
- hydroxyacetaldehyde 860.4 cm^{-1}
- CO 2055.3 cm^{-1}
- CO_2 2251.6 cm^{-1}

They used a high resolution ($1cm^{-1}$) and short wavenumber ranges were used to increase the speed of data collection to approx. 0.08s per scan.

More commonly it is used to measure just CO and CO_2 evolved during the pyrolysis of cellulose, with various equipment designs for heating the samples [72, 99, 100].

The solid residue may also be examined using FTIR allowing the examination of the functional groups in the material. By heating the material, cellulose or its derivatives to different temperatures it is possible to see the changes in the absorption peaks of the spectra. This gives an indication as to the chemistry of the char and the processes of formation [62, 128, 129].

1.6.5 Nuclear Magnetic Resonance Spectroscopy (NMR)

NMR has been used in a number of studies [47, 62, 130, 131], mostly to investigate the charred residue. By measuring ^{13}C, NMR can elucidate the structure of the carbonaceous residue from a pyrolysis experiment, or from various stages of heat treatment. Sekiguchi used NMR to monitor the increasing aromaticity of the carbon content of the char. He noted that the carboxyl and carbonyl groups are diminished and the aromatic groups are increased using ^{13}C-NMR [26].

1.6.6 Pyrolysis Gas Chromatography-Mass Spectrometry (py-GC-MS)

Gas chromatography-mass spectrometry (GC-MS) is a common technique and is the technique of choice for many analytical assays. Pyrolysis units are available for these instruments, allowing direct interface of pyrolysis with GC-MS, making a convenient technique to measure the pyrolysis products from the pyrolysis of a material. When optimised the technique is powerful in that it allows collection, separation, quantification, and identification of pyrolysates. Normally a flash pyrolysis technique is used, where the sample is heated very rapidly (several hundred degrees per second) to a fixed temperature and the pyrolysis products swept onto the column. Ramped systems may also be used, but in both cases some form of focussing of the pyrolysate occurs. Usually liquid nitrogen 'cryo-trapping' is used to hold all of the pyrolysate prior to the separation on the GC column, which improves the chromatography. One limitation of this technique is that the focusing and separation stage prevents the time/temperature resolution of the pyrolysis products being observed. Although the molecular fragmentation is what makes the identification of the compounds possible by mass spectrometry, another disadvantage is that the resulting molecular fragmentation of the pyrolysis products may be extremely complex. In such a complex matrix the fragmentation may lead to many similar fragment ions making identification much more difficult.

However, a number of researchers have used pyrolysis gas chromatography-mass spectrometry (py-GC-MS) to study the evolved products [21, 34, 57, 101, 132]. Two of these studies, by Pouwels, and Moldoveanu, have published extensive lists of cellulose pyrolysis products [21, 34].

1.7 Summary

After decades of research into the properties of cellulose combustion and pyrolysis there is some agreement over the mechanism of cellulose degradation. However, there are aspects that are not as clearly defined. This is particularly highlighted in the kinetics studies where there is still debate over the rate order and the other kinetic parameters. However, there are a number of general concepts that are agreed by a large number of researchers:

- cellulose pyrolysis proceeds via a number of complex consecutive and concurrent reactions. Of these there are two main pathways, one forming a char and another higher temperature route that forms volatiles that may decompose further. These reactions may be treated as first order reactions in determining of global kinetic parameters based on weight loss data.
- the source of the cellulose, and the conditions used in pyrolysis or combustion have varying influence on the exact mechanistic processes.
- the reactions involved in these processes include depolymerisation, fission, transglycosylation, dehydration and other rearrangement reactions.
- levoglucosan and a large number of volatile products are formed via the higher temperature pathways.
- the char formed may have both aliphatic and aromatic character. These chars decompose further via highly exothermic oxidation reactions.
- by contrast there has been little work on alginic acid and alginates in terms of their thermal decomposition.

1.8 Aims

Following the investigation of the literature the aims of the study can be summarised as follows:

1. to use a thermogravimetric analyser coupled with a Fourier transform infrared spectrophotometer to characterise the thermal decomposition chemistry of two polysaccharides, i.e. Cellulose and alginic acid.
2. use a multivariate data analysis technique to interpret the spectral analysis of the decomposition products.
3. identify differences, if any, between these two model compounds.
4. to use any identified differences to compare their thermal behaviours under known conditions.

5. to compare and deduce the mechanisms of formation of the identified evolved compounds and their residual chars.

CHAPTER 2 EXPERIMENTAL PROCEDURES

2.1 MEASUREMENT TECHNIQUES

The main measurement technique used in this study is Thermogravimetric Analysis coupled with Fourier Transform Infra-Red spectroscopy (TGA-FTIR). The techniques are discussed individually below but in the experimental setup the two instruments are coupled together by a heated transfer line.

2.1.1 Thermogravimetry

Thermogravimetry is a relatively simple technique in which the mass of a sample is continuously monitored and recorded while subjected to a temperature programme. This procedure is carried out in a designated atmosphere, normally a choice of oxidising or non-oxidising, and the mass of the sample is plotted against time or temperature [115, 116].

Modern thermogravimetric analysers (TGA) or thermobalances are available in various configurations but all have the same fundamental parts:

- the balance and its controller
- the furnace and temperature sensors
- a computer to control the furnace and record all of the data

The balances are extremely sensitive microbalances, generally capable of measuring changes of less than 1 μg, and usually have a maximum sample mass of up to ~30mg. With such equipment it is important to isolate the instrument from vibrations. Other considerations include the need to purge the balance region of the instrument with a dry, inert gas to prevent deposition of material from the furnace region. Electrostatic charge may also be an issue with such small weight changes and an antistatic spray or means to discharge static build up are required.

The furnace design is also important; in the case of this study a Perkin Elmer TGA-7e is used which contains a microfurnace that sits within the furnace tube of the instrument, directly surrounding the sample holder. This allows rapid heating rates, as the sample is close to the furnace [133]. The furnace also contains a thermocouple inside to allow the temperature sensing to be as close as possible to the sample to give an accurate measurement of sample temperature (Figure 2-1). Both the balance and furnace need to be calibrated before use. The balance is

calibrated easily with a certified mass within the range of the balance. The furnace is calibrated for temperature using ferromagnetic alloys of known Curie point. The sample is placed in the holder and a magnet is placed near to the furnace tube to give an apparent mass due to the magnetic force on the sample. The alloy's ferromagnetic properties are lost when the Curie point temperature is reached. The observed temperature is then compared to the known Curie point and a calibration prepared for the furnace, normally an operation carried out by the controlling software for the instrument. This technique may be coupled to other instruments such as gas chromatographs, mass spectrometers or Fourier transform infrared spectrophotometers, which allow the identification and quantification of compounds released on heating the sample in the TGA furnace. In this study the TGA is linked to a Perkin Elmer Spectrum 2000 Fourier transform infrared spectrophotometer.

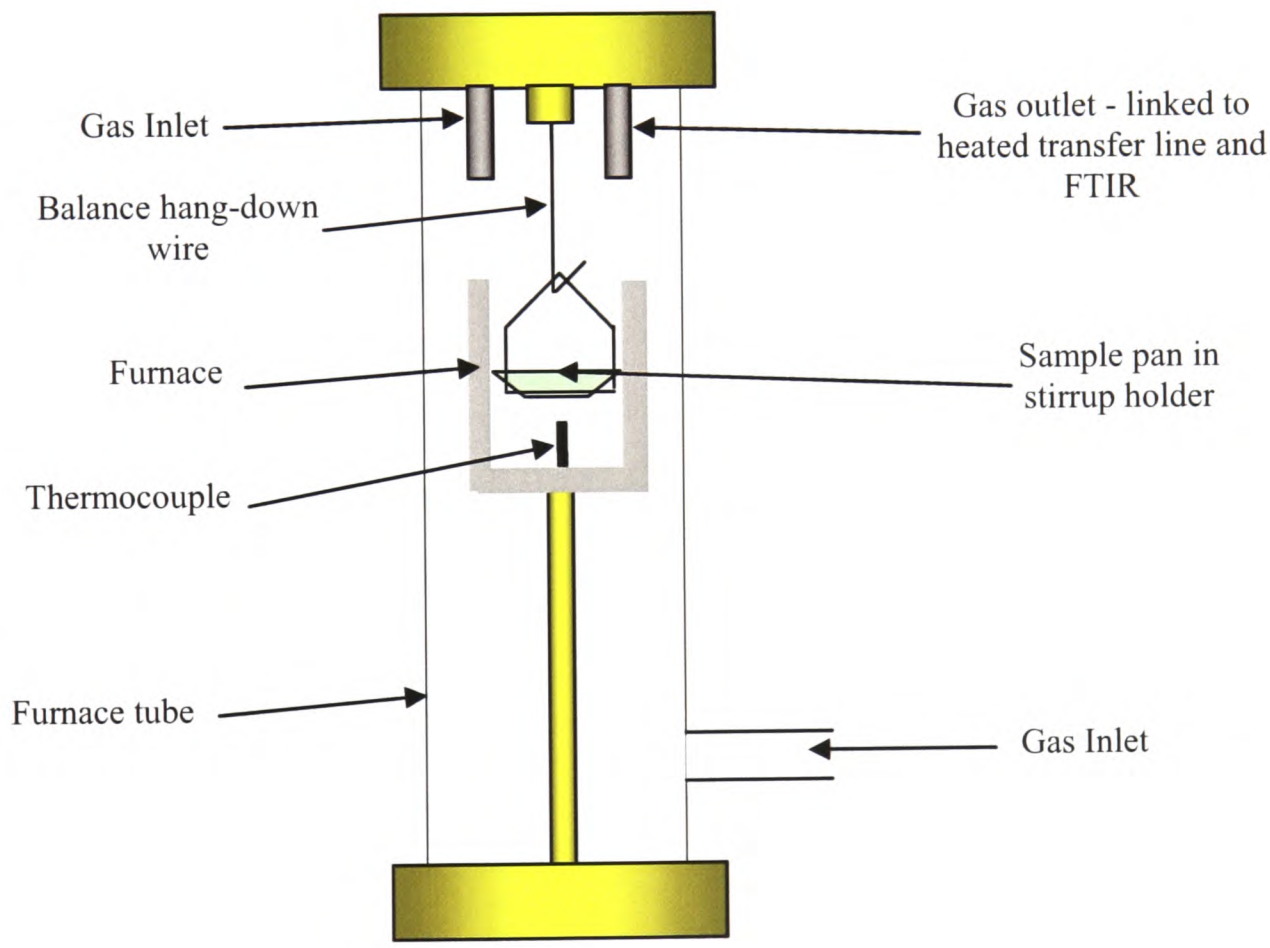

Figure 2-1. A schematic diagram illustrating the furnace design of the Perkin Elmer TGA7e.

2.1.2 Infra-Red Spectroscopy

Spectroscopy is the measurement of changes that occur at a molecular level due to the interaction of electromagnetic radiation with the material. Therefore, if radiation from the IR

region is passed through a compound that is 'IR active' (meaning it has a fixed dipole) some of the energy is absorbed to produce vibration, stretching, bending and rotation in the molecule, giving rise to an absorption spectrum. In very simple cases (i.e. diatomic molecules with a fixed dipole, e.g. CO) the effect on the dipole of the molecule is to produce vibrational changes leading to only a few absorption bands, however at higher resolution further complexity can be seen from the interaction of rotational absorptions. For more complex molecules there will be a combination of vibrations and rotations giving rise to a more complex absorption spectrum. The absorption of energy is plotted against wavelength to show the absorption bands, which are characteristic for the particular molecule. These resulting spectra can be used to obtain information about the functional groups of a molecule and may give clues to the structure of the compound and, by comparison with standard spectra, identification of a compound. The wavenumber region of $4000cm^{-1}$ to $1400cm^{-1}$ contains characteristic information about functional groups, a few examples are shown in Table 2-1.

Table 2-1. Examples of characteristic frequencies for common functional groups in organic materials [134].

Bond	Frequency (cm-1)
-OH	3600
$-NH_2$	3400
$=CH_2$	3030
$-CH_3$	2970 2870 1460 1375

The region from $700cm^{-1}$ – $1400cm^{-1}$ is known as the 'skeletal vibration' or more commonly the 'fingerprint' region of the spectrum. The skeletal frequencies are formed by linear or branched chain structures within a molecule, hence the term skeletal, which give complex bands of absorption that are characteristic of that compound. It is also termed the fingerprint region as it is possible to identify a compound or structure purely from this region of the spectrum [134, 135].

The instrumentation of an IR spectrophotometer (Figure 2-2 (a)) is most commonly a dual beam system that allows one beam to pass through the sample and a second to pass through a reference cell with exactly the same path length. Both beams are brought to a focus on a rotating sector mirror (Figure 2-2 (b)), which rotates at between 10 – 100 times per second. The mirror allows the detector to see the sample beam and then the reference beam alternately, and as the two beams have passed through an identical path length they are both reduced in intensity by atmospheric water and CO_2 equally, thus removing background interference. The rotating mirror also acts as a modulator, which in effect 'removes' stray radiation that does not have the modulation frequency of the mirror (10 – 100 rotations per second) therefore improving the signal-to-noise ratio.

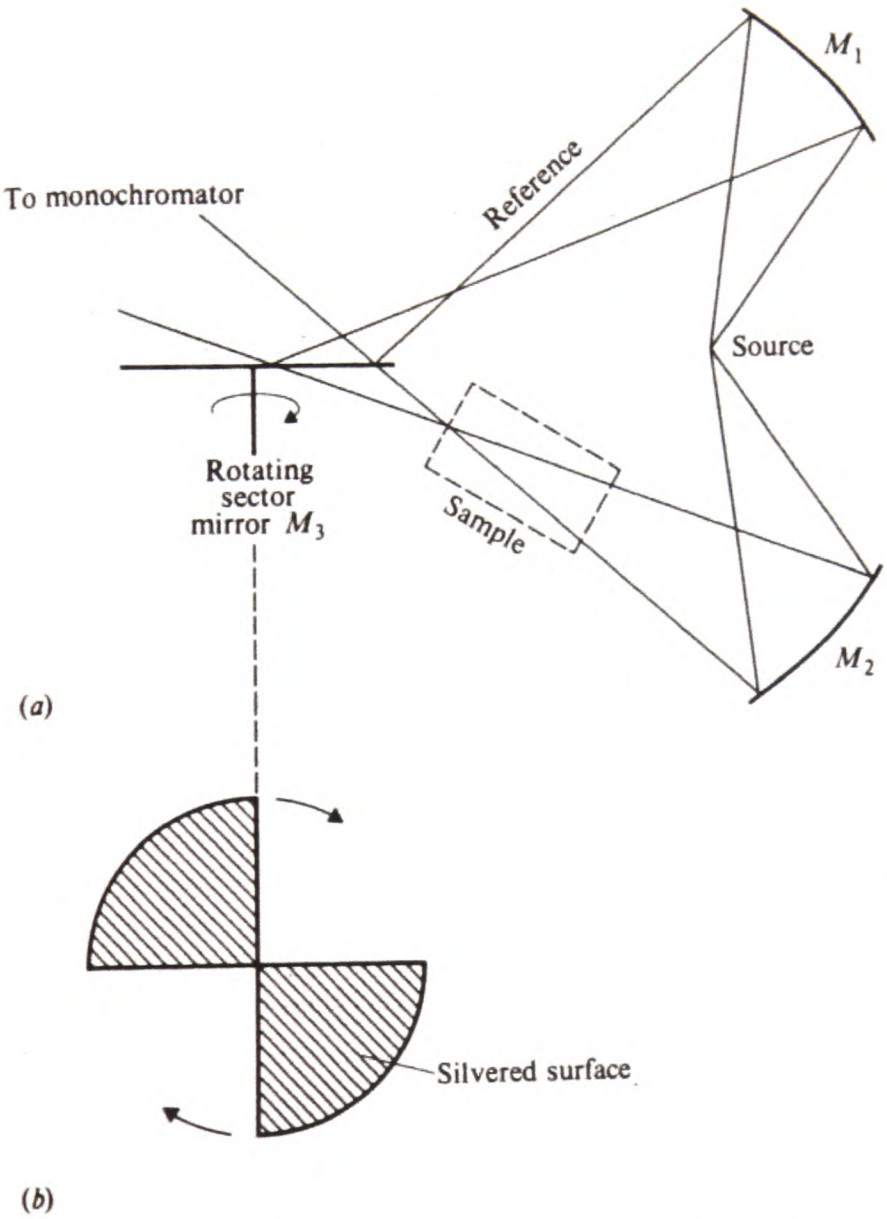

Figure 2-2. (a) Schematic diagram of a double beam infrared spectrophotometer. (b) A plan view of the rotating sector mirror [135].

2.1.3 Fourier Transform Infrared (FTIR)

One of the limitations of conventional IR spectroscopy is the time required to acquire the data, as the energy is swept through all of the frequencies from 4000 cm^{-1} – 700 cm^{-1} to obtain the spectrum in the mid-IR region. The development of Fourier transform spectroscopy greatly increases the speed with which data are acquired, cutting the time to collect an entire spectrum from 10 minutes to 10 seconds at similar resolutions [136]. The basis of the principle is that a 'white' source of IR radiation, containing all frequencies, is used and the data collected by a sufficiently fast detector. The path of the beam is split through a half silvered mirror (B) and reflected back towards the sample (Figure 2-3).

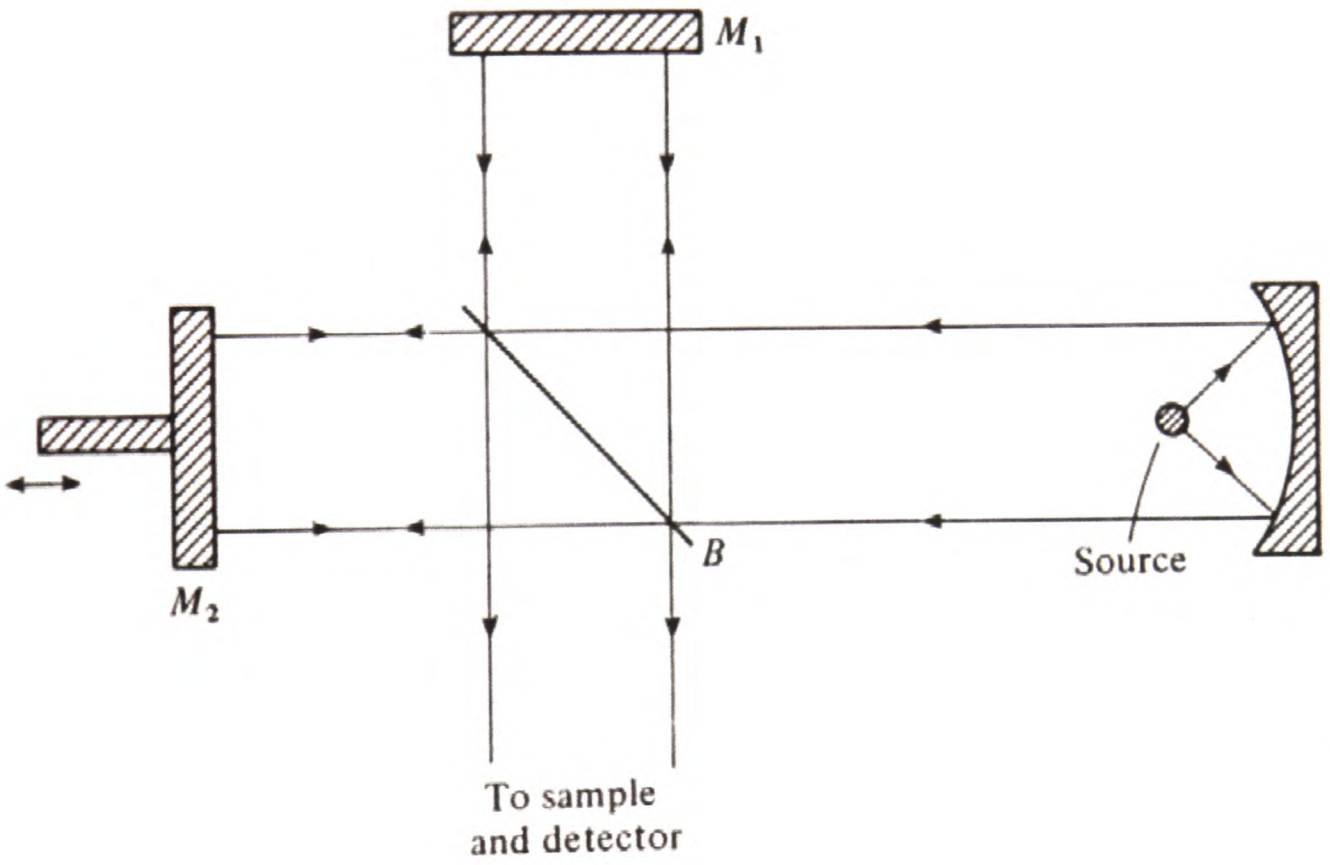

Figure 2-3. The interferometer unit of a Fourier transform spectrometer[135].

One of the mirrors (M_2) can be moved, which produces different path lengths for the parallel beams causing interference patterns to form as the post sample beam wavelengths combine constructively or destructively. The signal that is then measured comprises a complex mixture of frequencies, some of which have been absorbed by the sample. This is known as an interferogram. The data is then placed through the Fourier transform process (named after the mathematician Jean Baptiste Fourier), which is a method of integrating complex wave patterns;

thus a conventional spectrum is resolved from the interferogram [136]. This allows a complete wavelength range to be captured almost simultaneously, bringing the analysis time for a spectrum down to approximately 3 to 10 seconds, depending on the resolution required.

FTIR is a technique that is used frequently for measurement of combustion products, evolved gases, pollutant gases and many other areas that require continuous monitoring of a reaction or process. [120-125]. FTIR was chosen for this study due its ease of use, and ability to measure a number of species simultaneously and continuously. The TGA-FTIR technique allows the use of oxidative atmospheres, which may be problematic in GC techniques, and allows the evolved components to be plotted as a function of temperature accurately with a single experiment [126]. FTIR does have some disadvantages, the main being the lack of sensitivity compared to GC-MS, and the spectra of small molecules at high concentration may cause spectral interferences [137].

Separation of the co-evolved species in the spectrum can be problematic (though GC-IR is also a technique used in some studies, but sample trapping is required prior to the GC analysis [127]) and is one weakness of the basic FTIR set-up. An improved spectral technique is described below, and a method of processing the convoluted spectral data sets is discussed. It is important to remember that not all compounds are visible to IR, and also light scattering caused by particulates in a gas stream may also cause problems. However this broadband distortion of the spectrum baseline, caused by particulates, has been put to use as an additional measurement tool in the quantification of soot particles [121].

2.2 MULTIVARIATE ANALYSIS

Many instruments, with the aid of computer controlled operation and data collection, now produce copious amounts of data from an experiment. It is, therefore, important to ensure that maximum use is made of this wealth of data. The power and sophistication of modern computers have allowed chemometrics to become its own discipline, dedicated to extracting chemically relevant information from data produced in chemical experiments [138, 139].

One of the most important techniques used is that of multivariate analysis. Multivariate analysis involves the use of multiple variables from an analysis technique to characterise a sample, instead of a single (univariate) variable.

Multivariate analysis can be used for classification or quantification:

- classification or qualitative analysis – involves the grouping of samples based on similarities of multiple measurements, pattern recognition, and artificial neutral networks.
- regression analysis – allows quantification, and includes a variety of techniques, multivariate regression, multiple linear regression, principal component regression, partial least squares regression, target factor analysis

One approach to analysing multivariate data is by Factor Analysis (which is similar to Principal Component Analysis). These methods use matrix algebra to decompose the data matrices which yields mathematical descriptions of the component parts of the data. This has been exploited by analytical sciences to extract information, often hidden, from complex sets of data. The software uses the singular value decomposition (SVD) method for the factor analysis. The SVD produces factors which mathematically describe the main underlining changes in the column and row domain of the data matrix.

The extracted factors are structured such that the first accounts for the majority of the variation, the second the next largest variation, and so on. This means that after a number of factors have been identified they will account for most of the variation, which means any data not accounting for significant variation may be discarded.

Spectroscopic information or chromatograms gathered from pyrolysis and combustion of organic polymers are often quite complex and their interpretation requires appropriate mathematical treatments, especially for quantitative work. Data complexity can be due to imperfect chromatographic peak separation. In systems where chromatography is not possible the mixture of gases creates complex data set of largely overlapping spectra. These types of data need careful treatment to enable meaningful interpretation and quantification. Factor analysis is one technique used in chemometrics that has evolved over the past 30 years to tackle large data sets in behavioural science and over the last 15 years it has also been applied to chemical problems [140]. Factor analysis is a multivariate technique for reducing matrices of data to their lowest dimensionality by the use of orthogonal factor space and transformations that yield predictions and/or recognisable factors, as defined by Malinowski [140].

The data is expressed mathematically in a matrix, D, consisting of r rows and c columns. The SVD extracts factors or singular values structured such that,

$$D = \begin{bmatrix} d_{11} & d_{12} & \dots & d_{1c} \\ d_{21} & d_{22} & \dots & d_{2c} \\ \dots & \dots & \dots & \dots \\ d_{r1} & d_{r2} & \dots & d_{rc} \end{bmatrix} \qquad \textbf{Equation 2-1}$$

The symbol d_{ik} represents the data point associated with the ith row and kth column of the matrix. The first objective of factor analysis is to obtain a mathematical solution such that each point in the data matrix is expressed as a linear sum of product terms. The number of terms in the sum, n, is called the number of factors. Specifically, the solution should be in the form

$$d_{ik} = \sum_{j=1}^{n} r_{ij} c_{jk} \qquad \textbf{Equation 2-2}$$

in which r_{ij} and c_{jk} are called row (or scores) *factor* and column (loadings) *factor*, respectively. For data modelled by this equation, the data matrix can be broken down into the product of a row matrix and a column matrix:

$$\mathbf{D} = \mathbf{R}_{\text{abstract}}\mathbf{C}_{\text{abstract}} \qquad \textbf{Equation 2-3}$$

Where;

$$R_{abstract} = \begin{bmatrix} r_{11} & r_{12} & \dots & r_{1n} \\ r_{21} & r_{22} & \dots & r_{2n} \\ \dots & \dots & \dots & \dots \\ r_{r1} & r_{r2} & \dots & r_{rn} \end{bmatrix}$$

$$C_{abstract} = \begin{bmatrix} c_{11} & c_{12} & \dots & c_{1c} \\ c_{21} & c_{22} & \dots & c_{2c} \\ \dots & \dots & \dots & \dots \\ c_{n1} & c_{n2} & \dots & c_{cn} \end{bmatrix}$$

Since this solution is purely mathematical and is devoid of physical meaning, these matrices are called abstract matrices.

Methodologies for determining the number of factors and for calculating the abstract row and column matrices then form the fundamentals of factor analysis. Since the abstract solution should involve a physically meaningful number of factors, determination of n, the correct factor "size or window" is an important step. As a result of this step, an estimate of the complexity of the data space, information normally lacking for a chemical problem such as combustion of a biopolymer, is obtained.

Factor Analysis is ideally suited to determining the number of components in spectroscopic analysis [141]. The sum of Beer's law for a multi-component mixture is

$$A = \sum_{j=1}^{n_c} \varepsilon_j c_j \qquad \textbf{Equation 2-4}$$

Where A is the absorbance at a given wavelength in a cell of unit length; ε_j the extinction coefficient of the jth component; and c_j is the concentration of the component j. The sum is of the n_c components of the mixture. This equation is in the same format as that used to generate the linear vectors from the data matrix in Equation 2.2.

In the generalised matrix notation, M is the data matrix which is made up of the spectral data where the row information (R) corresponds to the wavenumbers and the column information (C) are the spectral intensity. M is equivalent to D in Equation 2.3.

$$M = RC \qquad \textbf{Equation 2-5}$$

The data is deconvoluted to give the significant row scores ($\underline{R}$) and the significant column scores ($\underline{C}$), removing the non-significant factors and system noise (E).

$$M = [\underline{R} \cdot \underline{C}] + E \qquad \textbf{Equation 2-6}$$

The transformation matrix (T) is described using the generalised inverse of the significant row factors ($\underline{R}^+$) mapped on to the test target in the row domain (R_t).

$$\underline{R}^{+} \in R_t = T \qquad \textbf{Equation 2-7}$$

Using the transformation matrix the predicted spectrum (R_p) is formed from the significant row factors.

$$\underline{R} \cdot T = R_p \qquad \textbf{Equation 2-8}$$

This predicted spectrum can then be displayed and if available tested against a library of reference spectra. The predicted spectral intensity (C_p) for the predicted spectrum is calculated form the significant column scores ($\underline{C}$), which contain the spectral intensity of the data matrix, multiplied by the inverse of the transformation matrix (T^{+}).

$$T^{+} \cdot \underline{C} = C_p \qquad \textbf{Equation 2-9}$$

The predicted spectral intensity is then available to be used with the calibration data for a predefined reference compound.

This technique is now embodied in software called InSight™ [142] coded in Matlab™ [143] language. All data analysis was performed through this software. In particular the software allows:

- the selection of a compound of interest to be used as a reference in its database
- the quantitative calibration of the reference compound within a user defined range
- deconvolution of complex time-resolved data to identify the compound from a mixture, e.g., pyrolysates or co-eluting chromatographic peaks
- the quantification of the compound against the calibrated range

2.2.1 The InSight™ Software

Unlike other common methods of data analysis and mathematical modelling that use least squares regressions, or neural networking approaches, the InSight™ method does not have to build a model for the data with the assumption that all samples will have the same basic matrix [142]. The system has a self-deconvolution system that enables it to deconvolute a signal with no knowledge of the signal constituents that make up the mixture [144]. This means that the data may be separated into the key factors provided the data are provided in a format that may be read by the algorithms.

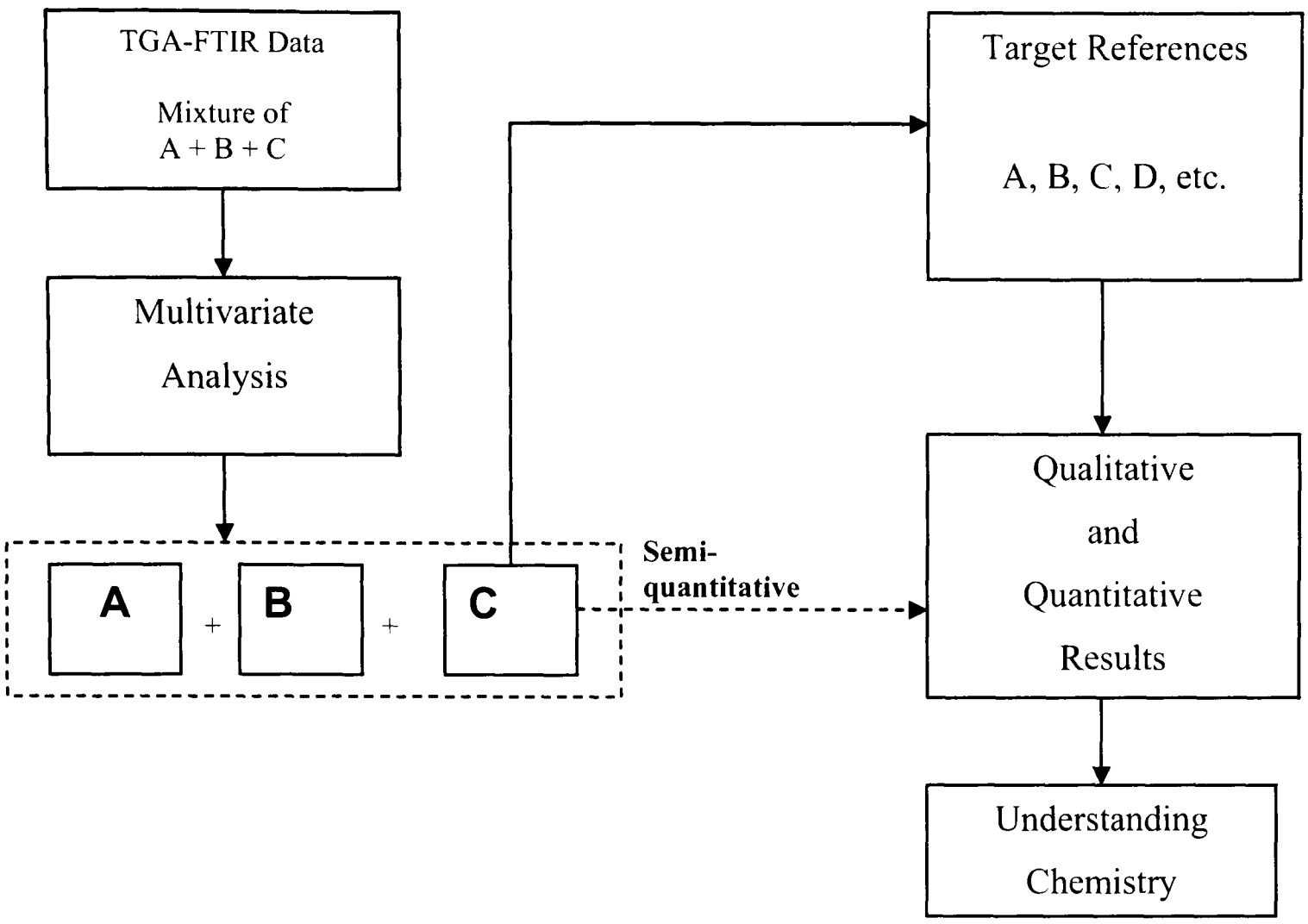

Figure 2-4. A schematic flow path of Target Factor Analysis (TFA) illustrating the process of analysis of FTIR data using the InSight software

For the purpose of this study the software was furnished with a library of pure compound spectra and calibration data to enable quantitative profiling for each of these reference compounds.

Sets of linear calibration spectra are prepared using a required compound, and from this set a single spectrum is selected to add to a master reference table. As many compounds may contain similar absorption frequencies, particularly within a homologous series of compounds (e.g. aldehydes), it is important that the reference spectra are as free from interference as possible [145]. These calibration spectra are arranged into separate data tables for each reference material and are linked to the master reference table. On evaluation of an unknown sample factor analysis is carried out on the experimental data to reduce the data to its component factors (Figure 2-4). The factors are then compared to the reference table for matches with the prepared pure compounds. If a match is found the software looks to the linked calibration table for the

identified compound and provides a concentration vs. time profile for the identified factor. Experience in the interpretation of IR spectra is required to interpret the resolved data to check that factors identified are real, rather than other artefacts.

It is also important to utilise this experience to establish that the compound has been correctly identified as many compounds share similar absorption features as a result of sharing similar chemistries. With all of these points in mind it is important to realise that representative reference spectra that are free from noise and interference are required to make the software's matrix calculations as robust as possible.

The software analysis process is shown visually in the following sequence of figures. Figure 2-5 shows the first step in the software process, which is to select a window to examine the whole data set. In the example shown the carbonyl region (1850 – 1650cm^{-1}) is selected for the extraction of formaldehyde from the FTIR data.

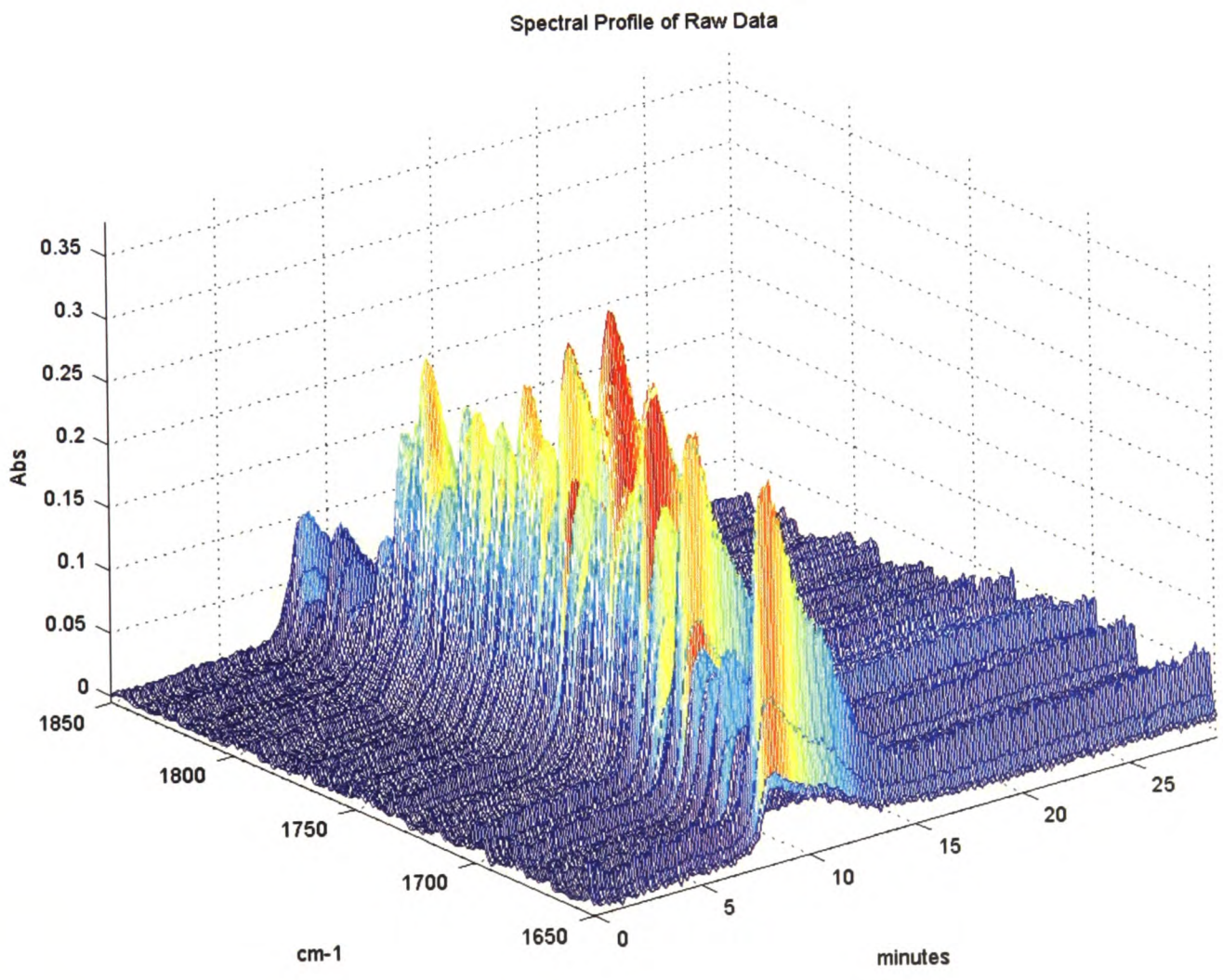

Figure 2-5. Spectral window from 1850 – 1650cm^{-1} extracted from complete spectrum file.

This window is taken such that it will include important, or ideally unique peaks for the compound of interest, in this case the C=O carbonyl function of formaldehyde. Once this is chosen the software performs the target factor analysis and provides statistics to indicate how many potential compounds, or factors, are present in this portion of the spectrum (Figure 2-6). This is shown by the three plots at the bottom of the figure which are (from left to right); the factor indicator function (Malinowski's IND plot [140]), the % significance level based on the F-test (%SL plot), and the cumulative variance plot (% variance plot).

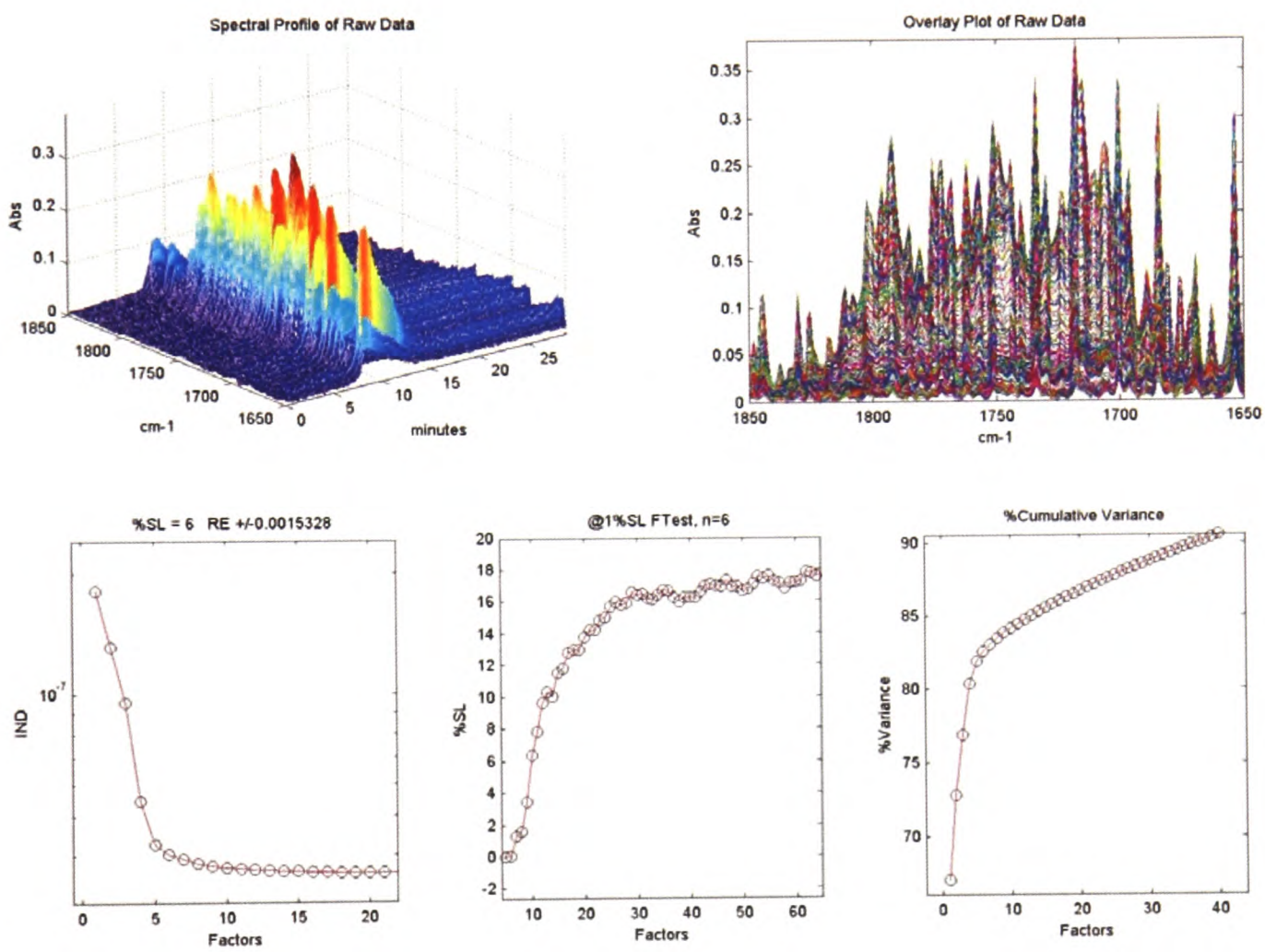

Figure 2-6. Analysis of the spectral window with the number of statistically extracted factors shown in the lower three plots.

The software then displays the extracted factors for verification by both statistical information and also by inspection of the spectral characteristics of each factor. This information is illustrated in Figure 2-7 where the factor number is shown down the left-hand side of each plot. Also displayed for each factor is an indication of the cumulative variance (V) that is described by that factor.

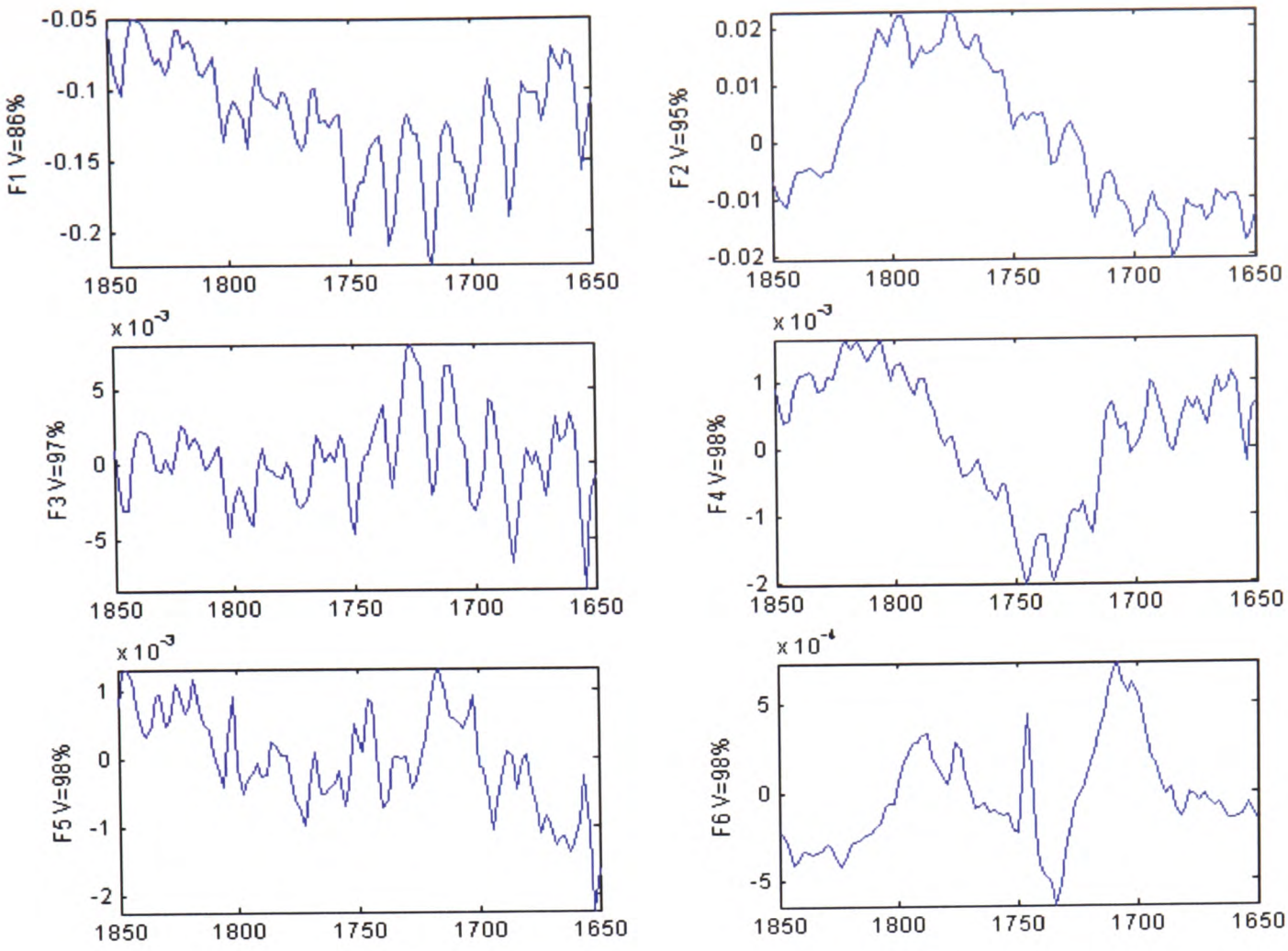

Figure 2-7. Factor extraction output taken from InSight™ software.

Once the factors have been selected then the software will produce a 'predicted spectrum' for this factor and compare it to the reference spectrum of the same compound. An example of this for formaldehyde is given in Figure 2-8. This overlay graph allows the user a visual check that the match is accurate for the particular target compound. The software can be set into an automated (configured) mode where all of the calibrated compounds in the reference library may be tabulated, along with the spectral windows used for the analysis. This can then be used to analyse a data set, automatically stepping through the configuration table testing the data for each of the references in turn. This configured mode in the software allows a rapid qualitative assessment of a large batch of samples against a large database of reference spectra. After all of the references have been tested a summary page is given for each of the references in the library (Figure 2-9). This gives information about the quality of the matching and also the shows the factor match graph (bottom) for visual inspection. The two other graphs show individual evolution profiles for the target compound (top) and an average profile (if a number of replicate samples are presented to the software) and a cumulative plot of evolved compound (middle)

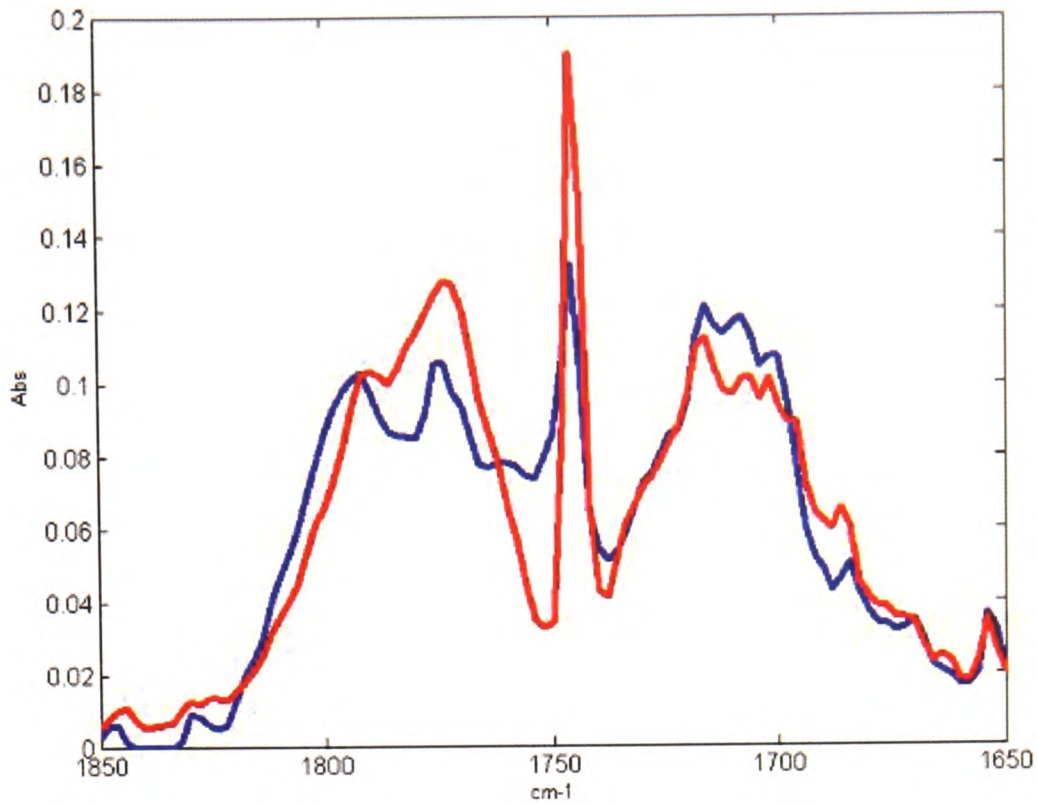

Figure 2-8. Factor match for formaldehyde. The 'predicted spectrum' is in blue and the reference spectrum is in red. The correlation for the match, R = 0.913.

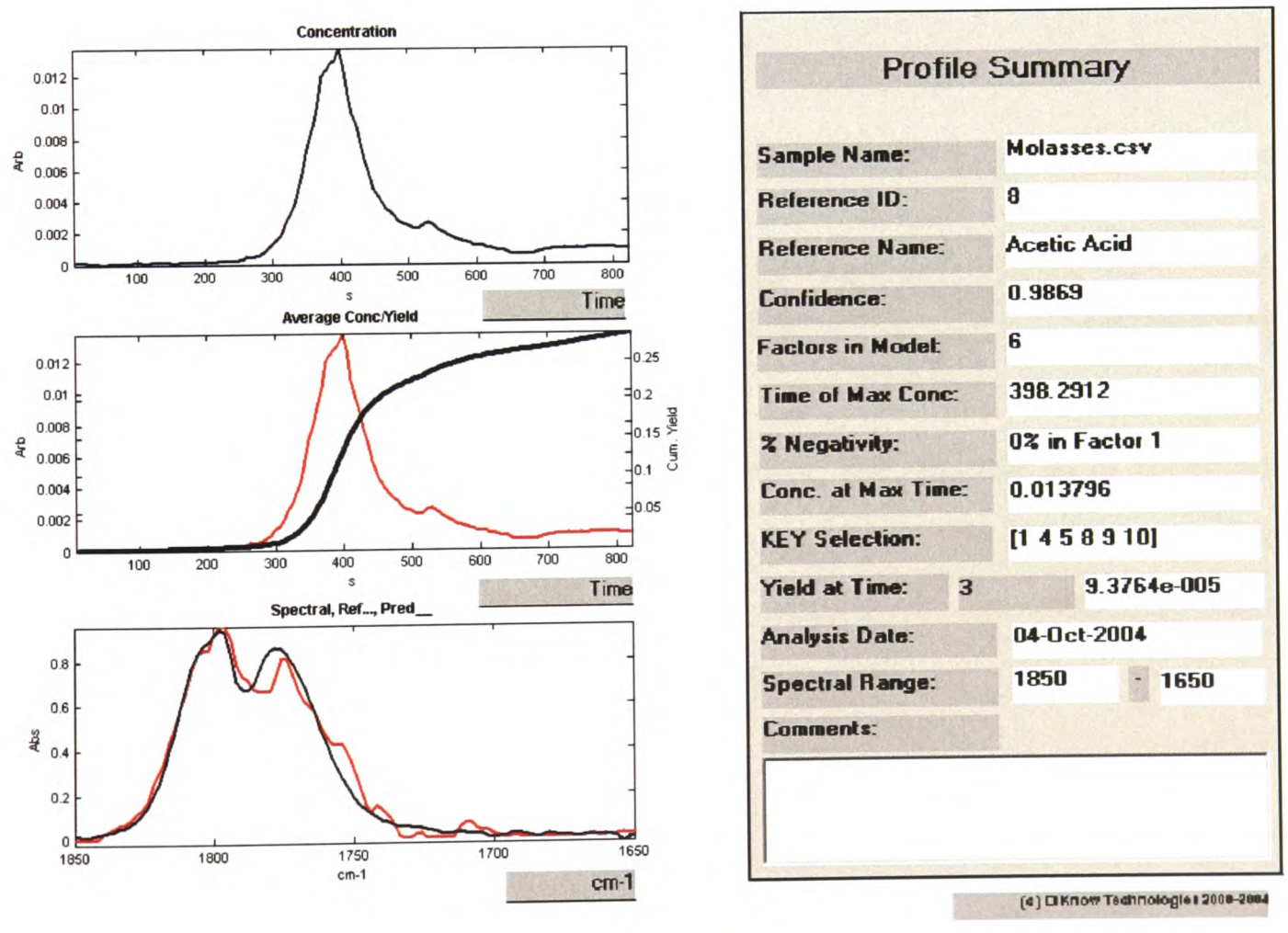

Figure 2-9. An example page from the configured mode of the InSight™ software showing the rapid qualitative matching process. The evolution profiles and factor matching is shown on the left side. The table on the right shows the confidence in the match and other information regarding the extraction process.

2.2.2 Quantitative Analysis

Once positive qualitative matching is achieved, it is sometimes desirable to gain quantitative information using InSight™. In order to get the best data from the software a two staged process is used – First, wide spectral windows (~200cm^{-1}) are used to allow accurate qualitative matches, followed by a second stage in which narrow spectral windows (~50cm^{-1}) are used. This second step allows the system to make the comparison with the calibration data using a small part of a unique peak for each of the identified compounds.

The conversion of the evolution profile to a cumulative amount of material is performed by the following equation:

$$\text{Total concentration} = \sum (C \times v \times t) \qquad \textbf{Equation 2-10}$$

where:

C = Concentration (μg/ml)

v = Flow rate (ml/min)

t = Scan time interval (min)

This is then divided by the initial mass of the sample (m) to give a proportional value:

$$\text{Total concentration per unit starting mass} = \frac{\sum (C \times v \times t)}{m} \qquad \textbf{Equation 2-11}$$

This equation results in a dimensionless proportion, the amount of a particular compound evolved from the amount of starting material (i.e. μg/mg). The information generated by the software is shown in Figure 2-10. This gives a summary of the qualitative extraction of the factors as well as calibration and quantification information.

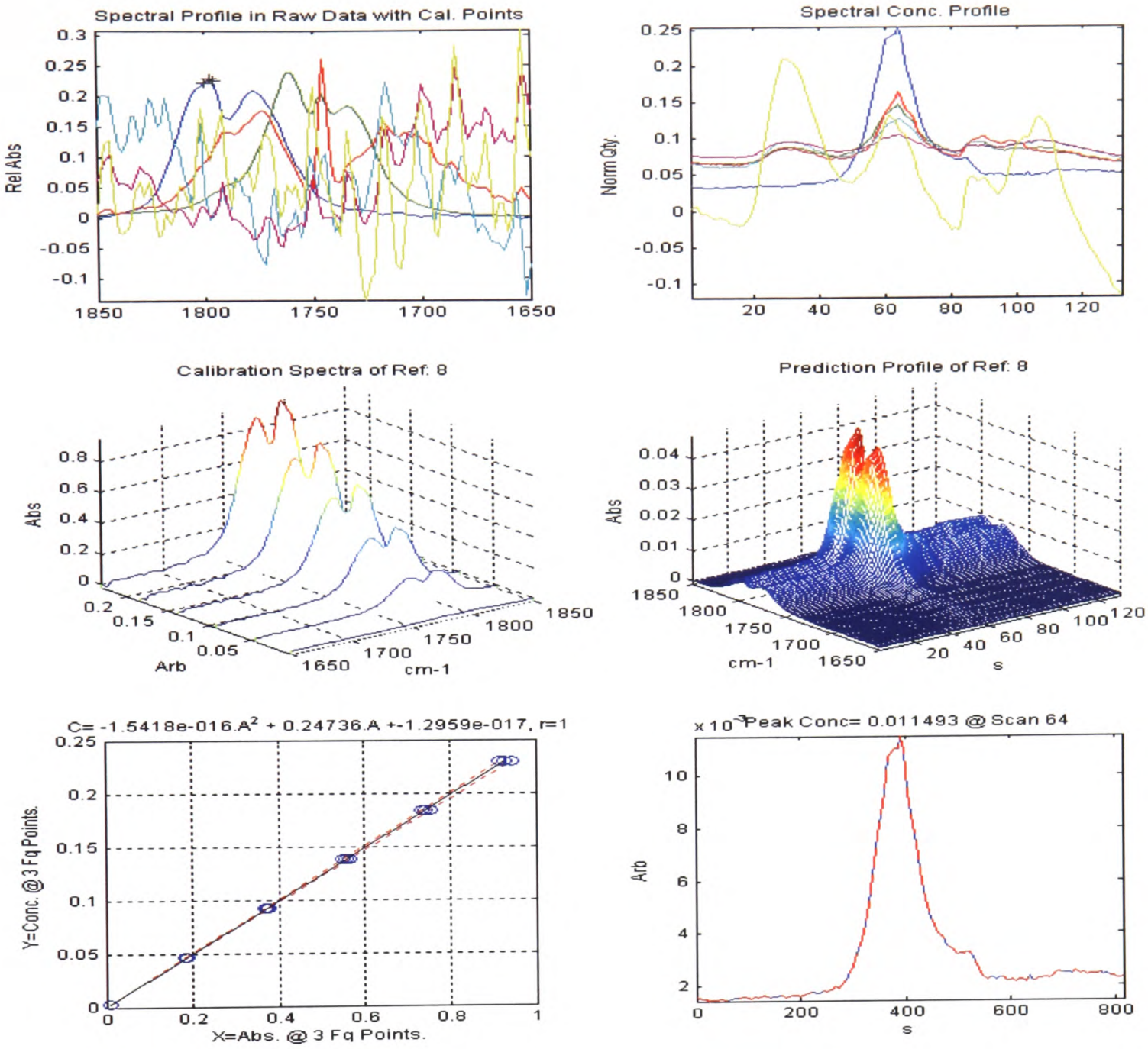

Figure 2-10. Quantitative analysis summary page from InSight™ software showing (l- r, top to bottom); the spectra of the extracted factors; The semi-quantitative evolution profiles for the extracted factors; a plot of the calibration standards for the spectral window for the selected target compound (acetic acid); 3-D plot of the selected factor; the Beer's law calibration plot; the quantified evolution plot of the extracted factor (acetic acid).

2.3 TESTING THE PARAMETERS OF THE TGA-FTIR

TGA-FTIR combined with multivariate analysis was used previously to analyse polysaccharide tobacco ingredients [146]. Subsequent to this work a longer pathlength cell (compared to the original 8 cm cell) was added to the FTIR in order to improve the sensitivity of the system. The new gas flow cell (2.5 m Cyclone™ cell, fitted with ZnSe optical windows and gold coated mirrors, supplied by Specac Ltd) allowed a higher sensitivity to be achieved with the FTIR. By using a mercury cadmium telluride (MCT) detector the FTIR could be used at a higher resolution than the previous regime, but maintained the scan speed to enable useful real-time measurements [147]. With these changes to the system it was important to establish the practical flow rates, sample sizes, and scanning parameters for optimal performance. A schematic for the experimental setup is given in Figure 2-11. The FTIR gas cell is linked to the TGA via a heated transfer line. The transfer line (1m, stainless steel with a Teflon® liner) is connected to the TGA such that the end is close to the furnace.

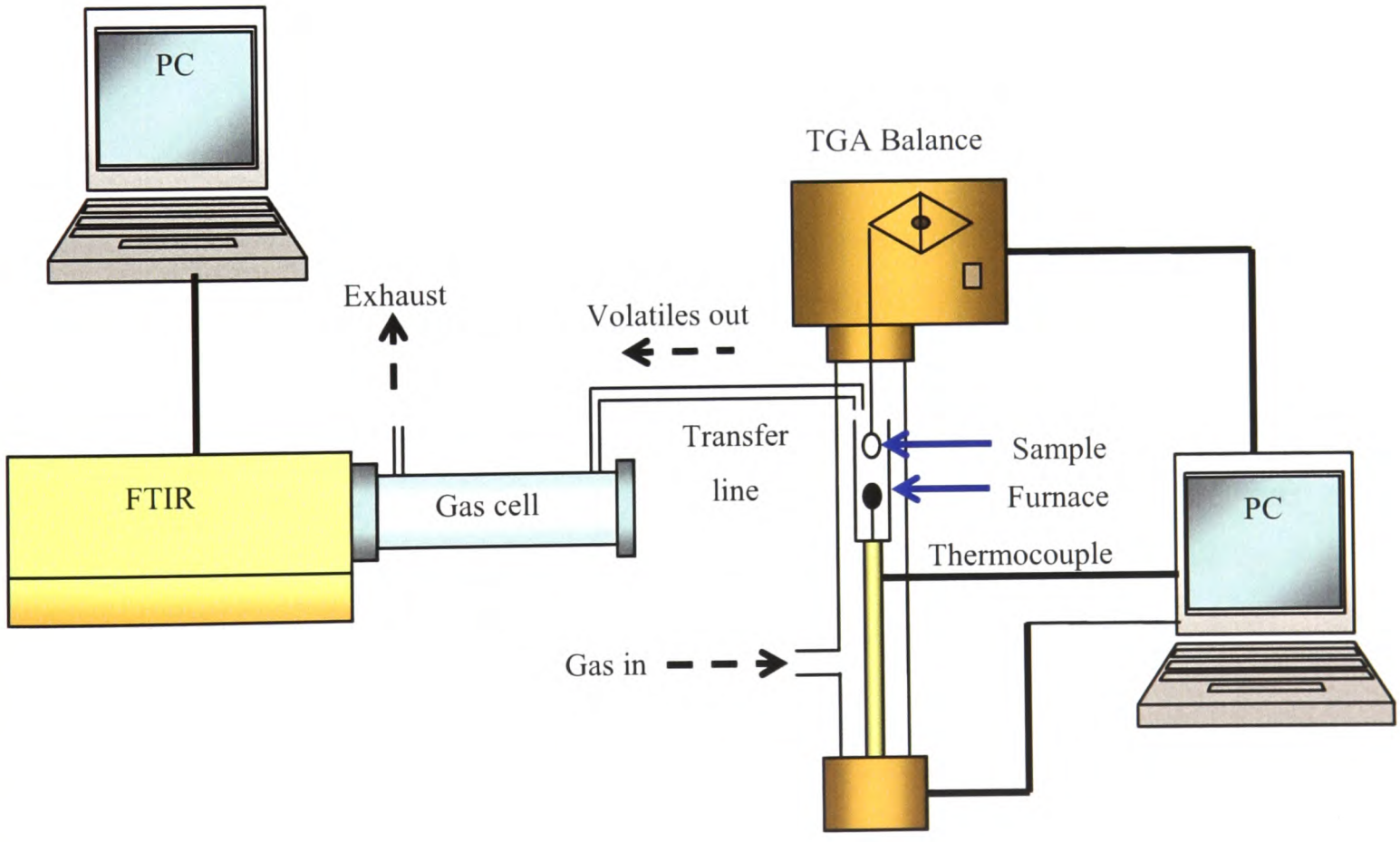

Figure 2-11. Schematic diagram of the TGA-FTIR equipment used in this study.

Following this parameter testing it was necessary to make a new calibration data set due to the changes in the system that affect the response of the FTIR signal with respect to the sample concentration:

- detector type – deuterated triglycerine sulphate (DTGS) to MCT, a faster response and higher sensitivity detector allowing the increase in resolution
- resolution – 4cm^{-1} to 2cm^{-1} – The increase in resolution effects the qualitative matching of the system. The reference spectra need to be collected under the same resolution as the samples.
- optical windows for the gas cell – KBr to ZnSe. The different optical materials have different characteristics in the amount of IR that will pass through the material. ZnSe windows absorb more of the IR energy than KBr, but have greater resistance to chemical attack and fogging than KBr
- pathlength of the cell - 8cm to 2.5m. This affects the calculation in determining the concentration of the material in the cell.

As all of these parameters affect the way the software measures the evolved gases it is important to ensure that the reference and calibrations spectra are collected with the same parameters as the samples.

2.3.1 Scanning Parameters

The FTIR scanning parameters were largely dependent upon the instrument and cell design. The FTIR potentially can scan from 7800 – 370cm^{-1} with its internal configuration, and with resolution of 0.2 – 64cm^{-1}. The ZnSe optical windows of the gas flow cell are transparent to IR in the range 20000 – 500cm^{-1}. The mercury-cadmium-telluride (MCT) detector used has a useful wavenumber range of 10000 – 750cm^{-1}, and is therefore the limiting part of the equipment in terms of the low wavenumber end. The normal range used in infra-red spectroscopy is 4000 - 625cm^{-1} [148], so the parameters chosen for the experimental scanning range were 4000 – 750cm^{-1}.

Resolution for the system was determined out of practicality. Ideally the higher the resolution the more detail is obtained. However scan rate decreases proportionally with increasing resolution, such that a scan from 4000 – 750cm^{-1} at 2cm^{-1} resolution takes approximately 6s, whereas the same scan at 1cm^{-1} resolution will take ~11s. As the experiments intended to monitor the changes in evolved gases as a function of the time or temperature program of the

TGA it was decided to take use $2cm^{-1}$ as a compromise between scan rate and resolution. Any events that occur faster than 6s will not be possible to detect.

2.3.2 Flow rate

The flow rate used in the gas cell was considered next. The gas cell has a volume of 190ml, so it seemed appropriate to maintain flow rates above $100mlmin^{-1}$ to maintain a suitable purge rate. Figure 2-12 shows the effect of changing the flow rate for a sample of formic acid held isothermally for 10 minutes at 60°C in the TGA.

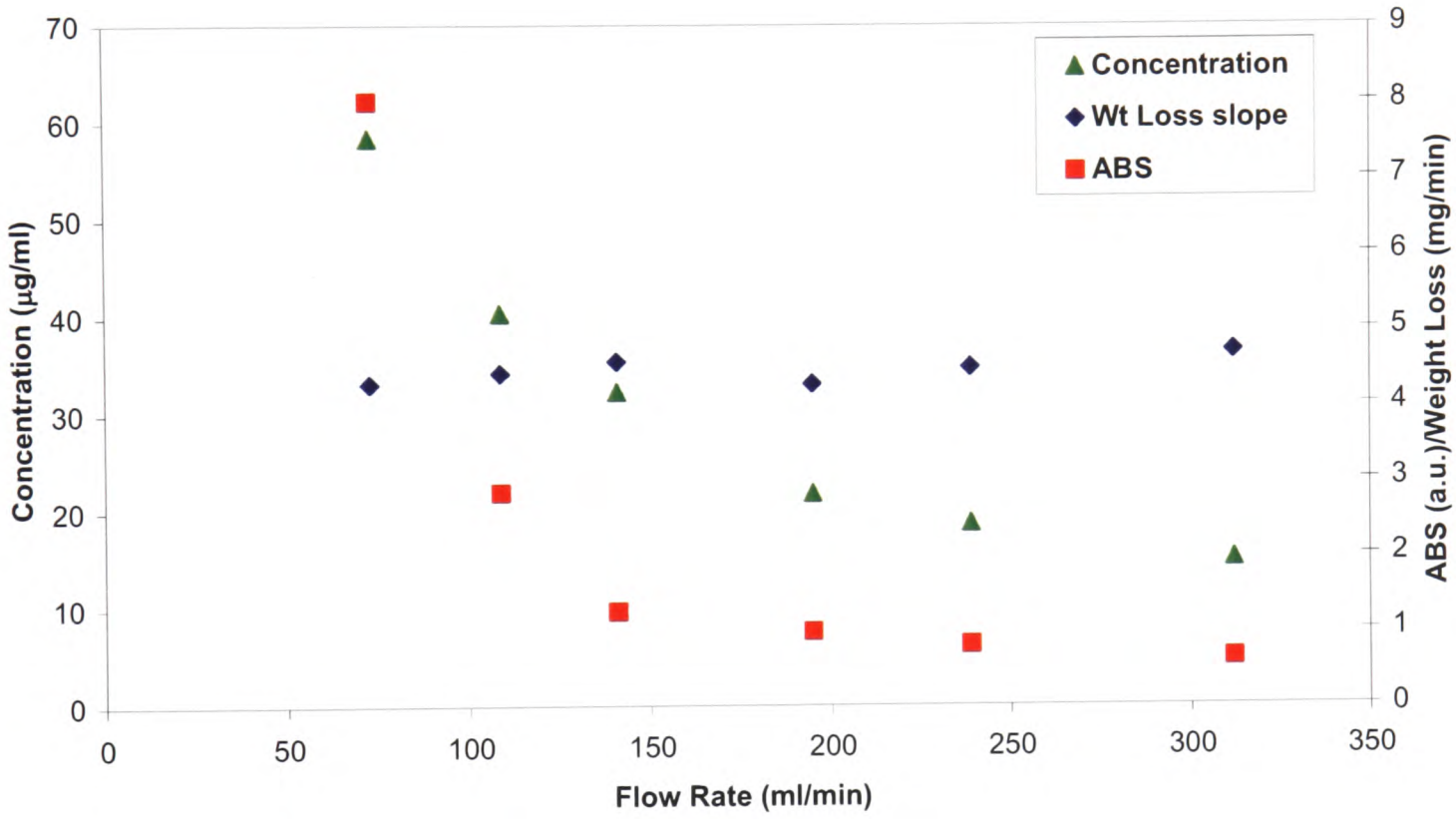

Figure 2-12. Peak absorbance, calculated concentration and TGA weight loss slope plotted vs. nitrogen flow rate for formic acid heated at 60°C for 10 minutes using a constant sample weight.

The graph shows that for a constant sample weight, under constant temperature the increase in flow rate decreases the observed peak absorbance in the spectrum and also the calculated concentration. However, above a flow rate of 200ml/min there is less effect on the concentration. The rate of weight loss of the sample in the TGA is not affected significantly by the change in flow rate for formic acid. The peak absorbance is the height in absorbance units of the largest peak in the spectrum. Concentration (C) is calculated by dividing the weight loss slope (w_l) by the flow rate (v), then converting to micrograms per unit volume.

$$C = \frac{W_l \times 1000}{v}$$ **Equation 2-12**

The transfer time from the TGA to the FTIR was also assessed. This was measured by placing formic acid into the sample pan using an isothermal temperature program. The time between the start of the experiment and the initial response on the FTIR was measured. The time between the sample weight reaching zero and the return of the FTIR signal to zero was also measured. The average of these times was used to determine the transfer time of the sample from the TGA to the FTIR. This experiment was repeated at different flow rates and the data are shown in Figure 2-13.

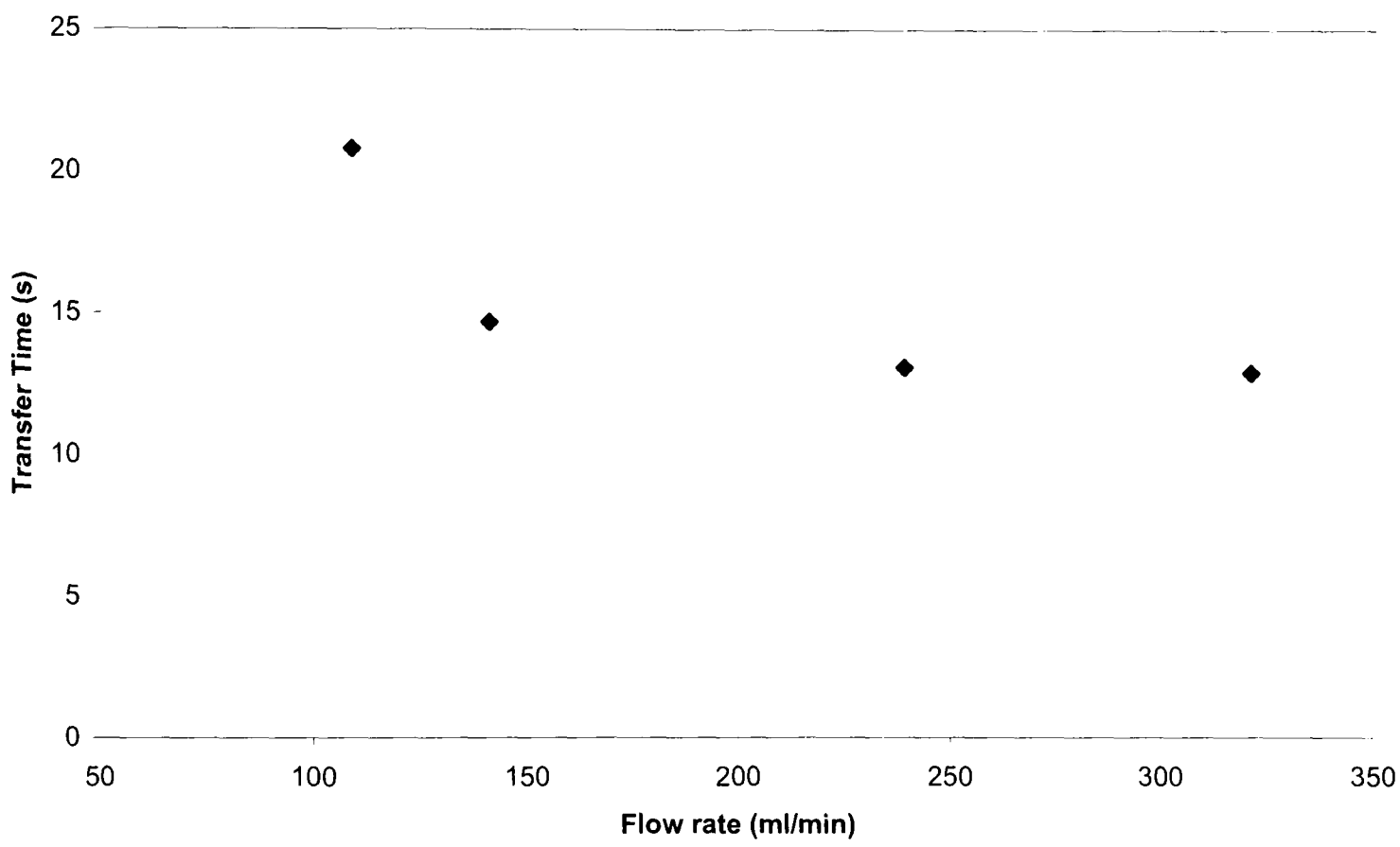

Figure 2-13. Transfer time between the TGA and FTIR plotted against purge gas flow rate, under constant sample weight and temperature.

Figure 2-13 shows that above about 200ml/min flow rate of purge gas there is little change in transfer time. This is thought to be caused by the physical configuration of the transfer line, which due to its narrow bore (~1mm diameter) acts as an impedance to flow beyond a certain point. From these experiments, consideration of the cell volume (190ml) and design of the transfer system, a flow rate of 250ml was chosen as the best flow rate for running samples and standards.

2.3.3 Sample Weight

Using formic acid under a constant flow rate (250ml/min) and 60°C isothermal temperature for 10 minutes the effect of changing sample mass was investigated. The results are shown in Figure 2-14.

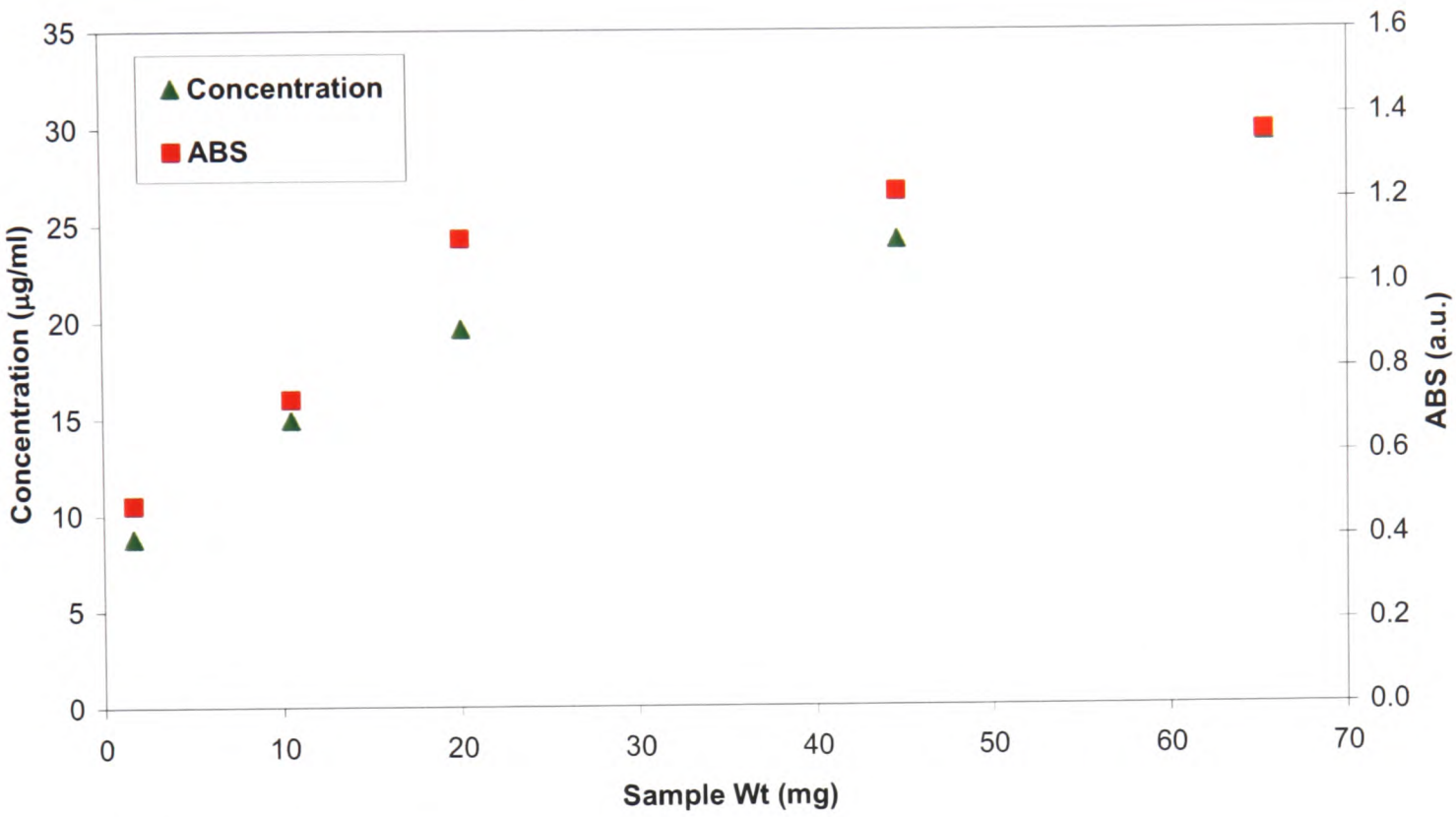

Figure 2-14. Peak absorbance and calculated concentration plotted vs. sample weight for formic acid heated at 60°C for 10 minutes using a constant flow rate of nitrogen.

The effect of changing the sample mass shows an increase in concentration, calculated as before. This indicates that for the best replication of sample information it would be important to keep a constant sample weight. However, it is difficult to assign a particular ideal sample mass as other factors need to be considered. Firstly, a high sample weight will lead to thermal lag, which is the temperature difference between the surface of the sample and the interior of the sample. Also the thermal inertia of the sample is increased leading to a divergence in the temperature program and the actual temperature of the sample. This effect would be accentuated with higher temperature ramp rates. The second aspect is that a smaller sample would produce lower amounts of evolved products on heating. Therefore a balance needs to be made to find a compromise between the thermal effects and the need to obtain measurable levels of evolved compounds.

2.3.4 Isothermal Temperature

The effect of changing isothermal temperature of a constant mass of formic acid under a constant flow rate is described by Figure 2-15.

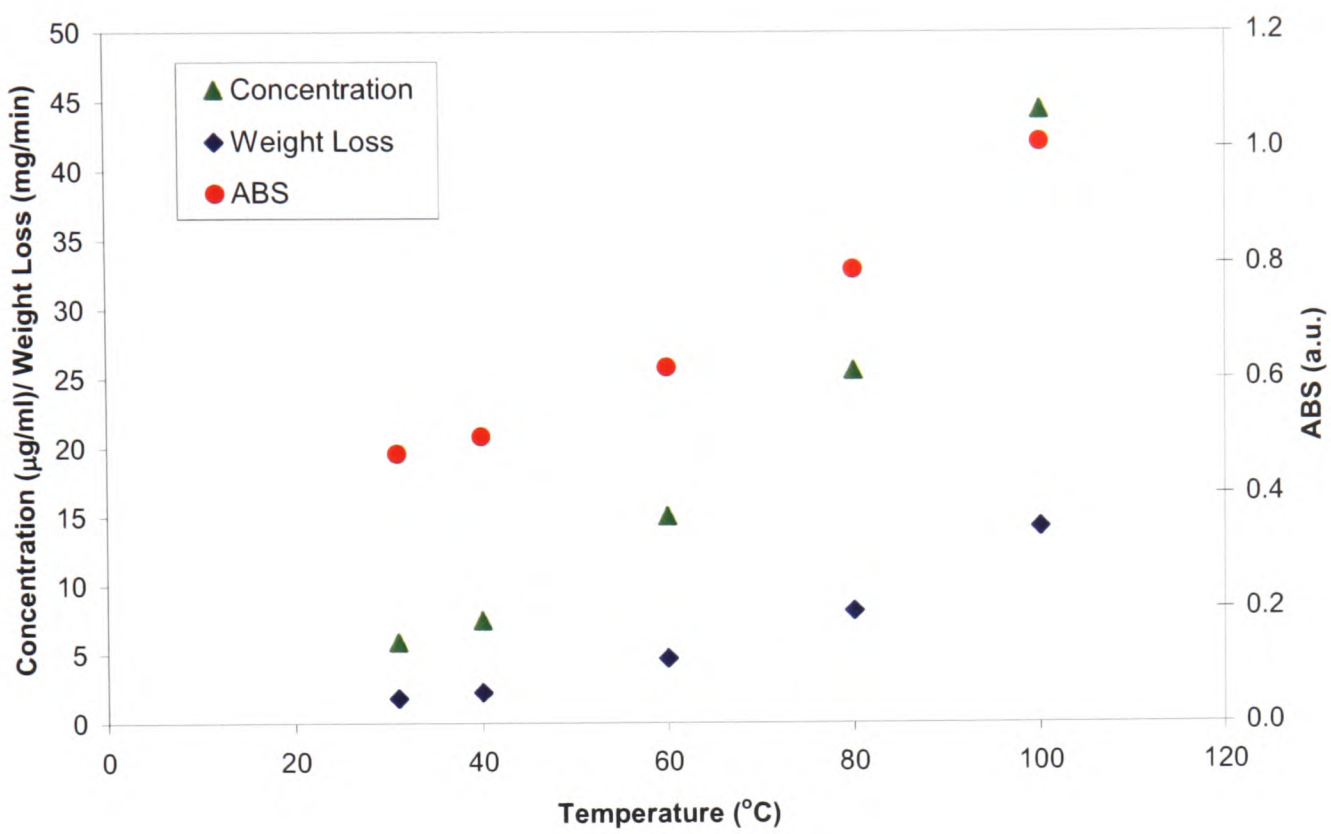

Figure 2-15. Peak absorbance and calculated concentration plotted vs. isothermal temperature for formic acid heated for 10 minutes using a constant sample weight and flow rate of nitrogen.

Increasing temperature has the effect of increasing concentration, as a result of the increased sample mass loss within the TGA. Changing the isothermal temperature provides a method of producing calibration data sets for liquid and solid samples that may be used with the InSight™ software. Though for formic acid the change in concentration with temperature is not linear, the software is capable of using non-linear calibration graphs.

2.4 CALIBRATION PROCEDURE

Based upon the findings of the previous section the procedure for generating the calibration data sets for use with the multivariate analysis software, InSight™, were established. The settings for the system are listed below –

TGA

Temperature program	10 minutes isothermal
Purge gas flow rate	250 ml/min, dry nitrogen

Transfer line temperature	220°C
Gas cell temperature	200°C

FTIR

Scan range	4000 – 750cm^{-1}
Resolution	2cm^{-1}
Scan time	6s, approx. (no co-addition)
Background spectra	nitrogen

These settings are the basic configuration for the system during calibration of system for the InSight™ software, however, it is possible to vary the TGA temperature programme and gas atmosphere (although the flow rate is optimal at 250ml/min) to more appropriate conditions for other experiments.

2.4.1 Calibration of Solid and Liquid Compounds

Pure compounds that are solid (paraformaldehyde for formaldehyde generation on heating) or liquid (ethanol, formic acid, etc) were introduced to the FTIR, via the TGA.

A known amount of the compound was placed in a DSC sample pan and crimped. The crimping of the pan does not seal the pan, but it does restrict the distilled vapour from leaving the pan too rapidly in a fashion similar to a diffusion tube. This allows closer control of volatile samples to be run without overloading the FTIR detector. However, as the crimped DSC pan can be placed onto the TGA balance the weight loss can be monitored for the compound under the conditions of use. This has a major advantage over diffusion tubes which would need to be calibrated over a period of time at each temperature required to provide the weight loss rate for a single compound. Individual pre-calibrated diffusion tubes can be purchased but at great expense and a separate one would be required for each compound required for calibration.

For calibration the DSC pan is heated using an isothermal temperature program for 10 minutes, under a known flow rate of dry nitrogen gas. The rate of weight loss was recorded, and this is linear under isothermal heating conditions. The observed spectrum was seen to increase to a constant absorbance, which was also recorded. The concentration that corresponded to this measured absorbance was calculated from the weight loss and gas flow rate information as shown in Equation 2.12. This data was plotted to ensure a good fit, and an example of one such

calibration is shown in Figure 2-16. The calibration graph for formaldehyde shows a good, non-linear fit with an intercept close to the origin. Beer's Law is non-linear at high values of absorbance and generally calibrations would be limited to spectra with absorbance peaks of less than 1. However, both linear and non-linear calibration data can be handled by the InSight™ software. Further to this as data is for the calibration points are taken across the whole wavelength range it is possible to use different regions of the spectrum for quantification to avoid peaks greater than one absorbance unit in size.

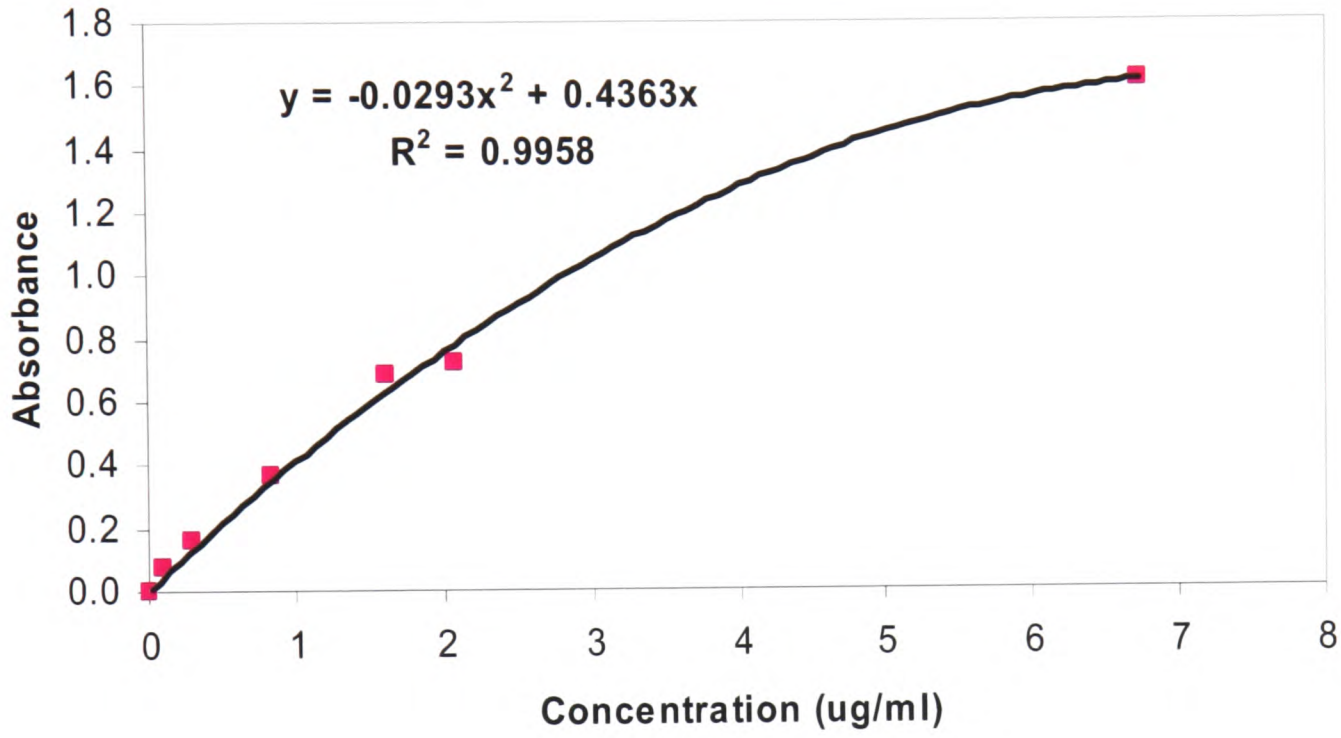

Figure 2-16. A graph of calibration data for formaldehyde with the equation and R^2 value displayed.

2.4.2 Calibration of Gas Phase Compounds

A number of the compounds chosen for calibration are gases (carbon monoxide, carbon dioxide, etc) or highly volatile liquids (acrolein, acetaldehyde, etc) at room temperature. These were obtained as certified concentrations within nitrogen in cylinders. A measured amount of the gas standards were then placed into gas tight bags and diluted with a known volume of dry nitrogen. The gas bag was massaged and then left to equilibrate for 10 minutes. The TGA was not required for the generation of the standard dilution so the gas bag was attached directly to the transfer line and the standard mixture drawn through the gas cell at a constant rate using a vacuum pump. The measured absorbance was plotted against the calculated concentration for

each standard material, an example of which is shown in Figure 2-17. As in the previous example the graph is non-linear but still has a good fit, which tends toward the origin.

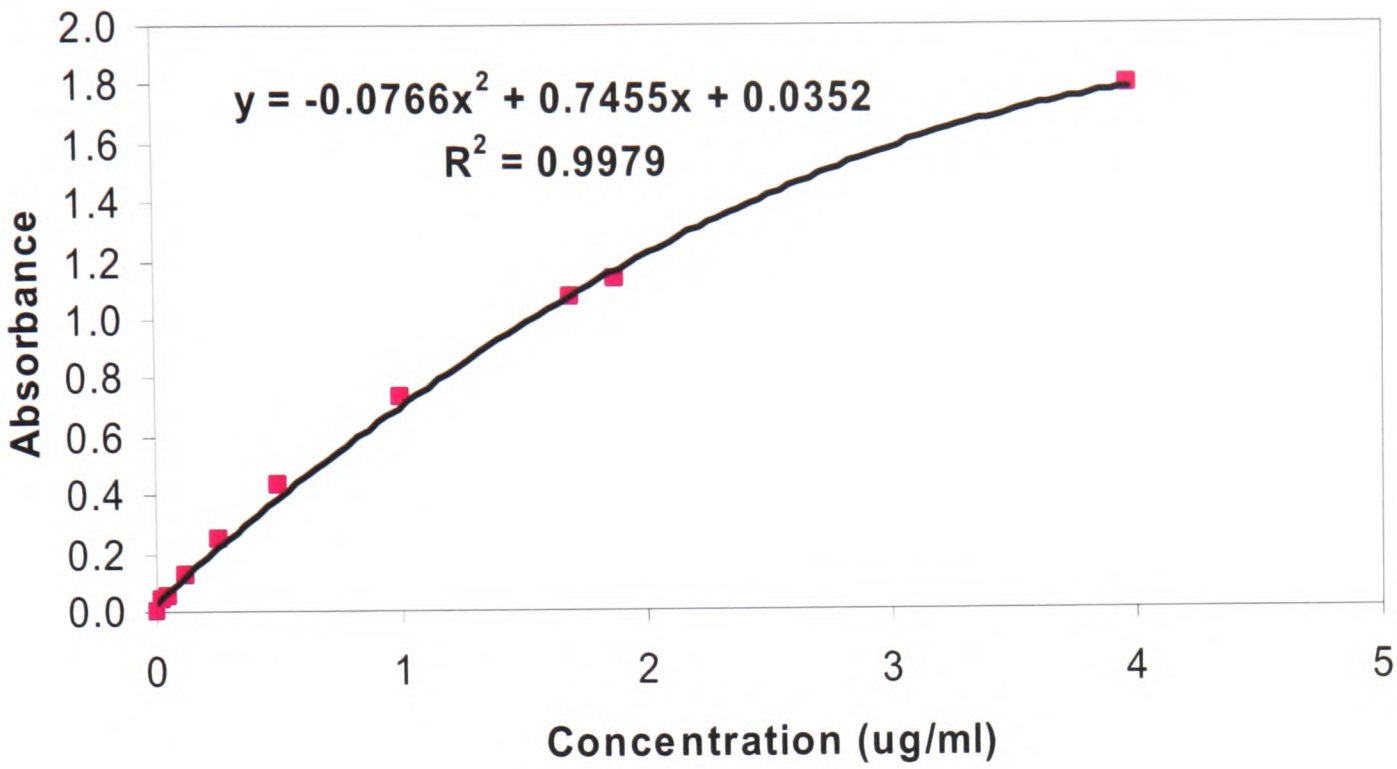

Figure 2-17. A graph of calibration data for methane with the equation and R^2 value displayed.

2.4.3 Testing the Calibrations

Following the calibration the standard samples were processed with the InSight™ software to give an indication of the accuracy of calculations made using the calibration graphs. Three are displayed below – formaldehyde, acetic acid and carbon monoxide, chosen as an example of a solid, a liquid and a gas sample respectively.

It can be seen from Figure 2-18 - Figure 2-20 that the accuracy of the calculation from the software is reasonable with values less than 3% from the expected average value.

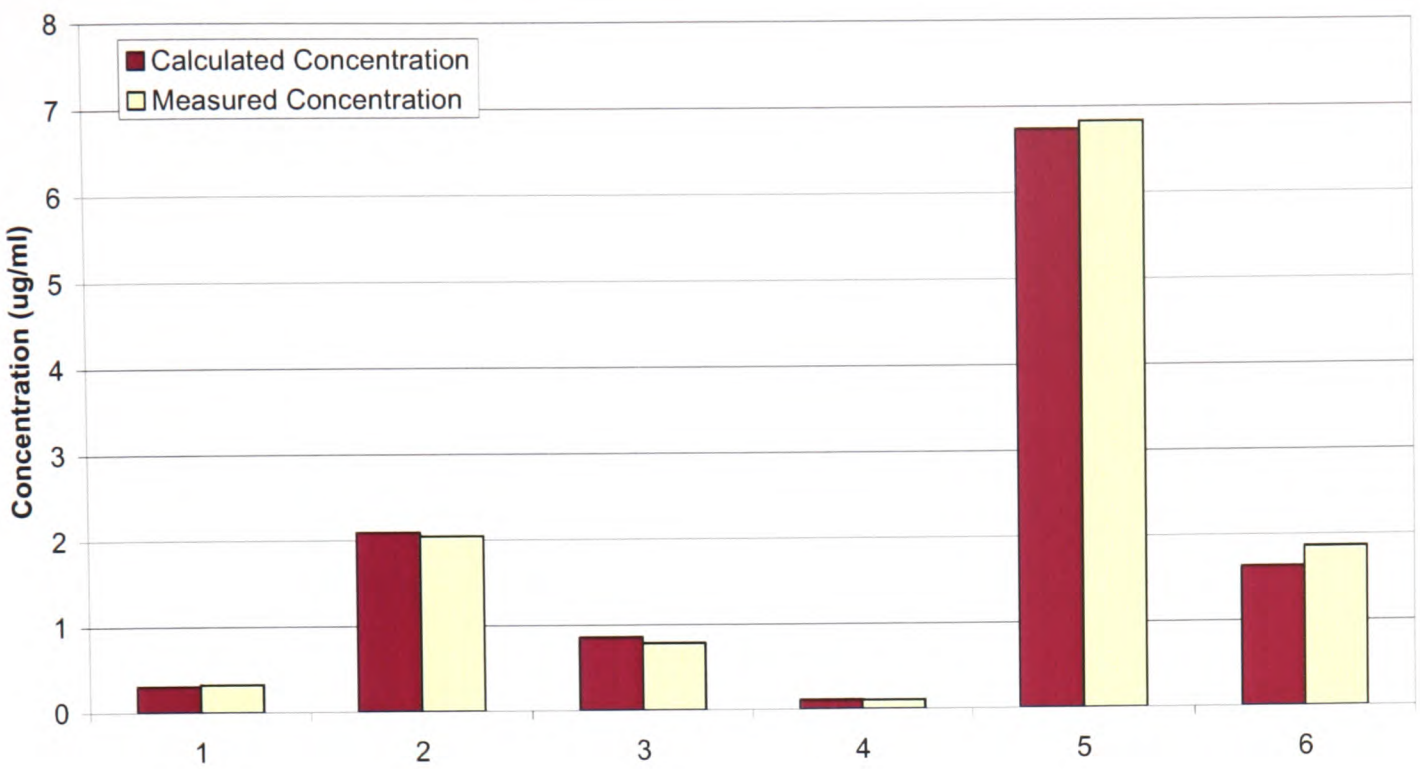

Figure 2-18. Comparison of calculated concentration of standards with the concentration measured using InSight™ for formaldehyde.

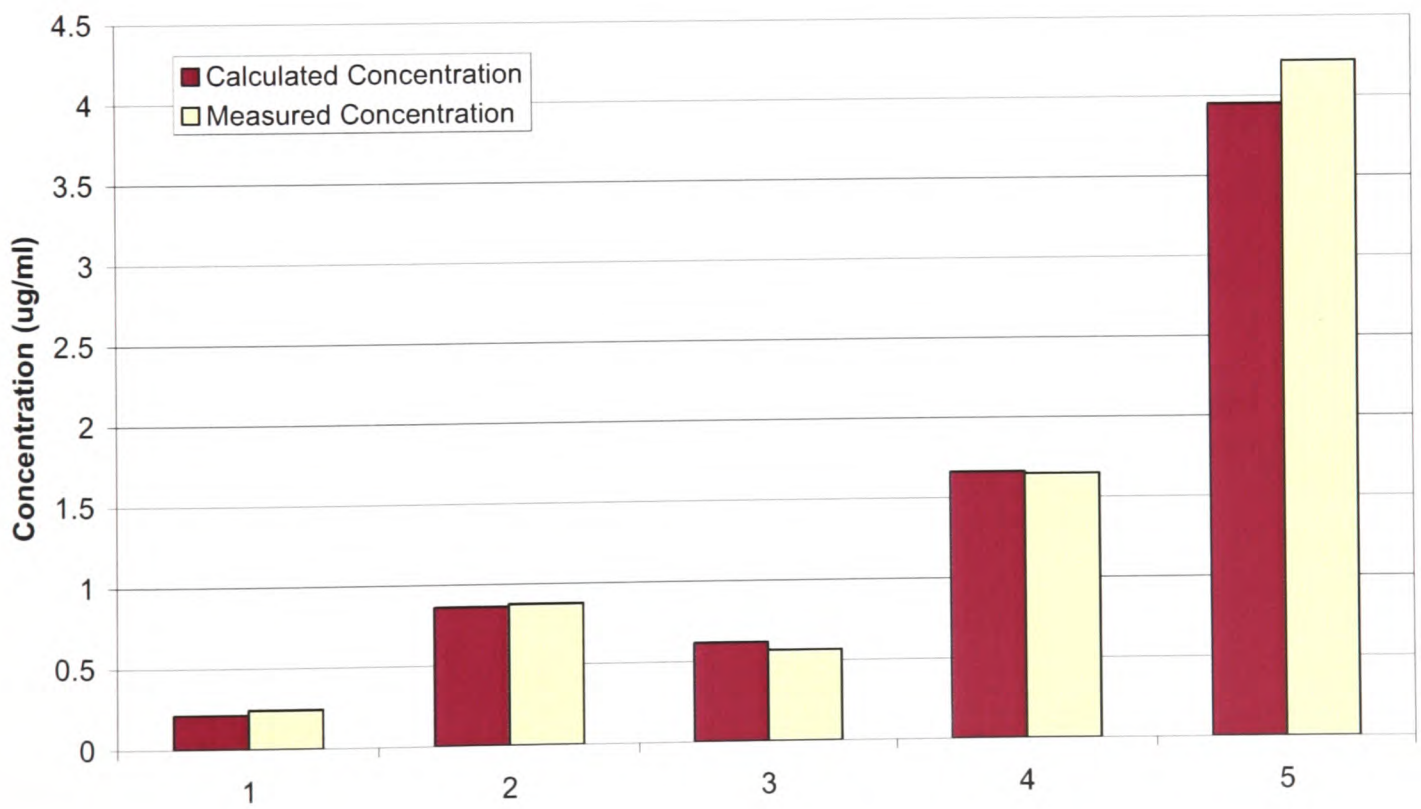

Figure 2-19. Comparison of calculated concentration of standards with the concentration measured using InSight™ for acetic acid.

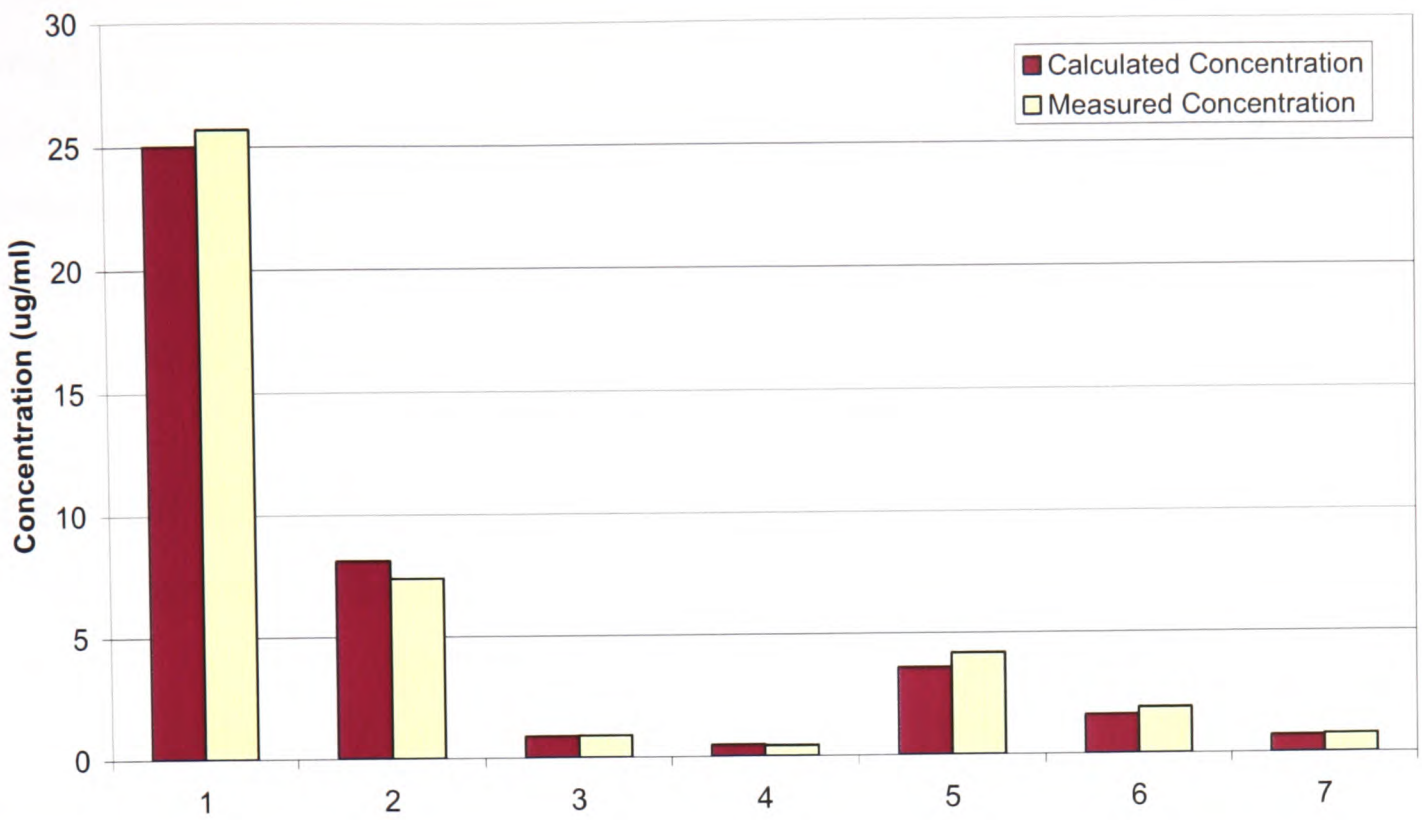

Figure 2-20. Comparison of calculated concentration of standards with the concentration measured using InSight™ for carbon monoxide.

2.5 MATERIALS

The materials used in the study are listed (Table 2-2) detailing the supplier and batch codes or lot numbers (more detail is given in Appendix A). Microcrystalline cellulose is produced by acid digestion of the amorphous region of the cellulose, which leaves the crystalline regions [45]. This process produces material with a low degree of polymerisation (DP ~200) [18].

Table 2-2. List of sample materials used in this study, with supplier and batch codes

Chemical	Supplier		CAS	Batch/Lot Number
Cellulose (microcrystalline powder)	Aldrich	High Purity	9004-34-6	05127H0
Alginic Acid	Acros Organics	97%+	9005-32-7	A015542301

Commercial alginates are normally a mixture of guluronic and mannuronic acid units, and being a natural product there will be some variability in the ratio of G:M units in the polymer across a sample and also between different batches. The alginic acid was chosen as it is primarily polymannuronic acid, although it is still a mixture of the two uronic acids. This allows better definition of the nature of the material used in the study and simplifies the chemistry.

In both cases the samples were stored in separate glass bottles in the same desiccator, over silica gel to maintain constant moisture content for each of the samples.

2.6 EXPERIMENTAL CONDITIONS

The comparison of the thermal decomposition of cellulose and alginic acid was divided into two sections. First the comparison of evolved gases from the two compounds using TGA-FTIR. Secondly examination of the residue remaining after subjecting the two compounds to different heat treatment temperatures and conditions.

2.6.1 Thermal Decomposition using TGA-FTIR

The two samples, cellulose and alginic acid, and a 50:50 mixture of the two were examined by TGA-FTIR using a single step temperature ramps. The conditions for the different samples are listed in Table 2-3.

The first 5 samples were all run in duplicate to examine the reproducibility of the technique and to assess the best weight of sample to use in the remaining experiments. The lower level (2mg samples) was chosen for practicality and the upper limit (20mg) was dictated by the size of the sample pan in the TGA.

The remaining experiments 6 – 28 study the effects of a range of temperature ramp rates and two different atmospheres for the materials. 10% oxygen in nitrogen was chosen as the oxidising atmosphere to simulate the oxygen deficient conditions of a cigarette burning zone [149]. A set of experiments (21 – 28) under these conditions was also run for a 50:50 mixture of the two materials to investigate any interaction between the two materials under the prescribed conditions. The mixture was prepared by weighing identical amounts of cellulose and alginic acid into a dry container and sealing the lid. The container was then placed in shaking device that tumbles the sample in three directions for 30 minutes to homogenise the sample.

Table 2-3. Table of experiments showing the conditions used in the TGA and the number of scans and interval between scans collected by FTIR.

Run	Sample	Flow Rate	Cellulose/ Alginic acid	Atmosphere	Ramp Rate	Scan Interval	Total Time	No of Scans
	mg	ml/min			C/min	min	Min	
1	4.922	242	C	N	30	0.0881	29	330
1a	4.820	211	C	N	30	0.0877	29	330
2	9.728	231	C	N	30	0.0879	29	330
2a	10.000	229	C	N	30	0.0880	29	330
3	14.540	232	C	N	30	0.0877	29	330
3a	15.085	232	C	N	30	0.0874	29	330
4	19.735	232	C	N	30	0.0872	29	330
4a	19.748	229	C	N	30	0.0878	29	330
5	1.921	231	C	N	30	0.0879	29	330
5a	1.948	231	C	N	30	0.0878	29	330
6	10.498	234	C	N	5	0.1205	170	1411
7	9.950	215	C	N	10	0.0924	85	920
8	9.615	225	C	N	60	0.0879	15	171
9	9.786	225	C	10% O	5	0.1256	170	1354
10	9.795	229	C	10% O	10	0.0879	85	968
11	9.620	230	C	10% O	30	0.0930	29	312
12	9.647	226	C	10% O	60	0.0928	15	162
13	9.225	215	A	N	5	0.0878	170	1937
14	9.387	211	A	N	10	0.0875	85	971
15	10.012	212	A	N	30	0.0868	29	334
16	10.233	209	A	N	60	0.0869	15	173
17	10.108	230	A	10% O	5	0.0924	170	1840
18	9.979	221	A	10% O	10	0.0923	85	921
19	9.568	223	A	10% O	30	0.0924	29	314
20	9.916	222	A	10% O	60	0.0932	15	161
21	10.237	210	50:50 mix	N	5	0.0878	170	1936
22	9.816	208	50:50 mix	N	10	0.0878	85	968
23	10.083	208	50:50 mix	N	30	0.0878	29	331
24	9.698	210	50:50 mix	N	60	0.0878	15	171
25	10.762	221	50:50 mix	10% O	5	0.0932	170	1825
26	10.035	221	50:50 mix	10% O	10	0.0932	85	913
27	9.504	215	50:50 mix	10% O	30	0.0932	29	311
28	9.806	214	50:50 mix	10% O	60	0.0879	15	171

2.6.2 Char Analysis

Char (the residue remaining after heating cellulose and alginic acid under nitrogen for a set temperature and time period) from both cellulose and alginic acid was prepared using a tube furnace. The samples were placed in pre-weighed ceramic sample boats and the weight of sample measured. The samples were placed into the tube, but outside of the furnace region, in flowing nitrogen for 5 minutes. To prevent any secondary reactions [53], a high flow rate of nitrogen used (~300ml/min) to ensure that the products formed were swept from the furnace tube quickly.

Table 2-4. Details of the samples heated at different isothermal temperatures for 1 hour under flowing nitrogen.

Sample	Temperature	Flow Rate	Sample Weight		% 'char' Formed
			Pre	Post	
	°C	ml/min	g	G	%
Cellulose	Untreated	-	-	-	-
	200	290	1.8187	1.6919	93.0
	300	310	1.9072	0.8016	42.0
	400	305	1.2099	0.1485	12.3
	600	305	1.9179	0.1412	7.4
	800	305	1.9378	0.0537	2.8
	1000	305	1.6712	0.0338	2.0
Alginic Acid	Untreated	-	-	-	-
	200	305	1.6638	1.2347	74.2
	300	310	2.0554	0.7815	38.0
	400	305	1.8484	0.4267	23.1
	600	305	1.8295	0.3628	19.8
	800	305	1.9001	0.2944	15.5
	1000	305	2.1497	0.2604	12.1

The samples were then pushed manually into the pre-heated furnace and remained there for 1 hour. After this time period the samples were taken out of the furnace and allowed to cool to room temperature in the nitrogen stream before being re-weighed. The residue was analysed with two different techniques: Firstly, an NA2100 Elemental Analyser (CE Instruments) was used to determine carbon and hydrogen contents. The oxygen content was assumed to form the rest of the 'char' mass.

Table 2-5. Details of the samples heated at different isothermal temperatures for 1 hour under flowing nitrogen containing 10% oxygen.

Sample	Temperature	Flow Rate	Sample Weight		% "char" Formed
			Pre	Post	
	°C	ml/min	g	G	%
Cellulose	Untreated	-	-	-	-
	200	295	1.7323	1.6421	94.8
	300	300	1.6064	0.5902	36.7
	400	303	1.9491	0.2069	10.6
	600	307	1.8309	0.0016	0.1
	800	296	1.7165	0.0000	0.0
	1000	307	1.7279	0.0000	0.0
Alginic Acid	Untreated	-	-	-	-
	200	297	1.9378	1.4108	72.8
	300	300	2.0802	0.6381	30.7
	400	303	1.8339	0.0443	2.4
	600	305	1.8128	0.0253	1.4
	800	295	1.8472	0.0020	0.1
	1000	295	1.9793	0.0000	0.0

The second technique was infra-red spectroscopy, using an Attenuated Total Reflectance (ATR) accessory (Golden Gate single reflection diamond ATR, Specac Ltd). ATR is a technique commonly used as an alternative to analyse solid samples that are difficult to prepare as KBR

discs or in paraffin oil (nujol). It has particular application in studying fibres which would cause scattering in transmittance spectroscopy, and is also commonly used to study surface coatings. The principle of the ATR technique involves using a transparent material in a trapezoidal prism (Figure 2-21a) through which the IR beam is passed through at such an angle the light is totally reflected internally through the prism (Figure 2-21b). In reality there is some loss in the energy due to some of the light passing beyond the prism surface at each reflection point. If a material is pressed firmly to the surface, this part of the beam will carry the IR spectra of the material through the prism with it (Figure 2-21c). The total energy is reduced as it is absorbed by the material, the transmitted energy is then said to be attenuated by the material in contact with the prism surface.

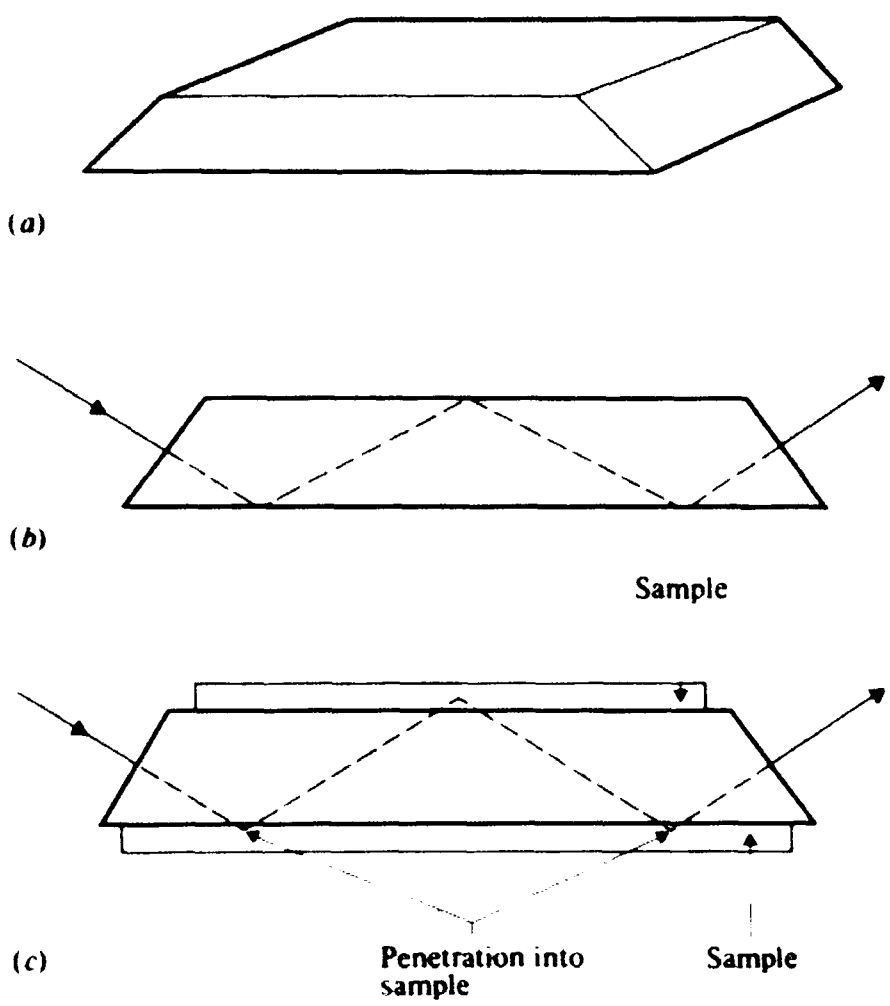

Figure 2-21. Mechanism of attenuated reflection. (a) Prism. (b) Beam path reflected through the prism. (c) Beam passes into surface of sample at the reflection points.

The ATR used in this study was a single reflectance type II diamond prism with an effective transmission range of 5200 – 650cm^{-1}. This has an effective pathlength of 4 microns and an active sampling area of 0.6mm diameter. The char residue samples were placed onto the sampling area and pressed down using the sample compression head using a setting of 70 cNm

on the torque wrench (The torque wrench allows samples to be positioned reproducibly against the optical window of the ATR). A background spectrum was recorded before scanning the sample for the purpose of automatic background subtraction. The sample was scanned from 4000 – 650cm^{-1} with a resolution of 2cm^{-1}. Ten scans were recorded and the averaged to give the final spectrum used in the analysis.

CHAPTER 3 RESULTS

3.1 Thermogravimetric Analysis

The 1st derivatives of the TGA (DTG) data are presented to show the effect of the changing conditions (sample weights, temperature ramp rate or atmosphere) for the three samples, e.g. Figure 3-1. The first derivative of the TGA curve is used as it shows any thermal events more clearly than TG itself. In the case of the three samples, cellulose, alginic acid, and the 50:50 mixture the very initial weight loss (~ 80 – 100°C) is likely to be loss of physically absorbed water. The moisture content of the samples was measured by near infrared (NIR) spectroscopy and the results are shown in Table 3-1. This technique is specific for water.

Table 3-1. Water content of the test samples as measured by NIR spectroscopy.

Sample	Water Content
	%
Cellulose	1.99
Alginic Acid	1.97
50:50 Mixture	2.02

3.1.1 Effect of sample weight

The first set of experiments (Table 2-3; no. 1 – 5) show the effect of changing the sample weight using cellulose as a sample material. In each of the experiments the ramp rate was 30°C/min and the atmosphere used was nitrogen.

Figure 3-1 shows that changing the sample weight has the effect of increasing the two peaks observed at ~80°C and 370°C. This is due to the larger sample mass and hence a larger mass of sample lost on heating. There is little effect on the temperature at which the peaks occur. The temperature of the peaks moves from 75°C to 85°C, and 366°C to 375°C with increasing ramp rate (Figure 3-4). This is likely to be evidence of thermal lag due to increasing mass.

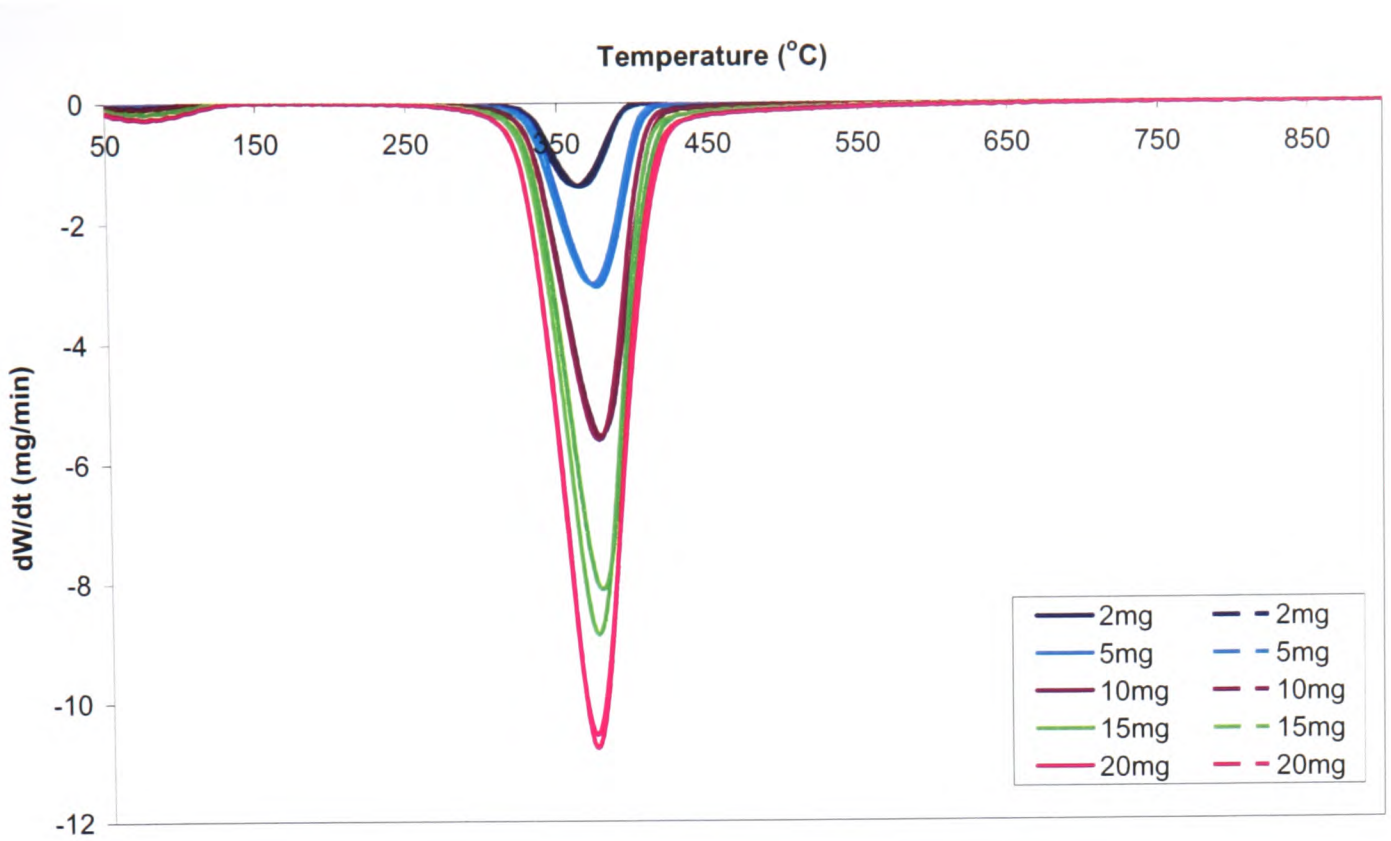

Figure 3-1. DTG data showing the effect of changing sample weight. Cellulose heated at 30°C/min under nitrogen. Two replicates are shown for each sample weight.

Figure 3-1 also shows the good reproducibility of the TGA by comparison of the replicate profiles which are almost perfectly superimposed over each other. The exception being the 15mg sample weight experiments, where some deviation is seen.

Figure 3-2 shows the effect of changing the sample weight on the total weight loss of cellulose under a constant heating rate and constant flow rate. It appears that increasing the sample weight slightly decreases the weight loss (or increases the residual char), although the effect is small. This could be due to temperature gradients through the sample material which in turn may lead to either incomplete pyrolysis in the sample. Alternatively, primary pyrolysis products may be trapped in the sample which could then react to promote the production of char [27, 63].

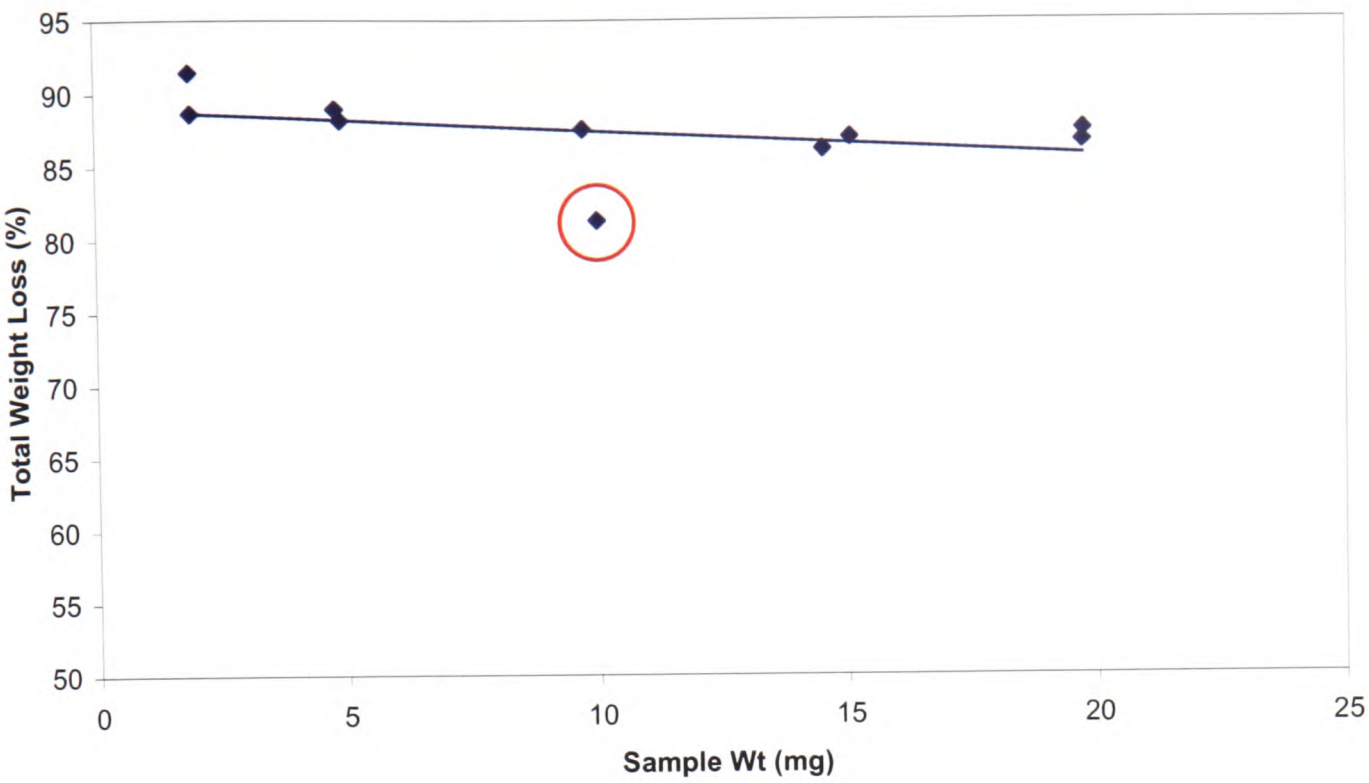

Figure 3-2. The effect of changing sample weight on the total weight loss, calculated from the peak areas of the DTG graphs (Figure 3-1) of cellulose heated at 30°C/min under nitrogen. The red circle indicates an outlier.

3.1.2 Effect of temperature ramp rate

The effect of changing the temperature ramp rate for cellulose under nitrogen is shown in Figure 3-3. There is a shift in the temperature at which the major weight loss effect is observed from 338°C - 399°C (Figure 3-4). There is little effect on the first peak, though there is an artefact visible in the 60°C/min which is due to electrostatic issues in the TGA furnace tube, which can cause the TGA sample pan to stick momentarily to the furnace wall. When the pan is released from the furnace wall, a sudden step change in the weight occurs which will appear as a small sharp peak in the DTG trace. Although the weight change is very small (less than 0.2mg) the effect is exaggerated by the derivative plot.

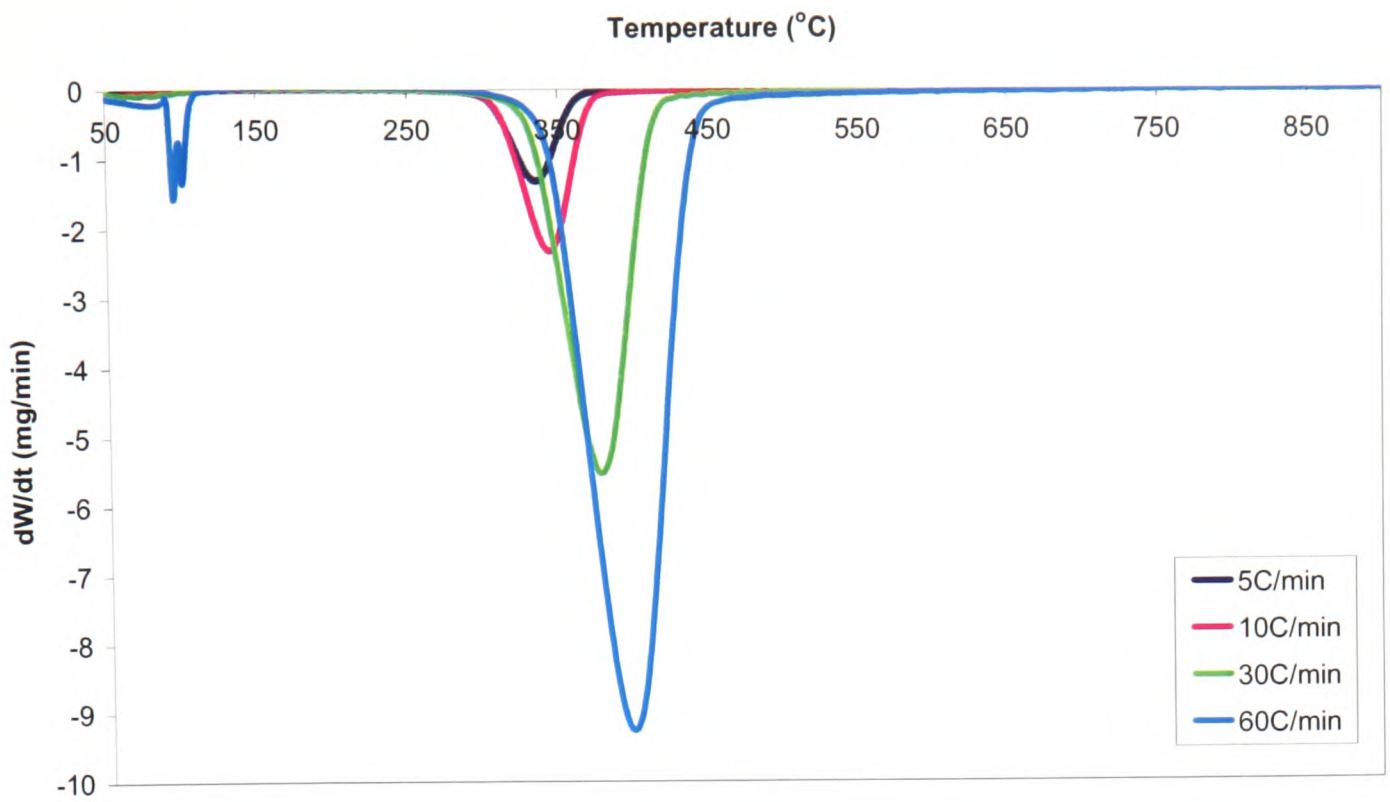

Figure 3-3. DTG data for cellulose under nitrogen showing the effect of changing the ramp rate. Sample weight - 10mg

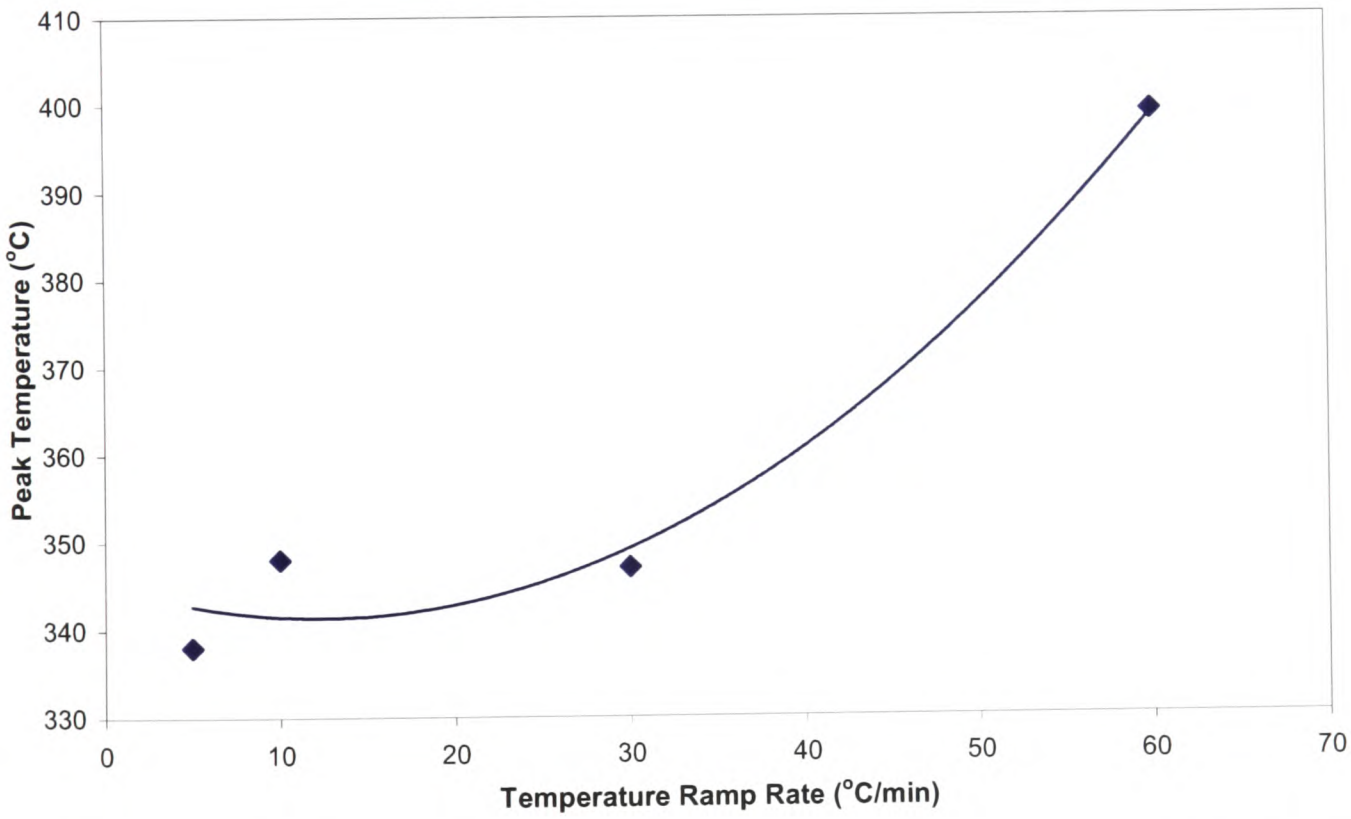

Figure 3-4. Temperature of peak weight loss event for cellulose vs. temperature ramp rate under nitrogen purge gas

This effect of increasing the temperature of the weight loss with increasing temperature ramp is repeated with alginic acid (Figure 3-5). There is almost no effect on the position of the peaks with changing ramp rate under nitrogen (Figure 3-6).

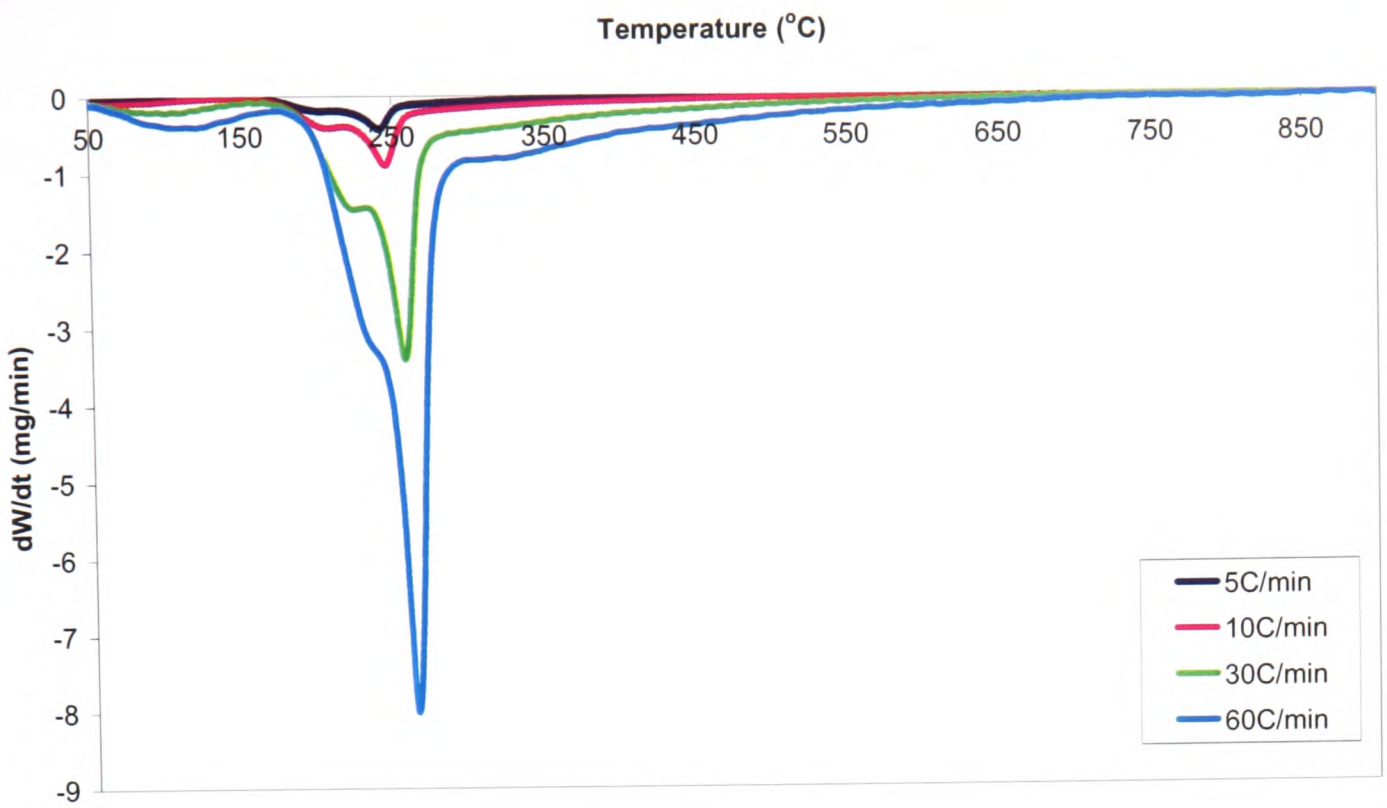

Figure 3-5. DTG data for alginic acid under nitrogen with increasing temperature ramp rates. Sample weight - 10mg

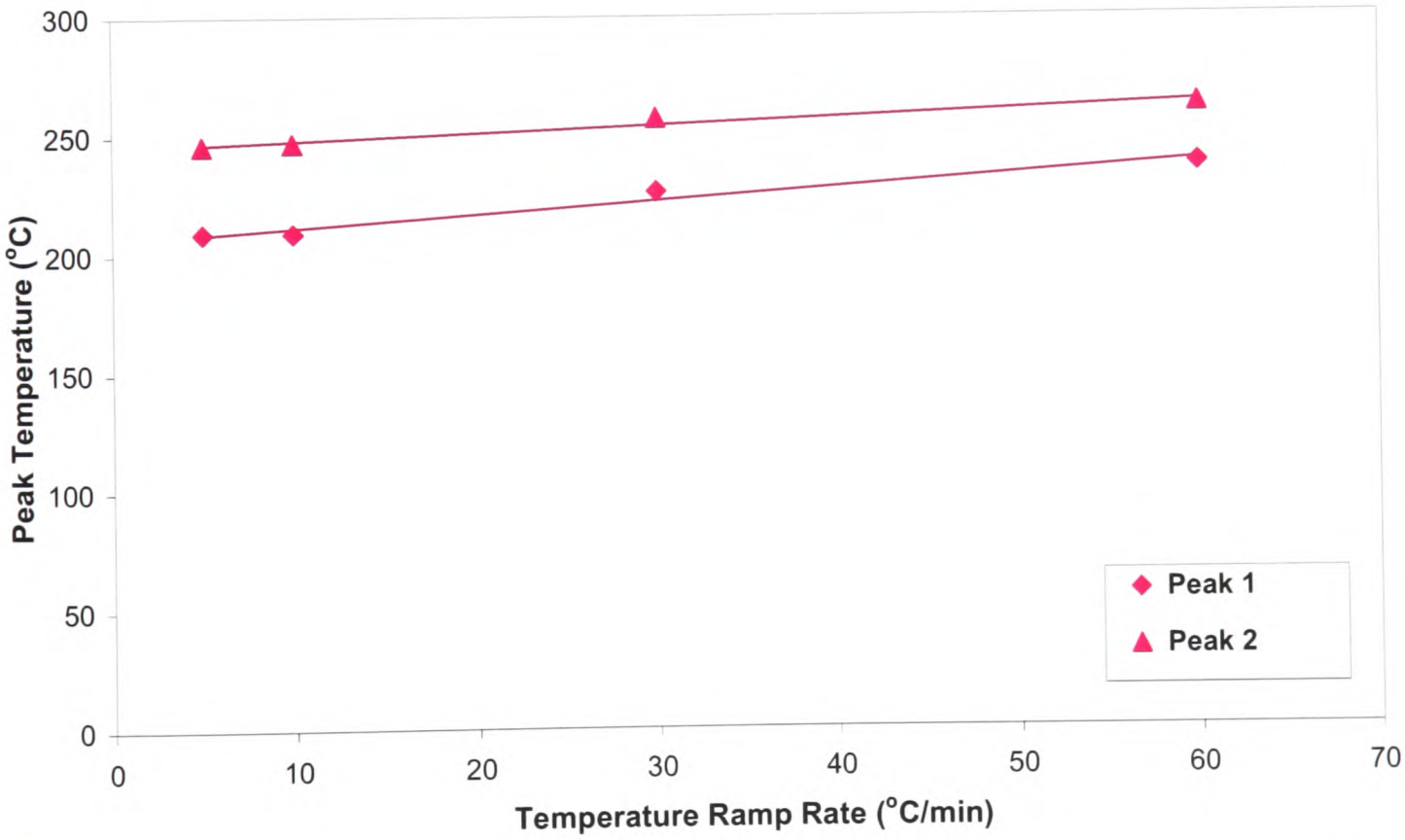

Figure 3-6. Temperature of peak weight loss events for alginic acid vs. temperature ramp rate. Peak 1 is the shoulder, peak 2 the major weight loss peak.

The same effect is also seen for a 50:50 mixture of cellulose and alginic acid (Figure 3-7). The 50:50 mixture under these conditions appears to contain all of the weight loss events observed form cellulose and alginic acid, indicating that there appears to be no interaction between the two samples.

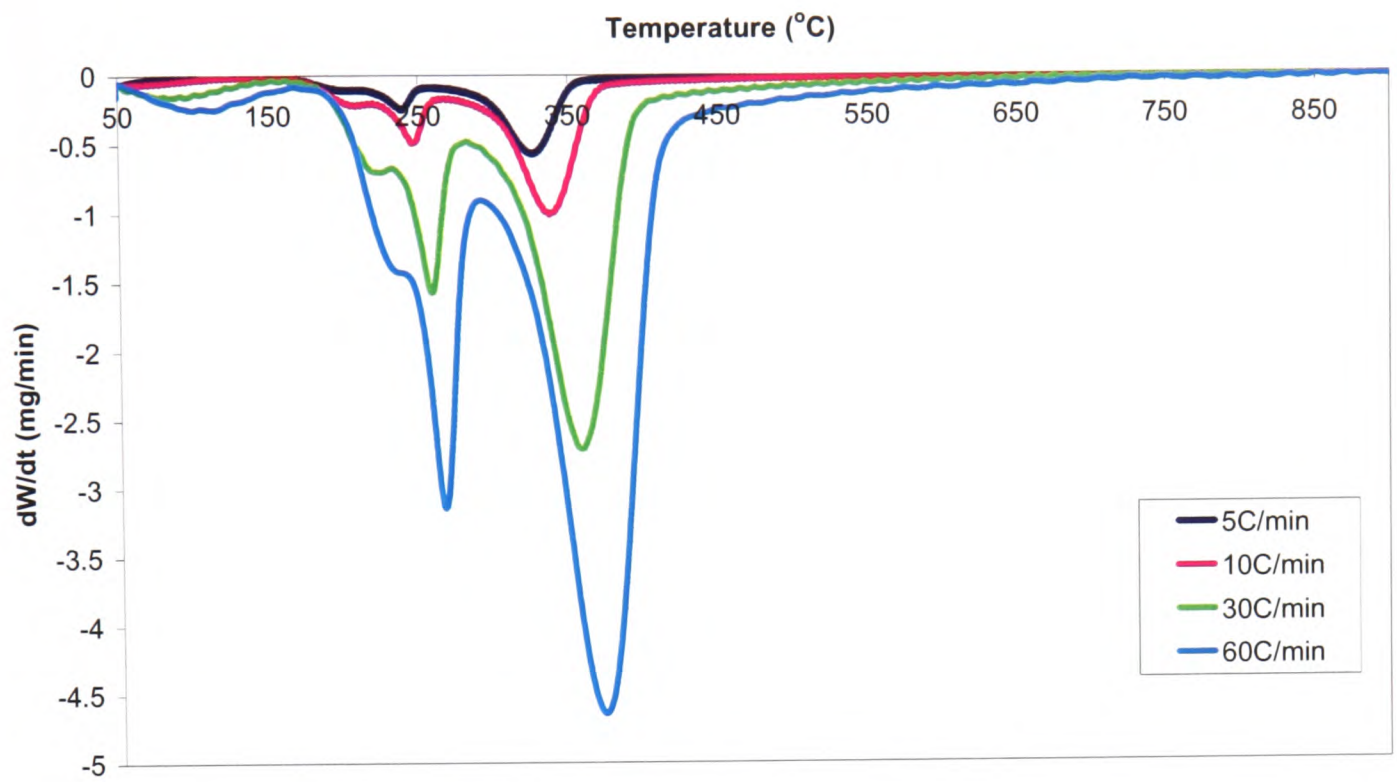

Figure 3-7. DTG data for 50:50 mixture of cellulose:alginic acid under nitrogen with increasing ramp rates. Sample weight -10mg.

The effect of changing the thermal ramp rate is displayed for each of the samples with a purge gas of 10% oxygen in nitrogen. Figure 3-8 shows the TGA data for cellulose with the oxidising atmosphere.

The same trend is seen as the nitrogen atmosphere samples (Figure 3-3) with the gradual increase in the temperature of the peaks at which the weight loss occurs with increasing ramp rate (Figure 3-9). With the change in atmosphere a higher temperature weight loss is observed at ~600°C. This is likely to be high temperature decomposition of the residual solid, most likely due to an oxidative process.

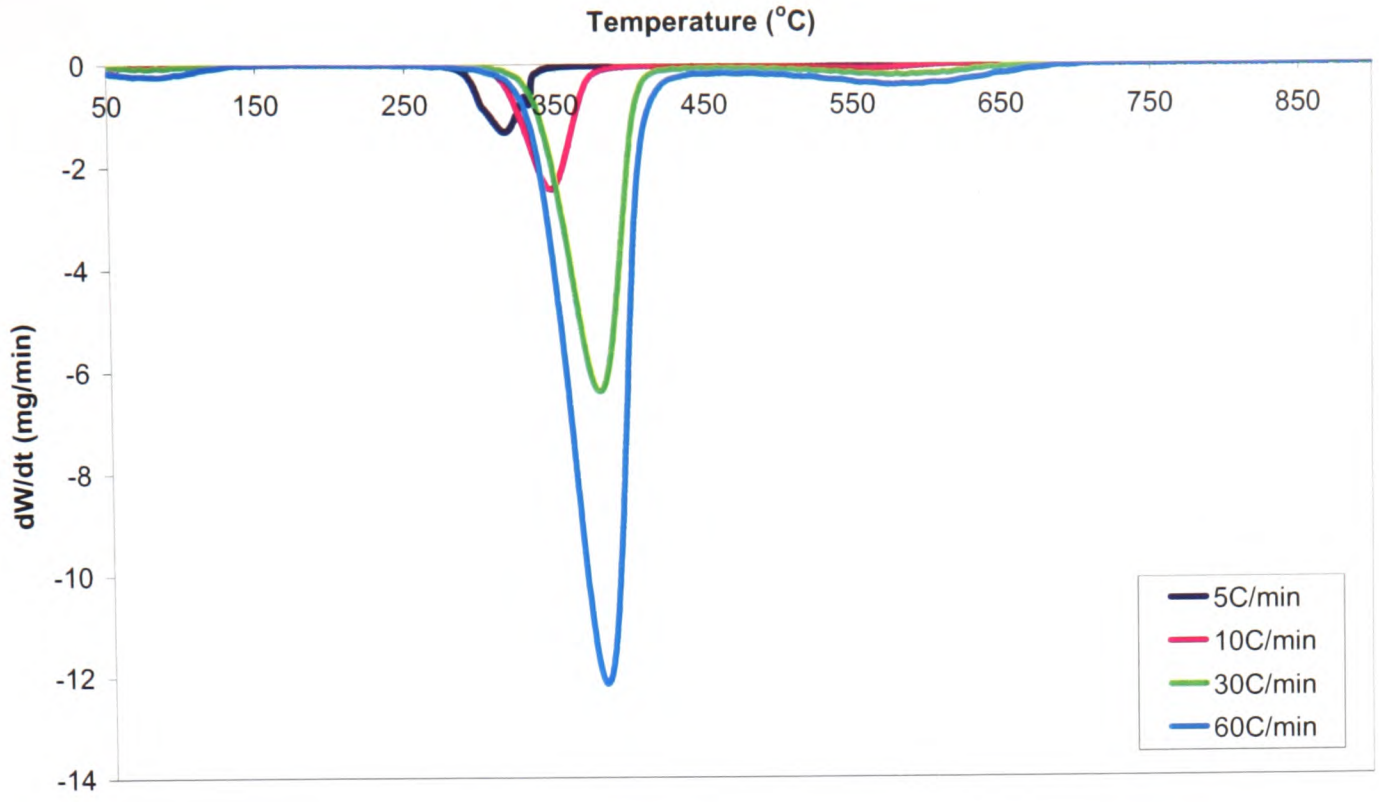

Figure 3-8. DTG data for cellulose under 10% oxygen in nitrogen, showing the effect of changing the ramp rate. Sample weight 10mg.

Figure 3-10 shows the alginic acid under the same conditions. Again similar effects are seen as in the experiments with nitrogen purge gas (Figure 3-5), increasing peak temperature of weight loss events with increasing ramp rate. As is the case with the cellulose samples there is the appearance of a higher temperature weight loss event. There is also the suggestion of another distinct weight loss event at ~340°C, though this only clearly visible at the 60°C/min ramp rate. Figure 3-11 shows the peak positions plotted against the ramp rate. Similarly to the non-oxidising case (Figure 3-6) there is little effect for the lower temperature peaks but for the additional high temperature peak the change in temperature is a little more pronounced.

The 50:50 mixture sample (Figure 3-12) shows the same trend as the nitrogen purge gas experiments (Figure 3-7). Unlike the nitrogen purge case experiments, the addition of 10% oxygen in nitrogen the higher temperature peak seen in cellulose is not observed in the mixture. This may be due to the weight loss being relatively small compared to the higher temperature peak observed in the alginic acid.

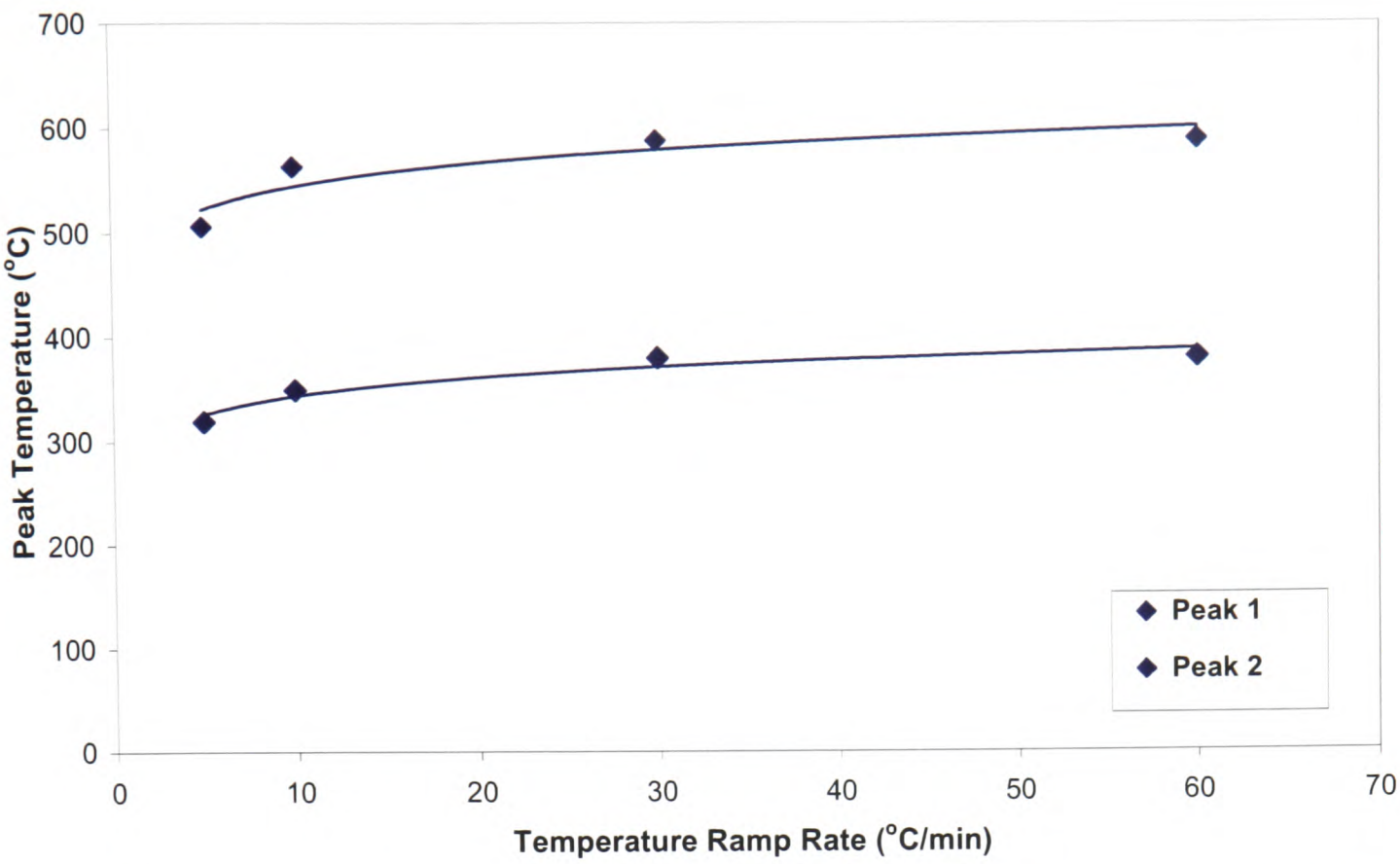

Figure 3-9. Temperature of peak weight loss events for cellulose vs. temperature ramp rate under 10% oxygen in nitrogen purge gas.

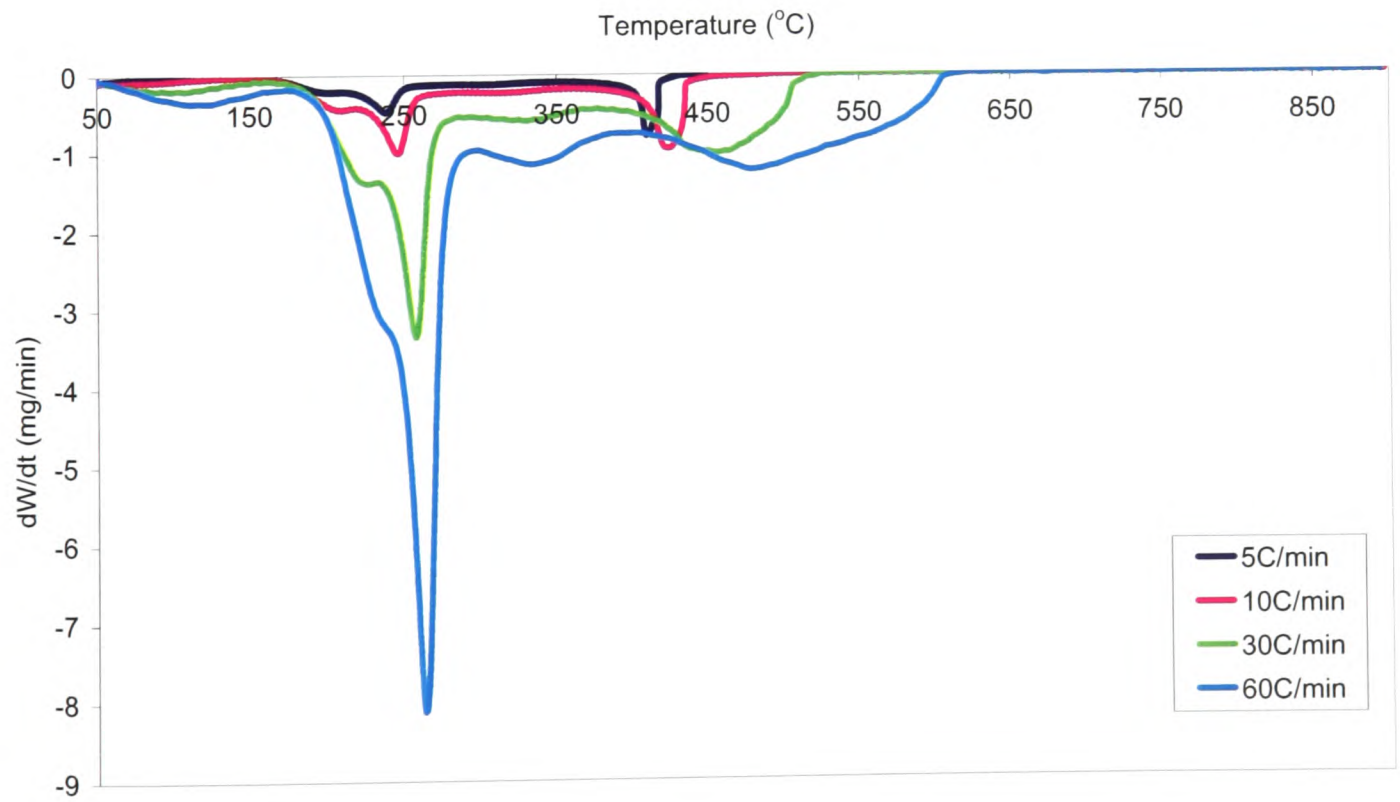

Figure 3-10. DTG data for alginic acid under 10% oxygen in nitrogen, showing the effect of changing the ramp rate.

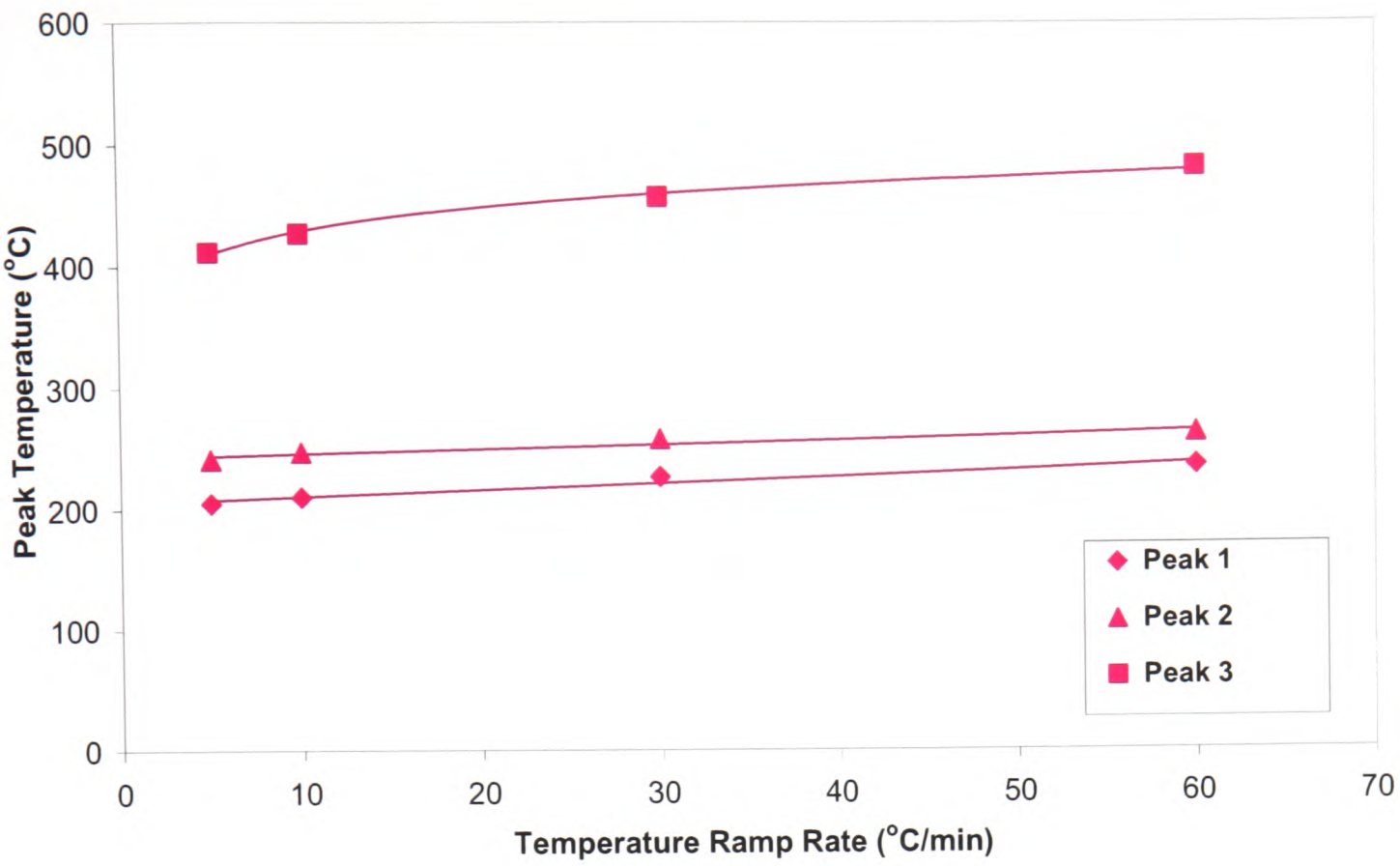

Figure 3-11. Temperature of peak weight loss events for alginic acid vs. temperature ramp rate.

The effect of the ramp rate on the total weight loss for the three samples is shown in Figure 3-13. This is more complex than the effect of increasing sample mass (Figure 3-2), as the 5°C/min ramp rate seems to be different to the other ramp rates. In the case of alginic acid the effect is quite pronounced, but in cellulose the effect is much less well defined. As is the case in much of this study the 50:50 mixture displays an effect that is somewhere between the two materials.

Under an oxidising atmosphere the temperature ramp rate has little effect on the total weight loss from the sample materials. This shows that the ramp rate does have some effect, particularly under non-oxidising conditions. Although thermal lag is an issue with increasing ramp rate [28, 67] it does not seem to have a great effect on the total weight loss from the sample materials. However, between 5°C/min and 10°C/min there is a marked decrease in total weight loss for alginic acid, under non-oxidising conditions, which may be an indication of temperature gradients in the sample, causing the production of more residual char [27, 63] as described previously in section 3.1.1.

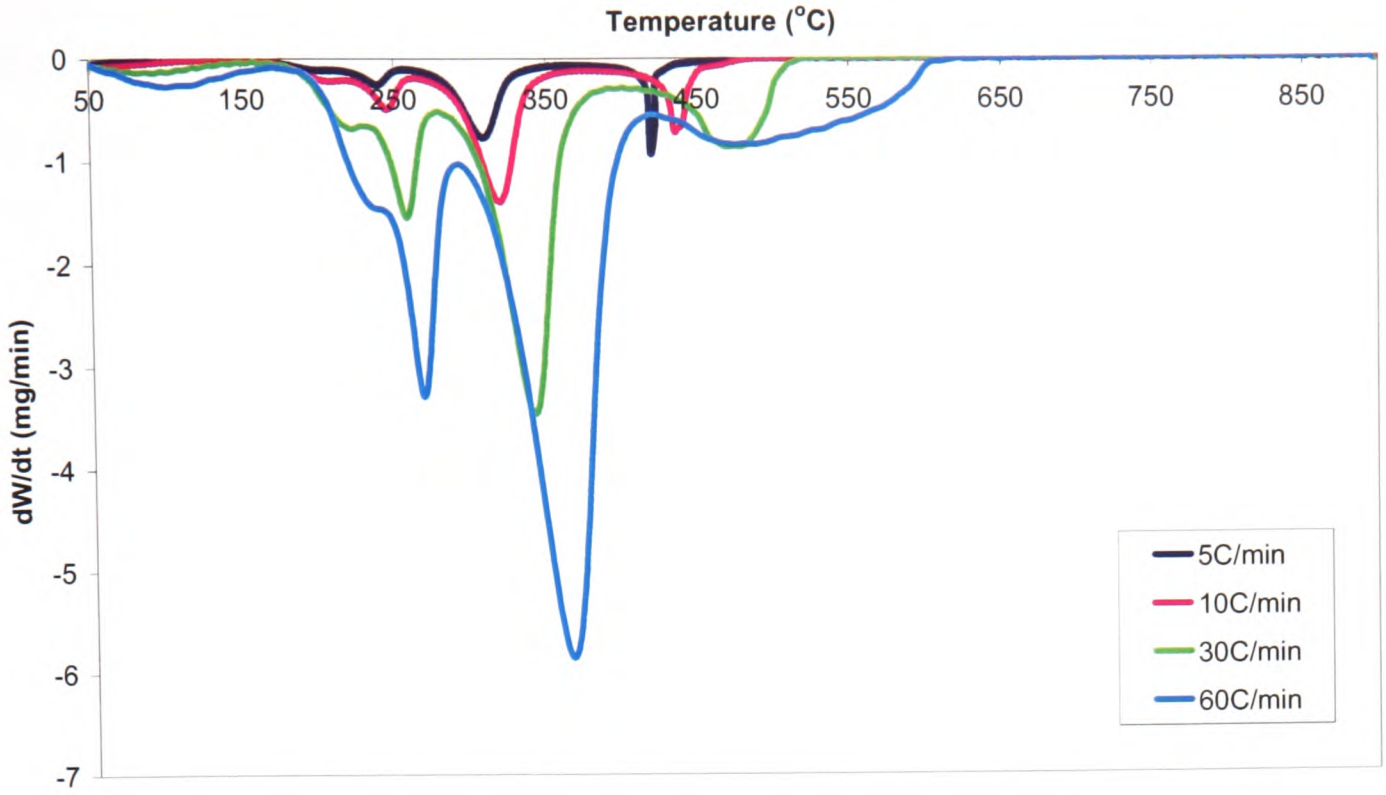

Figure 3-12. DTG data for 50:50 cellulose:alginic acid under 10% oxygen in nitrogen, showing the effect of changing the temperature ramp rate.

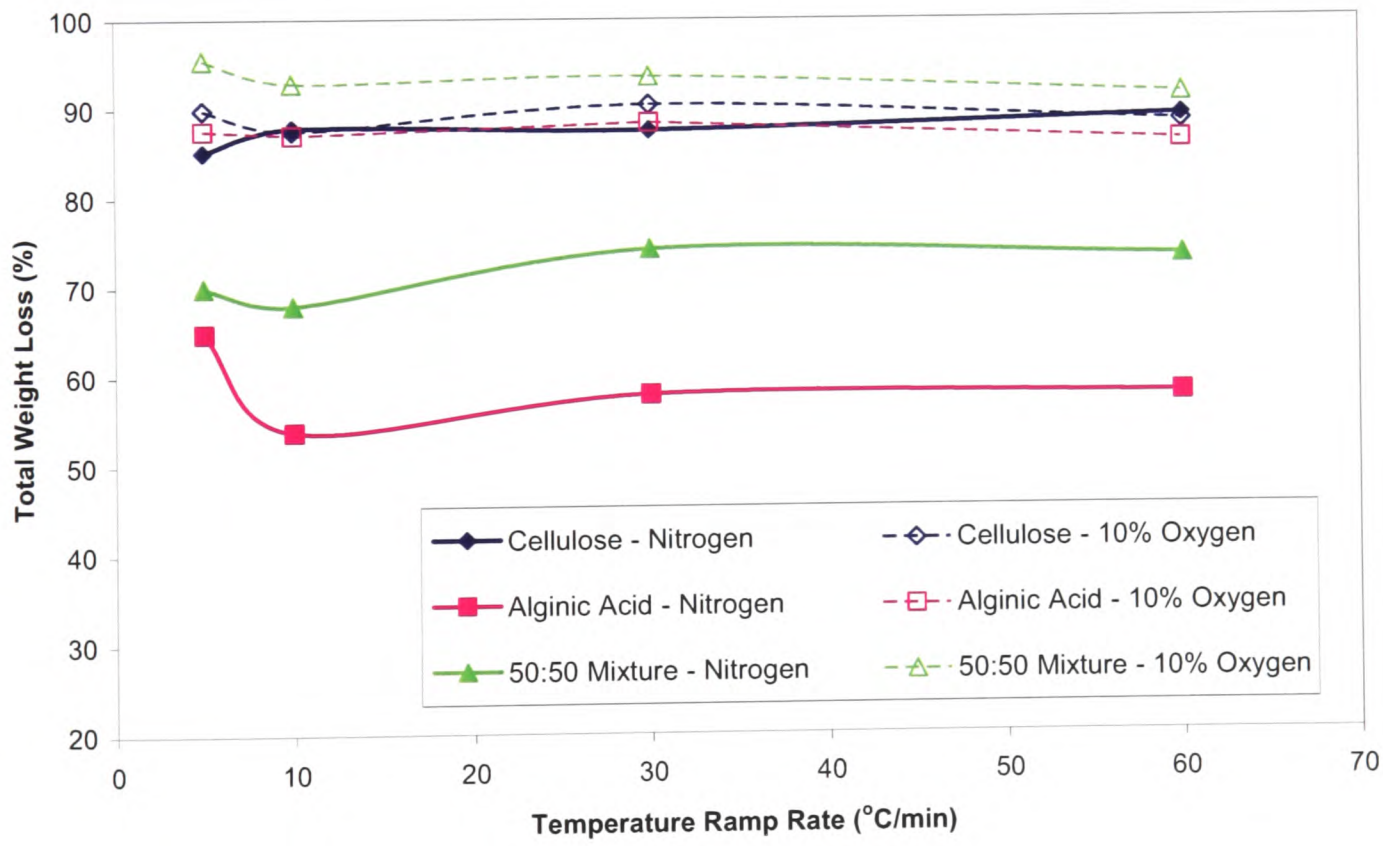

Figure 3-13. The effect of changing temperature ramp rate and atmosphere on the total weight loss from the three samples on heating. Sample weight is constant.

3.1.3 Effect of TGA furnace purge gas

The effect of changing the purge gas from a non-oxidising (nitrogen) to oxidising (10% oxygen in nitrogen) atmosphere is shown for cellulose in Figure 3-14. This shows clearly the additional high temperature peak (~590°C) in the oxidising conditions. Only one temperature ramp rate (30°C/min) is shown for purposes of clarity but the additional high temperature peak is seen at all ramp rates tested. The weight loss peak is also observed at about 10°C lower in temperature compared to the nitrogen experiments. The magnitude of the weight loss in the first event is about 90% of the sample mass in both oxidising and non-oxidising conditions (Figure 3-15). The initial weight loss for adsorbed moisture is around 2% which agrees with the water content of samples as measured by NIR (Table 3-1).

These observations are consistent with literature which also noted that the initial weight losses for the first event accounted for 89% of the mass under both oxidising and non-oxidising conditions [54].

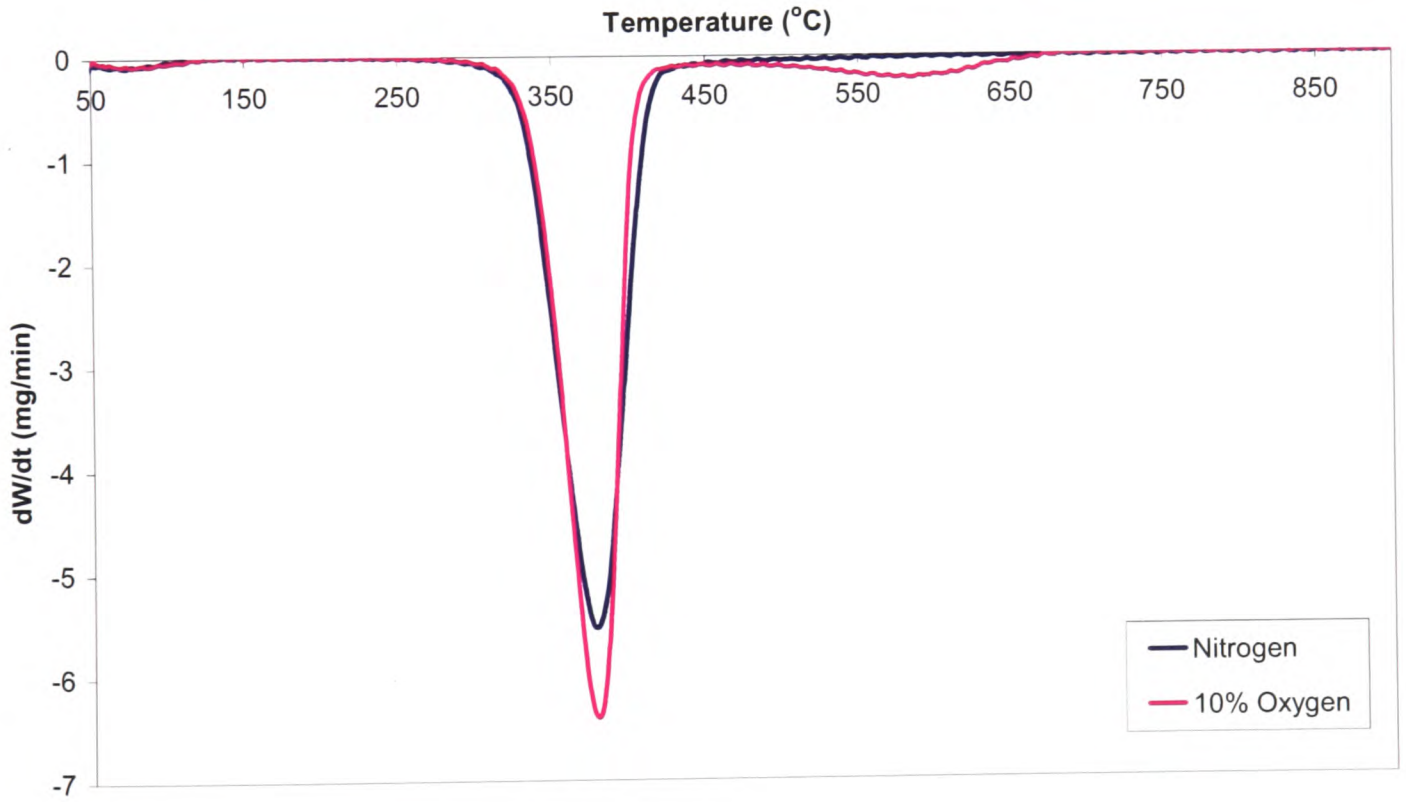

Figure 3-14. DTG data showing the effect changing atmosphere on cellulose with a temperature ramp rate of 30°C/min.

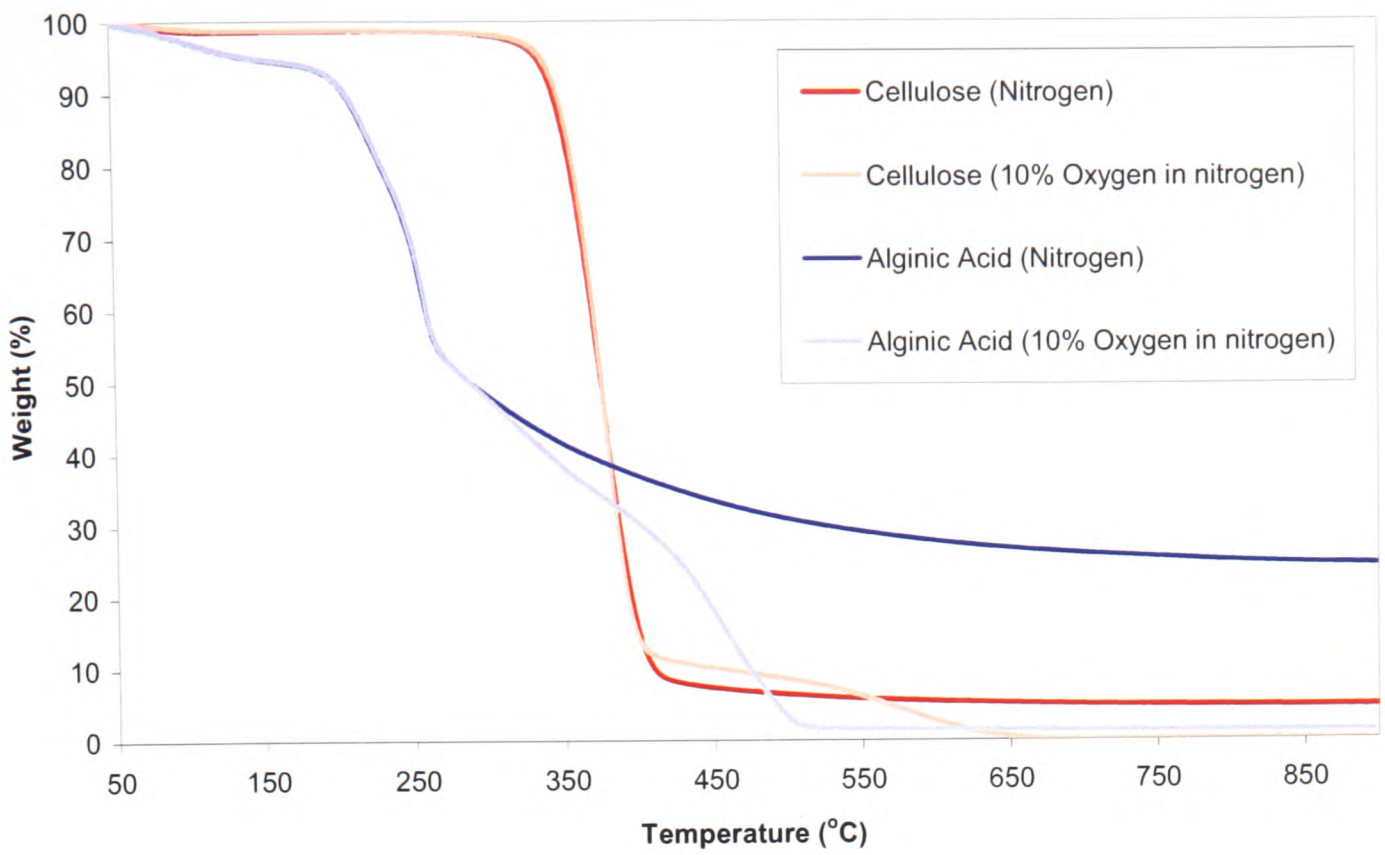

Figure 3-15. Comparison of % weight loss (TGA) for cellulose and alginic acid under oxidising and non-oxidising conditions with a temperature ramp rate of 30°C/min.

A high temperature peak (~450°C) is also seen with alginic acid (Figure 3-16). In the case of the alginic acid this higher temperature peak appears to be affected by the change in ramp rate (Figure 3-10). The peak becomes broader with increasing temperature and also the peak moves from ~410°C to ~480°C with increasing ramp rate. Additionally to this there is a peak at ~330°C visible which is additional to the non-oxidising condition. However, the peak is not visible in the mixture sample (Figure 3-17) due to the presence of the large peak at ~340°C most likely due to the cellulose in the mixture.

Similarly to cellulose the magnitude of the initial peaks of alginic acid weight loss are not affected by the presence of oxygen (Figure 3-15). It may be assumed that oxygen does not play a significant part in the initial thermal decomposition stages of alginic acid.

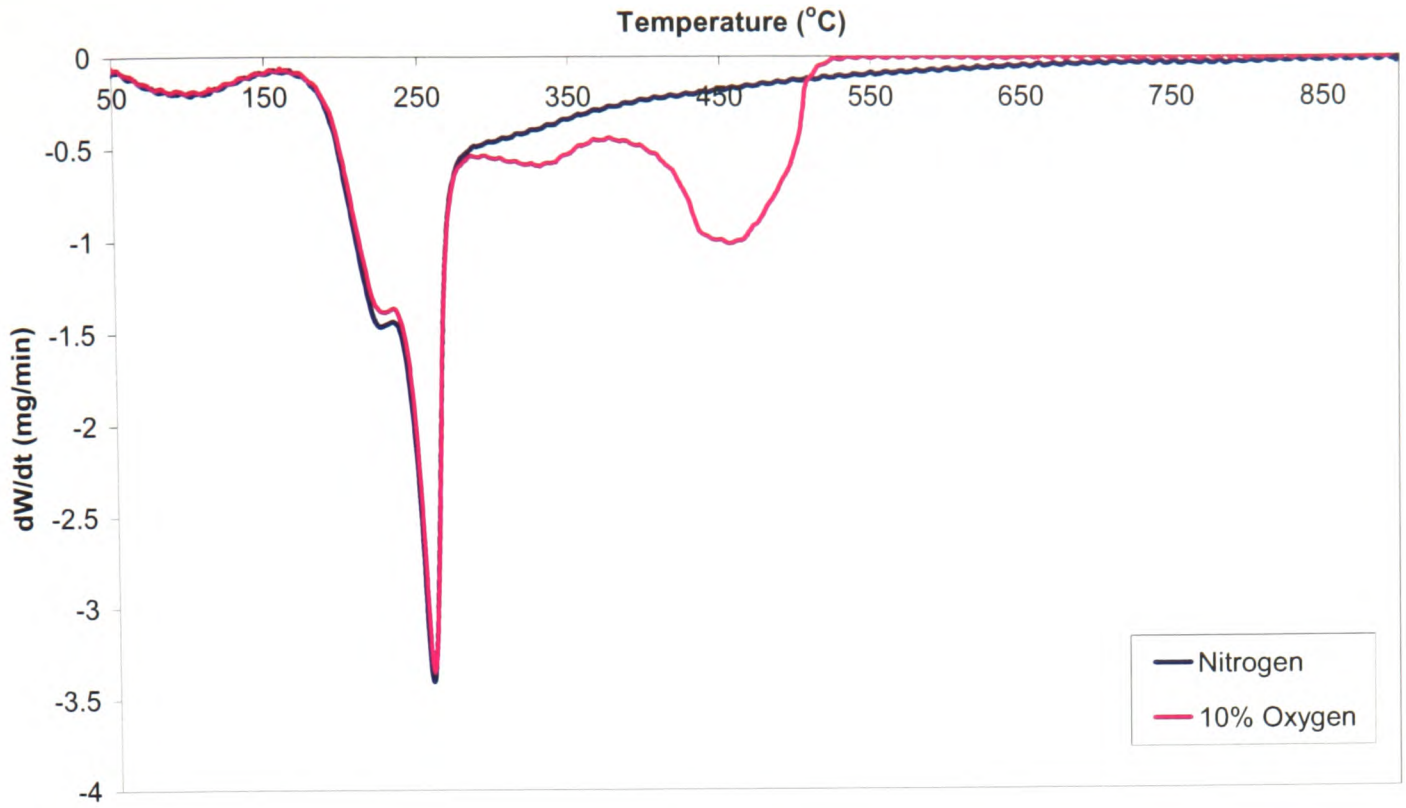

Figure 3-16. DTG data showing the effect changing atmosphere on alginic acid at a ramp rate of 30°C/min.

With the 50:50 mixture of cellulose and alginic acid in the oxidising conditions it is seen that the peak attributable to the cellulose in the mixture occurs at slightly lower temperature than the non-oxidising condition (Figure 3-17). However, this is not seen in the pure cellulose sample (Figure 3-14).

The 50:50 mixture samples under oxidising conditions (Figure 3-12) show this same temperature rate effect as seen in alginic acid (Figure 3-10).

Figure 3-18 shows the three sample materials heated at 30°C/min under a nitrogen atmosphere. Under these conditions is can be seen that there appears to be no interaction between the cellulose and alginic acid, as the features of both materials is seen in the 50:50 mixture.

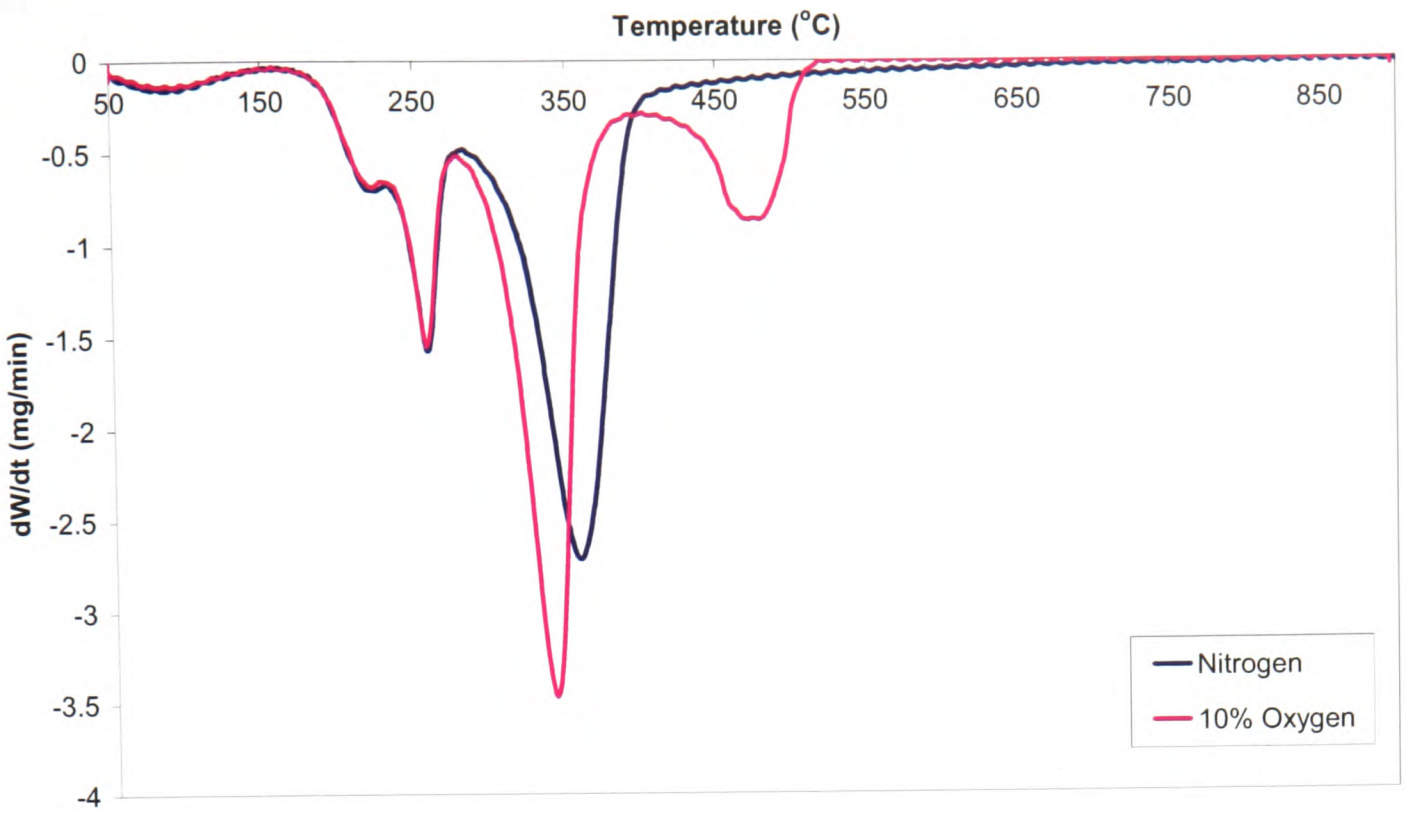

Figure 3-17. DTG data showing the effect changing atmosphere on 50:50 cellulose:alginic acid at a temperature ramp rate of 30°C/min.

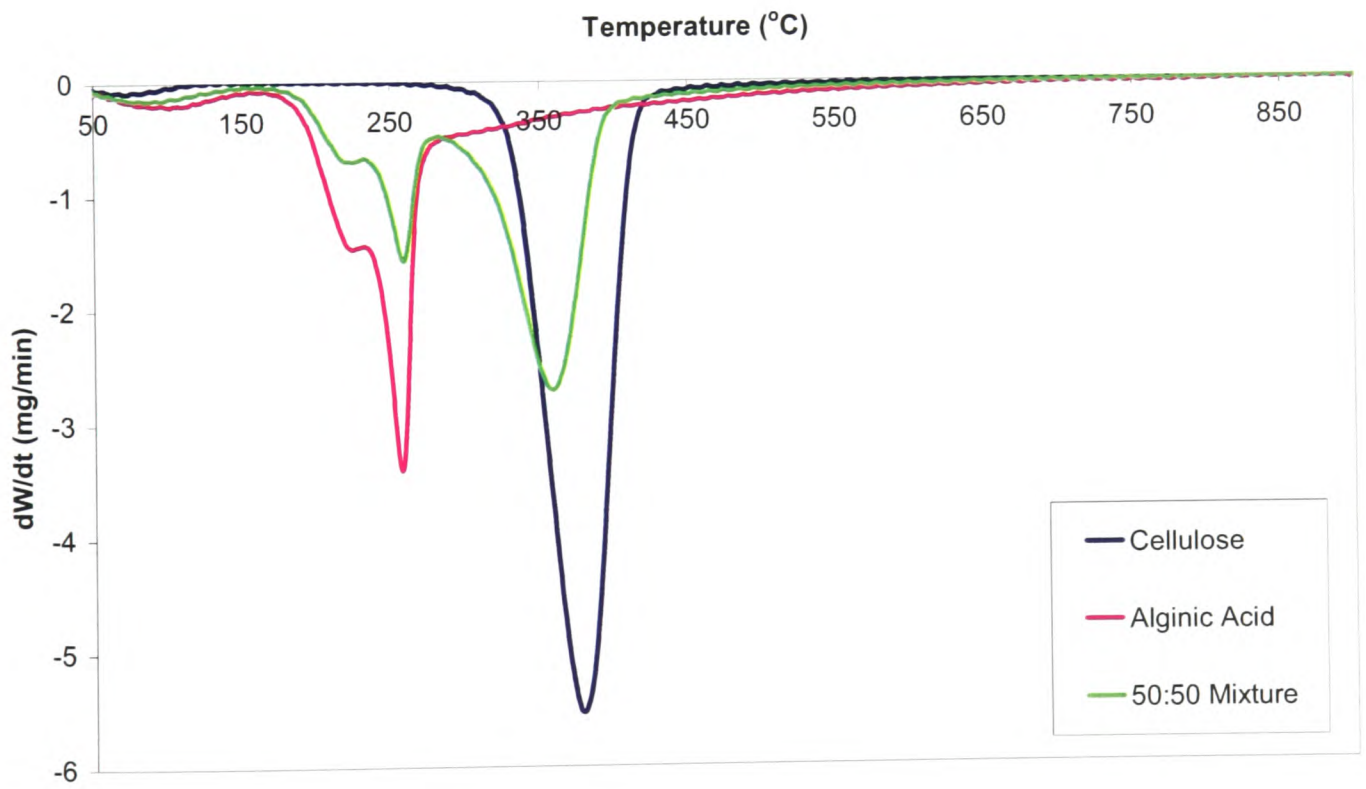

Figure 3-18. Comparison of the three samples, cellulose, alginic acid and 50:50 mixture in nitrogen with a ramp rate of 30°C/min.

At 30°C/min ramp rate under oxidising conditions (Figure 3-19) the additional high temperature weight loss event is not visible for cellulose (~600°C) in the mixture. This may be due to it

being a small curve in pure cellulose so in a 50:50 mixture it may not be visible as there is less cellulose in the sample.

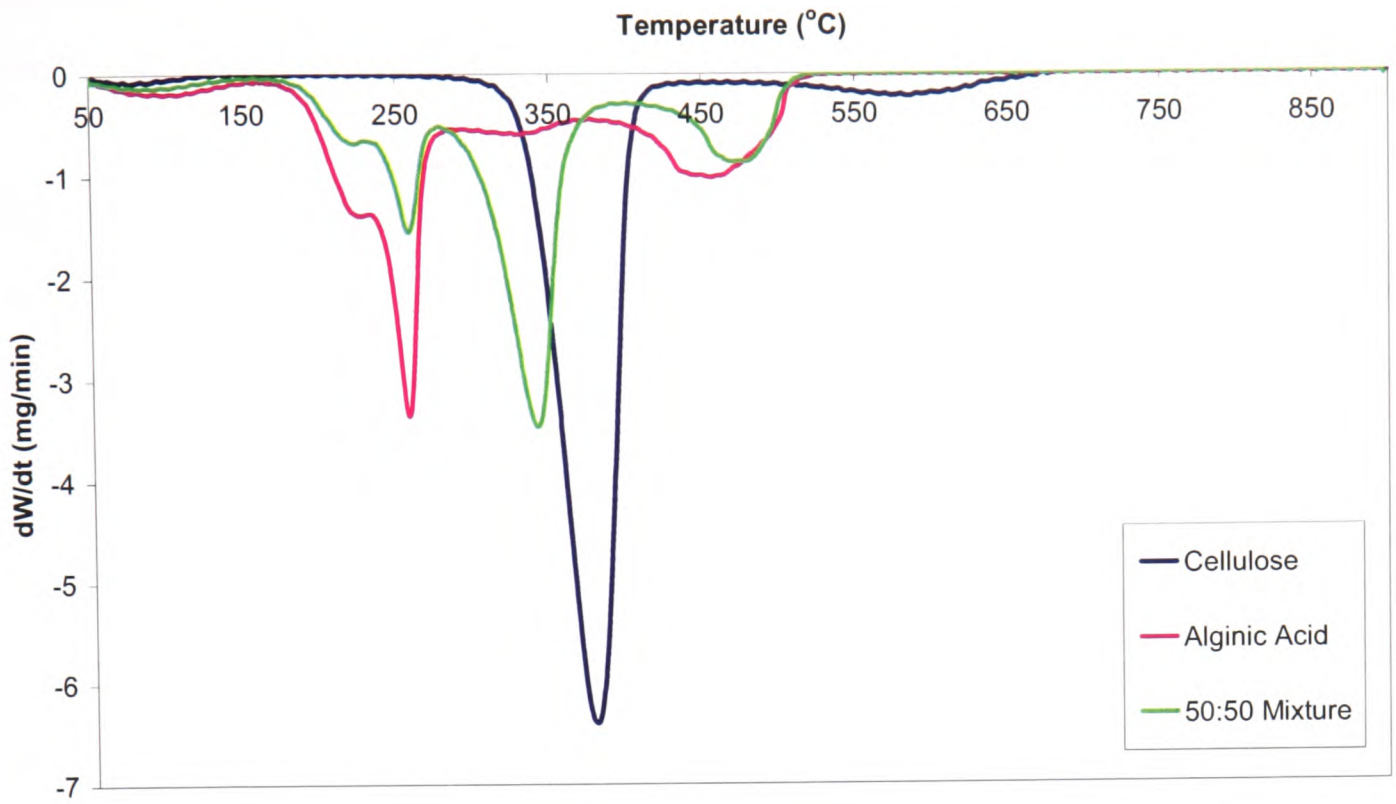

Figure 3-19. Comparison of the three samples, cellulose, alginic acid and 50:50 mixture in 10% 0xygen in nitrogen with a temperature ramp rate of 30°C/min.

3.1.4 Summary of TGA data

The TGA data shows that the two sample materials decompose differently under the same conditions – cellulose mainly in a single step (between 330°C and 390°C in this study) and alginic acid with two steps (200 – 240°C and 250 – 260°C). The values for cellulose are in good agreement with literature values [19, 38]. The 50:50 mixture of the two samples show a combination of weight loss events of the two samples. In the mixture the weight loss associated with the cellulose is at a slightly lower temperature range (330°C to 370°C). There are no additional peaks observed in the 50:50 mixture samples in non-oxidising conditions.

In both cases under oxidising conditions an additional high temperature peak is observed – at about 590°C for cellulose and between 410°C and 480°C for alginic acid. This is likely to be due to oxidation of the residual material as this is not seen in the non-oxidising conditions [54]. This additional higher temperature peak is also observed in the 50:50 mixture, but at lower temperature than the individual compounds. For cellulose the major weight loss peak occurs at slightly lower temperatures (320 – 380°C) but the alginic acid weight loss events occur at the

same temperature as the non-oxidising conditions. This may indicate that oxygen has no influence on the pyrolysis behaviour of the alginic acid. In both cellulose and alginic acid the magnitude of the weight loss in the early stages of thermal decomposition appears to be unaffected by the addition of 10% oxygen to the purge gas.

3.2 Multivariate Analysis of the Spectral Data

The TGA-FTIR system was calibrated with 32 compounds in the reference library of InSight™ (Table 3-2). However, not all of the calibrated compounds have been observed in the spectra from the experiments. Some are observed under only one atmosphere or from only one of the compounds but not both. The total numbers of compounds that are observed are also dependent upon the correlation level set in the software. This allows automatic rejection of qualitative matches below a pre-determined point. Any compounds found to have a correlation level below the threshold are likely to contain artefacts caused by the mathematical treatment. There are a large number of the compounds measurable in the evolved gases, so for brevity not all of the identified compounds are covered in the same detail. Only six compounds (carbon monoxide [Target Reference No. 3], carbon dioxide [Target Ref. 4], water vapour [Target Ref. 13], acetaldehyde [Target Ref. 15], acrolein (2-propenal) [Target Ref. 14], and acetic acid [Target Ref.17]) of the 32 references are examined in detail.

In order to make the data presentation manageable the FTIR data are divided into two groups –

- An overview of the qualitative identification of gas phase compounds is presented.
- Further detail of the quantitative analysis for six of the compounds chosen from the calibrated compounds for more in depth discussion.

Table 3-2. List of compounds calibrated in the InSight™ software showing the database reference number and the wavenumber window used for qualitative matching.

Reference. No.	Compound Name	Wavenumber Range (cm^{-1})	
		Upper Limit	Lower Limit
1	Acetylene	3370	3200
2	Ammonia	1100	800
3	CO	2200	2100
4	CO2	2410	2250
5	Ethane	3300	2800
6	Ethylene	3300	2800
7	Formaldehyde	1850	1650
8	Methane	3300	2800
9	Nitrous Oxide	3550	3480
10	NO	1950	1750
11	Propylene Oxide	1000	850
12	Ethylene Oxide	1000	850
13	Water Vapour	3550	3400
14	Acrolein (2-Propenal)	1850	1650
15	Acetaldehyde	1850	1300
16	1,3-butadiene	1000	800
17	Acetic Acid	1850	1650
18	Formic Acid	1850	1700
19	Propionic Acid	1200	750
20	Methanol	1150	900
21	Ethanol	1150	900
22	n-Propanol	1150	910
23	Acetone	1400	1150
24	3 Methyl-2-Cyclopenten-1-one	1500	1100
25	2,5-Dimethylfuran	950	750
26	Furfural	1050	750
27	2-Furanmethanol	1050	750
28	2-Butanone	1500	1200
29	2,3-Dihydrofuran	1200	800
30	Furan	1050	750
31	Levoglucosan	1000	800
32	Glyceraldehyde Dimer	1550	1250

3.2.1 Qualitative identification of compounds

The first stage of the InSight™ analysis is to qualitatively identify any of the compounds in the reference library. This was performed using a configured analysis mode that allows the software to scan each experiment for each of the 32 compounds in turn and display the match statistics. The configured mode may have a correlation coefficient limit set for each compound, such that compounds with a value less than this limit will not be displayed by the software. This gives a basic overview of the compounds that may be present in the gas mixture. This analysis can be described graphically as shown in Figure 3-20. This correlation map gives a quick indication of the compounds present in the gas phase with a correlation of 0.6 or better with the reference database. All values below 0.6 have been left black for the purposes of clarity. The left hand axis shows the sample type atmosphere and ramp rate abbreviated. For example, A-N-5 refers to alginic acid heated at 5°C/min under a nitrogen atmosphere. The column on the right is a key for the correlation level. The correlation map shows that a large number of the reference compounds can be observed in the FTIR analysis of the evolved gases from the samples.

In each of the data sets, it is clear that more compounds are identified at the higher temperature ramp rates. This is more visible in correlation maps with a higher correlation selected (Figure 3-21) and may be explained by the rate of release of the compound. At higher ramp rates the temperature at which a compound is evolved will be reached and exceeded more rapidly, meaning that an evolved species will be released during a shorter time period. Therefore, from a similar sample mass the total amount of evolved species should be similar, and if the compound is evolved in a shorter time period the time-resolved concentration will be higher. This means that some compounds that are evolved in small amounts may not be observed under a slower ramp rate as they may be below a limit of detection for the system.

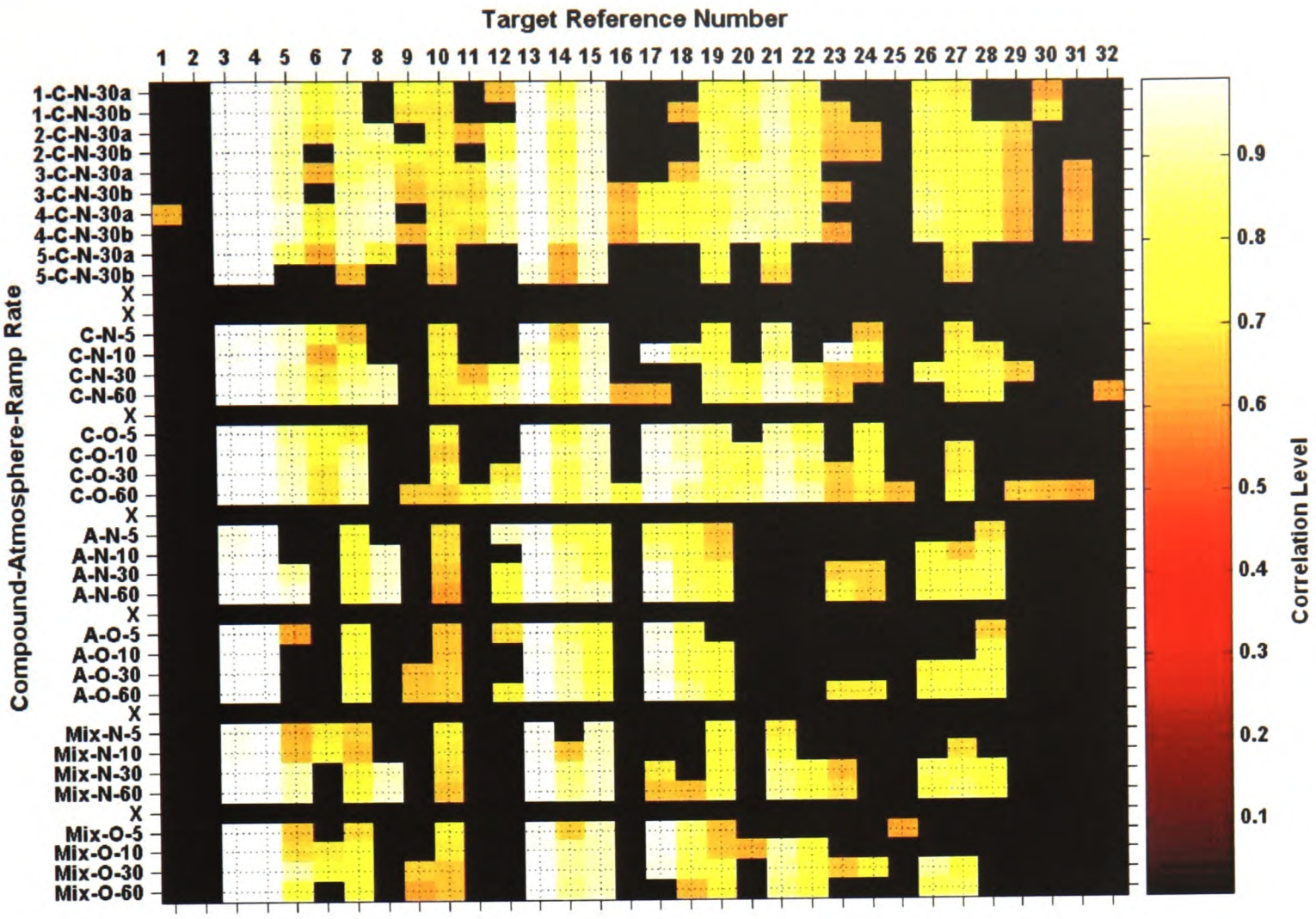

Figure 3-20. Correlation map for the TGA-FTIR experiments showing the correlation value for all compounds in the reference data set with a correlation ≥ 0.60.

It can be seen that there are similar compounds observed for both the cellulose and alginic acid samples. CO [Target Ref. 3], CO_2 [Target Ref. 4], water vapour [Target Ref. 13] are seen in all of the experiments as may be expected. There are also a number of the other compounds that are common to both samples, and no additional compounds observed in the 50:50 mixture experiments which may indicate that no interaction is occurring. By adjusting the cut-off level for correlation to 0.8 there is more confidence in the qualitative matches identified by the software (Figure 3-21).

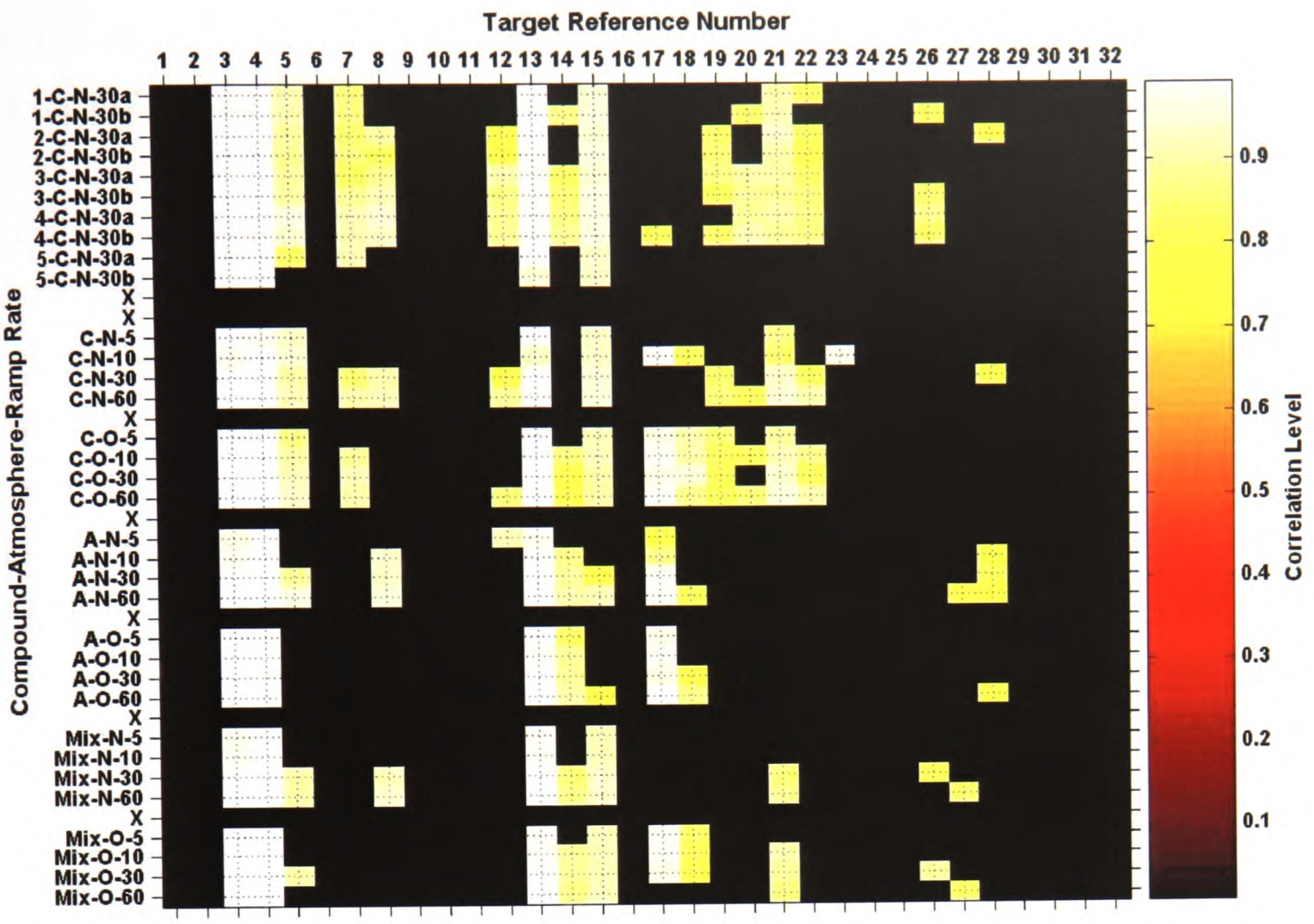

Figure 3-21. Correlation map for the TGA-FTIR experiments showing the R value for all compounds in the reference data set with a correlation ≥ 0.80.

It is clear from the first phase of experiments (1-C-N-30a through 5-C-N-30b) that the effect of changing the weight has the effect of changing the number of qualitative matches observed. Experiments 1 and 5 are the lowest sample weights (5mg and 2mg respectively) and consequently show the lowest number of compound matches. There is little difference between experiments 3 and 4 (15mg and 20mg) but the amount of CO_2 evolved tends to overload the FTIR detector. Another concern with the high sample weight is the potential for thermal lag. Therefore 10mg sample mass was used in the remainder of the experiments.

Generally, there are fewer compounds that are positively matched at this level (correlation coefficient ≥0.80) in comparison to Figure 3-20, but it is still possible to see water, CO, CO_2, acetaldehyde [Target Ref. 15], acetic acid [Target Ref. 17] and formic acid [Target Ref. 18] for both compounds in both atmospheres. A number of compounds are only seen in the cellulose experiments – formaldehyde [Target Ref. 7], propionic acid [Target Ref. 19], methanol [Target

Ref. 20], ethanol [Target Ref. 21], n-propanol [Target Ref. 22] and acetone [Target Ref. 23], although the latter is only seen in under nitrogen. Methane (both cellulose and alginic acid) [Target Ref. 8], furfural (cellulose only) [Target Ref. 26] and 2-furanmethanol (alginic acid only) [Target Ref. 27] are only seen under nitrogen atmosphere.

In the 50:50 mixtures there are no additional compounds observed. However, a number of compounds are not observed in the mixture that are seen in the individual compounds (formaldehyde, ethylene oxide, propionic acid, methanol, n-propanol and 2-butanone). Four of these (formaldehyde, propionic acid, methanol and n-propanol) are only observed in one of the compounds. It may be that they are actually evolved, but with a lower initial sample mass (effectively 5mg), the evolved compounds are below the limit of detection for the instrument. Formic and acetic acids are only observed in the oxidising atmosphere for the 50:50 mixture samples, despite the fact that they are observed in the nitrogen atmosphere experiments for both compounds.

3.2.2 Quantitative analysis of selected compounds

Six of the calibrated reference compounds (carbon monoxide, carbon dioxide, water vapour, acetaldehyde, acrolein, and acetic acid) were selected for further assessment of the quantitative evolution profiles measured by FTIR. These six compounds were chosen because CO, CO_2 and water vapour are major pyrolysis products, and acetaldehyde, acetic acid and acrolein are different classes of small organic molecules that are relevant to fire toxicity. It is prudent at this point to visually check the qualitative matches to be sure that the mathematical correlation is a true indication of the presence of the compound. Where necessary after this visual assessment of matching, a manual check of the data is made to verify the match and evolution profile.

Figure 3-22 shows the IR spectra of the six compounds that are examined quantitatively. The individual graphs also are marked with a box that indicates the wavenumber window that was used in the InSight™ software to qualitatively identify the compounds prior to the quantification.

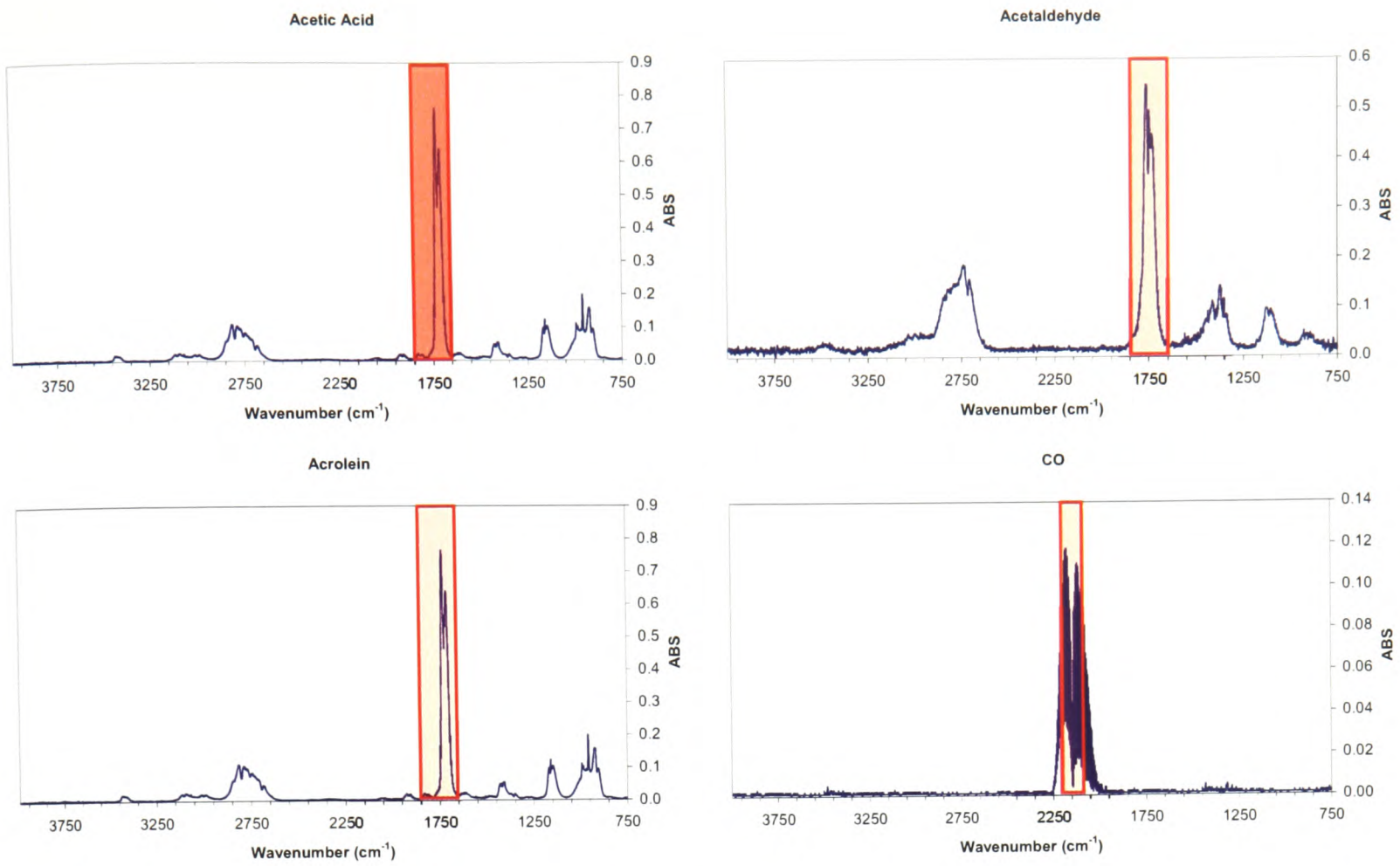

Figure 3-22. IR spectra of the six compounds used for quantification, with a box indicating the window used for analysis with InSight™.

Figure 3-23 shows the evolution profiles for six compounds evolved when the sample were heated at 5°C/min under a nitrogen atmosphere. It can be seen that there is no observed formation of acetaldehyde from alginic acid or acrolein from cellulose under these conditions. In all cases the evolved compounds are formed at the temperatures where the major weight loss events occur for each of the samples as shown in the TGA graphs. The CO profiles also show that in all of the samples there is an increase in evolution above 650°C. This may be due to high temperature decomposition of the residue with the oxygen coming from the substrate.

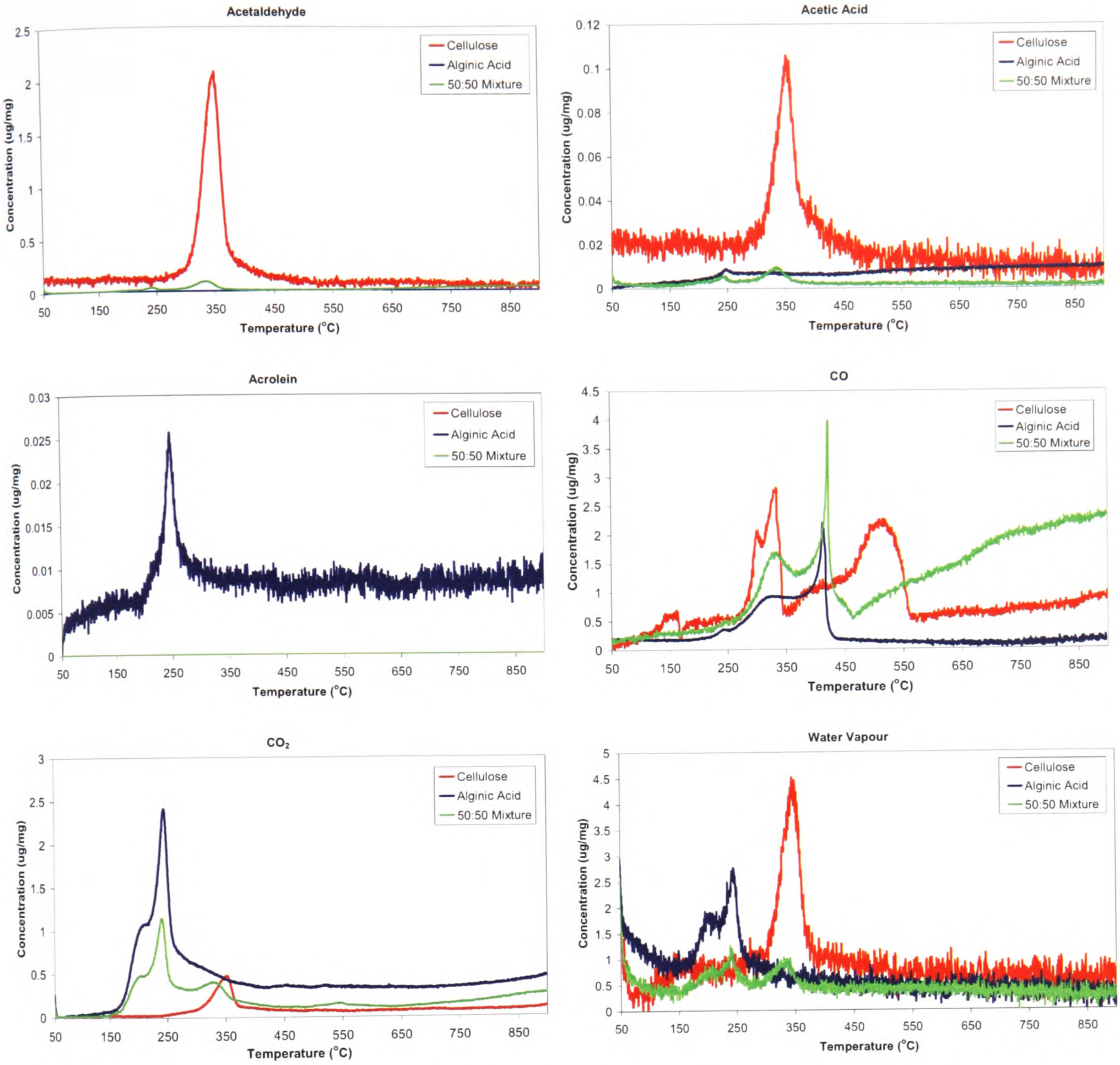

Figure 3-23. Evolution profiles for acetaldehyde, acetic acid, acrolein, CO, CO_2 and water vapour from cellulose, alginic acid and a 50:50 mixture of the two heated at 5°C/min under nitrogen.

Under nitrogen with 10% oxygen similar effects are seen (Figure 3-24). The evolution of the compounds relates to the major weight loss peaks of the TGA data. However, under the oxidising conditions there is no acrolein observed from any of the samples. In the evolution profiles for CO and CO_2 there are additional high temperature peaks of formation, which are consistent with the TGA information. In the water profile an additional peak can be seen for alginic acid at ~400°C, which is not observed for cellulose.

As was noted in the TGA information the 50:50 mixture shows no additional peaks, however under oxidising conditions (Figure 3-24) the high temperature peak seen in CO_2 formation in cellulose is not observed.

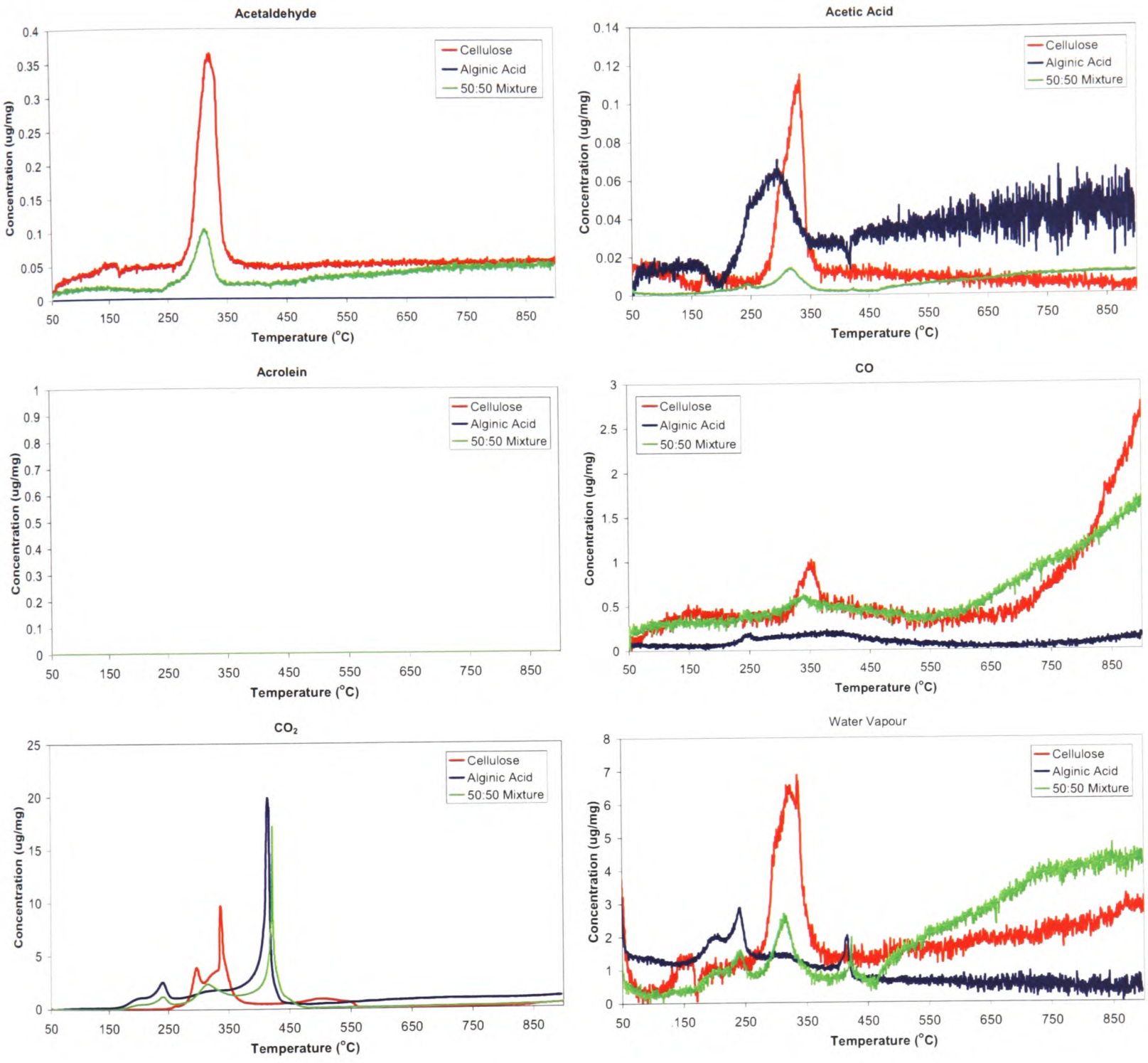

Figure 3-24. Evolution profiles for acetaldehyde, acetic acid, acrolein, CO, CO_2 and water vapour from cellulose, alginic acid and a 50:50 mixture of the two heated at 5°C/min under 10% oxygen in nitrogen.

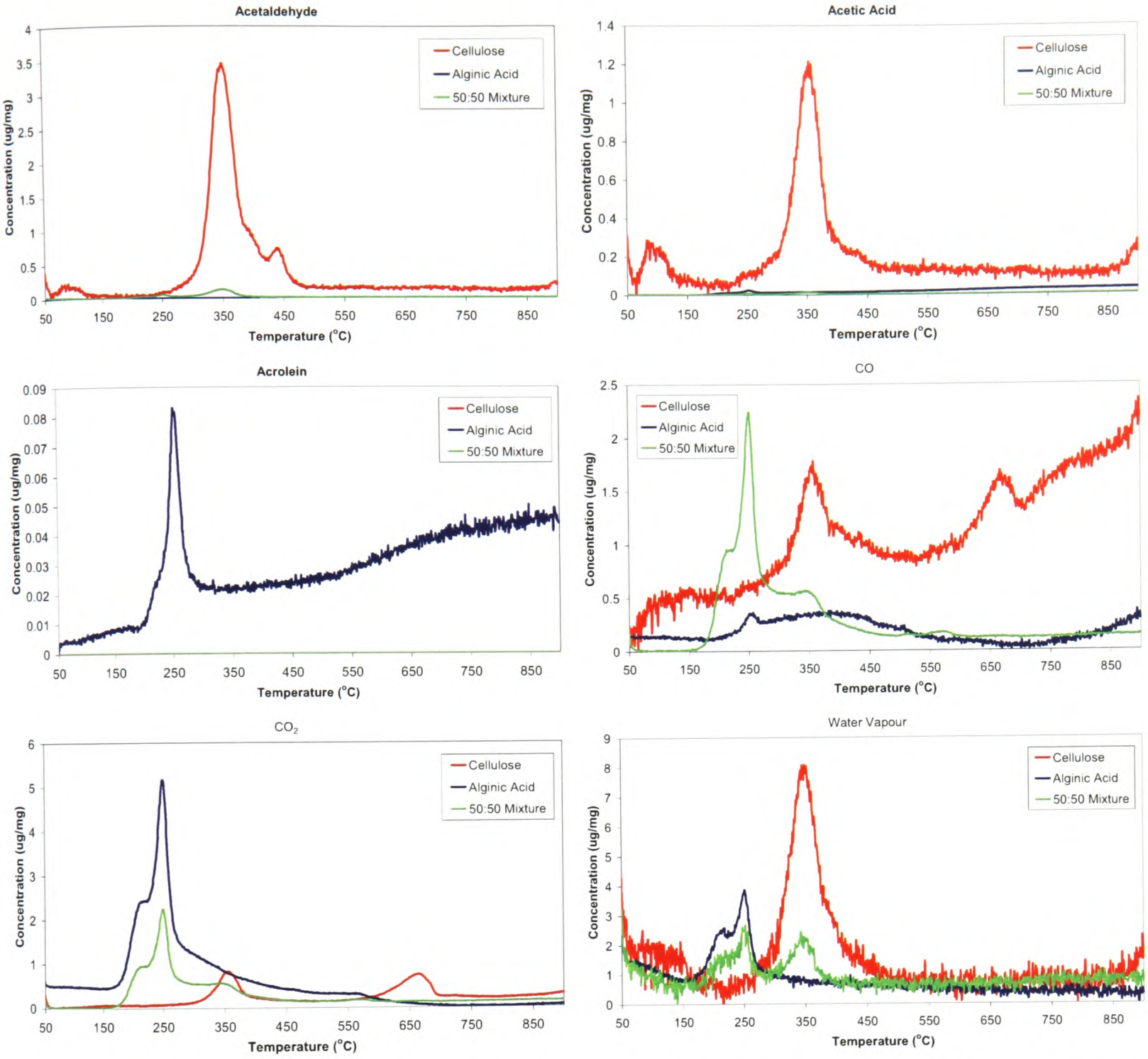

Figure 3-25. Evolution profiles for acetaldehyde, acetic acid, acrolein, CO, CO_2 and water vapour from cellulose, alginic acid and a 50:50 mixture of the two heated at 10°C/min under nitrogen.

At a temperature ramp rate of 10°C/min (Figure 3-25) similar effects are seen for all of the observed analytes as in the 5°C/min ramp rates. Acetaldehyde is not observed from alginic acid under either atmosphere. Acrolein is formed from the degradation of alginic acid only, and only under non-oxidising conditions. The CO_2 evolved from cellulose under nitrogen shows a second peak at ~650°C. This peak is not observed under oxidising conditions (Figure 3-26).

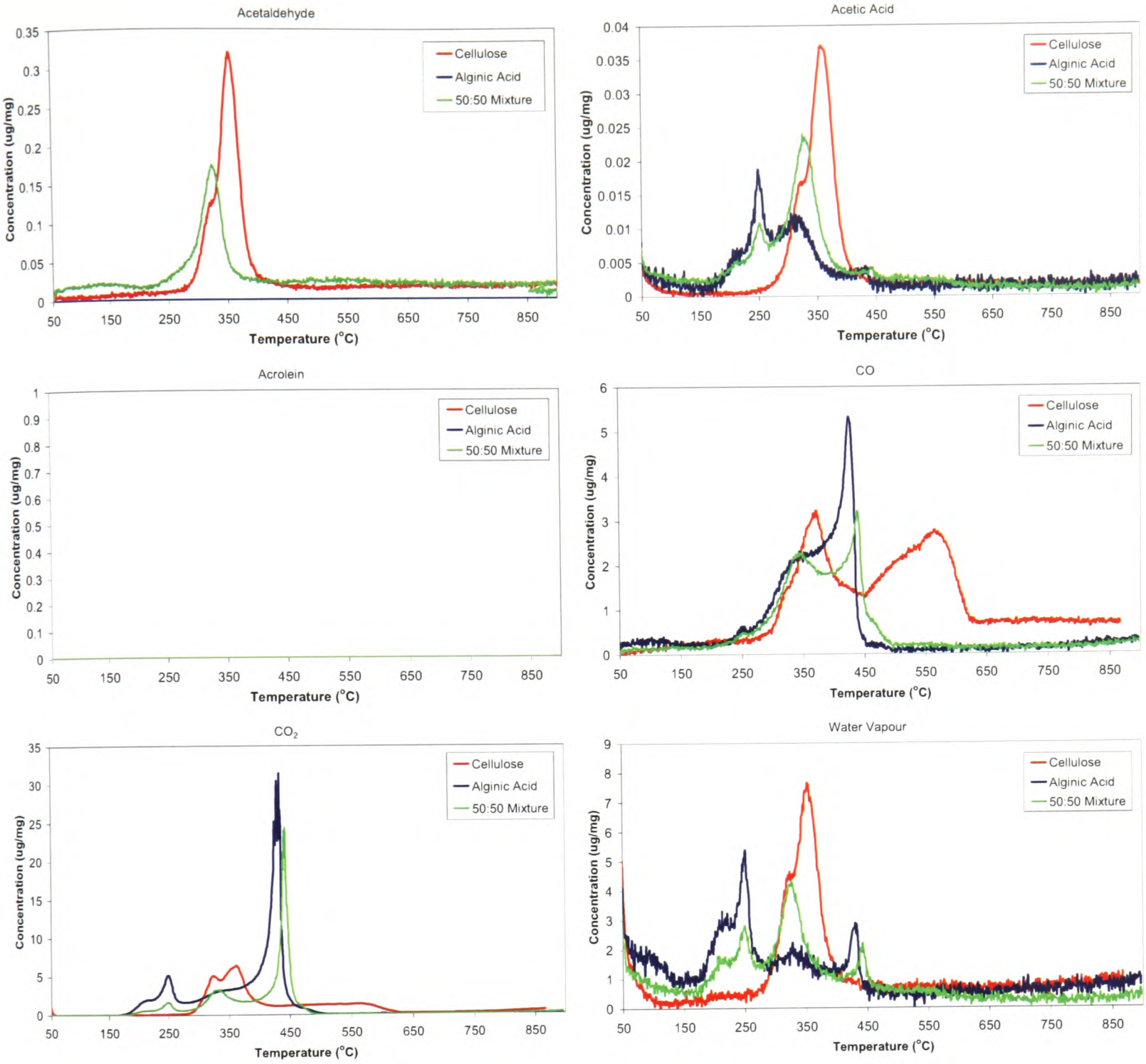

Figure 3-26. Evolution profiles for acetaldehyde, acetic acid, acrolein, CO, CO_2 and water vapour from cellulose, alginic acid and a 50:50 mixture of the two heated at 10°C/min under 10% oxygen in nitrogen.

Although most of the features that have been noted for the 5 and 10°C/min are present some differences are observed at 30°C/min. Acetaldehyde is observed from the alginic acid under non-oxidising conditions (Figure 3-27), and this is reflected in the 50:50 mixture sample. Under non-oxidising conditions (Figure 3-28) acrolein is seen for cellulose and the 50:50 mixture. The concentration of the acrolein peak observed is larger than that for alginic acid which indicates that it is likely to be an effect of the temperature ramp rate rather than being below the limit of quantification at lower ramp rates.

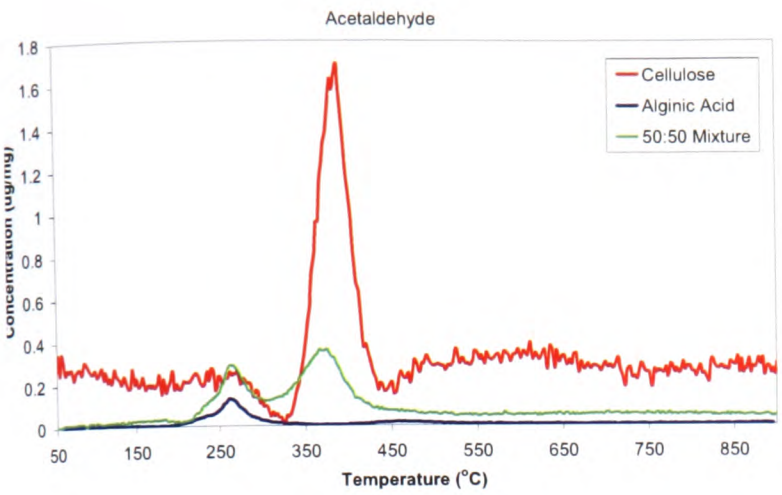

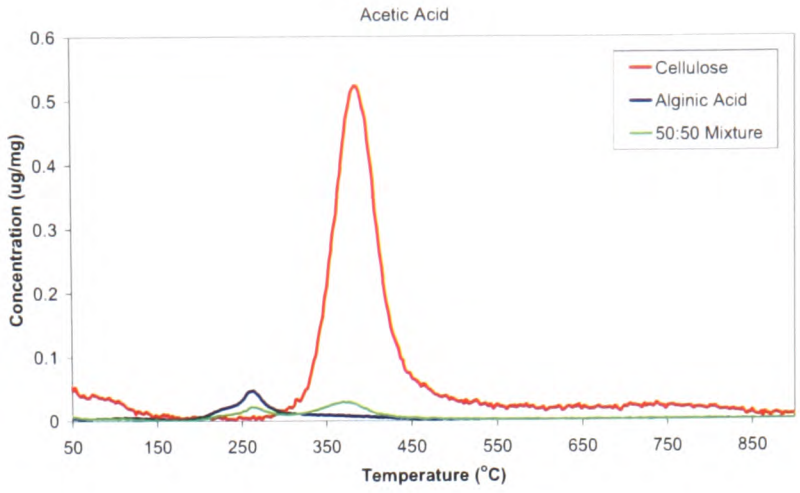

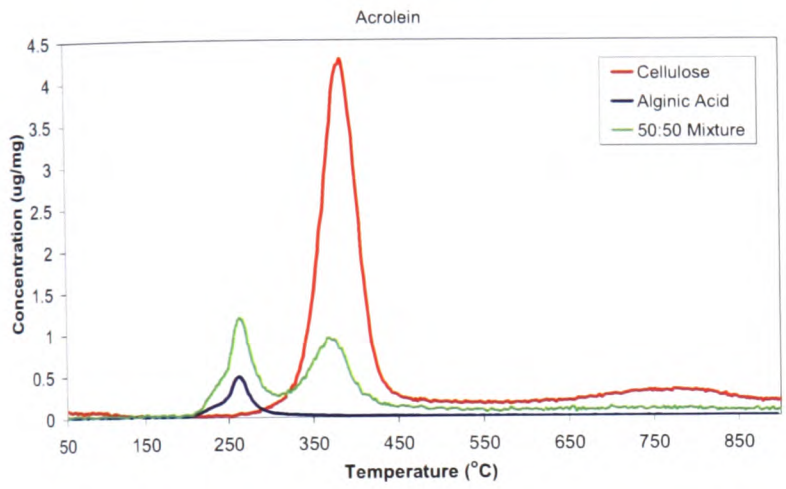

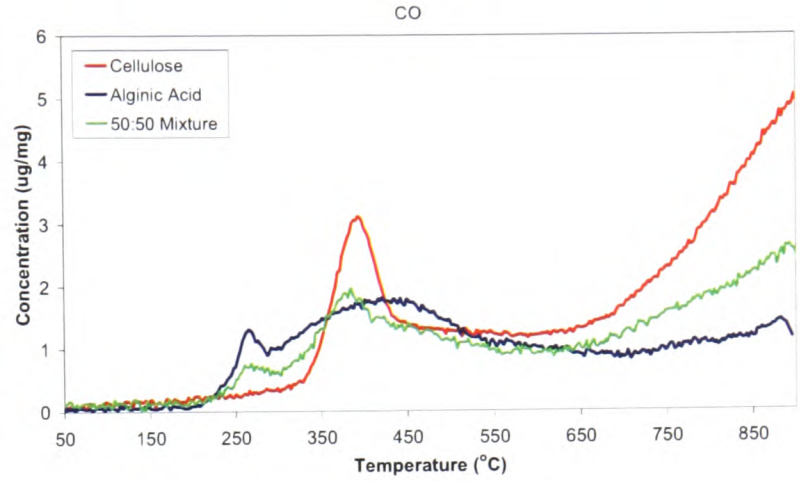

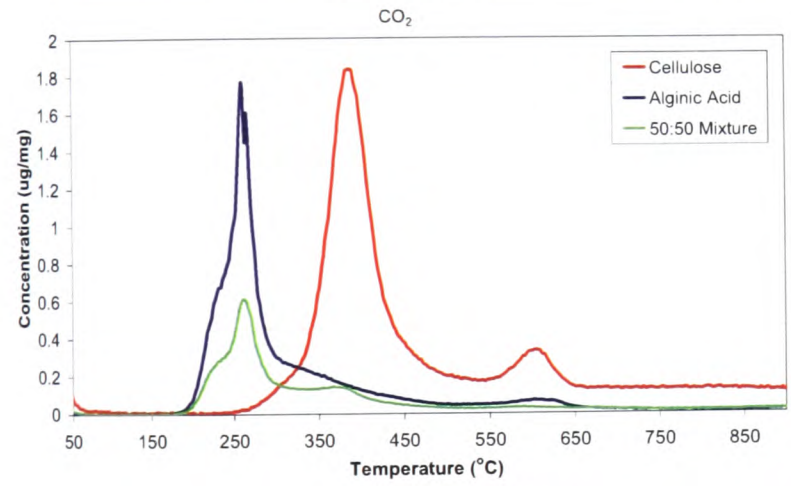

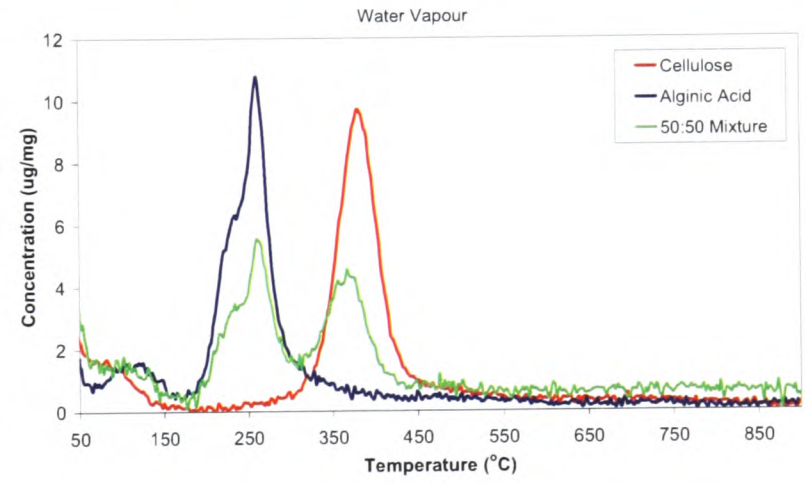

Figure 3-27. Evolution profiles for acetaldehyde, acetic acid, acrolein, CO, CO_2 and water vapour from cellulose, alginic acid and a 50:50 mixture of the two heated at 30°C/min under nitrogen.

An effect of concentration observed by the increasing ramp rate is seen in the CO_2 for alginic acid and the 50:50 mixture under oxidising conditions (Figure 3-28). The CO_2 peak at ~450°C is a conglomeration of sharp peaks, which is an artefact of the FTIR detector reaching overload. This effect is seen in the 60°C/min samples of alginic acid and 50:50 mixture (Figure 3-30). This indicates that for the same sample mass, under the same conditions alginic acid degrades to form more CO_2 than cellulose.

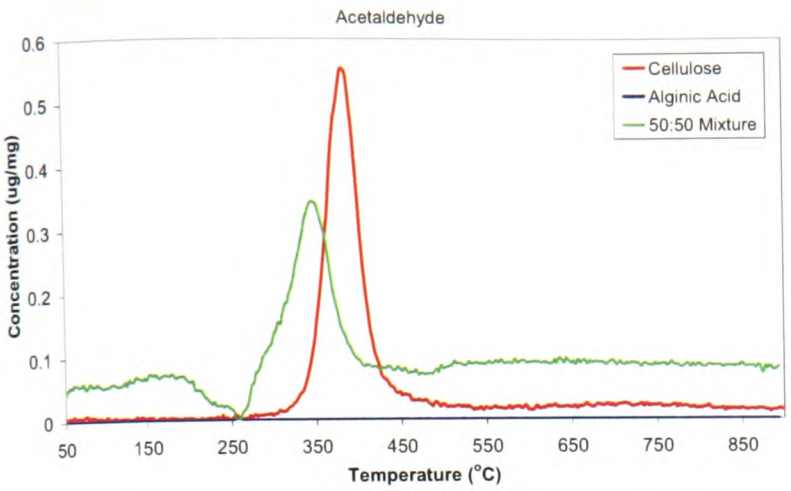

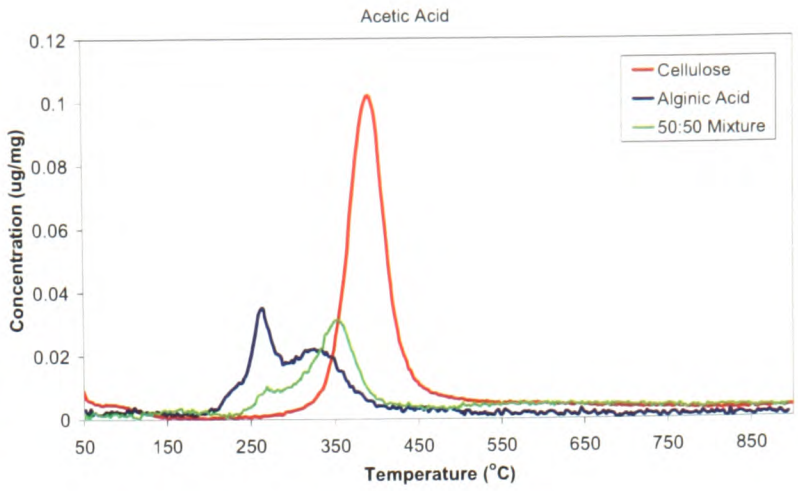

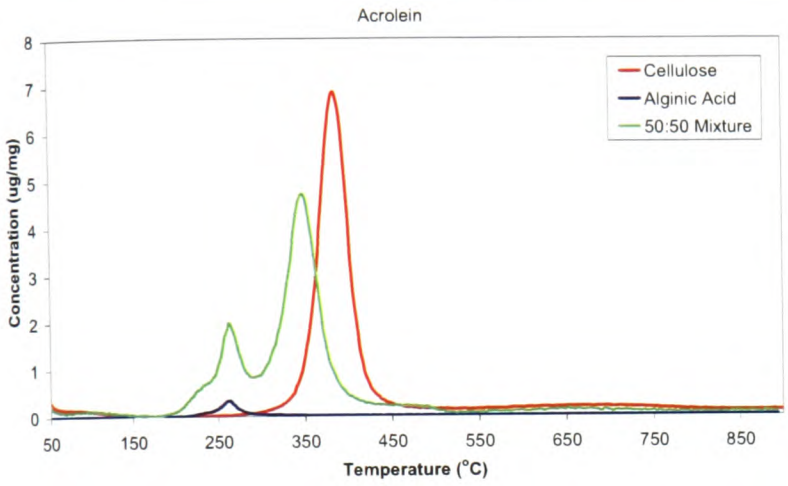

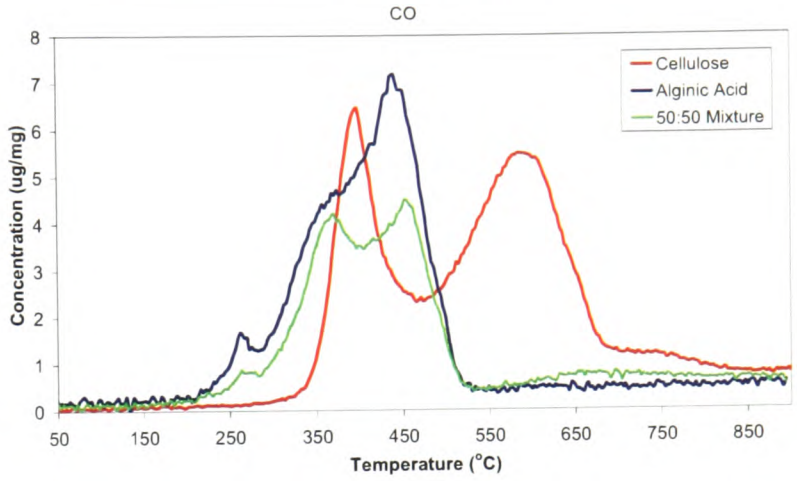

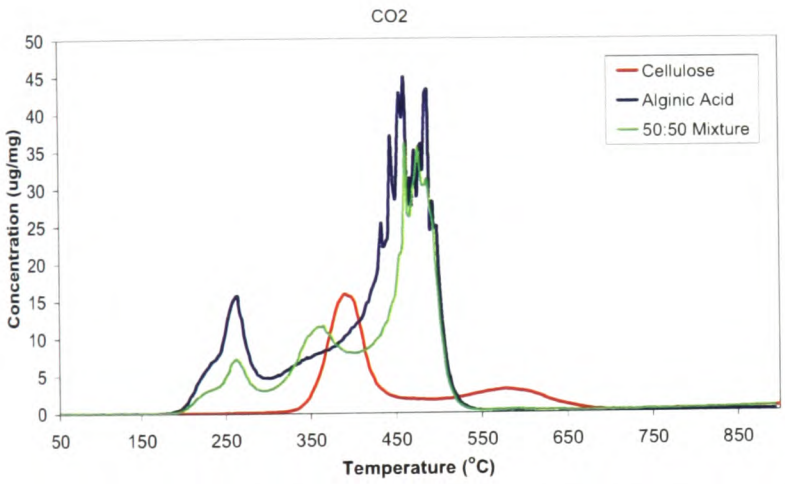

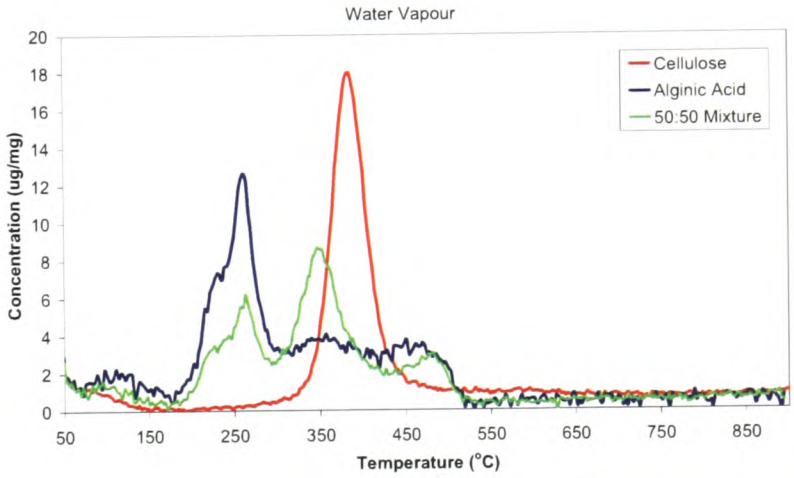

Figure 3-28. Evolution profiles for acetaldehyde, acetic acid, acrolein, CO, CO_2 and water vapour from cellulose, alginic acid and a 50:50 mixture of the two heated at 30°C/min under 10% oxygen in nitrogen.

The evolved compounds observed from the experiments run at 60°C/min under nitrogen (Figure 3-29) and 10% oxygen in nitrogen (Figure 3-30) follow the trends observed previously.

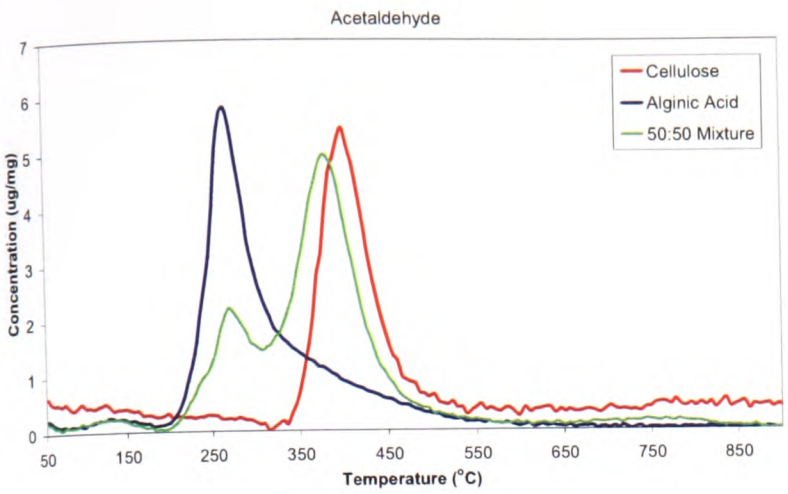

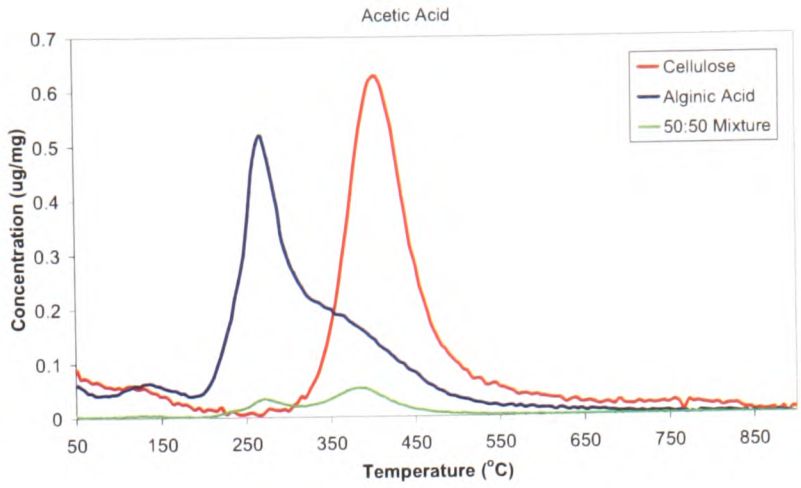

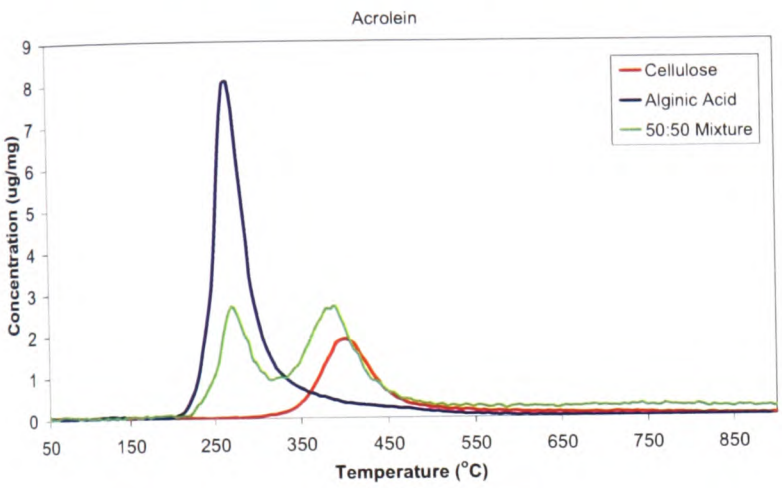

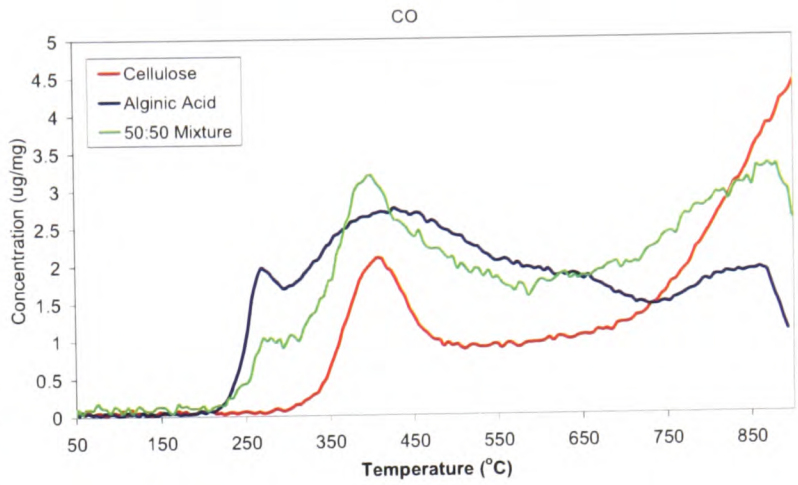

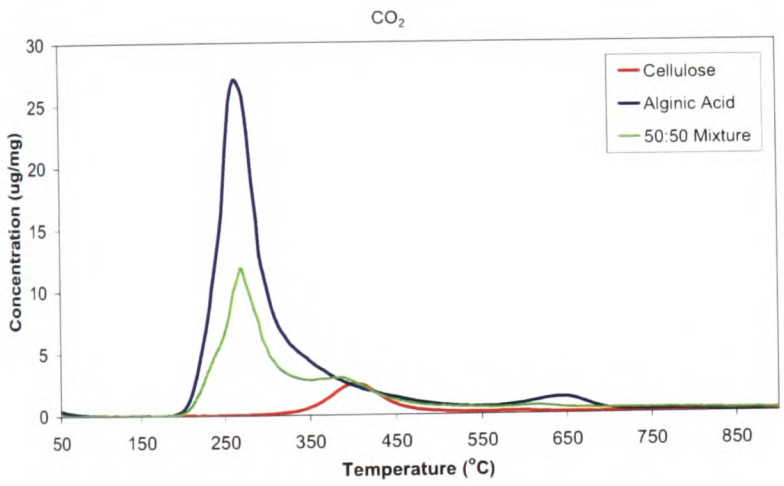

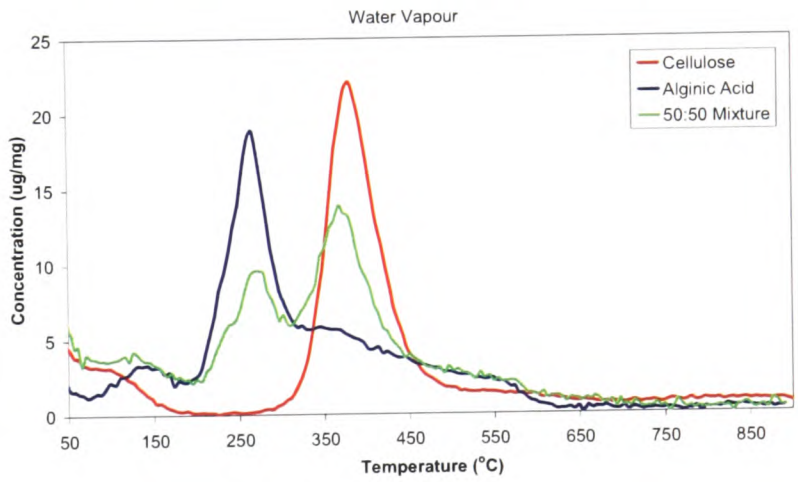

Figure 3-29. Evolution profiles for acetaldehyde, acetic acid, acrolein, CO, CO_2 and water vapour from cellulose, alginic acid and a 50:50 mixture of the two heated at 60°C/min under nitrogen.

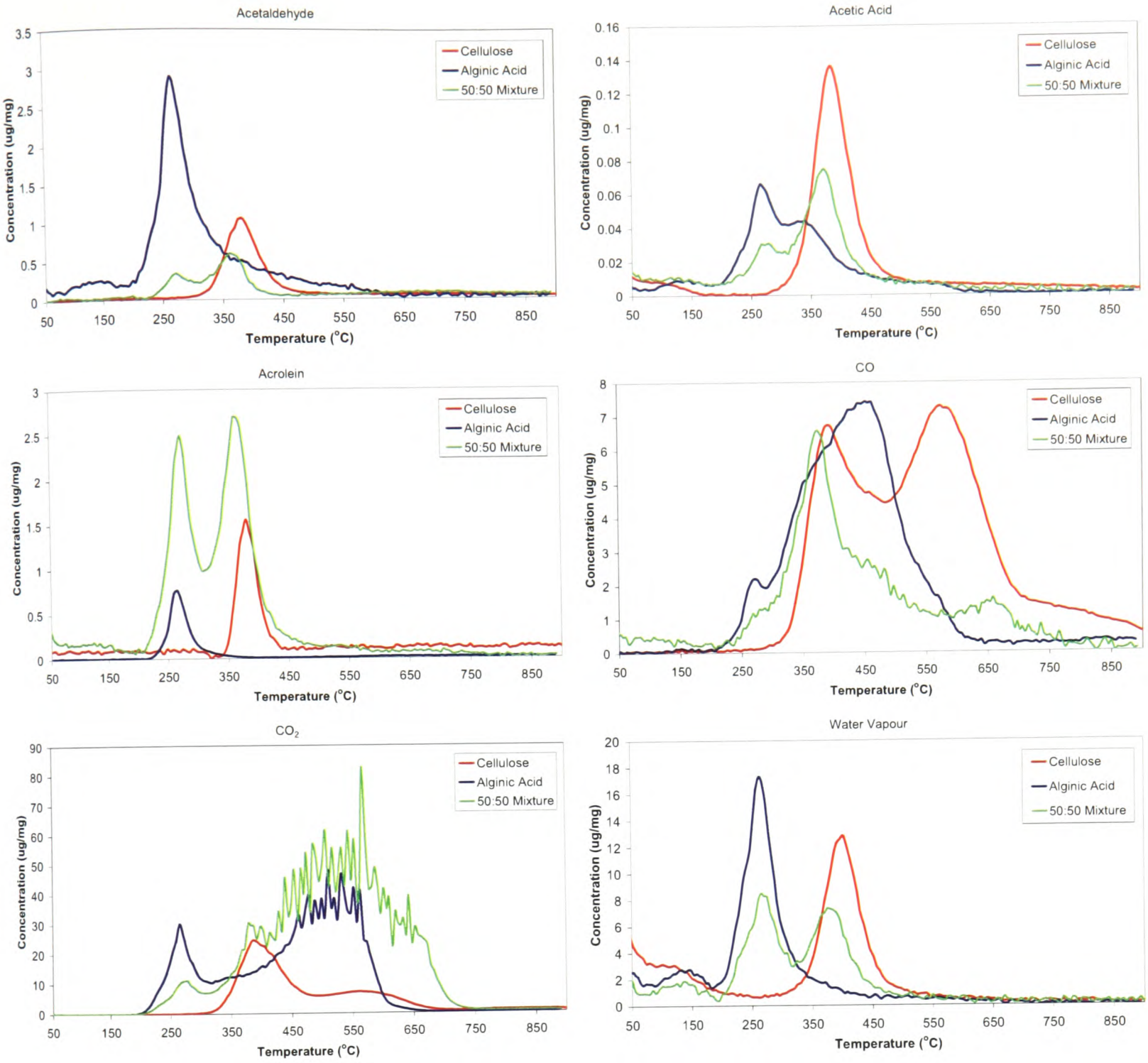

Figure 3-30. Evolution profiles for acetaldehyde, acetic acid, acrolein, CO, CO_2 and water vapour from cellulose, alginic acid and a 50:50 mixture of the two heated at 60°C/min under 10% oxygen in nitrogen.

The total concentration of the peaks observed in the evolution profiles (Figure 3-23 to Figure 3-30) make it possible to highlight trends observed by the changes in atmosphere and temperature ramp rate for each of the samples. The concentration scale is in µg/mg and in some of the graphs the results indicate more than 1000µg/mg. This is likely to be due to two sources of error; firstly, the observed concentrations of the compounds may be outside of their calibrated range (calibrated range for each compound is given in the Appendix B). As the calibrations are generally non-linear then this may lead to significant error in the measured concentration values. Secondly, as the total concentration is simply the area under the curve, any deviation from the

baseline is not accounted for in the calculation. In addition to this, the CO_2 at high ramp rates (particularly for alginic acid samples) show some overloading of the detector in the FTIR which contributes to errors in measuring the peak area.

However, the absolute concentration values of the compounds are not considered here, and are only used for comparative purposes.

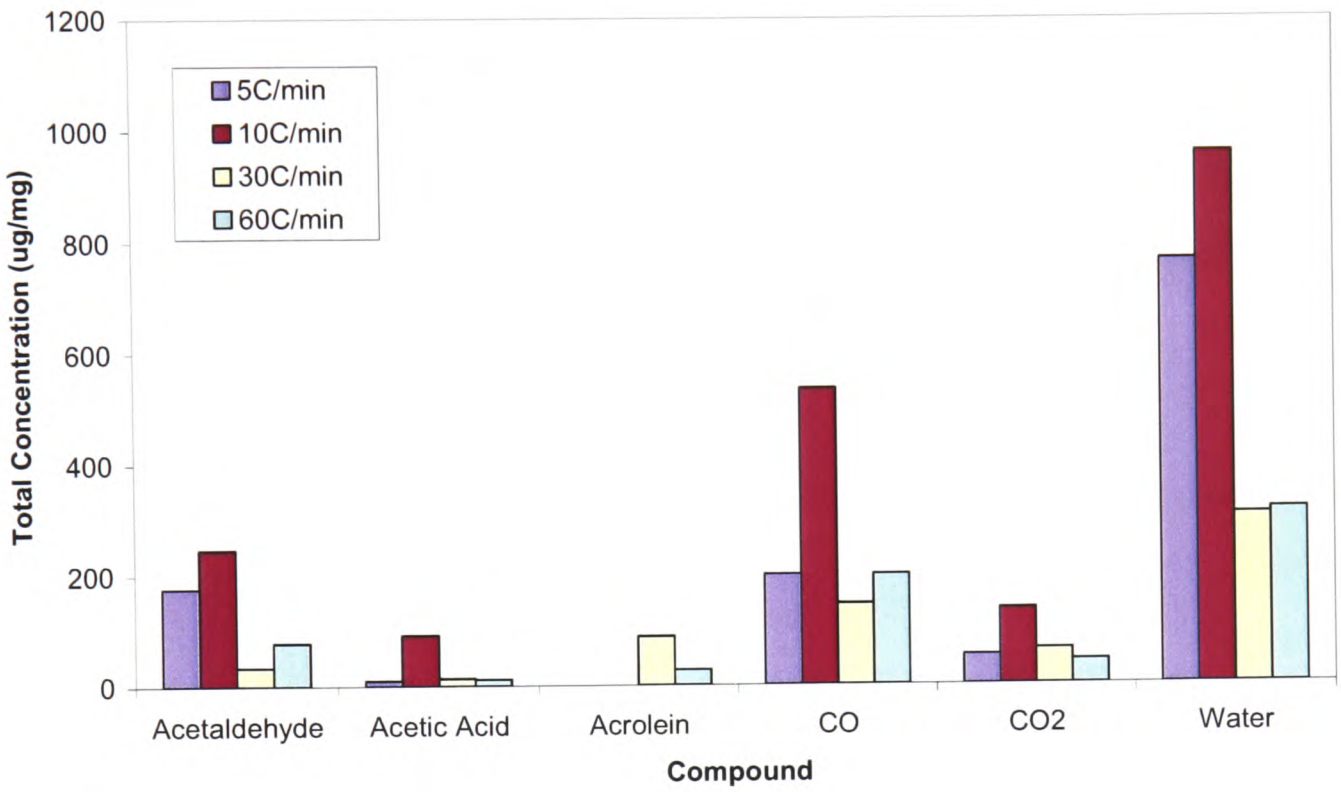

Figure 3-31. Effect of temperature ramp rate on the total evolution of six compounds from cellulose heated under nitrogen purge gas.

Figure 3-31 shows cellulose heated in a nitrogen atmosphere. There appears to be no effect as a result of heating rate on the selected compounds, with the exception of water that appears to have a trend of decreasing evolution with increasing ramp rate. Although in this series the 10°C/min sample has a larger total for each analyte compared to the other ramp rates.

Under an oxidising atmosphere (Figure 3-32) overall the amount of each of the analytes is reduced for acetaldehyde, acetic acid and acrolein, increased for CO and CO_2 and relatively unchanged for water vapour. Multipliers have been added to the acetaldehyde, acetic acid and acrolein to make them visible on the axis with the other compounds in the same graph.

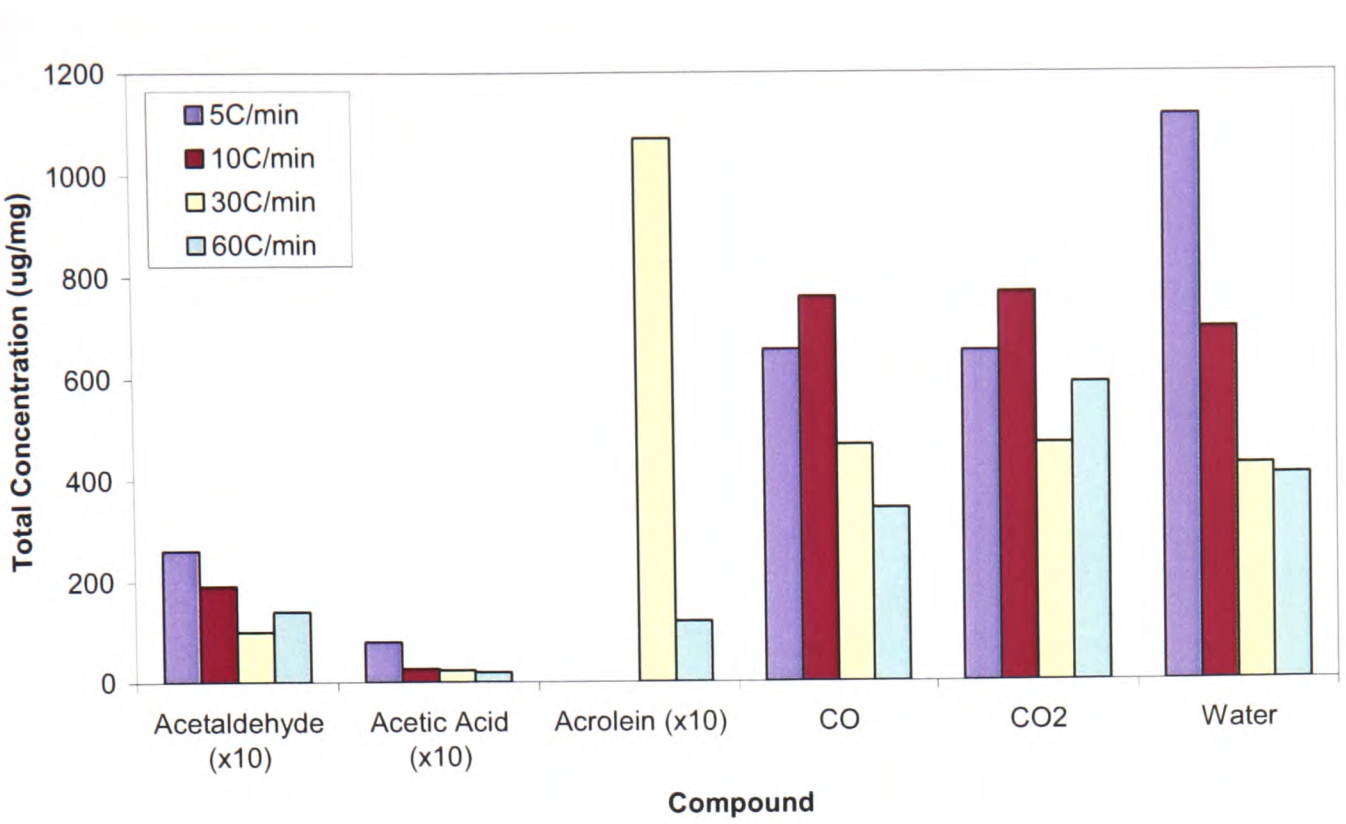

Figure 3-32. Effect of temperature ramp rate on the total evolution of six compounds from cellulose heated under 10% oxygen in nitrogen purge gas.

These increases in CO and CO_2 are due to the oxidation at higher temperature of the residue. CO also displays different trend with decreasing CO with increasing ramp rate at the higher rates when compared to the non-oxidising conditions.

Alginic acid heated under nitrogen purge gas is shown in Figure 3-33. Similarly to cellulose the water vapour appears to decrease with increasing temperature ramp rate. CO is increased with increasing ramp rate, and acrolein appears to have a similar trend. There appears to be no trend in any of the other analytes.

Under the oxidising conditions (Figure 3-34) the CO and CO_2 are increased, and water appears to be slightly elevated too. All of the other measured compounds are unaffected by the change in atmosphere, unlike cellulose. The CO appears to have no trend under the oxidising atmosphere, compared to the non-oxidising atmosphere. Acrolein shows a similar effect, although it is not present for the two lowest ramp rates (5°C/min and 10°C/min), under 10% oxygen in nitrogen purge gas.

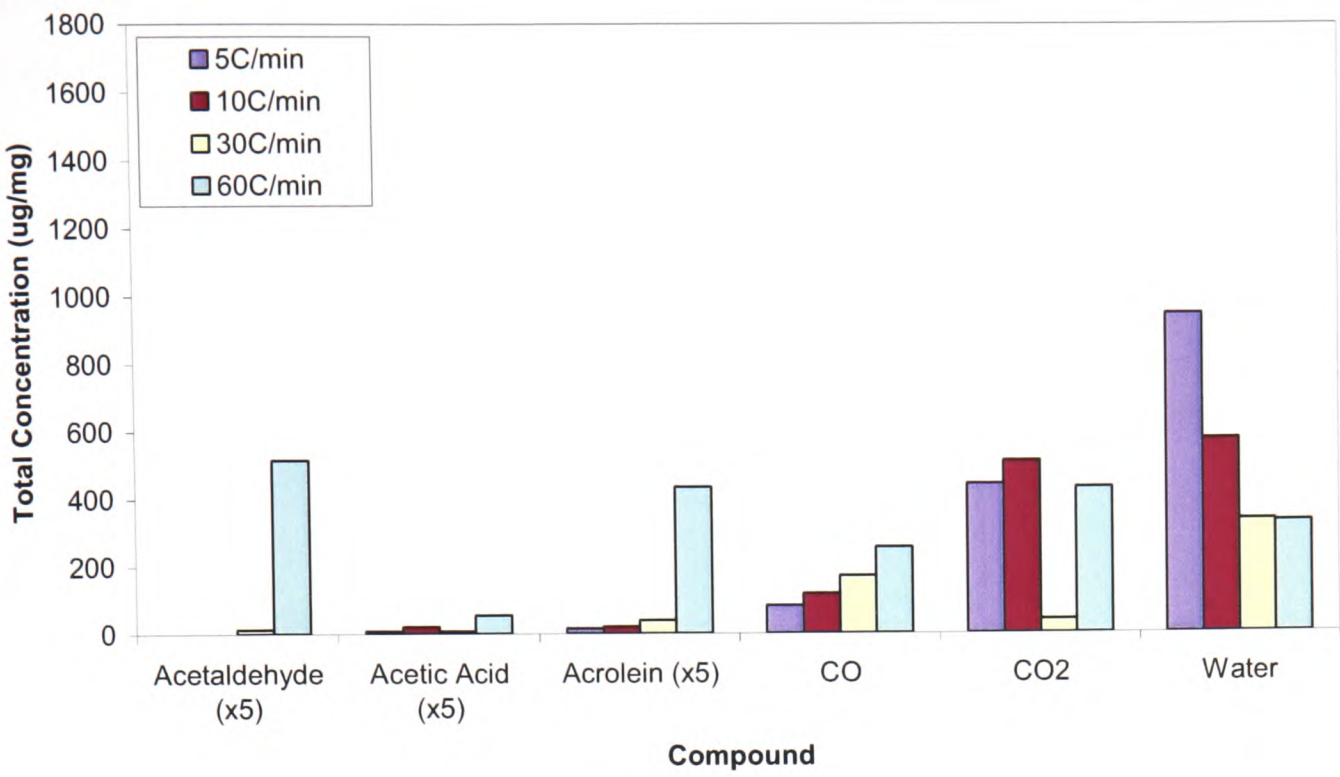

Figure 3-33. Effect of temperature ramp rate on the total evolution of six compounds from alginic acid heated under nitrogen purge gas.

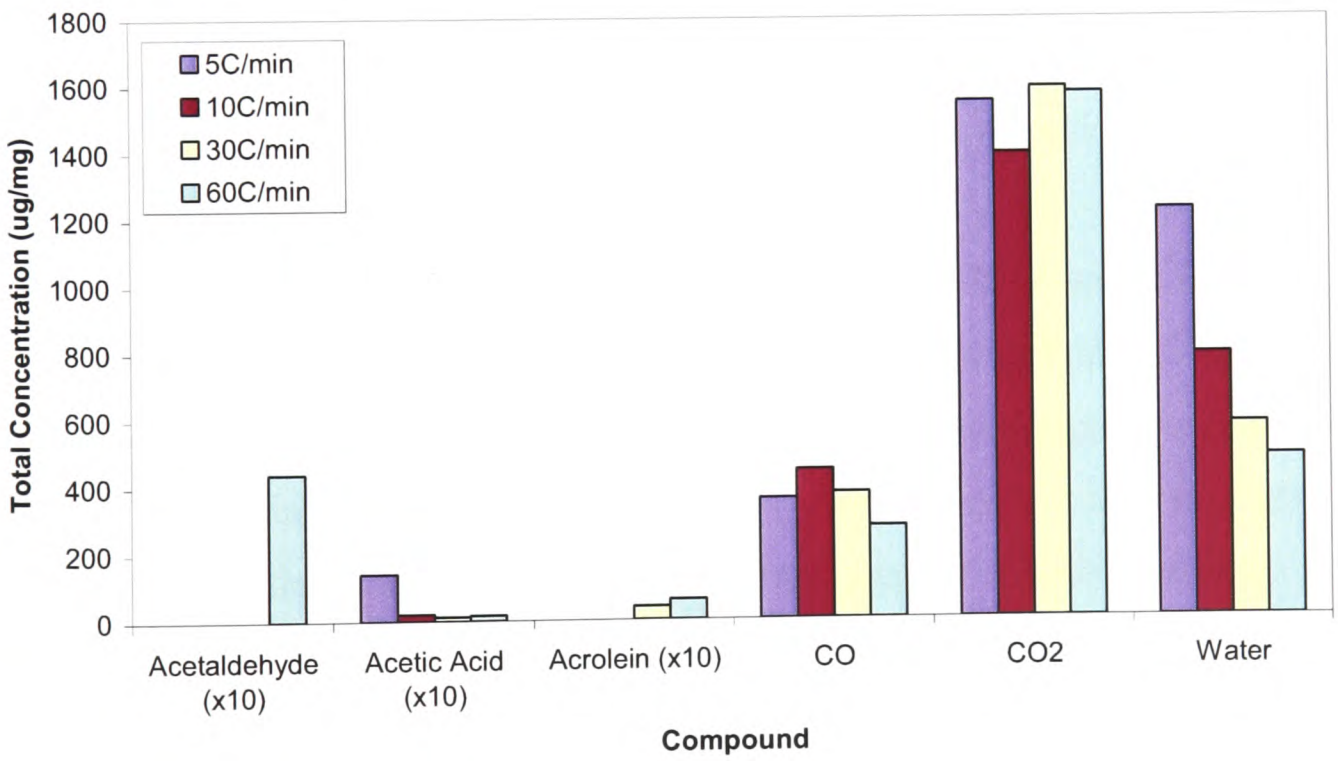

Figure 3-34. Effect of temperature ramp rate on the total evolution of six compounds from alginic acid heated under 10% oxygen in nitrogen purge gas.

The 50:50 mixture shows some similar effects to the two pure compound samples. Figure 3-35 shows that the trends are similar to those seen in cellulose (Figure 3-31) with no trends being observed as a result of changing temperature ramp rate, except for water vapour.

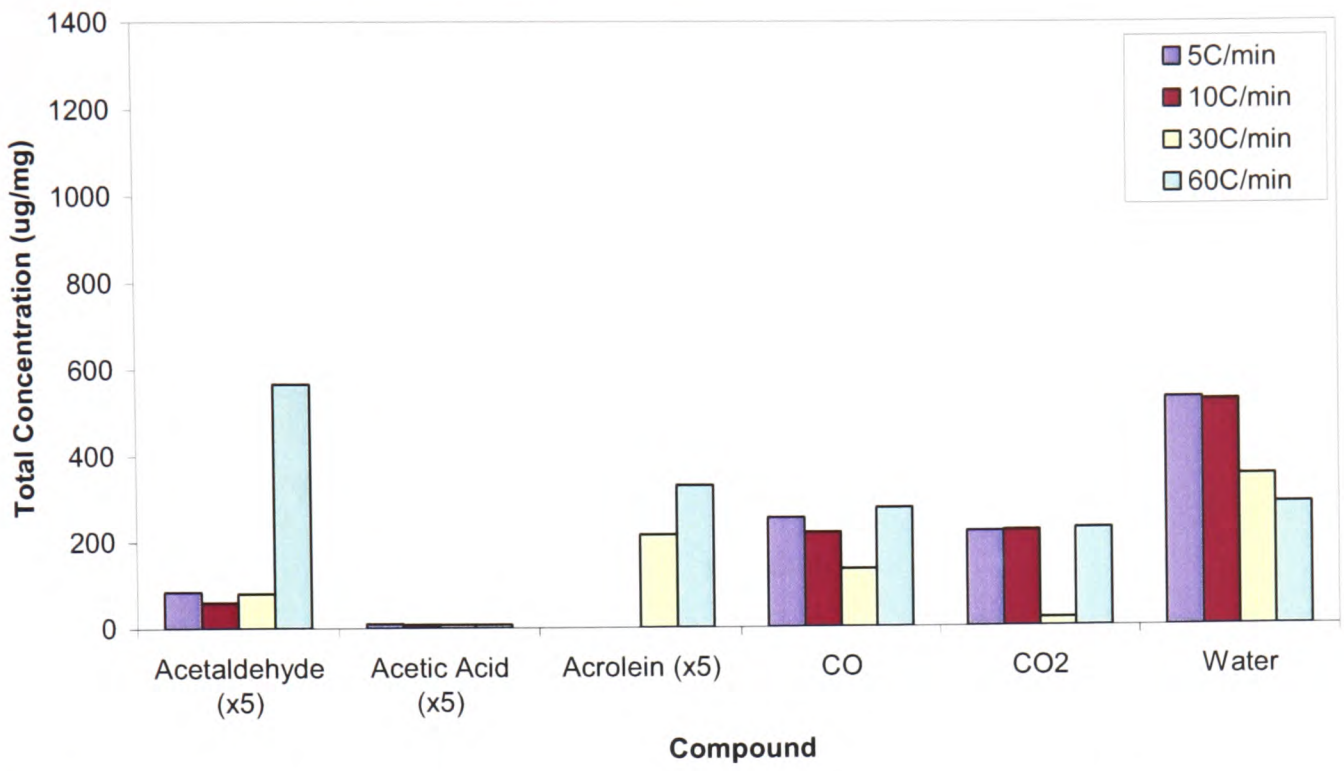

Figure 3-35. Effect of temperature ramp rate on the total evolution of six compounds from a 50:50 mixture of cellulose and alginic acid heated under nitrogen purge gas.

Similar to the pure samples, the CO and CO_2 are raised in the oxidising conditions compared to the non-oxidising conditions (Figure 3-36).

CO_2 in the 60°C/min sample is off-scale and is due to the detector overloading of the FTIR shown in Figure 3-30. As a result the CO_2 column is omitted from this figure as the calculation of peak area gives a total that is unrealistic. The CO concentrations show the same trend as cellulose, decreasing with increasing ramp rate. Acetaldehyde, acetic acid and acrolein show no real trend in similar fashion to cellulose. Water vapour follows the same trend as the other samples and decreases with increasing temperature ramp rate under both atmospheres.

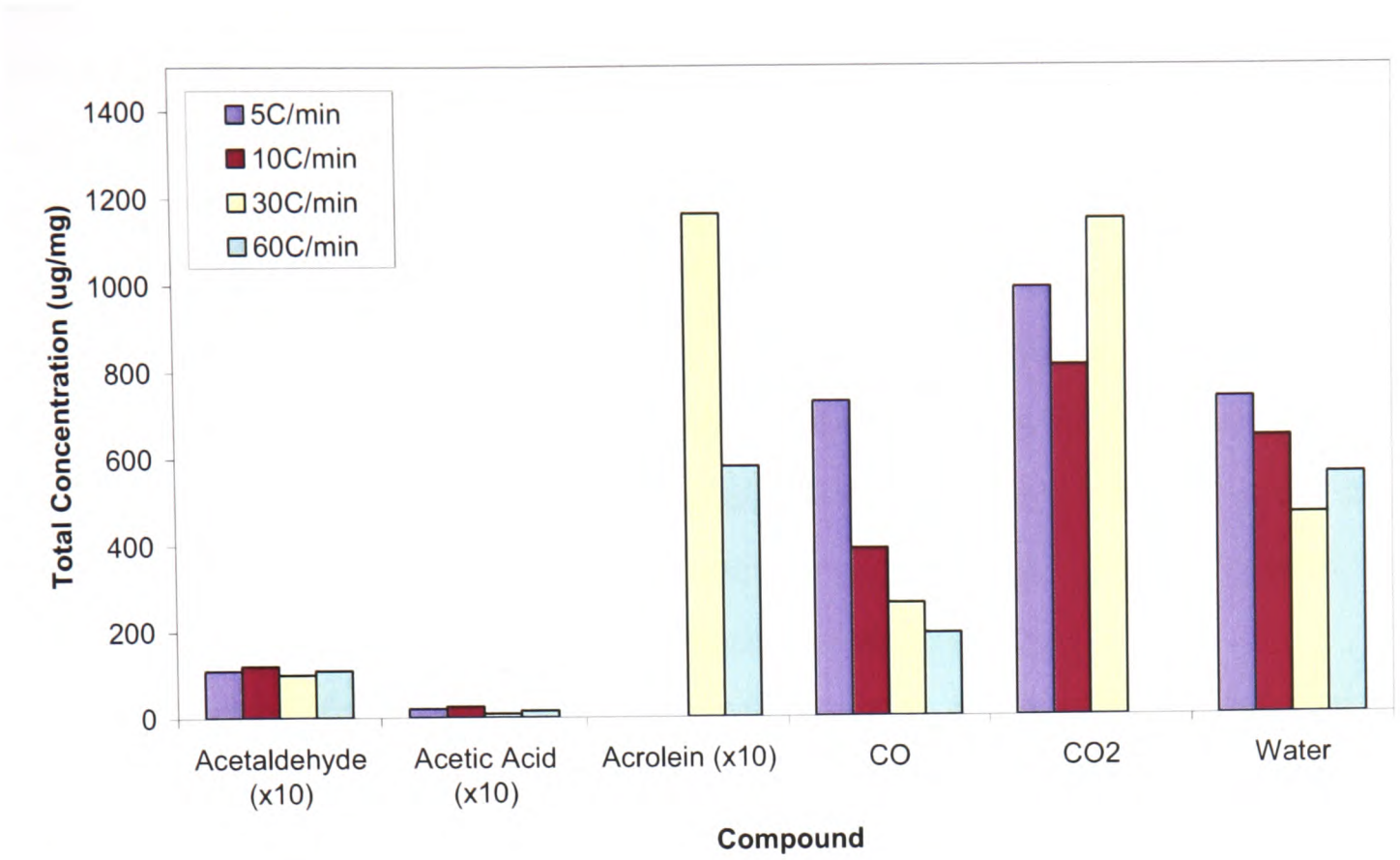

Figure 3-36. Effect of temperature ramp rate on the total evolution of six compounds from a 50:50 mixture of cellulose and alginic acid heated under 10% oxygen in nitrogen purge gas.

3.2.3 Summary of FTIR data

The qualitative matching of the software demonstrates that it is important to determine a correlation level (R) that gives consistent and accurate identification of the materials analysed. In the case of this study a qualitative match of $R \geq 0.80$ was used. However, visual comparison of the extracted factors was still made with the reference spectra prior to quantitative data being accepted. This allows confidence in the evolution profiles that are presented for the six chosen analytes from the qualitative matches – acetaldehyde, acetic acid, acrolein, CO, CO_2 and water vapour.

Acetaldehyde is formed by cellulose under both atmospheres, with more formed in non-oxidising conditions compared to oxidising conditions. In the alginic acid experiments acetaldehyde is only observed under higher temperature ramp rates, and again in higher amounts under nitrogen purge gas. The mixture of the two samples shows the same peaks as each of the samples, indicating that there is no interaction in acetaldehyde formation.

Acetic acid is observed as a decomposition product for both cellulose and alginic acid under both atmospheres at all temperature ramp rates. The alginic acid samples show a double peak under the oxidising conditions, at 250°C and 300°C approximately, though at the highest

temperature ramp rate the peaks tend to merge. Similarly to acetaldehyde the acetic acid is formed in lower amounts under the oxidising conditions. The mixture of the two samples, under either atmosphere, shows the same peaks as each of the samples, indicating that there is no interaction in the evolution of acetic acid.

Acrolein is not observed in cellulose under either condition at the two lower ramp rates (5 and 10°C/min), nor is it measured in alginic acid under oxidising conditions at these lower ramp rates. Generally the amount of acrolein observed is higher in the cellulose samples compared to alginic acid under the equivalent conditions. There are no additional peaks observed in the 50:50 mixture samples, although under oxidising conditions the peaks appear larger than the individual samples, but the total values appear much the same.

For CO formed from the samples the trends seem more complex. Under non-oxidising conditions there is either no trend or a rising trend with increasing ramp rate, but under oxidising conditions the trend is decreasing with increasing ramp rate. Under oxidising conditions for alginic acid the second broad peak (~450°C) is increased and there is a second high temperature peak for cellulose (~570°C). However, this additional peak seen in cellulose is not observed in the mixture sample, though the remainder of the profile maps to the two unmixed samples. This may be an indication of some interaction between the samples. Perhaps this is due to the CO evolution from the alginic acid occurring at slightly lower temperature, causing the cellulose reaction to occur at the same lower temperature due to the presence of similar reaction precursor compounds.

CO_2 follows similar trends for all of the samples, under both atmospheres, although the first peaks occur at different temperatures for the two materials (lower temperature for alginic acid – 250°C vs. 350°C). The higher temperature peak (~550 – 600°C) is observed for both samples in both atmospheres. The mixture sample maps onto the evolution profiles for the two unmixed samples.

Water vapour shows the same trend for all of the samples under both atmospheres, with a decrease in evolution with increasing ramp rate. The amount of water vapour measured is also slightly increased in the oxidising conditions compared to the nitrogen atmosphere.

Despite the lack of higher CO peak under oxidising conditions for the mixture compared to cellulose, there appears to be little interaction between the samples.

3.3 Char Analysis

The char residues formed using the tube furnace as described in the experimental section were analysed using an elemental analyser and also by ATR spectroscopy. Only char residues from pure cellulose and alginic acid samples were prepared. No 50:50 mixture sample was prepared for the char analysis section of the study as the compounds are similar in elemental composition it was felt that little information could be drawn from the data provide by elemental analysis. The resolution of the ATR was not thought to be sufficiently high enough for the pure samples to detect interactions between them in a mixture.

Initially, the weight of char formed was plotted against the heat treatment temperature, shown in Figure 3-37.

The literature values by Shafizadeh and Sekiguchi [47] for cellulose show some agreement with this study at temperatures above 400°C, although a much smaller temperature range was examined.

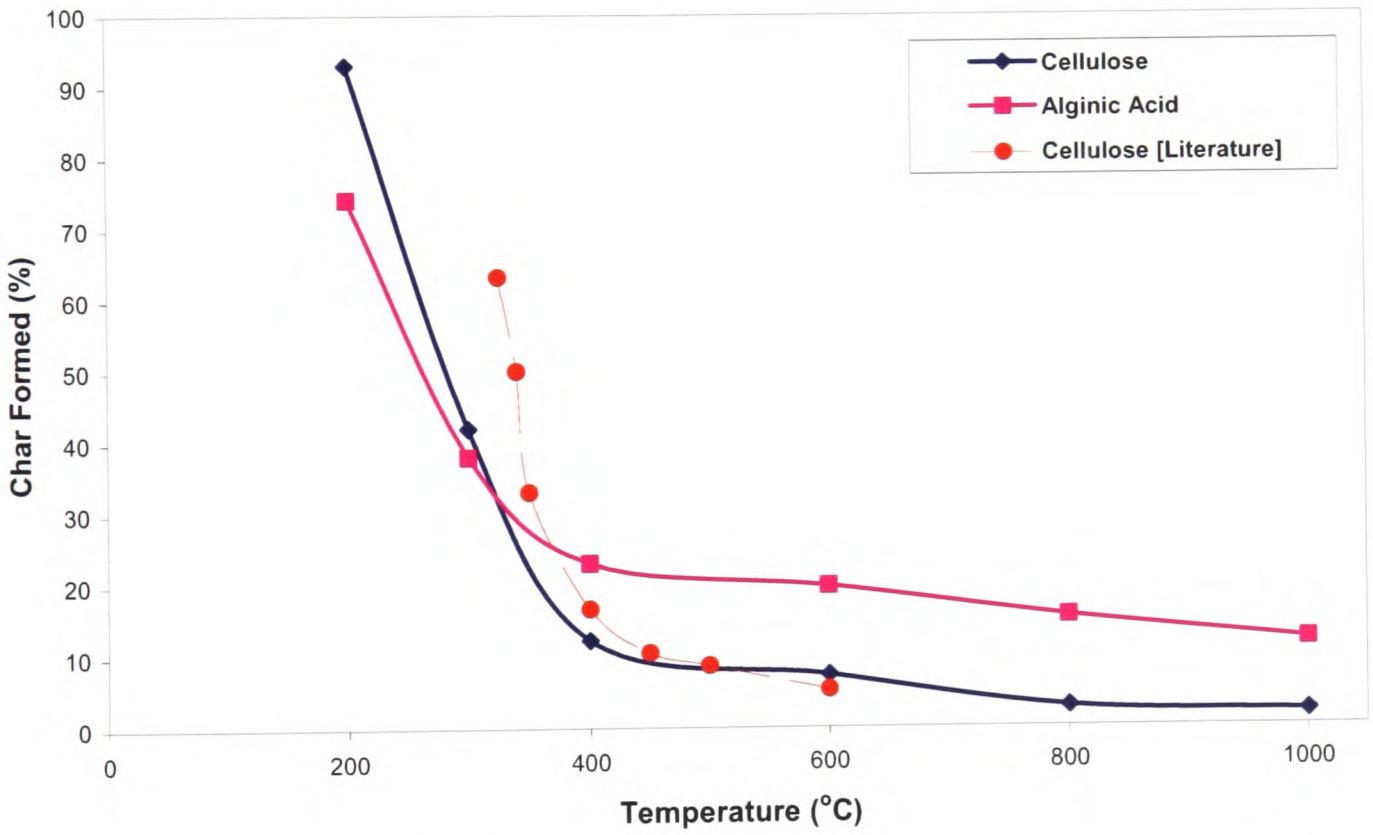

Figure 3-37. A graph showing the percentage of char formed in nitrogen as a function of heat treatment temperature. Literature data are also plotted for comparison [47].

Below 400°C there is significant difference in the absolute values, but the overall trend is similar with the point where the largest weight loss occurring at 400°C. The variation in absolute values may be explained by the difference in the methodology of the preparing the char. In the literature [47], samples of cellulose were only treated for 5 minutes in 60ml/min

nitrogen flow rate at the heat treatment temperature, rather than 1 hour and approximately 300ml/min as used in this study. The alginic acid (Figure 3-37) has more residual char at higher temperature than the cellulose sample

3.3.1 Elemental analysis of the char samples

The data for the untreated samples is shown in Table 3-3. In both cases the measured result is in good agreement with the theoretical values for the untreated samples. The measured values are also in good agreement with those quoted from the literature for cellulose.

Table 3-3. Elemental composition for untreated cellulose and alginic acid.

	Cellulose $(C_6H_{10}O_5)n$			Alginic Acid $(C_6H_8O_6)n$		
	%C	%H	%O	%C	%H	%O
Theoretical	44.4	6.2	49.3	40.9	4.6	54.5
Measured	43.9	6.2	49.9	38.5	5.4	56.1
Literature [47]	42.8	6.5	50.7	-	-	-

Figure 3-38 shows the elemental composition of the char obtained from cellulose, which is also consistent with the literature values provided by Shafizadeh [47], despite the difference in methodology for the char preparation.

In this study only the carbon and hydrogen are measured and oxygen is assumed to make up the remainder of the elemental composition of the residue. However, the value for oxygen is consistent with both the theoretical composition for both samples and also with the literature values in the case of cellulose.

Figure 3-39 shows the results for alginic acid pyrolysed under nitrogen. Overall the trends look similar to that of cellulose; however, the total weight of char formed is higher (Figure 3-37). The % carbon measurements at the two highest temperatures show a similar effect to that of cellulose.

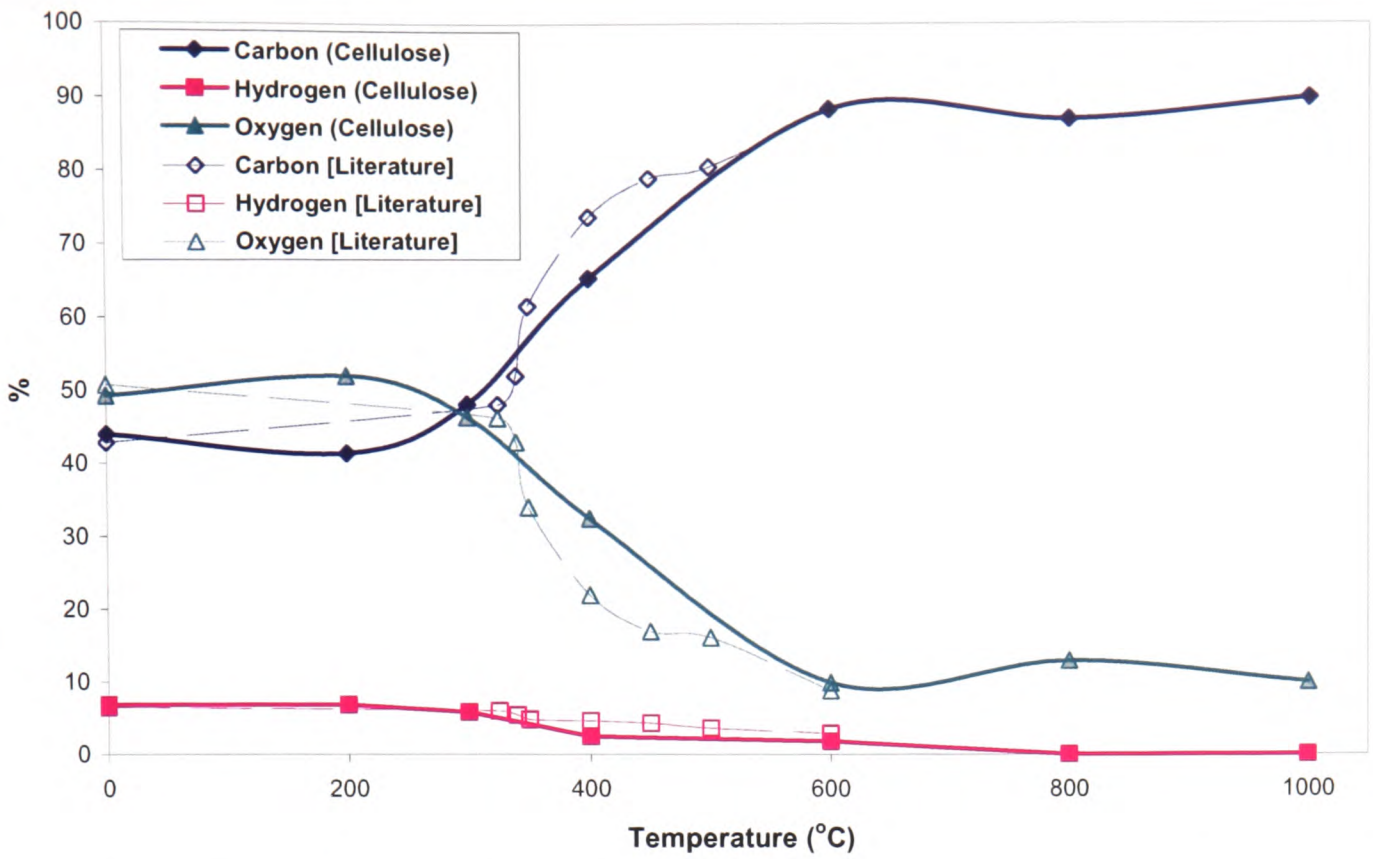

Figure 3-38. Elemental composition of cellulose chars vs. temperature of char formation compared with literature data [47].

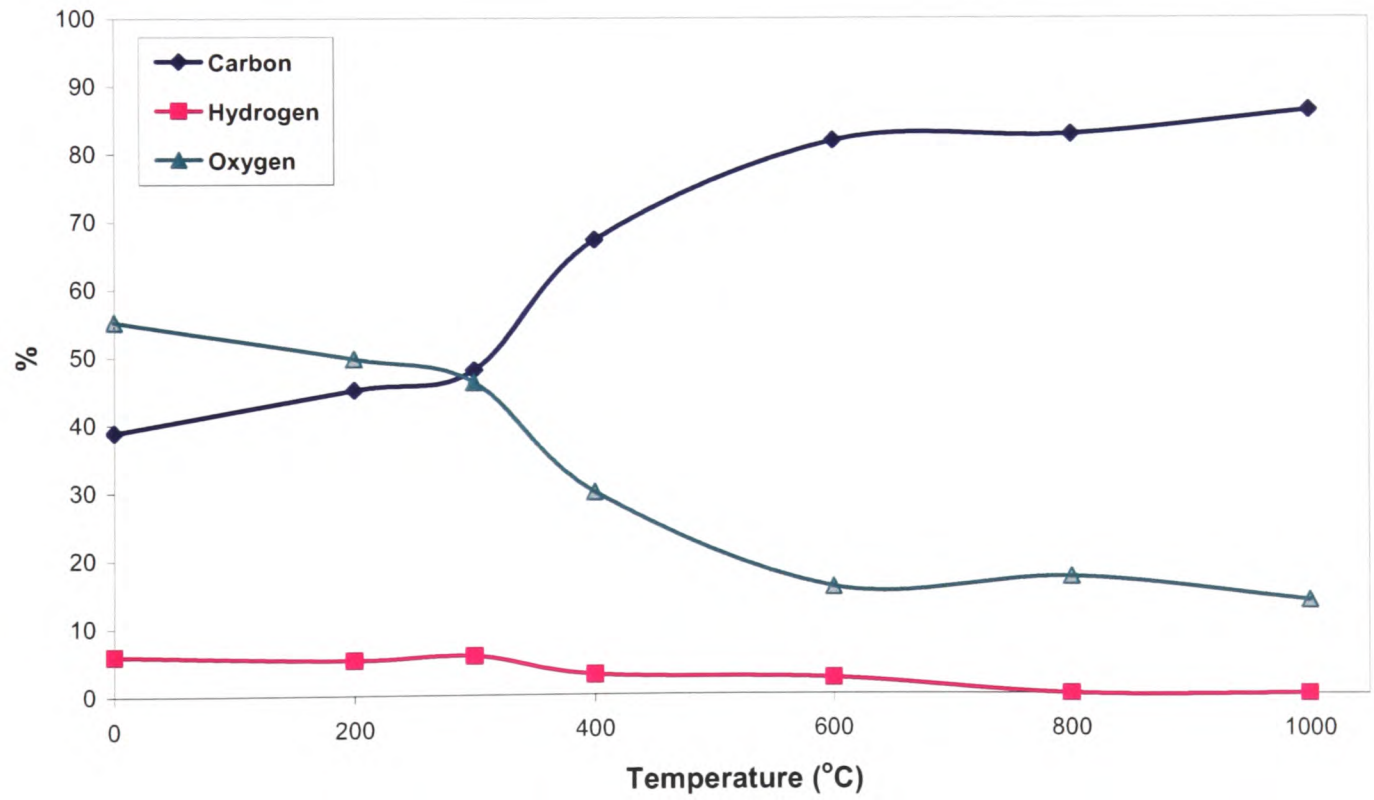

Figure 3-39. Elemental composition of alginic acid chars vs. temperature of char formation.

Figure 3-40 shows the comparison of the changes in elemental composition of cellulose and alginic acid overlaid. It can be seen that the alginic acid shows slight changes in the composition of the char at lower heat treatment temperatures than cellulose but the major

changes begin above 300°C. Above 400°C the trends are similar although there is a slightly lower carbon content above 600°C. This would imply that there is less aromatic structure to the alginic acid char at high temperature compared to that of cellulose.

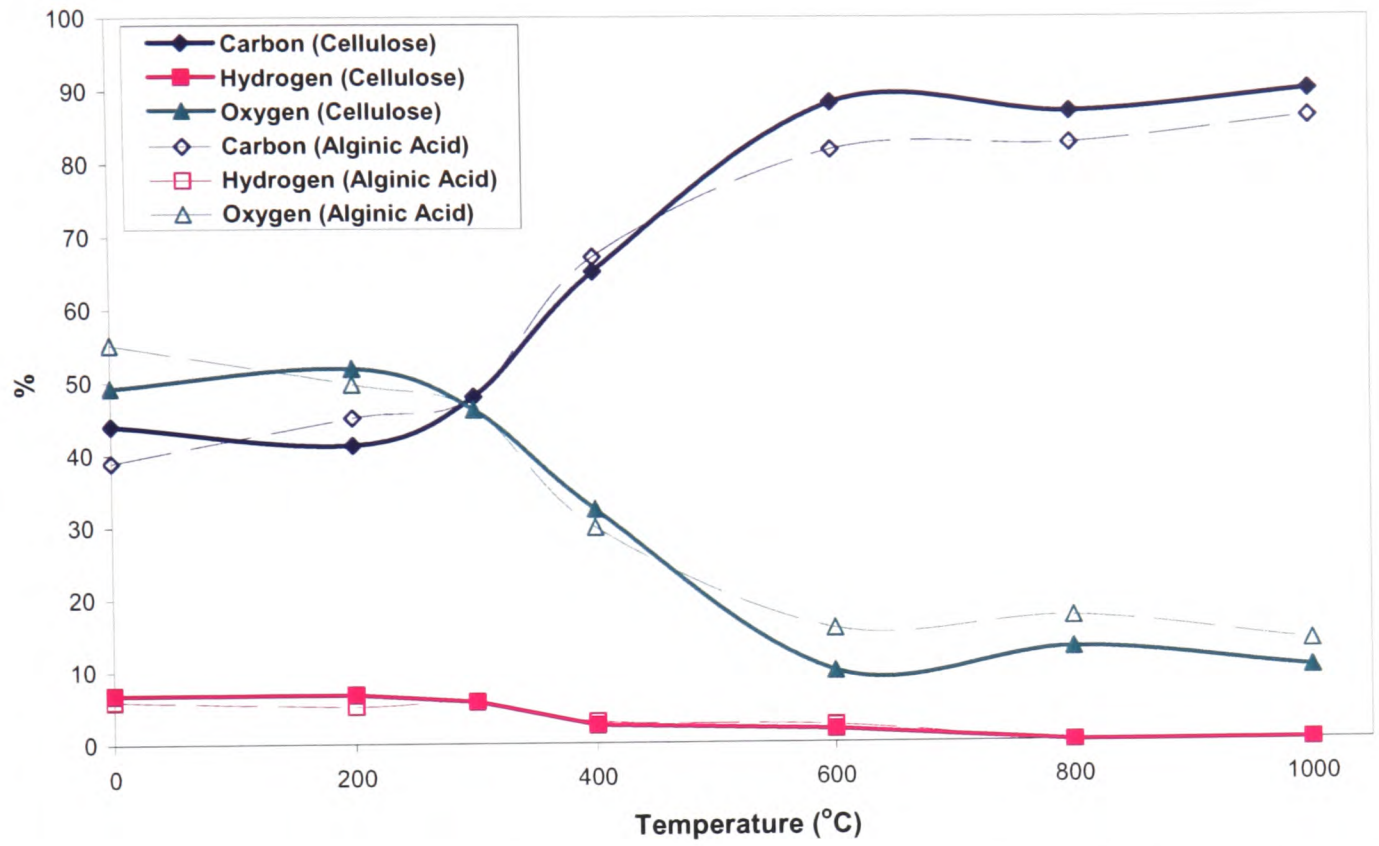

Figure 3-40. Comparison of the elemental composition of cellulose and alginic acid chars formed at different heat treatment temperatures under nitrogen.

The calculated empirical formulae of the two samples at the different HTTs under the two different atmospheres are shown in Table 3-4. It can be seen that both sample's residues become increasingly carbonaceous with increasing temperature. In the case of hydrogen the instrument was not capable of detecting the element at very low concentrations, so there is likely to be some hydrogen at the higher temperatures. In the case of the oxidising conditions the same trends are seen but at lower temperature, indicating that oxygen has some accelerating effect on the process. However at higher temperatures, 600°C and above for cellulose and 1000°C for alginic acid, there is no residue detected.

Table 3-4. Empirical formulae for cellulose and alginic acid as a function of heat treatment temperature, calculated using the elemental analysis of the chars and normalised to $C_6H_xO_y$.

	Heat Treatment Temperature (°C)	Nitrogen			10% Oxygen		
		C	H	O	C	H	O
Cellulose	0	6	10	5	6	10	5
	200	6	11.9	5.7	6	12	5.7
	300	6	8.8	4.3	6	3	2.5
	400	6	2.8	2.2	6	0.9	2.2
	600	6	1.5	0.5	-	-	-
	800	6	-	0.7	-	-	-
	1000	6	-	0.5	-	-	-
Alginic Acid	0	6	8	6	6	8	6
	200	6	8.3	5	6	7.5	4.9
	300	6	8.8	4.3	6	2.7	2.9
	400	6	3.2	2.0	6	-	1.5
	600	6	2.1	0.9	6	-	1
	800	6	-	0.9	6	-	0.9
	1000	6	-	0.7	-	-	-

3.3.2 ATR spectroscopy of the char samples

The char samples were analysed using an ATR accessory with the FTIR. This allows an infrared scan of the sample surface to taken, as described in the experimental section. The main difference between the two raw materials is the functional groups on the glucose rings, an alcohol for cellulose (Figure 1-1) and a carboxylic acid for alginic acid (Figure 1-27). The lower temperature changes in alginic acid may be due to the carboxylic group being more reactive than the alcohol group under these conditions.

The ATR technique allows discrimination between the two untreated samples of cellulose and alginic acid (Figure 3-41). The cellulose spectra show a number of key features of the molecule.

There is prominent peak at 3500cm^{-1} due to the OH groups and a smaller peak at 3000cm^{-1} representing CH bonds.

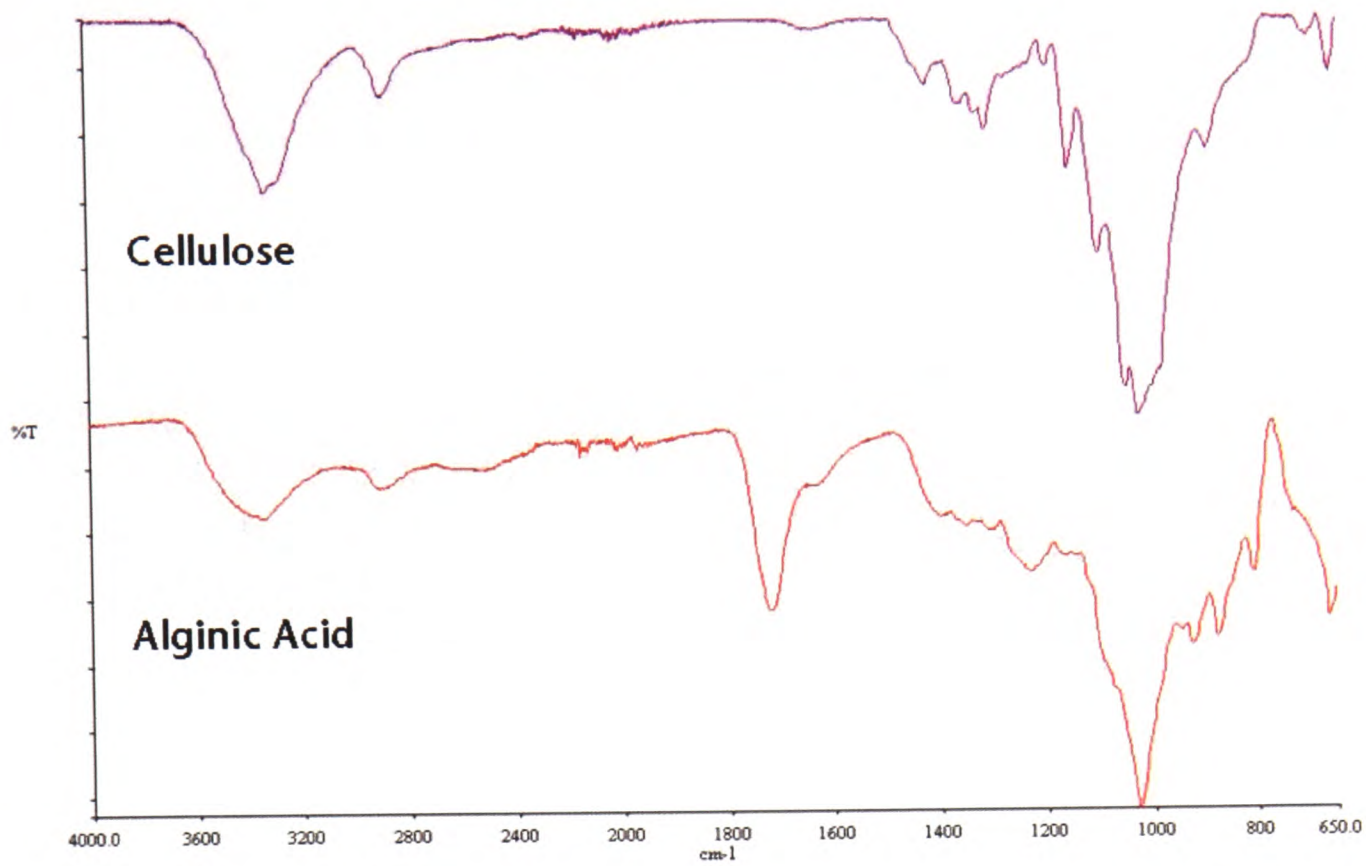

Figure 3-41. Comparison of the infrared spectra of cellulose and alginic acid using ATR.

The region between 900 and 1200cm^{-1} is due to a combination of OH bonds and the glucosidic links between the monomer units. These features are consistent with the known structure of the material [62]. The alginic acid shows some of the same features as cellulose, but there is an additional carbonyl peak at 1700cm^{-1} due to the carboxylic functional group (-COOH).

Figure 3-42 shows the infrared spectra of cellulose chars formed at different heat treatment temperatures under nitrogen. The spectrum of untreated cellulose is also shown in the figure. The residue from the 200°C heat treatment sample shows little difference to the untreated sample of cellulose. At 300°C there are some changes as peaks begin to emerge at 1600 and 1700cm^{-1}. These are attributed to the formation of C=C bonds in the molecule (1600cm^{-1}) and formation of some carbonyl functionality (1700cm^{-1}) as the cellulose decomposes. At 400°C and 600°C these two new peaks increase in size, in particular the 1600cm^{-1} peak as the carbonyl functionality is also decomposed at higher temperature. The hydroxyl peak and the saturated CH peaks at 3500 and 3000cm^{-1} respectively are almost completely gone. Also the peaks between 900 and 1200cm^{-1} are diminished indicating break down of the polymer structure and further loss of the hydroxyl groups on the glucose rings. Above 800°C the spectra are consistent

with that of a sample of pure powdered carbon. These findings agree with the findings of Sekiguchi and Shafizadeh [62], despite the differences in the methodology and the cellulose source.

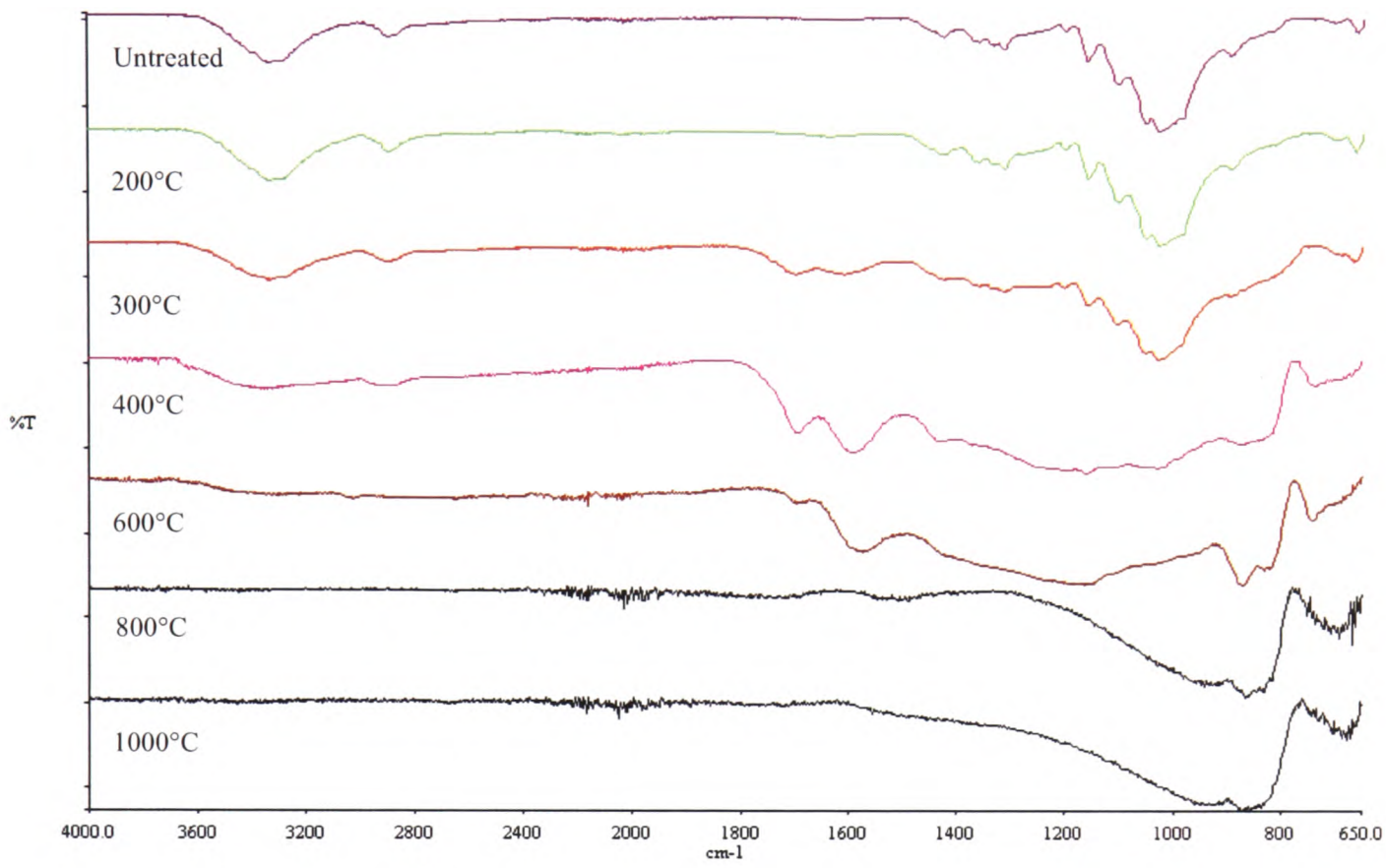

Figure 3-42. Infrared spectra of cellulose char formed at different heat treatment temperatures under nitrogen.

With an oxidative atmosphere (10% oxygen in nitrogen) a similar pattern emerges for cellulose compared to non-oxidising conditions (Figure 3-43). The principle difference is that the full oxidation of the residue occurs at a lower temperature, such that there is no measurable residue from the 800°C and 1000°C samples.

The 600°C sample residue is also similar to that of the pure carbon powder sample. There is also a small peak at 1400cm^{-1} which could be an ether bond (-C-O-C-) which may be related so some residual glycosidic bonding in the polymer structure or some cross-linking.

The spectra of alginic acid char formed in non-oxidising conditions are shown in Figure 3-44. A similar pattern of changes occurs, in that the peaks at 3500 and 3000cm^{-1} are diminished with increasing temperature. The same occurs with the carbonyl peak at 1700cm^{-1}.

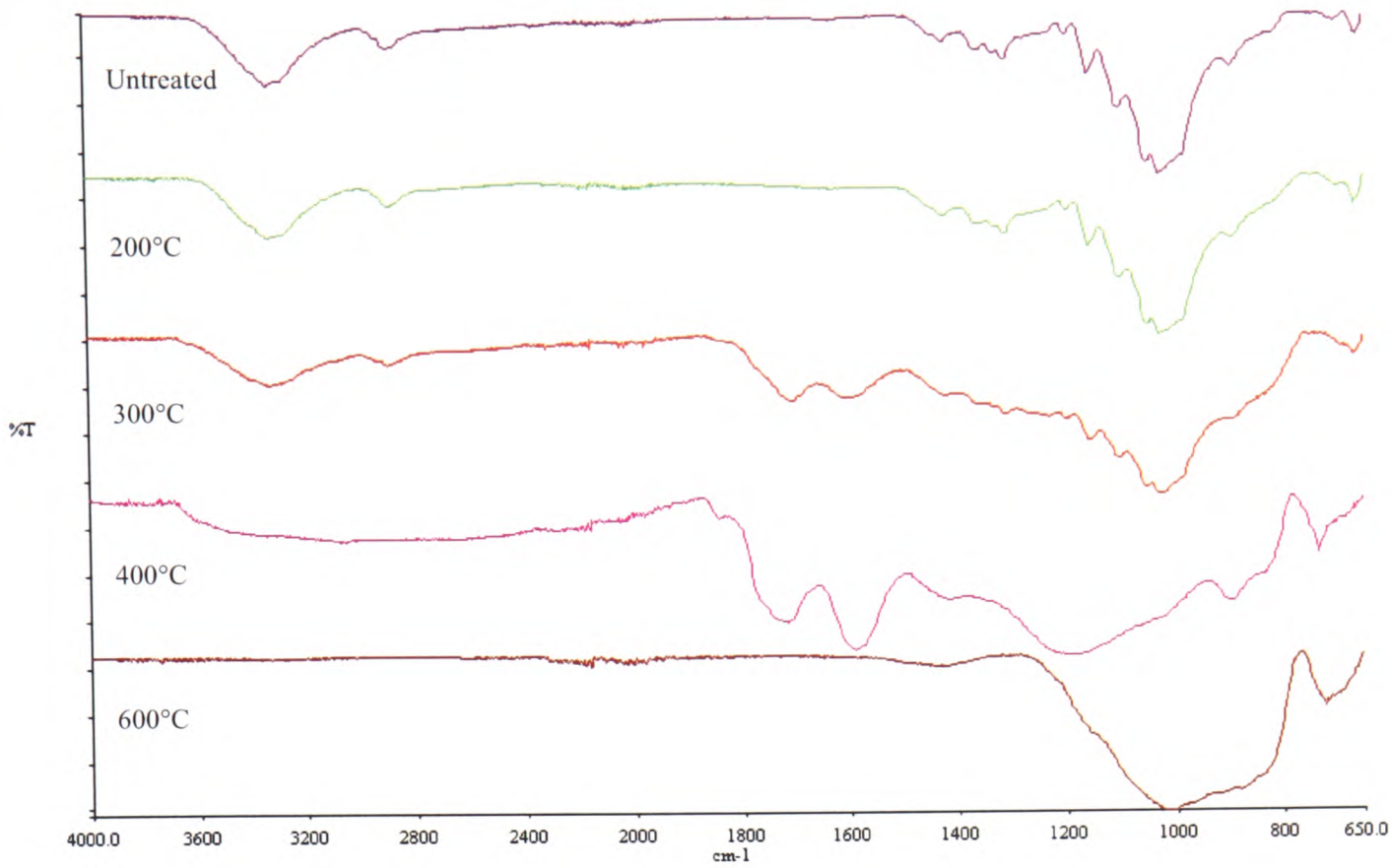

Figure 3-43. Infrared spectra of cellulose char formed at different heat treatment temperatures under 10% oxygen in nitrogen.

These changes appear to occur at lower temperature to cellulose, the C=C peak at 1600cm^{-1} is visible at 200°C whereas in the cellulose tested it appears at 300°C (Figure 3-42). A peak is observed at 1100cm^{-1}, particularly at 400°C and 600°C which may be attributable to an ether bond (-C-O-C-) which could be the remaining glycosidic bonding of the polymer chain [128].

As in the case of cellulose, for alginic acid in an oxidising atmosphere there is some similarity when compared with non-oxidising conditions. However, there are some notable differences, in particular a new peak at 1400cm^{-1} is observed at 300°C, which is particularly prominent at 400°C. This is likely to be an ether functionality, which is commonly related to the glycosidic bonds in the polymer backbone.

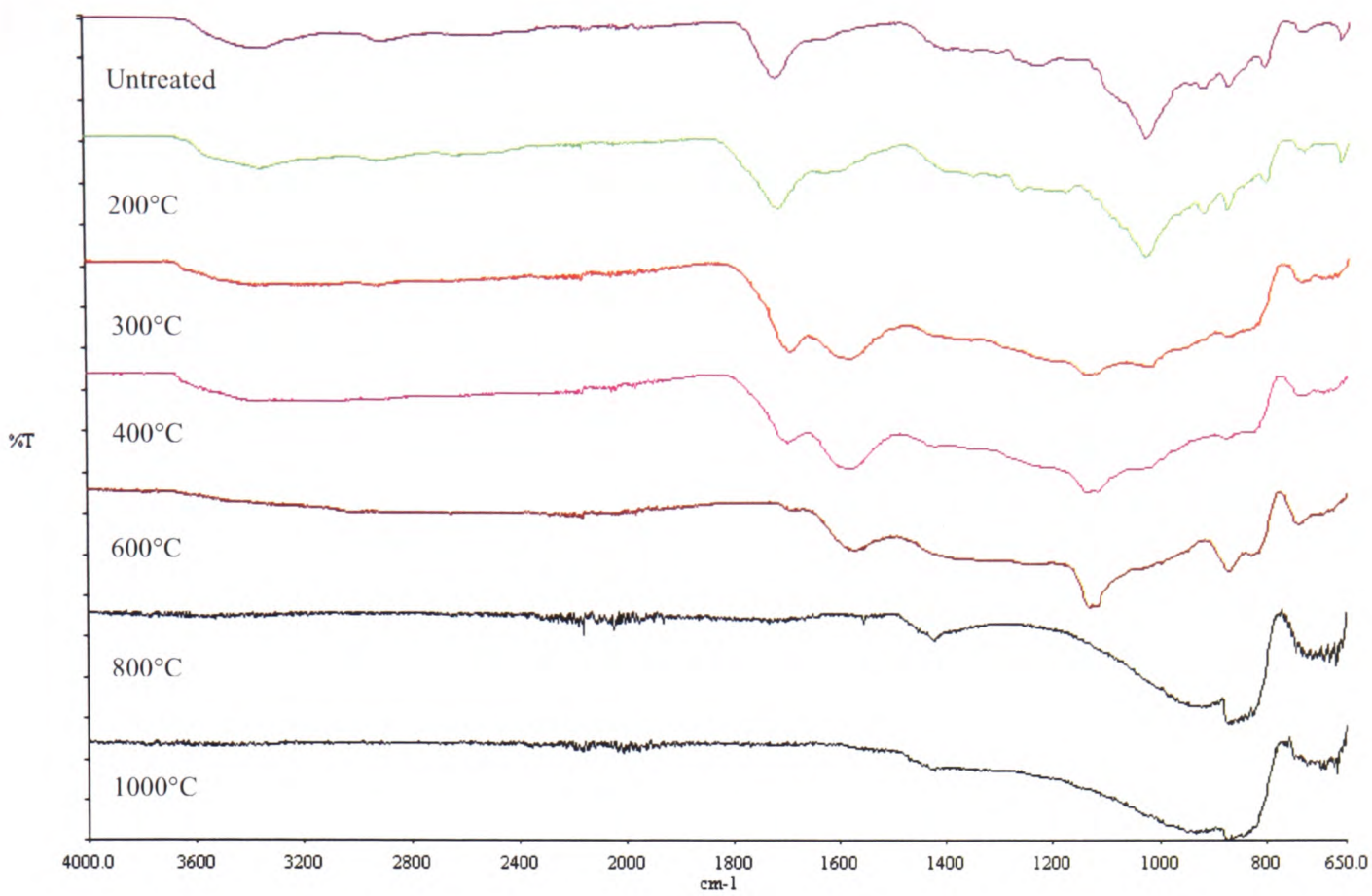

Figure 3-44. Infrared spectra of alginic acid char formed at different heat treatment temperatures in a flow of ~300ml/min nitrogen.

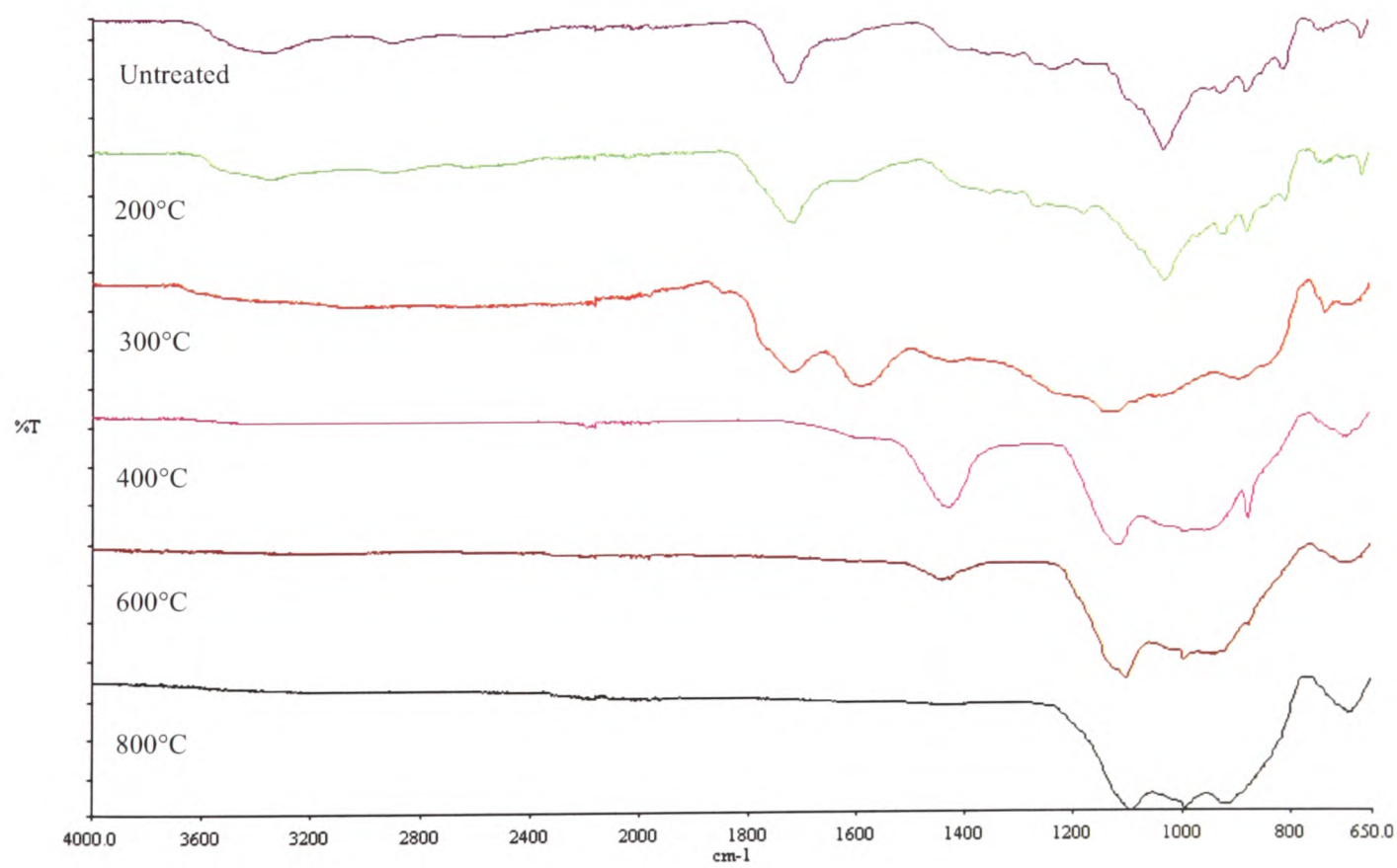

Figure 3-45. Infrared spectra of alginic acid char formed at different heat treatment temperatures in a flow of ~300ml/min nitrogen containing 10% oxygen.

Also by 400°C the peaks observed at 1600cm^{-1} and 1700cm^{-1} in the samples prepared under nitrogen are not present. As in the case of cellulose there was no residue from the 1000°C sample, but unlike cellulose spectra resembling carbon is not observed until 800°C. These differences are most obvious in the spectra of the chars prepared at 400°C, as shown in Figure 3-46.

This comparison clearly shows different features in the spectra which imply a different mechanism of decomposition occurs in an oxidising atmosphere at this temperature. There are three distinct peaks which could relate to ether (-C-O-C-) bonds at 1400, 1100 and 880cm^{-1}. Of these peaks only one, at 1100cm^{-1}, is visible in the sample prepared in nitrogen, but this more likely due to the glycosidic linkages

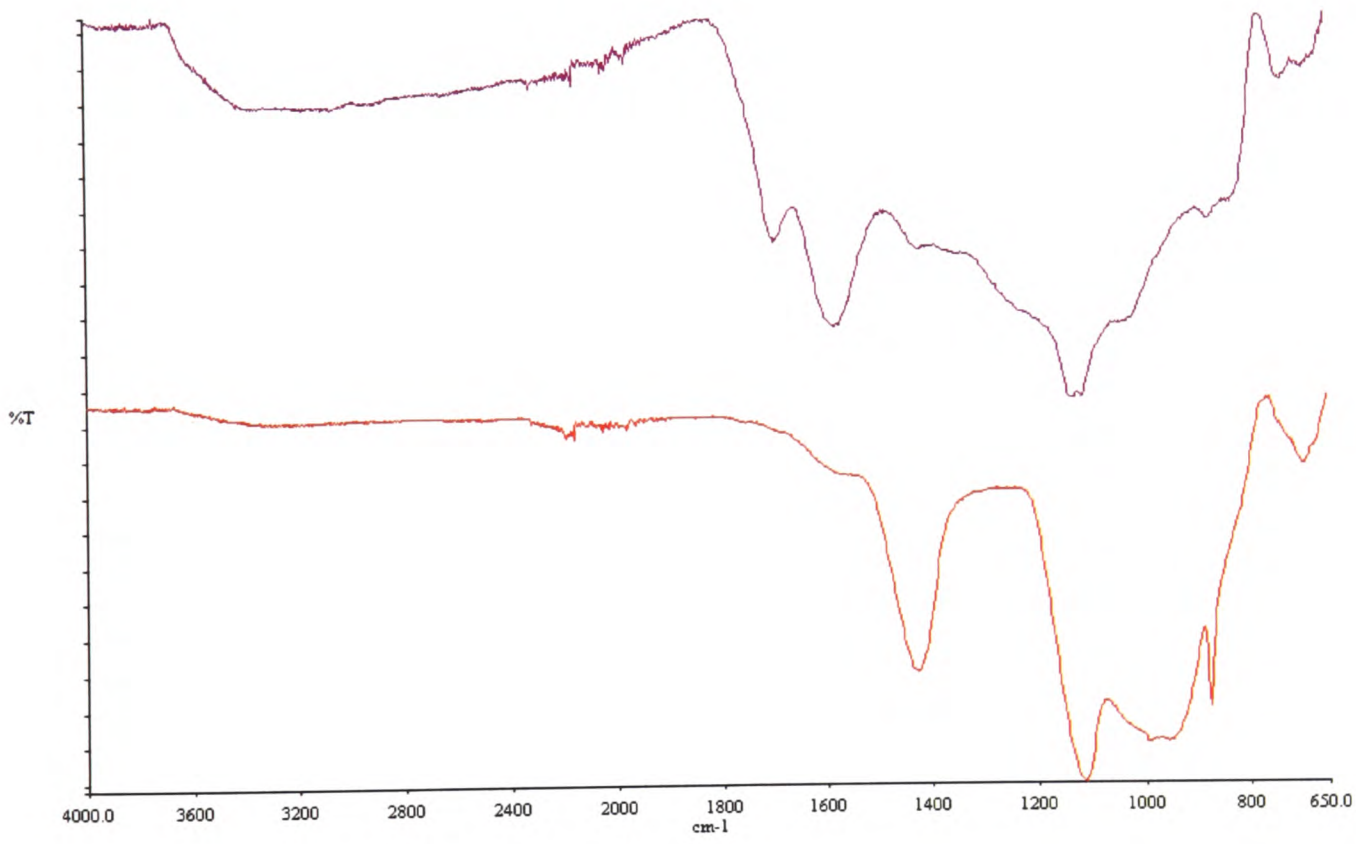

Figure 3-46. Comparison of the spectra of alginic acid char prepared at 400°C under nitrogen and 10% oxygen in nitrogen.

3.3.3 Summary of the char analysis

The char characterisation shows some agreement for cellulose below 400°C and good agreement above 400°C. Alginic acid shows similar amounts of char formed at temperatures below 400°C and more above 400°C compared with cellulose. The elemental composition of the chars from

the two samples is similar at lower temperatures. However above 600°C there is a lower amount of carbon in the alginic acid compared to the cellulose char. This may imply that there is less aromatic character in the char compared with cellulose chars. Using the ATR analysis it is possible to observe the different functional groups as a function of char preparation temperature and decomposition atmosphere. However, these changes in functional groups alone are not enough to depict a complete structural picture for the complex char combustion and pyrolysis reactions.

The cellulose chars formed under nitrogen in this work display characteristics in their spectra that are cited in the literature [62]. It is also seen that the effect of preparing the cellulose chars in an oxidising atmosphere appears to lower the temperature at which the changes in the spectra occur. However, there appears to be no difference in the spectral peaks observed. This would indicate that the rate for cellulose decomposition up to 400°C is accelerated by the presence of oxygen, but the mechanistic pathways remain much the same. At high temperature, above 400°C, under the mixed oxygen/nitrogen the cellulose residues are more completely oxidised with little residue remaining above 800°C.

Price and Horrocks [101], who studied burn retardants in cotton fabrics, produced a model for cellulose decomposition. Their detailed model of cellulose combustion showed some oxidative processes use the oxygen already contained within the cellulose molecule. This agrees with the findings here, in that the mechanism is accelerated by atmospheric oxygen but not changed by it. Alginic acid, however, does appear to show some differences below 400°C with the addition of oxygen. In particular the emergence of the ether functionalities and the more rapid loss of the carbonyl and C=C bond peaks (1700 and 1600cm^{-1} respectively). At higher temperatures a more complete oxidation of the residue is observed, in similar fashion to cellulose but at higher temperature, 800°C vs. 600°C.

CHAPTER 4 DISCUSSION

This section is divided into three parts. The first part examines the experimental technique and in particular the data mining process used to make the qualitative and quantitative measurements in this study. The second part considers the experimental results for cellulose in the context of the literature available. The final section discusses the alginic acid results to elucidate its thermal degradation pathway, achieved partially through comparison to the cellulose picture depicted in the second part.

4.1 Using Multivariate Analysis to Treat TGA-FTIR Spectra

FTIR is a method of making real-time measurements of the evolved gases from the thermal degradation processes occurring in the TGA under the conditions described in this work.

As discussed in the experimental section of this study there is no physical separation of the evolved gases which means that the spectra observed represents complex mixtures of gases and volatile compounds. This necessitated the use of a multivariate technique to mathematically separate the constituents of these mixtures. The Target Factor algorithm used for analysing the time and temperature resolved data from the experiments is embedded in the InSight™ software module, which was modified for this study to allow rapid analysis of large numbers of species. However, the ability for the Factor Analysis algorithms to correctly identify the number of components in an unknown mixture is dependant on the spectra of the components being distinguishable from one another. This means that correct selection of the spectral window is important. By performing this analysis over a wide wavenumber range, a whole section of spectra can be analysed rather than just a major band which will give statistically a more accurate result. In this study the author used a wavenumber window (generally 200cm^{-1} in width) to capture a section of a spectrum with a number of finger-print absorption peaks. Other studies have used FTIR to measure evolved gases in real-time [94, 120, 124], but in those studies they used an individual absorption peak to identify and quantify their target compounds. This method is only useful when the targeted compound can be unambiguously associated with the absorption peak. This is seldom the case when an FTIR technique is used to investigate the thermal degradation mechanism of a complex substance.

4.1.1 Multivariate Analysis by InSight™

The ability to perform the complex mathematical operations of multivariate techniques is only really practical via computers. The mathematical solution, multivariate analyses, is complex and for this study was encapsulated in a core software module, (InSight™, DiKnow Ltd, 84 Rushdean Road, Rochester, Kent, UK.) that facilitated not only the separation, but the qualitative and quantitative measurement of selected compounds from complex spectra.

By automating the analysis to search the data set for each of the pre-determined target reference compounds a rapid overview could be generated for each experiment. As the matching process is a mathematical correlation between the reference spectra and the extracted factor within a given spectral region (usually a window of 200cm^{-1}), there is potential for compounds with similar functional groups to have high correlations although the match may not be correct. As a result the need to select an appropriate correlation level is paramount, as can be seen in comparison of Figure 3-20 with Figure 3-21. By selecting a high correlation threshold a large amount of detail can be lost, however the use of a higher correlation does not necessarily improve the accuracy of the matching. In this study the correlation level used was correlation coefficient $\geq$ 0.80; this somewhat arbitrary level provides acceptable compromise for an overview of the compounds formed by heating the samples. It is then up to the operator's judgement, based on the samples under investigations, to accept or reject the software's identification.

The quantification steps using the software were also carried out under an automatic mode. For each of the target compounds, a visual check of the matching quality was made. Once considered acceptable, it was carried out manually using a narrower spectral range. The absorbance of the sample spectra was then converted to concentration using a predetermined calibration graph for the particular compound. The concentration is taken from an average of a number of points (usually 3) across the spectrum in the set spectral window. By using a smaller wavenumber window (~50cm^{-1}) there is less chance of inaccuracy caused by points being taken from peaks and troughs in the spectrum, and from other factors such as baseline drift, or artefacts in the extracted spectrum.

4.2 Thermal Degradation Pathway for Cellulose

The thermal degradation mechanism for cellulose has been extensively studied as reviewed in the introduction chapter. However, despite these efforts, there are still some discrepancies over

the exact mechanism of decomposition. In this section, parallels between the results of this study and those commonly agreed in the literature are drawn with the intention to develop the most appropriate reaction pathway for the thermal degradation of cellulose under the current experimental conditions. Where difference occurs, the likely mechanism underlying the experimental trends is proposed through examination of the data presented in Chapter 3.

4.2.1 Analysis of Cellulose Char

The TGA work shows the effect of changing the sample mass on the thermal decomposition of cellulose. It appears that the sample mass has little effect on the temperature at which degradation occurs (Figure 3-1), however the increased sample mass does lead to increased char yields (Figure 3-2). This will have direct implications on the nature or the amount of volatiles produced. It may also show that char formation is likely to be affected by mass transport, i.e. a larger sample will restrict the release of primary pyrolysis products and they in turn contribute to some secondary char formation. This may take place via either vapour phase or via solid state reactions [26, 53, 61]. Increasing the ramp rate (Figure 3-3 and Figure 3-4) has the effect of raising the temperature at which this main thermal degradation step occurs. This evidence is clearly linked to the sample's thermal lag. This is caused by the fact that the sample temperature is measured by a thermocouple that is in close proximity to the sample pan, but not in actual contact with the pan. A larger sample mass will therefore require more energy to produce a constant temperature increase. At a high heating rate, the larger the sample the wider the temperature gap between the sample and the set furnace temperature. In this study with a 10mg sample mass, with a ramp rate of 60°C/min the deviation of sample temperature from the programmed temperature after 1 minute run time was 12°C. At the slower ramp rates the deviation is lower, 5°C deviation for 30°C/min ramp rate; and less than 1°C for the 5°C/min and 10°C/min ramp rates. However, the instrument automatically adjusts the heating power to bring the sample temperature into step with the programme as rapidly as possible. All of the TGA and DTG plots in the study are of sample temperature.

The work shows a single weight loss event that occurred between 330 – 380°C, which agrees with the range of temperatures quoted in the literature [19, 38, 52, 54], i.e., 280 – 385°C. The addition of 10% oxygen to the furnace gas shows no effect on the thermal degradation process below 450°C (Figure 3-14), but above this temperature a second weight loss event is observed.

In similar fashion to the non-oxidising samples there is a slight increase in the observed temperature at which the degradation occurs (Figure 3-8 and Figure 3-9).

Under non-oxidising conditions a residual char remained, but under oxidising conditions this char was close to zero on further heating to above ~650°C, possibly oxidised. This supports the high temperature oxidation of the char as one of the decomposition routes [26, 61, 69, 70].

The 1400cm^{-1} peak detected from the cellulose char (Figure 3-43) can be attributed, at least partially, to an ether bond (-C-O-C-). The presence of the ether bonds during the thermal degradation of cellulose is still being debated in the literature [36, 43, 44]. A hypothetical route responsible for the inter-chain ether linkage has been proposed before, Figure 4-1 [21]. The evidence gathered from this work weighs positively towards such an intermediate step.

The mechanism described by Figure 4-1 involves a displacement process of an acetal oxygen from a neighbouring chain at the glycosidic linkage. Moldoveanu [21] suggests that this is energetically more favourable than reactions occurring at the hydroxyl groups at C2, C3, or C4 positions of cellulose with the elimination of water. Furthermore, a glycosidic bond would produce a weak peak at 1100cm^{-1} in cellulose char obtained at 400°C [47, 128]. Therefore it seems that the peak at 1400cm^{-1} is most likely to be evidence of ether bonds forming in the char.

Generally, polymers with no cross-linking will melt on heating, whereas, cross-linked polymers will undergo an irreversible degradation process [6].

Visual observation of the cellulose during the TGA experiments show that it appears to melt but a solid char remains after heating (an irreversible degradation process). This indicates that the cellulose is not cross-linked initially, but some cross-linking occurs during the decomposition process. This loss of the small peak at 1100cm^{-1} shows that the glycosidic bond is also broken during the decomposition process, which is described by Figure 4-2.

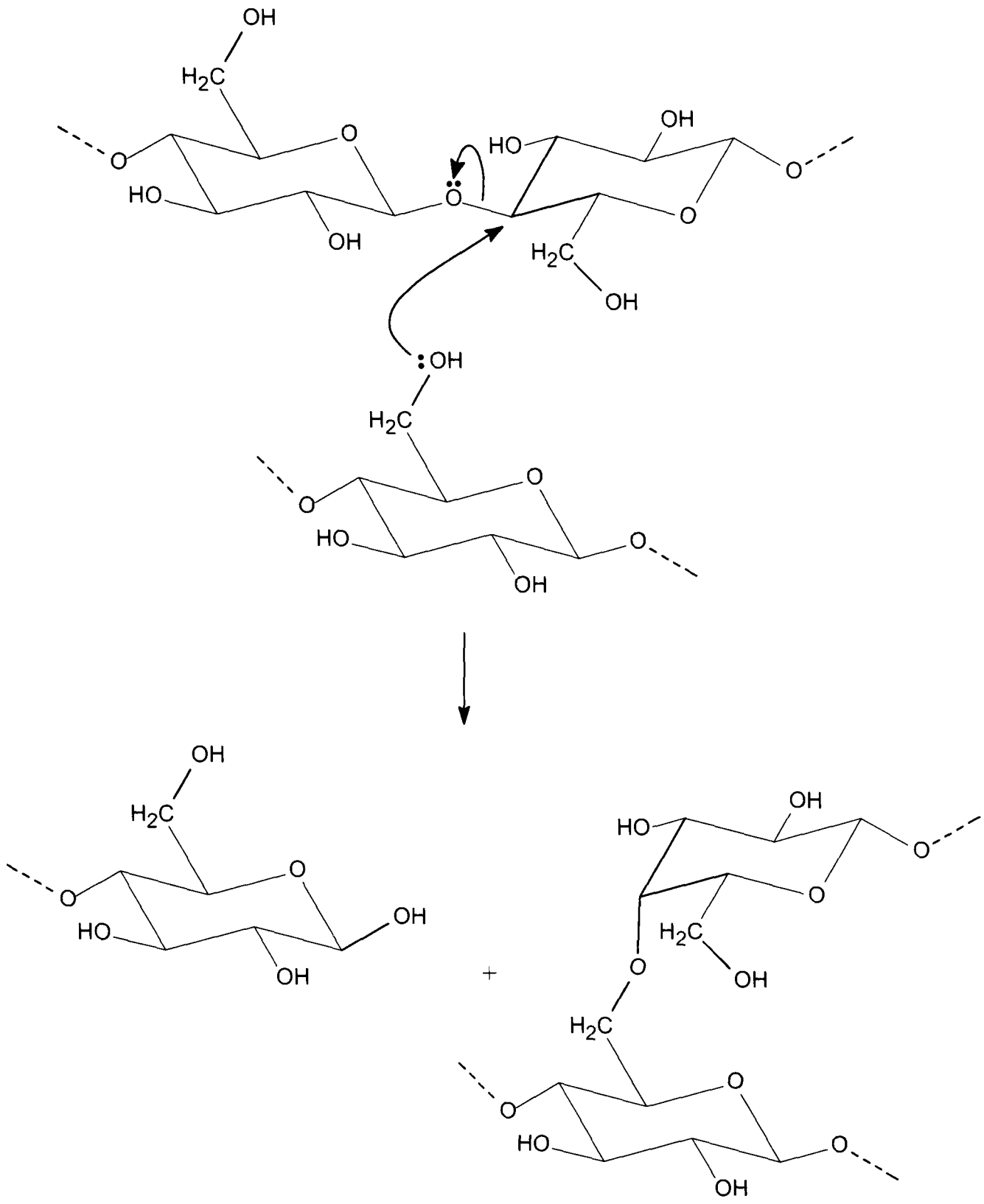

Figure 4-1. Potential mechanism for the formation of inter-chain ether bonds in cellulose [21].

The breaking of the glycosidic bond under heating shows the formation of two different end groups, one levoglucosan and the other a hydroxyl group.

The char analysis also showed the appearance of the 1700cm^{-1} peak, due to the presence of C=O bonds. These bonds began to appear at 300°C and reached a maximum at 400°C. They then decreased in intensities at 600°C in non-oxidising conditions (Figure 3-42) and were completely absent in oxidising conditions at the same temperature (Figure 3-43). This formation of the C=O bond may be analogous to the oxidation process for glucose (Figure 4-3).

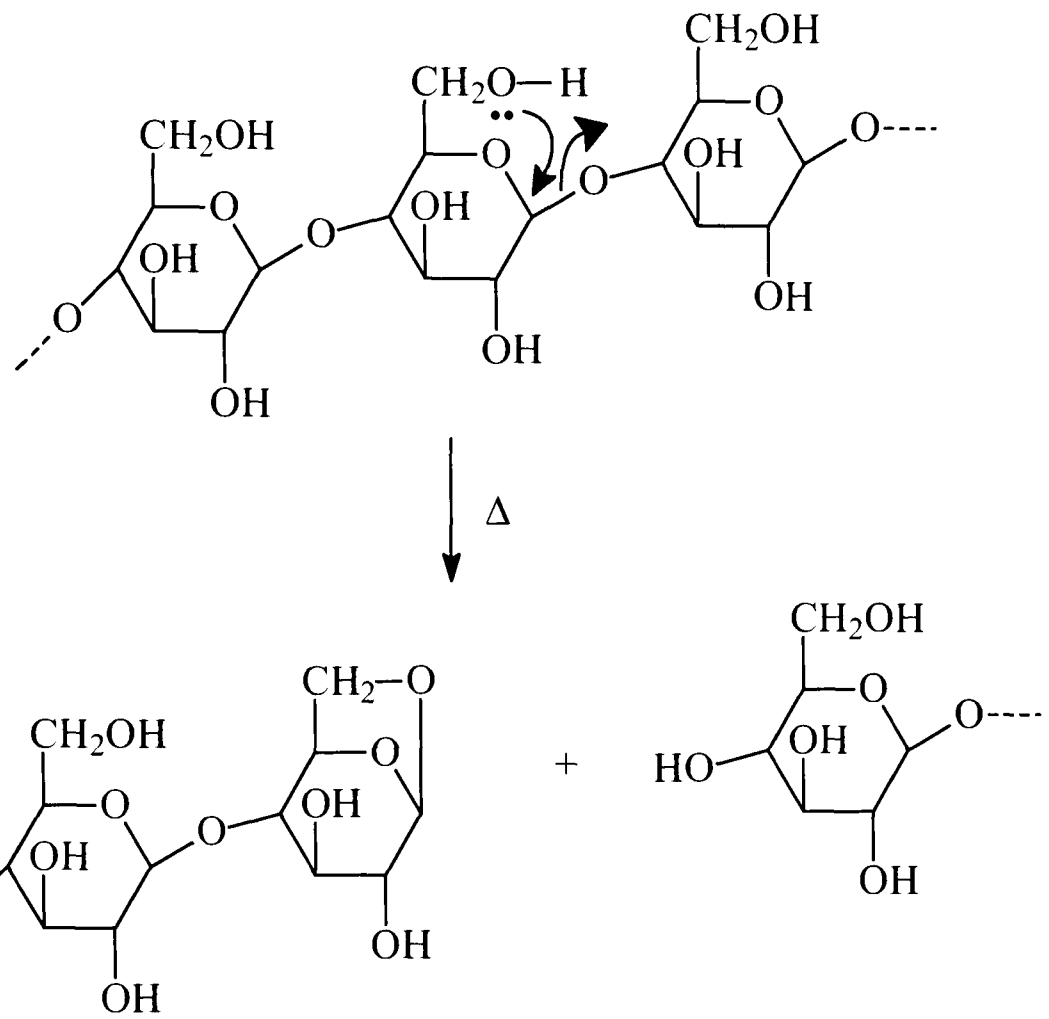

Figure 4-2. Cleavage of the glycosidic bond in cellulose |21|.

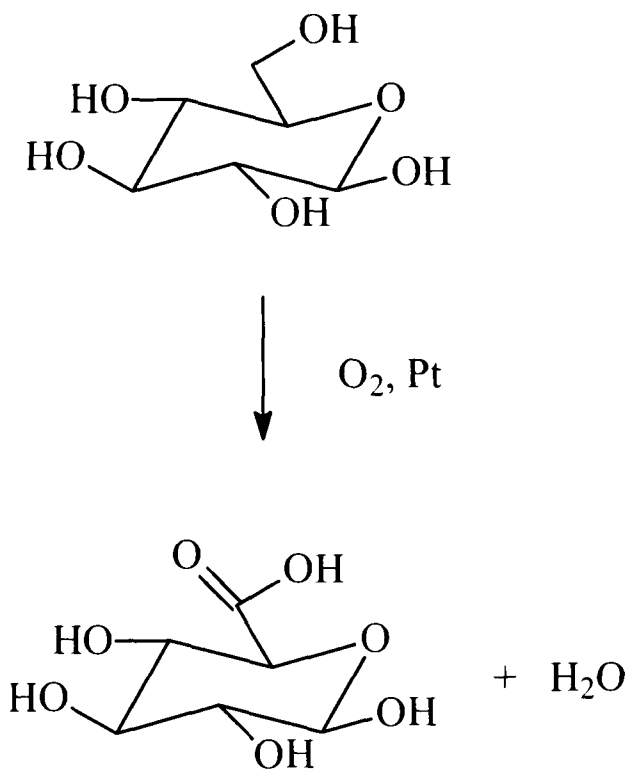

Figure 4-3. Mechanism for the oxidation of glucose |150|.

In this mechanism, the oxidation of the primary hydroxyl group to a carboxylic acid takes place over a platinum catalyst in the presence of oxygen. At higher temperatures this reaction needs no catalyst. However, for cellulose, the appearance of the C=O bond peak also occurred under non-oxidising conditions; therefore oxygen liberated from the cellulose itself must contribute to the oxygen molecule required for the reaction.

The char results (Figure 3-42 and Figure 3-43) clearly indicated two different char types: [47, 62, 63], one with aliphatic character dominating at lower temperatures and another with increasing aromatic character at higher temperatures. The addition of oxygen into the reaction atmosphere did not change the initial char formation process other than to accelerate it; this is reflected by the changes in absorption features at lower temperatures (Figure 3-43). However, at temperatures higher than 650°C, the char material is completely combusted.

Under non-oxidising conditions, the char prepared at 800 and 1000°C shows similar infrared characteristics to activated carbon (Figure 4-4). Similar spectra are observed for the cellulose char sample formed at 600°C under oxidising conditions (not shown). The increase of carbon content in the residue, from 40% in untreated cellulose to over 90% at 1000°C, illustrates that the unsaturated char broke down further to an almost pure carbon at these temperatures. The empirical formula of the char residue changes from $C_6H_{10}O_5$, cellulose, to $C_6H_0O_{0.5}$ under nitrogen at 1000°C (Table 3-4). Under oxidising conditions the change is from $C_6H_{10}O_5$, cellulose, to $C_6H_{0.9}O_{2.2}$ at 400°C with no detectable solid remaining beyond this temperature. This last feature was not observed by Shafizadeh and Sekiguchi [47] in their study of cellulosic char, as they used a maximum of 600°C under nitrogen which produced empirical formula of $C_6H_{3.2}O_{0.9}$ (Figure 3-37).

The results presented in this work cannot answer the fundamental question on the char formation under inert atmosphere. Nevertheless, the above discussion highlights the fact that the nature and character of the cellulose char strongly depended on the preparation method. These properties also change with increasing temperature and often more than one type of structure can be observed. This may account for the many different views found in the literature.

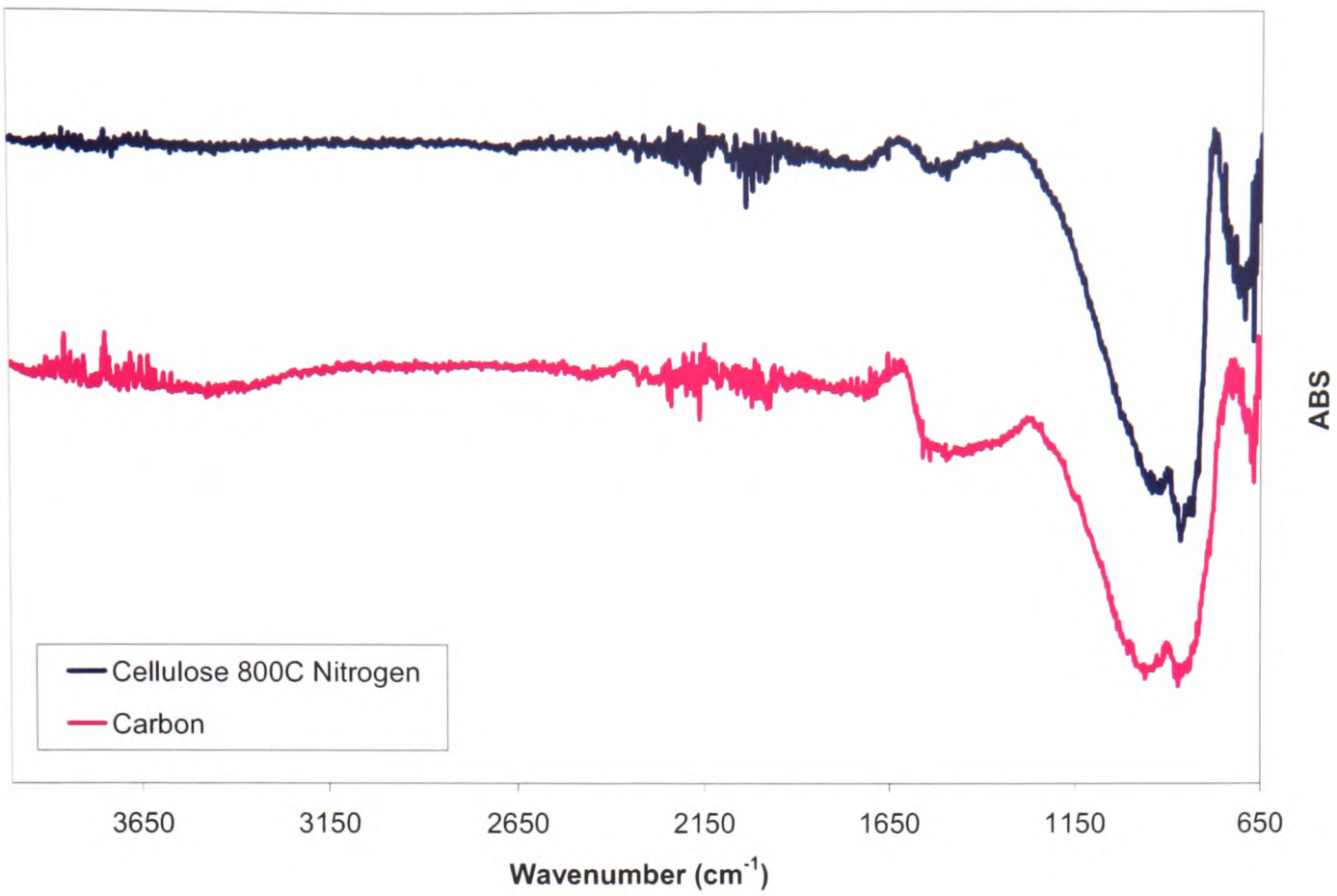

Figure 4-4. Comparison of ATR spectra of activated carbon with cellulose char formed at 800°C under nitrogen.

4.2.2 Spectroscopic Analysis of Volatiles from Cellulose

Qualitative identification and quantitative profiling of the volatiles released from the degrading cellulose are the main task of the multivariate analysis. The dominant gases evolved from the cellulose experiments (Figure 3-20 and Figure 3-21) are consistent with the literature [21, 34]. The major difference between the gas atmospheres is that methane was only observed in the non-oxidising condition.

Evolution profiles (yields vs. time or temperature), rather than the absolute quantities of the quantified compounds, are presented because they provide detailed information about the thermal decomposition process. For example, profiling allows the temperatures of formation to be clearly identified for individual reaction steps, which, after linking to other compounds being generated or consumed at the same temperature regions, aids the construction of a mechanistic pathway for the overall decomposition of the sample.

Six of the qualitatively identified volatile compounds were chosen for quantitative analysis – acetaldehyde, acetic acid, acrolein, carbon monoxide, carbon dioxide and water vapour. The selections represent major combustion gases – CO, CO_2 and water; and the remaining three are carbonyl compounds that are likely to be important decomposition products of cellulose that are sufficiently abundant to be detected. The quantitative profiles for these six compounds under

different atmosphere and temperature ramp rates are shown in Figure 3-23 through to Figure 3-30.

The results showed that these six compounds formed closely to the main weight loss step measured by the TGA. The peak evolution temperature for the compounds was always slightly higher (~20°C), for example the CO_2 profile in Figure 4-5, which is almost certainly due to the effect of the delay in transfer from the TGA to the FTIR. Therefore the observed thermal lag in this work may come from three sources: the delay by the transfer line (approximately identical for all evolved species as the gas flow rates were kept constant), the different sample weight (discussed before), and finally the effect of ramp rate.

The low ramp rate (5 and 10°C/min) experiments, showed no acrolein from the cellulose under either atmosphere. However, at the two higher ramp rates (30°C/min and 60°C/min), acrolein was detected under both atmospheres.

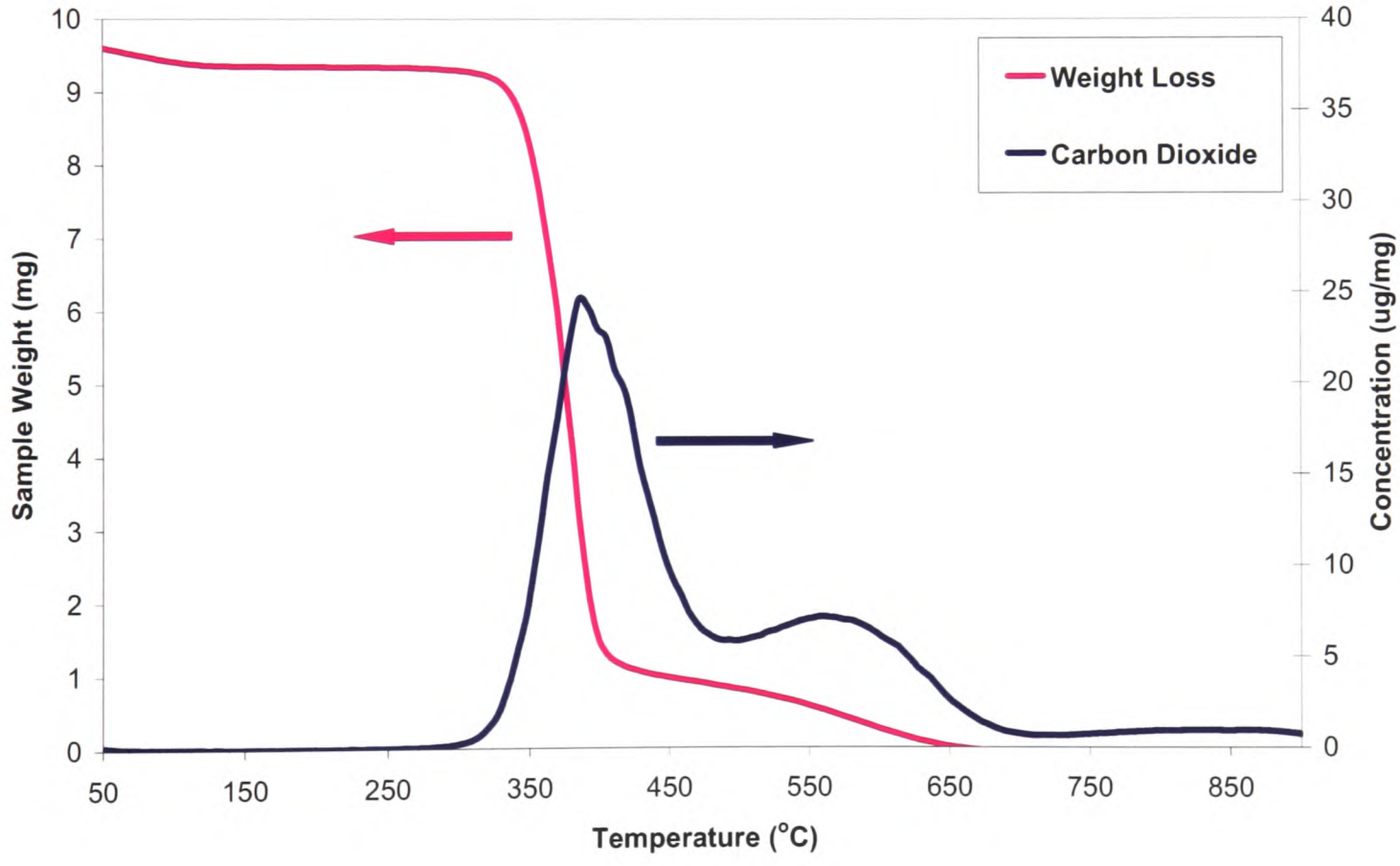

Figure 4-5. Weight loss curve of cellulose compared with the evolution profiles for carbon dioxide demonstrating that the evolution profiles reflect closely the weight loss events for the sample.

Acetaldehyde was detected under both oxidising and non-oxidising conditions. Under oxidising conditions the amount of acetaldehyde decreased with increasing ramp rate (Figure 3-32), but

under non-oxidising conditions there was no clear trend (Figure 3-31). This indicates that the presence of atmospheric oxygen was not required for the formation of acetaldehyde, but it did have an effect on the amount of the compound formed. A possible route is for ring opening to occur with elimination of a hydroxyl group,

Figure 4-6 , followed by the scission of the C4-C5 bond. This eliminates an enol group which may then rearrange to form acetaldehyde. Similar mechanistic steps may be true for other aldehydes.

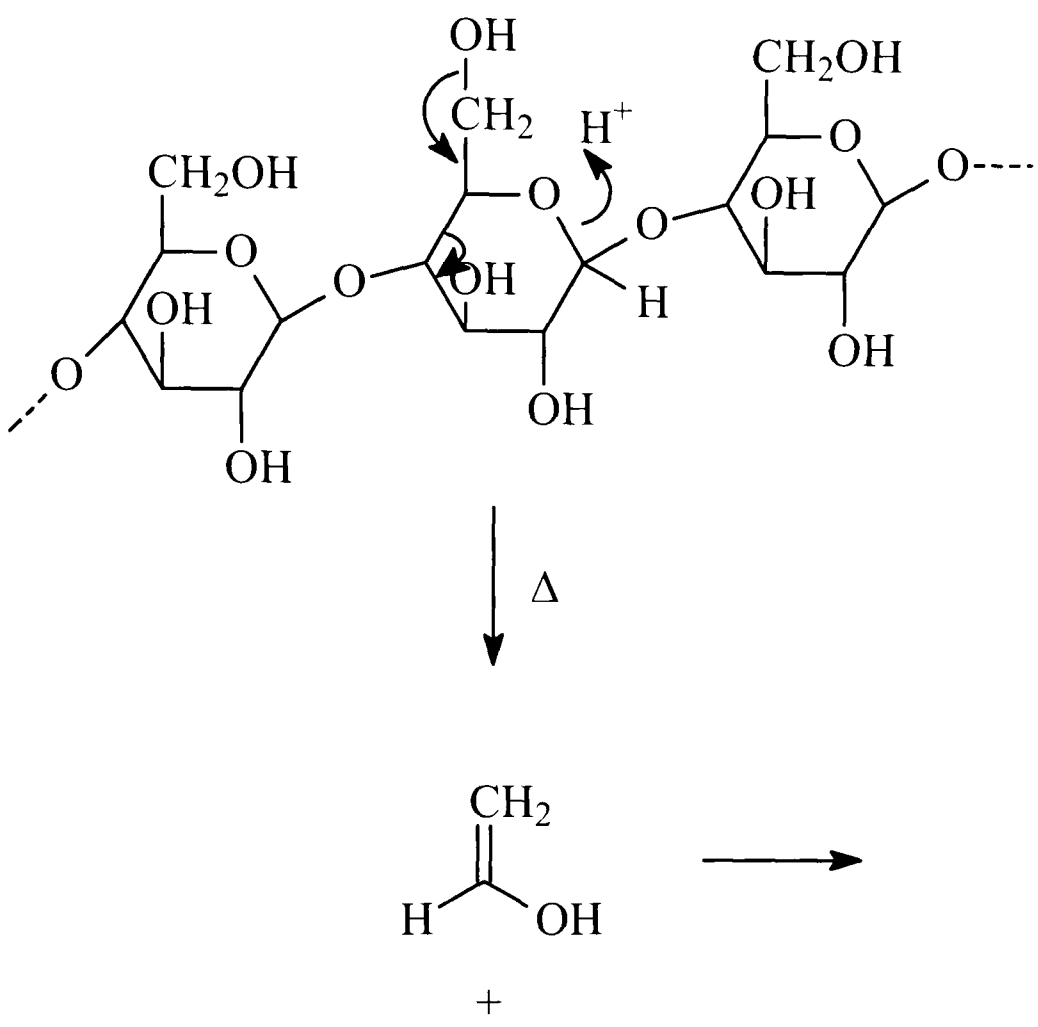

Figure 4-6. Proposed route for the formation of acetaldehyde via chain scission of the cellulose molecule.

Another example of a chain scission mechanism is given in Figure 1-23. In Figure 1-23, the eliminated compound is hydroxyacetaldehyde which is a potential route for the formation of acetic acid. Figure 4-7 shows that the hydroxyacetaldehyde (a) dehydrates rapidly at temperatures above 200°C to form ketene (b) which will recombine with water to form acetic acid (c). Sanders et al [107], show acetaldehyde as a direct product of cellulose via dehydration

of open chain cellulose fragments; and also as secondary pyrolysis products of anhydrosugars (Figure 1-25).

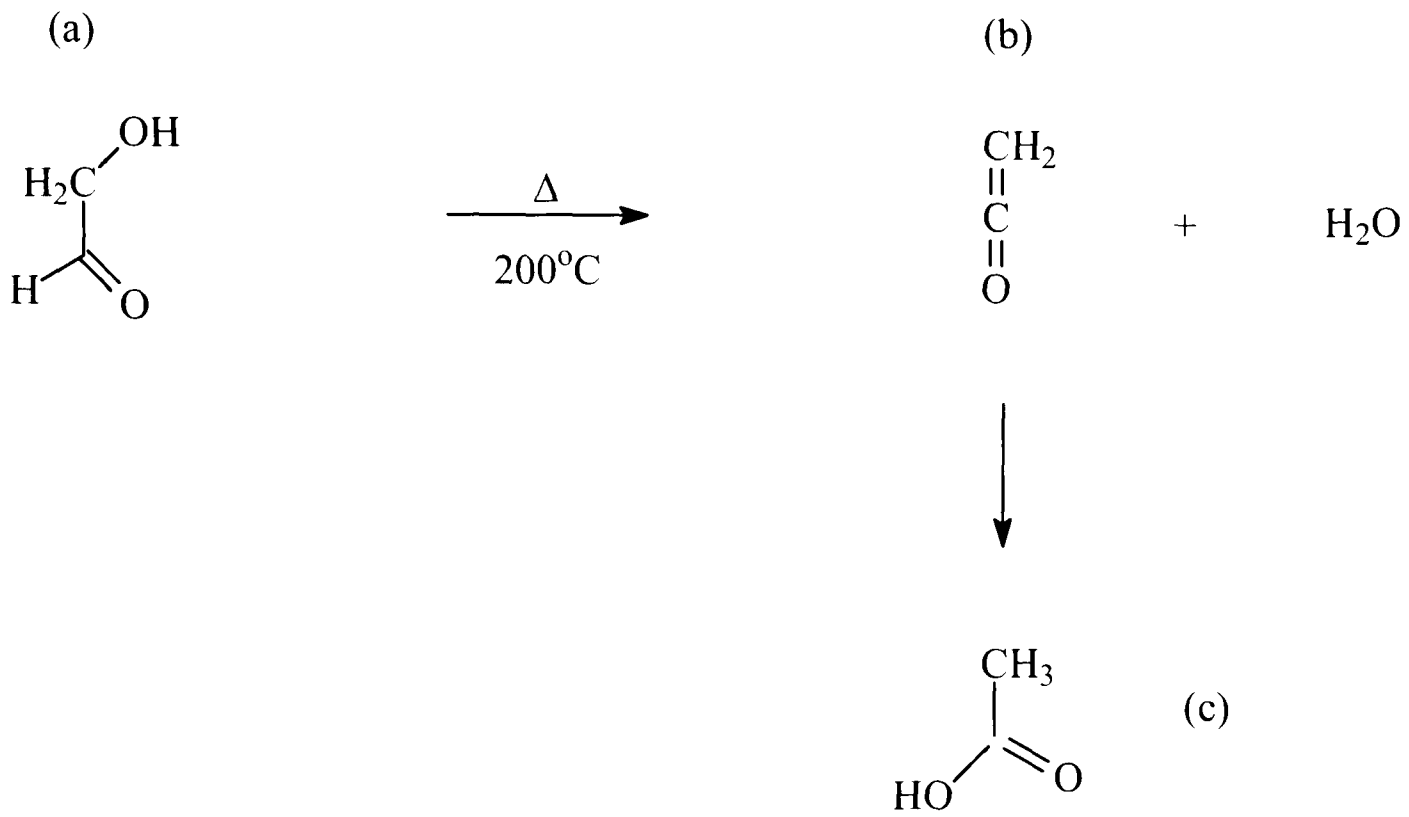

Figure 4-7. Reaction of hydroxyacetaldehyde (a) to form acetic acid (c) via a ketene (b) intermediate step [12].

CO and CO_2 formation is thought to be further oxidation of the primary decomposition products and the oxidation of the residual char. The total amount of acetaldehyde, acetic acid and acrolein in oxidising conditions (Figure 3-32) is decreased compared to those in non-oxidising conditions (Figure 3-31). This indicates that oxidation of the primary compounds is a method for the formation of CO and CO_2. In non-oxidising conditions this must occur via the oxygen available within the cellulose structure. The CO and CO_2 concentrations are increased in oxidising conditions which is likely due to the oxidation of the residue via the oxidation of carbon at active sites in the char, described in section 1.2.5 [65, 69]:

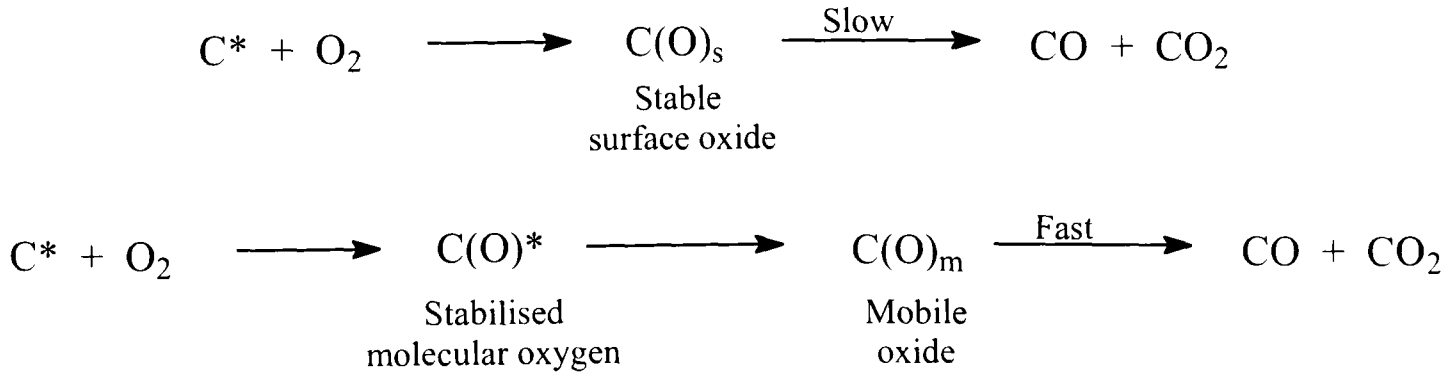

The change in ramp rate had little effect on the totals of the six analytes measured in this study (Figure 3-31) under non-oxidising conditions, with the exception of water, which does appear reduced with increasing ramp rate.

Under oxidising conditions the increasing ramp rate had the effect of decreasing all of the gas phase analytes, with the exception of CO_2 (Figure 3-32). A possible reason for this could be in the larger range of temperatures experienced by the primary products during their residence time in the furnace will be greater allowing secondary reactions and oxidation to occur. This would explain the increased amount of CO, CO_2 and water under these conditions.

Under non-oxidising conditions methane is identified as an evolved compound (Figure 3-21) but it is not present under oxidising conditions. At temperatures below 800K in oxygen, methane oxidises through a complex series of reactions.

Figure 4-8 shows a simplified mechanism [151] for this process, however other researchers have identified hundreds of mechanistic steps, both elementary and reverse, involving 33 species [24].

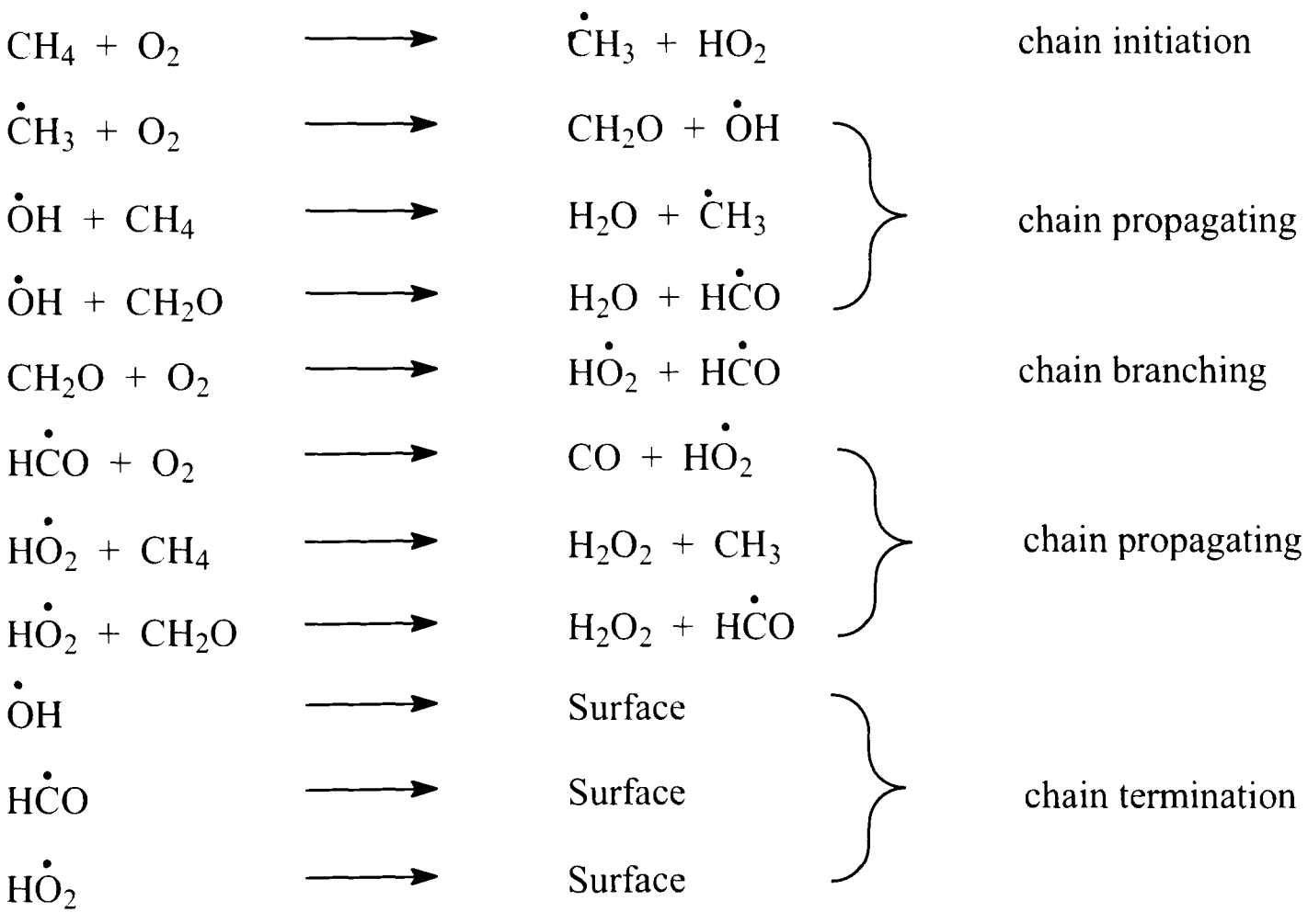

Figure 4-8. Simplified mechanism for the oxidation of methane at low temperatures [151].

It is therefore clear that there are numerous mechanisms for formation of smaller molecules from cellulose during thermal degradation. Moldoveanu [21] shows that a number of smaller molecules may be derived from the cellulose monomer ($C_6H_{10}O_5$) with elimination of CO, CO_2, formaldehyde or water (Figure 4-9).

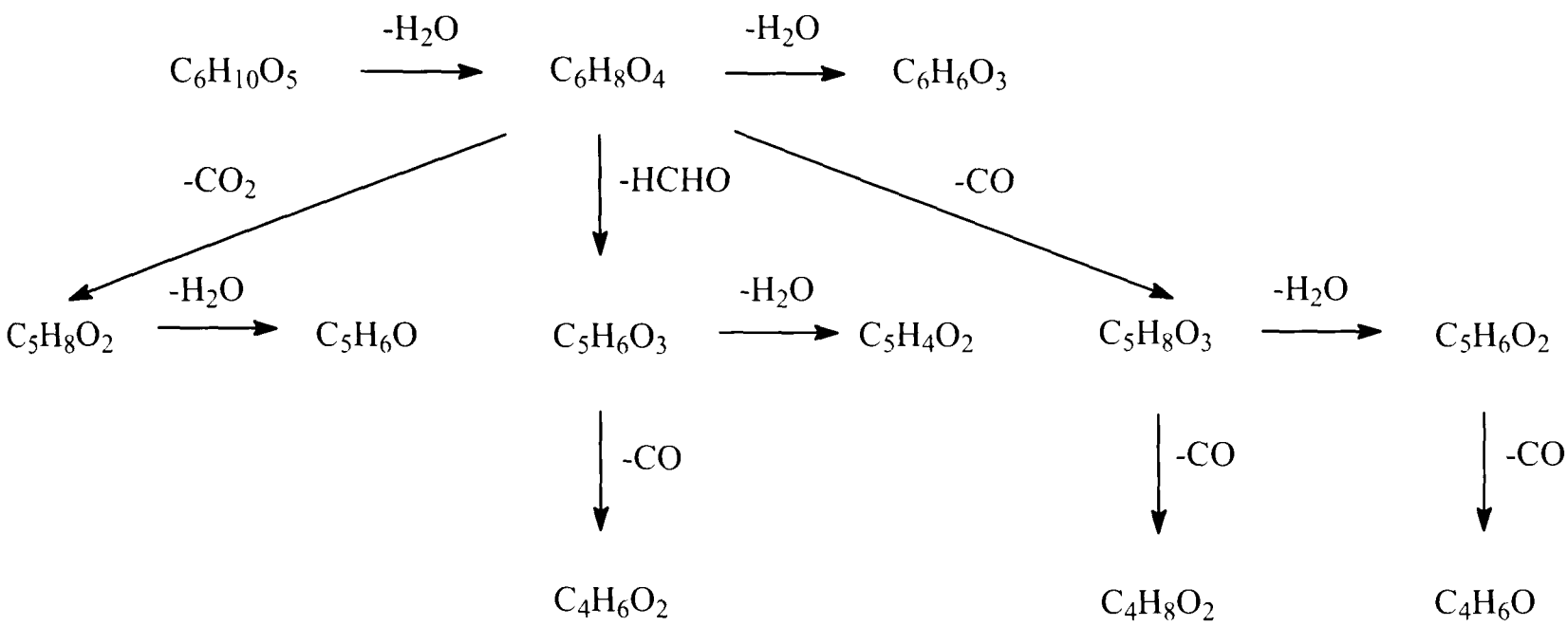

Figure 4-9. Formation of small molecular weight compounds from the cellulose monomer, deoxyglucose [21].

4.2.3 Cellulose summary

Both the solid residue and the evolved volatiles from cellulose degradation have been discussed in the chapter. Where possible mechanisms of formation are identified and compared with the literature. The exact nature of the active cellulose (cellulose*) is unclear from this study, and in the opinion of this work, it is not important as far as the rest of the decomposition routes are concerned. It is important to note, however, that preliminary structural change took place, as seen in the char study at 300°C and its loss of water as well as the evolution of CO and CO_2.

Above 300°C the major weight loss can be caused by two distinct reaction paths, which occur simultaneously. The first path led to the formation of a char residue with formation of CO, CO_2 and water vapour, and possibly other molecules. The second path is the formation of volatile products, along with CO, CO_2 and water vapour. The spectroscopic data detected a range of different compounds between 400°C and 550°C under both atmospheres. These two pathways

are concurrent and the presence of 10% oxygen did not significantly promote or depress either of the pathways.

The effect of the oxidative atmosphere became clearer above 600°C. Under non-oxidising conditions the solid residue and any high boiling point compounds were converted into a more carbonaceous char. This was not the case in the oxidative atmosphere: the remaining char was gradually degraded into smaller molecular species such as CO at high temperatures. Above 600 – 650°C there was no measurable solid residue remaining. The IR spectra showed an additional peak of CO and CO_2 at these temperatures, and additionally the water profile showed some tailing. Without additional atmospheric oxygen the thermal energy will not break down the remaining structure fully.

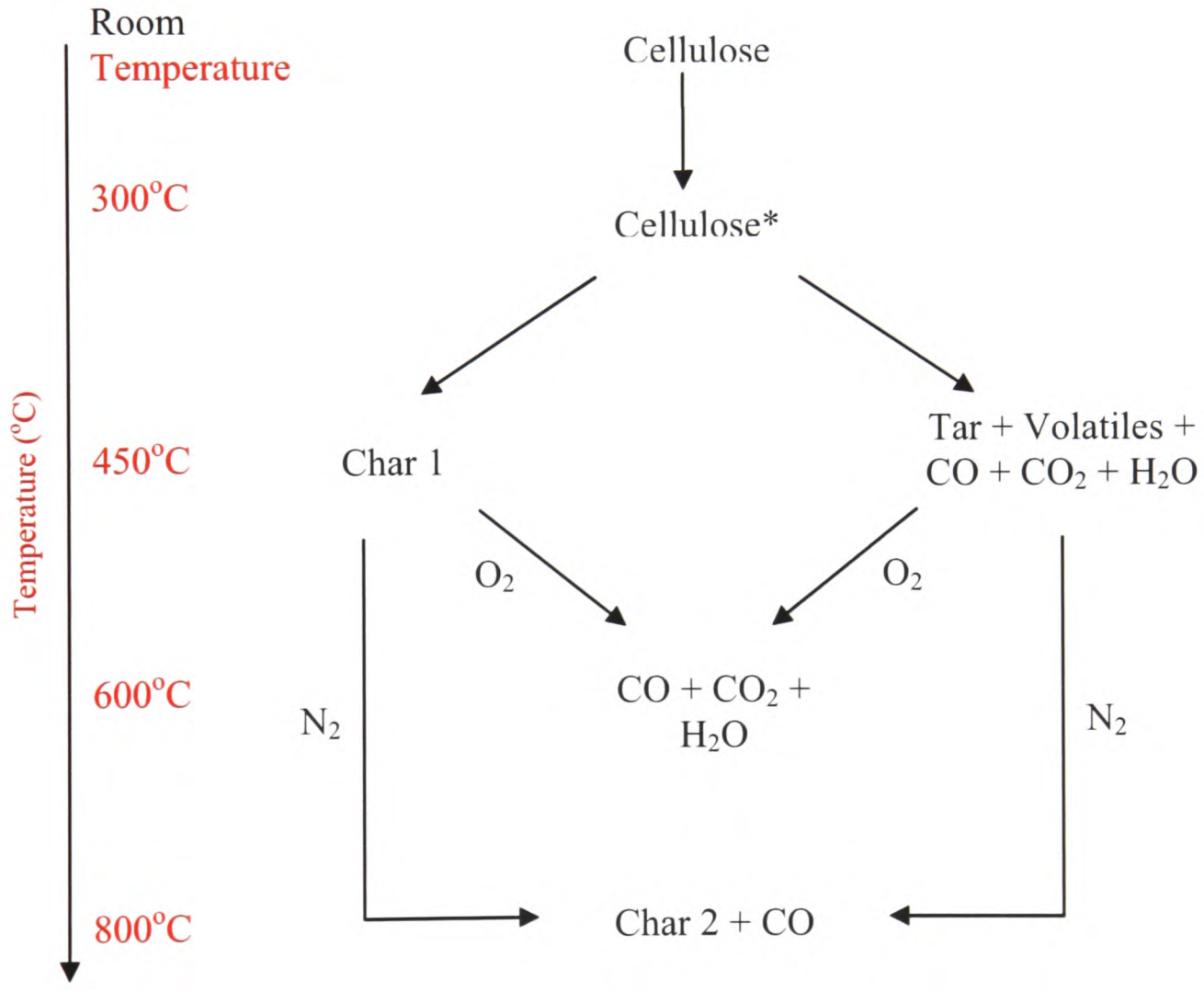

Figure 4-10. Summary of the thermal decomposition of cellulose described by the results of this study. The temperature scale is approximate, based on the temperature of peak evolution of the compounds evolved during the experiments.

Figure 4-10 summarises the thermal decomposition behaviour of cellulose as discussed in this chapter. Not all of the mechanistic details reported in the literature have been resolved in this work, however the pathway constructed here related closely to the most commonly agreed mechanistic pictures drawn from previous studies [53, 101]. The experimental approach used in this work is also by no means a thorough exploitation of the full capability of the TGA-FTIR-Multivariate technique. What this work clearly demonstrates is the efficiency with which the technique can be applied to establish a broader reaction mechanism for unknown materials. This will be further demonstrated by the example of alginic acid in the next section.

4.3 Thermal Degradation Pathway for Alginic Acid

In this section discussions are focused on establishing a reaction pathway for the thermal decomposition of alginic acid based on its known structural similarities to cellulose.

Alginic acid differs structurally from cellulose mainly at the functional group at C6; an alcohol group in cellulose and a carboxyl group in alginic acid. This is clearly reflected by their respective IR spectra (Figure 3-41). Alginic acid is also a block co-polymer containing β-D-mannuronic and α-L-guluronic acid monomers. These are epimers (at C5) of each other, so the two monomers have the same chemical formula and functional groups.

4.3.1 Analysis of Alginic Acid Residue

The weight loss of alginic acid (Figure 3-5) is more complex than that of cellulose. The temperature at which the decomposition occurs was lower, ~240°C vs. ~330°C. This may imply that there are different mechanisms of decomposition at different temperatures, such as depolymerisation, defragmentation and cleavage of the glycosidic bond. Figure 4-11 shows a potential mechanism for the cleavage of the glycosidic bond. This is based around the mechanism for cellulose (Figure 4-2) in which the two differing end groups are left in the polymer chain, levoglucosan and a glucose end group. In the case of alginic acid one of the end groups will have a mannuronic acid end group and an equivalent of levoglucosan on the other side of the break (2,3-dihydroxy-6,8-dioxa bicyclo [3.2.1.] octan-7-one).

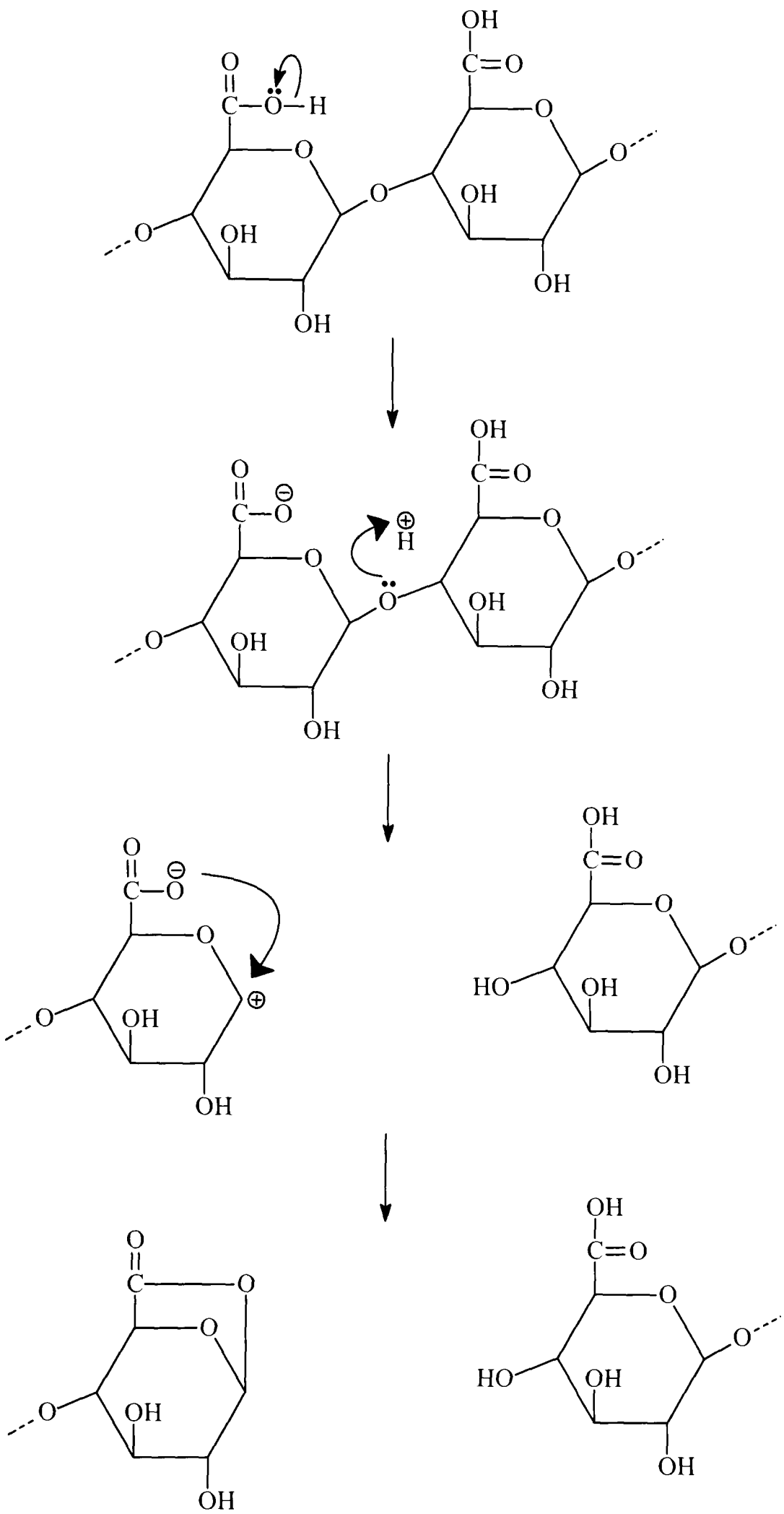

Figure 4-11. A proposed mechanism for the cleavage of the glycosidic bond in alginic acid.

Further fragmentation of the polymer may occur from this 'anhydro-mannupyranose' end group with the elimination of CO_2 (Figure 4-12). This opens the ring of the end group which may lead to further fragmentation into smaller volatile molecules.

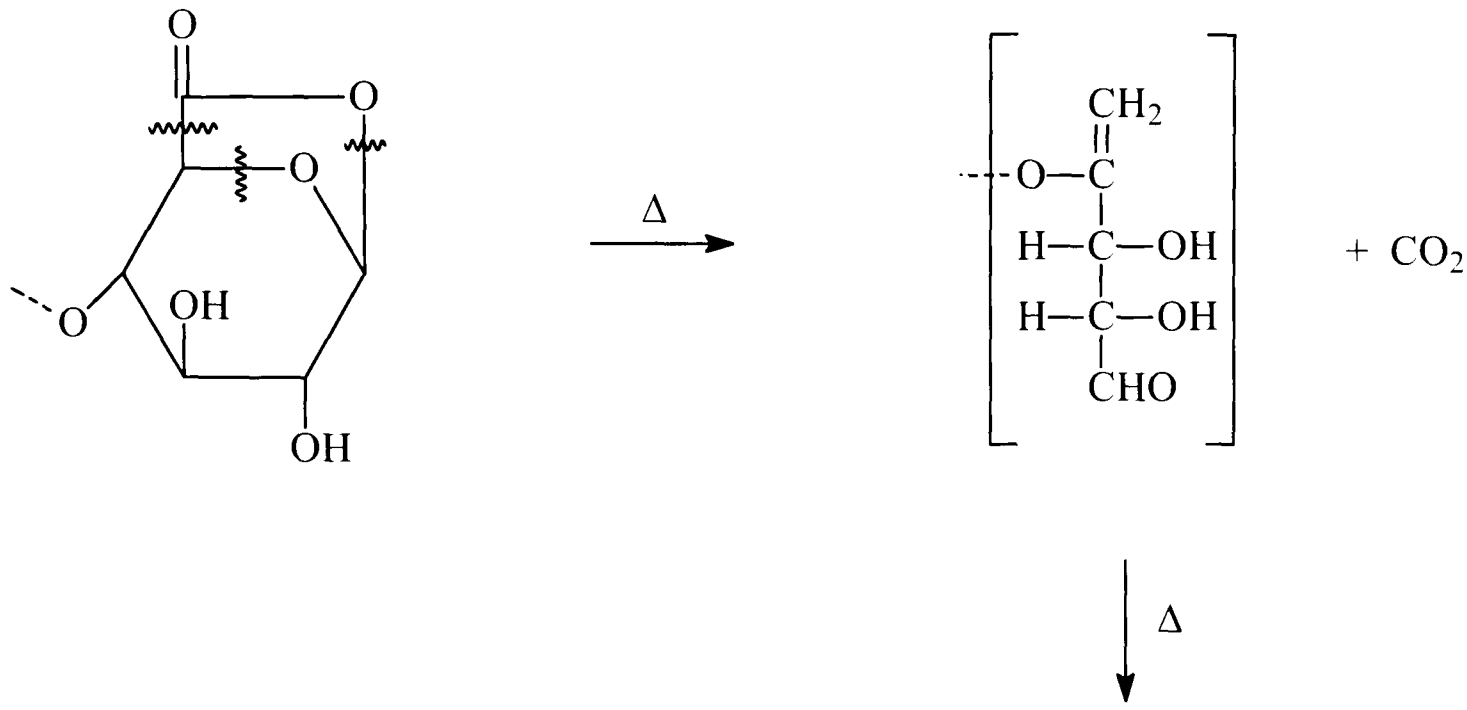

Figure 4-12. Fragmentation of the 'anhydromannupyranose' end group with the elimination of CO_2.

Under oxidising conditions (Figure 3-10) there were two additional peaks at higher temperature. This difference is seen clearly in the comparison of the 30°C/min samples shown in Figure 3-16. These additional weight losses can also be seen in the TGA profiles (Figure 3-15) and in a similar fashion to cellulose, the initial weight loss was not affected by the 10% oxygen atmosphere. Overall it was seen that the alginic acid gave more residue than cellulose under non-oxidising conditions, but with the addition of 10% oxygen to the furnace gas there was no residue (Figure 3-15). This increased char under non-oxidising conditions suggests that cross-linking is likely to occur, as cross-linked polymers tend to char rather than melt. However, the elemental composition of the char, shown in Figure 3-39, showed a similar pattern to that of cellulose (Figure 3-40). This implies that the alginic acid has a similar char forming process to cellulose, in that there is a general trend to a more carbonaceous composition at higher temperatures.

The char appeared to become more unsaturated with increasing temperature, seen in the changes in empirical formula from $C_6H_8O_6$ to $C_6H_0O_{0.7}$ at 1000°C under nitrogen; and $C_6H_0O_{0.9}$ at 800°C

in oxidising condition (Table 3-4). This increasing unsaturation of the alginic acid was also observed in the ATR spectra of the alginic acid residue as a peak appearing at 1600cm^{-1}. The peak reached maximum intensity at 600°C under nitrogen and 300°C in oxidising conditions. Above these temperatures the spectra appears similar to that of carbon under non-oxidising conditions, as seen with the cellulose sample (Figure 4-4).

The formula seemed to change in a slightly different way depending upon the atmosphere. From the information in Table 3-4 there appeared to be more rapid loss of oxygen at lower temperatures under oxidising conditions than under non-oxidising conditions. The hydrogen appears to be lost rapidly under oxidising conditions with none detected above 400°C. This may indicate that under oxidising conditions the primary mechanism of decomposition is accompanied by elimination of water. The vapour phase FTIR also showed a greater amount of water under oxidising conditions (Figure 3-34) than under non-oxidising conditions (Figure 3-33).

The carbonyl function was diminished in the char of alginic acid with increasing temperatures (Figure 3-44), indicating that the carboxyl functional group is more reactive than the alcohol function in the cellulose molecule. Figure 4-13 shows a potential route for the loss of the carboxylic function via elimination of water followed by the elimination of CO to give a double bond in the structure at C4 – C5.

This effect was repeated under oxidising conditions (Figure 3-45), but occurred even at lower temperatures. The oxidising conditions also produced a large peak at 1400cm^{-1} that may imply the presence of an ether functionality (Figure 3-46). This peak was dominant at 400°C with the carbonyl peak (1700cm^{-1}) completely diminished. At 600°C this ether functionality became undetectable. Figure 4-14 shows a potential mechanism for the formation of C-O-C bonding using a mechanism analogous to the formation of an ester from a carboxylic acid and an alcohol group on an adjacent molecule.

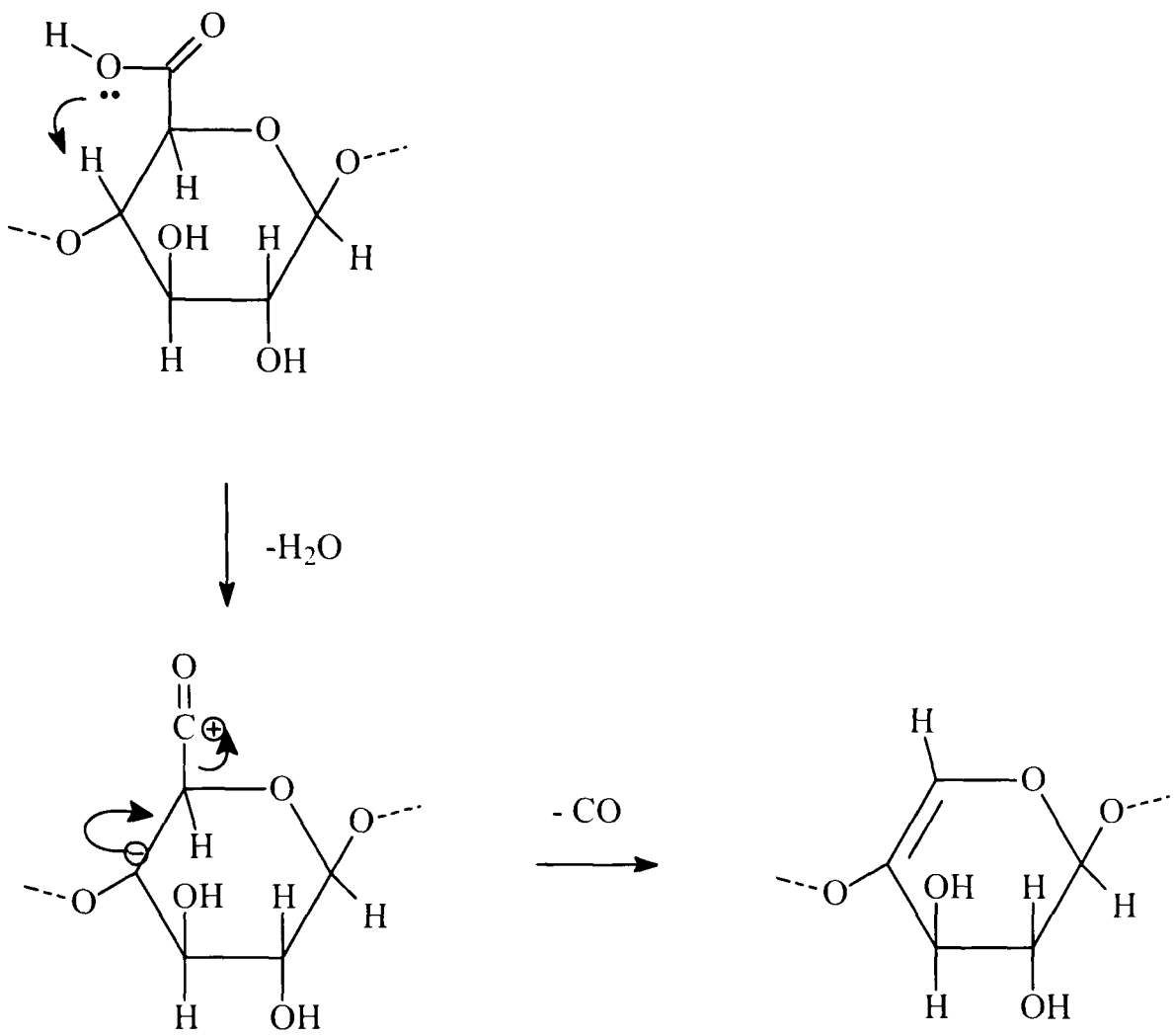

Figure 4-13. Proposed mechanism for the elimination of CO and water from alginic acid.

Though the peak at 1400cm^{-1} could represent an ether functionality, rather than an ester, there is a possibility that other peaks associated with esters could be unresolved in the broad peak between ~1200 and ~800cm^{-1} (Figure 3-44). An ester may also give peaks at around 1700cm^{-1}, and there is evidence of a second peak overlapping with the carbonyl peak at 300°C (Figure 3-44). It appears that the glycosidic bond is unbroken by this process as the peak at 1100cm^{-1} is present at higher temperatures (600°C in nitrogen and 800°C in 10% oxygen; Figure 3-44 and Figure 3-45) which indicates that the cross-linking does not involved the glycosidic bond as in cellulose (Figure 4-1).

With the addition of oxygen to the nitrogen there is a general acceleration of the charring process, with the changes in spectra seen at lower temperatures than under nitrogen. The residue is also completely oxidised under oxidising conditions, possibly in the same manner as cellulose (Section 4.2.1).

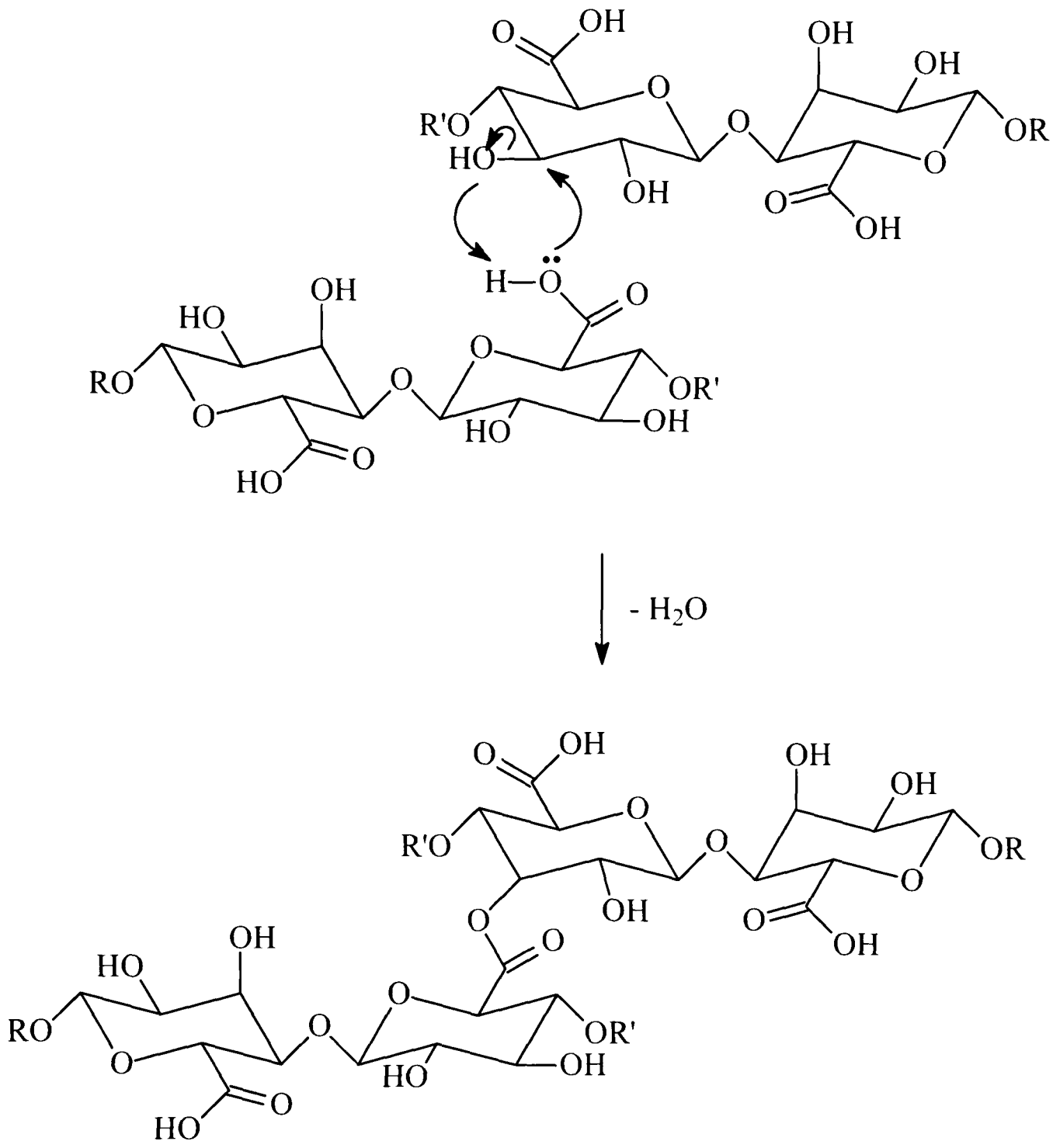

Figure 4-14. A potential route for the formation of the inter molecular cross-links in alginic acid.

Overall the charring process in alginic acid showed some similarity to cellulose. There was a changing structure of the char with increasing temperature. However, the chemistry of the cellulose char was not affected by the presence of oxygen in the purge gas, other than an acceleration of the process, i.e. the same spectral features were observed at lower HTT. The alginic acid char shows a prominent peak at 1400cm^{-1} under oxidising conditions that is not present under non-oxidising conditions. This indicates that there are two different forms of char formation at low temperatures that are dependant upon atmosphere. At higher temperatures (above 400°C) the char appears to have the same IR spectra, similar to that of an activated carbon sample.

The total amount of char residue for alginic acid was greater than cellulose (approximately 25% of starting weight compared to 5%, respectively) under nitrogen. Under oxidising conditions there was no residue left for either material above 800°C. However, there was residual char remaining for alginic acid at a higher temperature (800°C) than cellulose (600°C) which may be due to the larger amount of material to be fully oxidised. There does not appear to be any relationship between the amount of char formed and the ramp rate used in this study, which may be due to the high final experimental temperature of 900°C.

4.3.2 Spectroscopic Analysis of Volatiles Evolved from Alginic Acid

A number of the evolved products from alginic acid were similar to those of cellulose. However, formaldehyde, propionic acid, methanol, ethanol, n-propanol, acetone and furfural were all absent compared with cellulose. Only one compound, 2-furanmethanol, was observed in the qualitative analysis of alginic acid that was not observed in cellulose.

The numbers of evolved volatile compounds identified from alginic acid on heating were only affected by the change from nitrogen to the 10% oxygen atmosphere (Figure 3-21). Under non-oxidising conditions, the following additional compounds were found – methane, 2-furanmethanol, and 2-butanone. Butanone was also observed at 60°C/min under oxidising conditions. In similar fashion to the case of cellulose that these volatile compounds could react further to CO, CO_2 and water, and therefore occur in smaller amounts under oxidising conditions and are not detected. As in the case of cellulose many of the small molecules may be formed by defragmentation of the polymer via a number of routes. A proposed fragmentation of the polymer chain is shown in Figure 4-15. In this proposal the fragmentation occurs in two stages, first the fragmentation of one of the uronic acid groups, followed by the decomposition of the intermediate to give formaldehyde and CO_2.

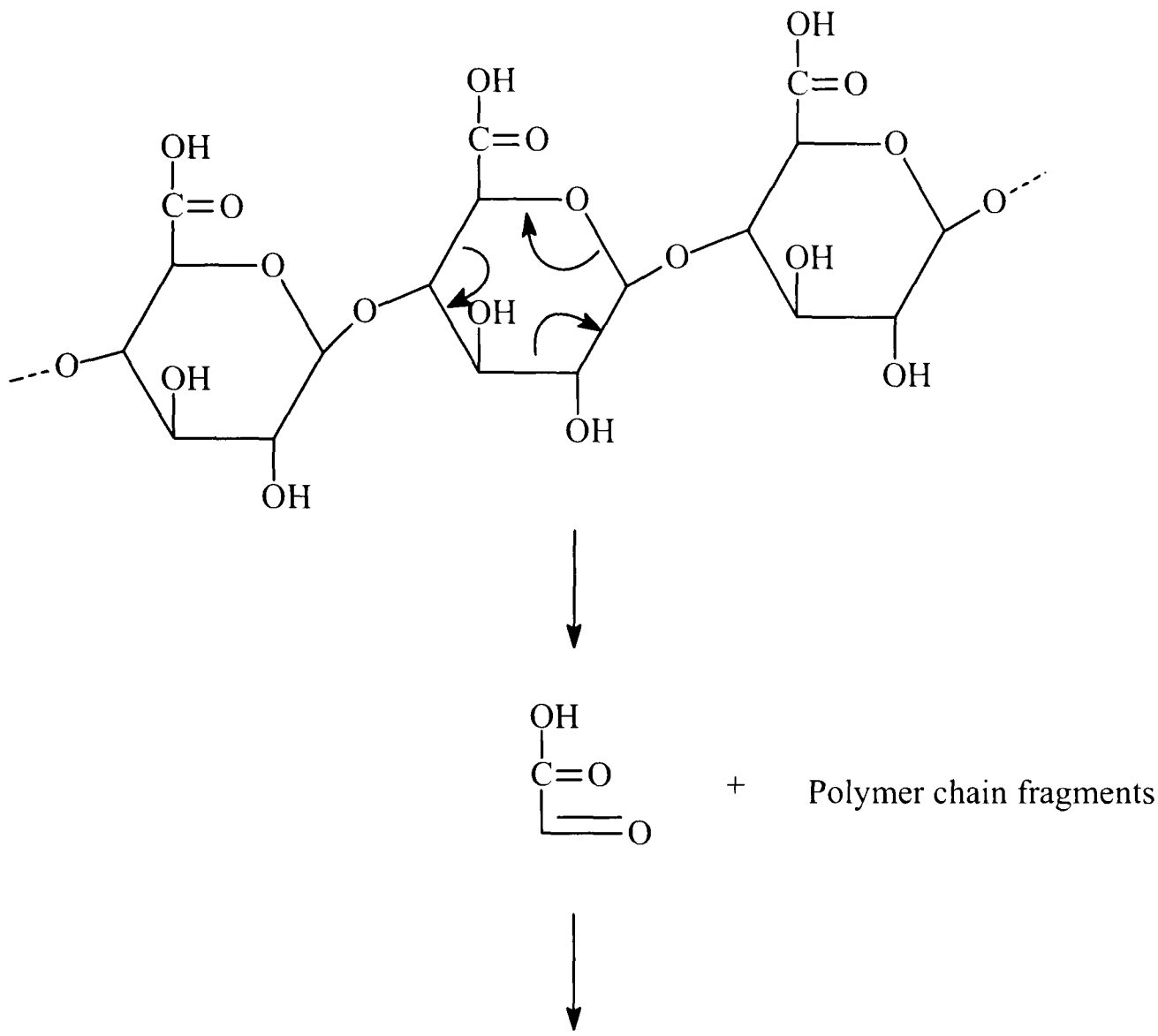

Figure 4-15. Proposed mechanism for the defragmentation of the alginic acid polymer chain

The CO_2 evolution profile for alginic acid and the 50:50 mixture sample went above the scale of the FTIR detector at the higher temperature ramp rates, 30°C/min (Figure 3-28) and 60°C/min (Figure 3-30) under oxidising conditions. This indicates that these samples appeared to break down more readily and produce more CO_2 under these conditions. This is likely to be due to additional oxygen available within the molecule and residue, combined with the addition of oxygen into the furnace gas. An alternative to this could be the formation of furanose end groups (Figure 4-16).

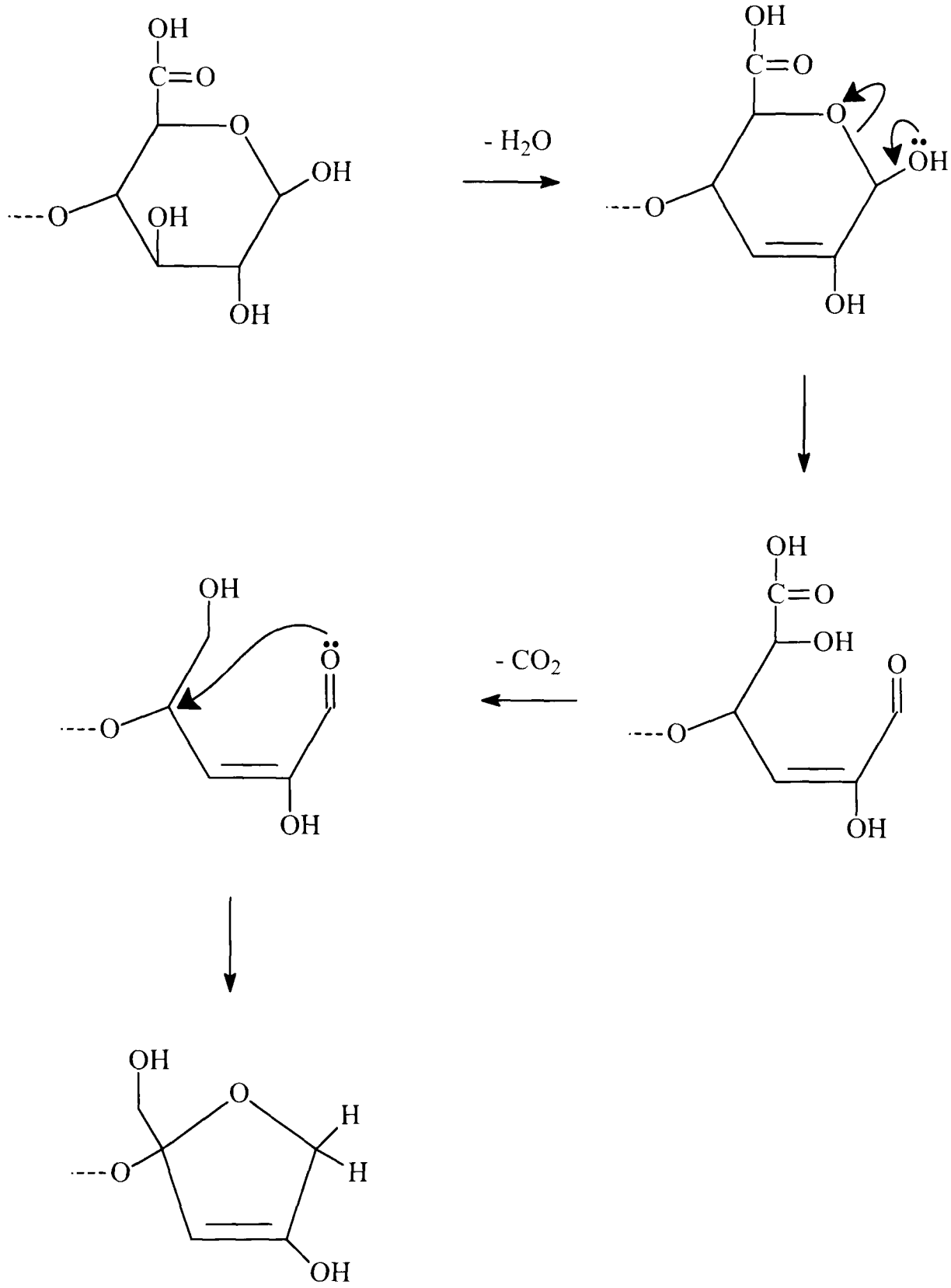

Figure 4-16. Proposed formation of a furanose end group with the elimination of water and CO_2 from alginic acid.

This mechanism eliminates water, increasing the conjugation in the molecule, followed by ring opening and the cleavage of the C5 – C6 bond. The elimination of the CO_2 molecule from the intermediate, leaves the remaining end fragment to close at C4, forming a furanose end group to the polymer chain. Breaking of the glycosidic bond is a potential route to the formation of furan groups in the evolved volatiles.

Acetaldehyde is only observed in the evolved gases from alginic acid at the two higher ramp rates (30 and 60°C/min under nitrogen; 60°C/min in oxidising conditions). It is still in small

amounts under these conditions, less than cellulose under the same conditions. There is also less acetaldehyde measured under oxidising conditions (Figure 3-34) than non-oxidising conditions (Figure 3-33). Acetic acid was observed to have a shoulder in the alginic acid experiments, the initial peak at ~260°C and the shoulder at ~340°C, under either atmosphere and at all temperature ramp rates (Figure 3-23 to Figure 3-36). There was no trend in the amount of acetic acid measured with respect to ramp rate, but there was less of the compound quantified under oxidising conditions. Acrolein was observed at all temperature ramp rates under nitrogen, but only at the two highest ramp rates under oxidising conditions. The formation of these small volatile molecules is likely to be through fragmentation of the polymer structure, and as Moldoveanu [21] illustrates for cellulose (Figure 4-9) there are many potential routes for the formation of these compounds.

CO was observed to increase with increasing ramp rate under nitrogen but with 10% oxygen there was no trend with increasing ramp rate. The total amount of CO formed was not greatly affected by changing atmosphere. The CO was seen to evolve at two temperatures, ~250°C and 420°C under non-oxidising conditions with a rising trend from 650°C towards 900°C, likely due to high temperature breakdown of the residual char. Under oxidising conditions the peak at ~450°C is more pronounced, but there is no observed CO above ~550°C. It may be that CO is oxidised to CO_2 above 550°C.

The amount of observed CO_2 was not affected by the change in ramp rate; however, the amount was approximately three times higher under oxidising conditions. The CO_2 had a peak at ~260°C, with a shoulder at ~200°C and then a small secondary peak at ~600°C. Under oxidising conditions the secondary peak is much larger and broader than the initial peak. The higher amount of residual char observed for alginic acid compared with cellulose under non-oxidising conditions (Figure 3-15) will also contribute to the higher amount of CO and CO_2 observed under oxidising conditions. This is likely to be through high temperature oxidation of the carbonaceous char as described previously for cellulose in section 1.2.5.

Water is observed with the same 260°C peak with the front shoulder as CO_2. It has a smaller peak at 350°C, and under oxidising conditions a small peak at 450°C under oxidising conditions. Water vapour was seen to decrease with increasing ramp rate, as was the case for cellulose. The total amount of water formed was unaffected by changing the atmosphere. The elimination of water from an alcohol with the formation of a carbon to carbon double bond is a well know reaction, and this concept may be extended to the alginic acid molecule (Figure 4-17).

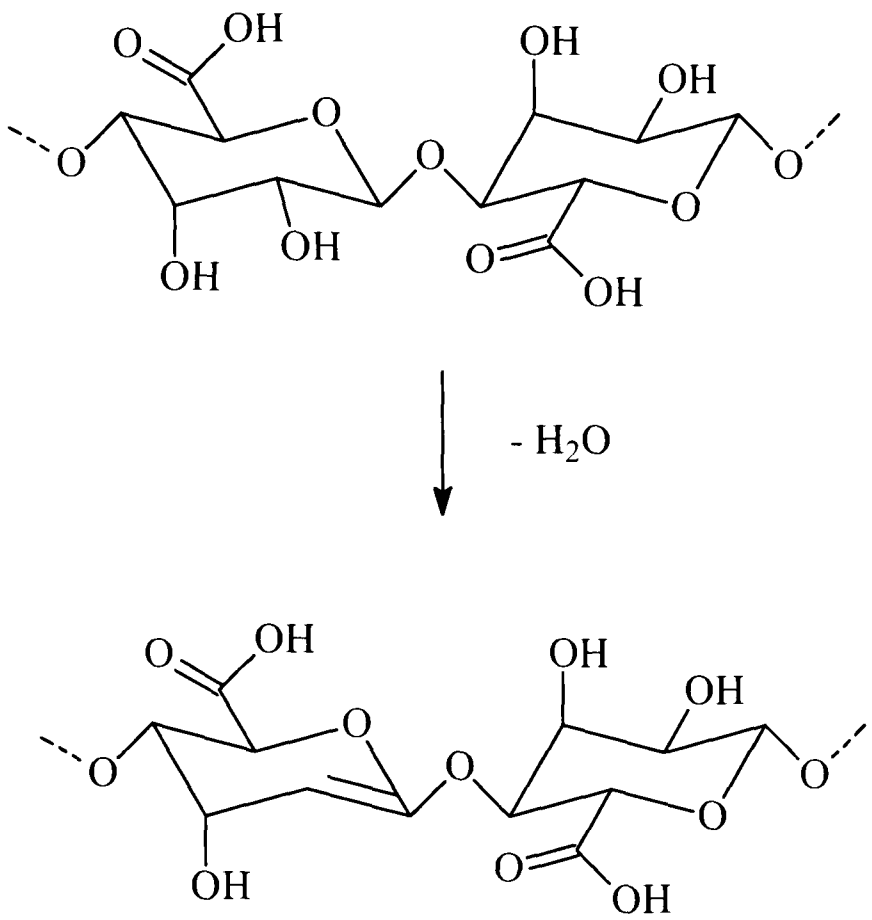

Figure 4-17. Proposed formation of double bonds by the elimination of water from alginic acid.

Generally the amount of the quantified volatiles, acetaldehyde, acetic acid and acrolein was lower for alginic acid than for cellulose under similar conditions. This would suggest that the elimination of small molecules, such as water, CO and CO_2 is the most likely route for decomposition for alginic acid. This is likely to lead to the greater amount of char that was observed for alginic acid, in comparison with cellulose. Elimination of these molecules is also likely to account for the increasing unsaturation of the remaining polymer.

However the presence of the other quantified volatiles, particularly under non-oxidising conditions, shows that polymer breaks down by other routes, such as fragmentation of the anhydrosugars units or perhaps depolymerisation.

4.3.3 Alginic acid summary

From the information gathered it is only possible to describe the changes that occur in alginic acid on heating. Through the char analysis some of the changes that occur structurally can be observed, and through the volatile phase data some of the products evolved can be identified. However, only some of the mechanisms that may result in the observed features may be proposed. It is clear from cellulose that many of the products of decomposition can be identified, but no one has proposed definitive chemical mechanisms for the formation of all of

them. Regardless of this a pathway for the thermal decomposition of alginic acid is shown in Figure 4-18. The pathway for alginic acid is more complex than that for the cellulose, as there are more intermediate steps which in turn were more sensitive to the reaction atmosphere.

For cellulose decomposition it is thought that there are two competing initial reactions, one favouring char and one favouring formation of volatiles [12, 34, 35, 46, 47]. The balance between these reactions may shifted by increasing the heating rate – higher rates favouring volatile formation, lower rates favouring char formation; although this was not apparent from this study, which may be due to the high final temperature (900°C) of the analyses. For alginic acid it appears that a similar effect may occur, although perhaps formation of the char is slightly more favourable than the formation of volatile compounds. The formation of char is also associated with the evolution of CO, CO_2 and water, which was also seen to be at least as high for alginic acid as cellulose, and in the case of CO_2 higher under oxidising conditions. The examination of the remainder of the volatile phase also showed that there were, quantitatively, less of the other volatiles measured for alginic acid compared to cellulose in this study. This allows a separation of the char formation and volatile forming pathways, as in cellulose.

The char pathway is less complicated than that of the volatile route, in that there is only the change of structure of the char from the aliphatic char (Char 1) to the carbonaceous char (Char 2) under nitrogen. Under oxygen char 1 is still visible indicating that the route of formation is likely to be the same, but a different residue (Char 3) is observed at 400°C, that starts to become more like Char 2 at 800°C but above this temperature there is no residue.

The volatile pathway, again is unaffected by change in atmosphere up to 300°C, as is the char. This shows that the mechanisms of formation are linked, i.e. both char and volatiles are formed in this temperature range as competing reactions. It appears that the reactions are primarily due to decarbonylation and dehydration reactions, as these are the primary evolved compounds at temperatures below 300°C. Above 300°C the addition of oxygen changes the chemistry of the volatiles observed, with additional peaks of acetic acid, CO and water observed at 350°C. At ~450°C further CO and water are observed, and at higher temperature (600°C) CO_2. Above this temperature there is no remaining char. Under nitrogen there is only the evolution of small molecules, such as methane, CO, CO_2 and water at higher temperature, 550°C, but there is a residue of highly carbonaceous char (for HTTs up to 1000°C) that remains unchanged structurally above 600°C.

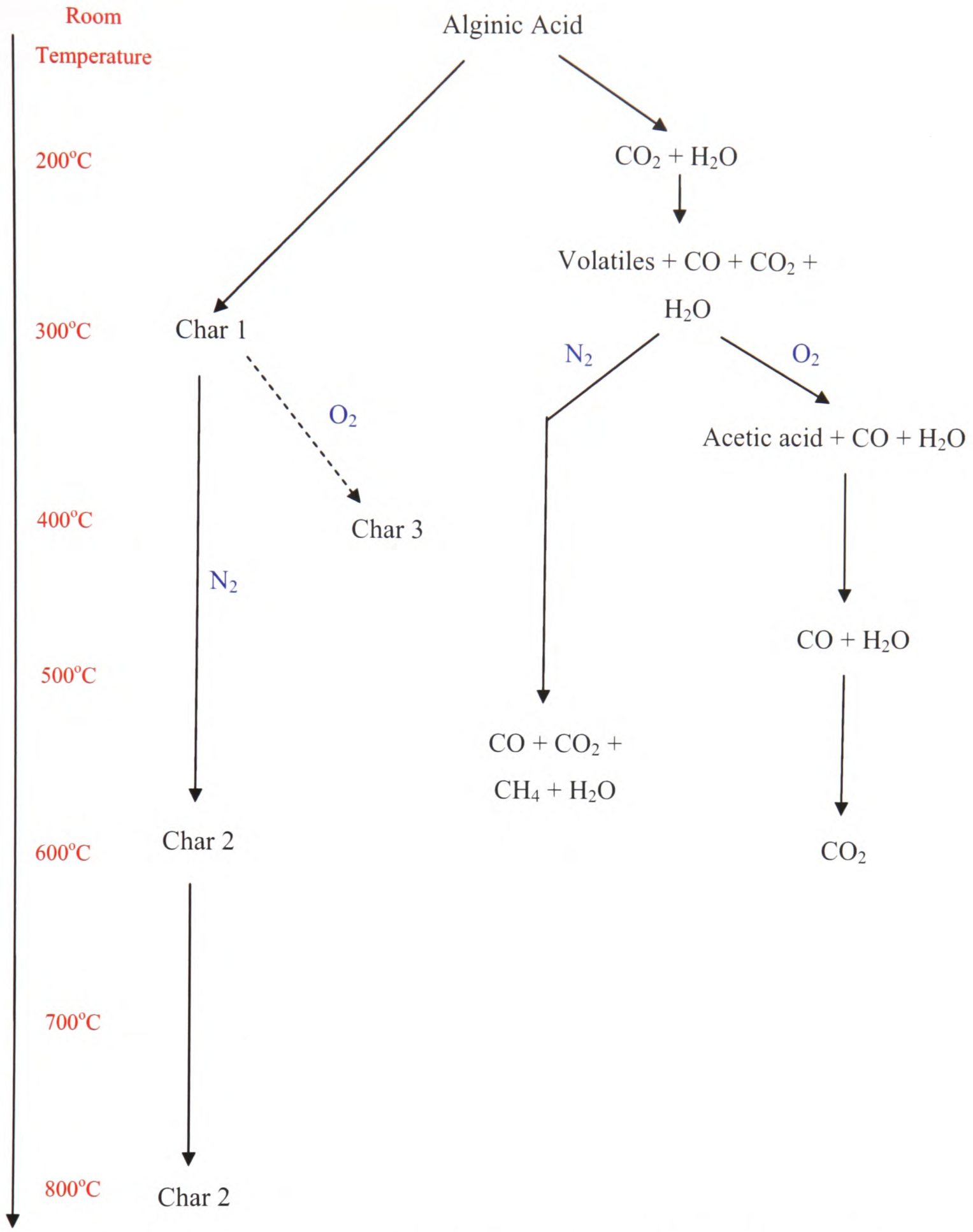

Figure 4-18. Proposed reaction pathway for the thermal decomposition of alginic acid based on the results of this study.

So it appears from Figure 4-18 that decomposition of alginic acid is a more complex process than that of cellulose (Figure 4-10) as the addition of oxygen appears to change the chemistry rather than accelerate the same set of reaction as is the case for cellulose. This is seen through

examination of the char residues; for cellulose the chars were similar under the different atmospheres whereas in alginic acid different functional groups were observed. Under nitrogen the amount of char formed by alginic acid was higher than that of cellulose. In both cases the addition of oxygen causes the residual char to be oxidised completely.

4.3.4 Effects of Mixing Alginic Acid with Cellulose

On the whole there appears to be no interactions between the two compounds when mixed in 50:50 ratio. The main weight losses in non-oxidising conditions (Figure 3-7) are observed for each of the two compounds, at the temperatures expected based on the TGA information for the pure compounds. Under oxidising conditions (Figure 3-12) the same effect is seen with no obvious interactions between the two compounds in the mixture. However the peak seen at ~340°C from alginic acid is not visible under these conditions. Figure 3-17 shows that the peak associated with cellulose at ~350°C in nitrogen atmosphere occurs at lower temperature (~340°C) in oxidising conditions. The individual compounds do not show this effect of lowering the peak temperature of the weight loss events on changing the atmosphere. Comparison with the individual compounds under nitrogen (Figure 3-18) shows that this effect occurs only under oxidising conditions (Figure 3-19). Analysis of total weight loss from the samples shows that the 50:50 mixture shows a mixture of the effects of the two individual compounds (Figure 3-13).

This may help explain the lack of higher temperature CO and CO_2 peaks that are observed under oxidising conditions (Figure 3-24, Figure 3-26 and Figure 3-28). Under the lowest temperature ramp rates the effect is not as apparent as the higher ramp rates. It may be that the CO and CO_2 evolution of alginic acid, which occurs at slightly lower temperature, causes an acceleration effect of similar processes, with the same precursors, in the cellulose leading to a single high temperature peak in the mixture instead of two. However the effect is not observed at the highest ramp rate (Figure 3-30), which may be an effect of thermal lag in the sample which is more apparent at higher ramp rates. Additionally the peaks are larger and broader, and in the case of CO_2 particularly, the signal is close to detector overload in the 30°C/min and 60°C/min ramp rate samples under oxidising conditions.

Water vapour was seen to have the same peaks as the cellulose and alginic acid combined. The overall trend of water was to decrease with increasing ramp rate which is similar to that of both of the unmixed samples (Figure 3-35) although under oxidising conditions the effect is not as

clearly defined (Figure 3-36). CO had a decreasing trend with increasing ramp rate in similar fashion to cellulose. Generally the amount of CO, CO_2 and water vapour evolved on decomposition were increased under oxidising conditions compared to non-oxidising.

There are no other apparent trends of total formation as a result of changing ramp rate which also gives rise to the conclusion that there is no interaction between the two materials.

CHAPTER 5 CONCLUSIONS

It is the purpose of this section to compare the results and discussion of the study with the initial aims of the work that are described in section 1.8. As part of this study the analysis technique has also been developed, operational parameters tested and a calibration library of reference compounds prepared. The technique established has found use outside of this study for analysis of some aldehydes as pyrolysis products of saccharide ingredients [146].

It is always the case with any study that there are other experiments that could be performed to add more information, and this study is no exception. However this aspect of the conclusions will be considered in section 5.2.

5.1 Review of the Aims of this Study

The goal of this study was to provide insight into the thermal decomposition of polysaccharide compounds through the use of two model compounds; a well characterised material, cellulose, and alginic acid which is less studied. A number of stages were necessary to meet this goal, the foremost being a detailed literature review of the two model compounds proposed for use in the study. From this it was discovered that there was a wealth of information surrounding the thermal decomposition of cellulose but little on alginic acid. Therefore it was proposed to investigate the thermal degradation process of alginic acid, using cellulose as a model system. The aims of the study were:

1. to use a thermogravimetric analyser coupled with a Fourier transform infrared spectrophotometer to characterise the thermal decomposition chemistry of two polysaccharides.
2. use a multivariate data analysis technique to interpret the spectral analysis of the decomposition products.
3. identify differences, if any, between these two model compounds.
4. to use any identified differences to compare their thermal behaviours under known conditions.
5. to compare and deduce the mechanisms of formation of the identified evolved compounds and their residual chars.

The development of the TGA-FTIR system has been essential to the analysis of the sample compounds in this study. The system facilitated two different aspects of studying the carbohydrate compounds, cellulose and alginic acid; first the analysis of the charred residue from various heat treatment temperatures (HTT) of the samples by use of an attenuated total reflectance (ATR) accessory; i.e. the solid phase could also be analysed. The analysis of the char showed the changing structure of the materials of the range of HTT used in the study. Secondly, the direct analysis of the volatile phase pyrolysis products of the materials by use of the gas flow cell.

The main challenge for this part of the work was in creating a stable, reproducible system that was capable of measuring IR spectra in such a way as to make the data suitable for factor analysis. There was also the need for producing a method that would allow the calibration of a wide range of volatiles, semi-volatiles and gases to make the analysis quantifiable. The use of the FTIR in ATR mode allowed a secondary method of analysis of the char residue of the materials, in addition to the elemental analyser. The methodology of the TGA-FTIR was successful and has been used to study other polysaccharide compounds in parallel with this work [146]. The ATR examination contributed greatly to the study in giving more structural information about the chars. This in combination with the analysis of the volatiles provided a powerful tool for studying the thermal decomposition processes.

It is difficult to separate the multivariate analysis from the thermal technique, as this is the power behind the 'real-time' analysis of the volatile phase of the decomposition. The qualitative analysis of the volatiles was made possible with the use of Target Factor Analysis (TFA) encapsulated in InSight™. TFA was use to separate the mixture and qualitatively identify selected compounds in the volatile phase. The qualitative assessment was based upon the selection of spectral windows that contained the most unique aspects of the target compounds spectrum. The evaluation of the equipment showed that differentiation of such series of compounds was achieved up to C_4 but became much more difficult beyond that. By setting a high correlation level for the acceptance of predicted spectral matches against reference spectra it was possible to quickly draw out a pattern of compound formation. The quantitative assessment of the evolved compounds proved to be extremely useful in distinguishing trends between the two samples. It was this feature that allowed the differences in the relative amounts

of gases and water vapour to be compared with the amount of volatile compounds evolved from the two materials.

Overall the combination of the TGA-FTIR instrument combined with the multivariate analysis has formed a powerful tool for a rapid assessment of decomposition characteristics of saccharide materials.

The results of the qualitative analysis showed a number of similarities in the compounds that were evolved on heating. This is not surprising considering the similarity in the structure of the two polymers. However, it was still possible through quantitative assessment of selected compounds, acetaldehyde, acetic acid, acrolein, CO, CO_2 and water vapour, to show some differences in behaviour of cellulose and alginic acid under the conditions examined. This gave some indication of the decomposition route of the two materials, and in combination with the char analysis made it possible to draw a picture of the decomposition routes for the two compounds. The decomposition route of for cellulose was in line with those published in the literature and although it was not possible to identify the structure of active cellulose, changes were observed in the region before the main weight loss. This gives confidence in the interpretation of the processes involved in the decomposition of the alginic acid, which produced similar compounds on heating.

The reaction pathway for alginic acid is more complex than that of cellulose since changing the reaction atmosphere appeared to change the chemistry of the thermal decomposition process. However, the types of compounds evolved were seen to be similar to that of cellulose which is not surprising considering the similarity in structure. When the quantitative data was examined more differences were noted, mainly in the fact that less carbonyl compounds were observed in favour of more CO, CO_2 and water vapour. In combination with the increased char this suggests that the primary decomposition mechanism is likely to be dominated by elimination reactions, with increasing unsaturation occurring in the remaining material. However, the fact that the other volatile materials are observed shows that other reactions are still occurring in parallel, such as defragmentation of the molecule and depolymerisation.

In summary this study has produced:

1. a clear schematic thermal decomposition pathway for alginic acid not reported in the literature before.
2. established a flexible analytical protocol for materials analysis using a TGA-FTIR setup.

3. demonstrated the usefulness of the multivariate data analysis, in the form of Target Factor Analysis for the treatment of complex mixtures.
4. confirmed and enhanced previous cellulose decomposition pathway understanding by adding time and temperature information for selected evolved compounds to previous knowledge in this area.

5.2 Further Work

As is previously noted it is the reality of any study that additional experiments, other techniques and other approaches could be used to supplement the work reported in this study. Such studies could include the following:

1. increasing the number of reference compounds that were calibrated within InSight™. Using a larger range of compounds, in particular more cyclo- compounds (both 5- and 6-membered rings) may have provided the opportunity to observe further (if any) differences between cellulose and alginic acid.
2. Rigorous kinetic analysis of the TGA weight loss data is another area that would add to the understanding of the process of decomposition of both materials. Using an isoconversional technique such as those developed by Flynn [84] and Ozawa [82] may have given global reaction values of activation energy and pre-exponential factors for both compounds. Kinetic analysis of the evolved compound profiles from the deconvolution process may also be examined to perhaps give more information of the formation of individual compounds. This data could be useful in the design of reactor processes that may potentially use the compounds, in similar fashion to other biomass sources, in the generation of energy or other chemicals of industrial interest.
3. Additional techniques that could have been used to supplement this study could have included, other thermal analysis techniques such as Differential Scanning Calorimetry (DSC) which would have added information regarding the transitions that occur during the decomposition process, such as glass transitions (T_g) and whether the processes are endo- or exothermic.
4. Pyrolysis gas chromatography mass spectrometry (py-GC-MS) is another analytical technique that would have proved useful to the study in identification of higher molecular weight decomposition products than is possible with FTIR. However, this

technique would not be able to show the compound formation as a function of temperature and/or time. The additional identification of potentially hundreds of compounds could be a good addition to this work.

5. NMR studies of the residues formed at the different HTTs could provide more information as to the structure of the chars. As it is, the FTIR allows only the identification of the functional groups, and the changing of these with temperature provides the opportunity to speculate over the structural changes.

CHAPTER 6 REFERENCES

1. Leffingwell, J. C., "Basic chemical constituents of tobacco leaf and differences between tobacco types," *Tobacco: production, chemistry and technology*, edited by D. L. Davis and M. T. Nielsen Blackwell Science, 1999.

2. Food Product Range Guide. 2001. I.S.P. Alginates UK Ltd.

3. Aspinall, G. O., *Polysaccharides*, Pergamon Press Ltd, Oxford, 1970.

4. *Encyclopedia of food sciences and technology*, Vol. 1, John Wiley & Sons 1992.

5. Whistler, R. and Daniel, J. R., "Functions of polysaccharides in foods," *Food additives*, edited by A. L. Branen, P. M. Davidson, and S. Salminen Marcel Dekker, Inc, New York, 1990, pp. 395.

6. Nicholson, J. W., *The chemistry of polymers*, 2nd ed., RSC, Cambridge, 1997.

7. Shafizadeh, F., "Cellulose chemistry, perspective and reterospect," *Pure Applied Chemistry*, Vol. 35, No. 2, 1973, pp. 195-208.

8. Brink, D. L., Charley, J. A., Faltico, G. W., and Thomas, J. F., "The pyrolysis-gasification-combustion process energy considerations and overall processing," *Thermal uses and properties of carbohydrates and lignins*, edited by F. Shafizadeh, K. V. Sarkanen, and D. A. Tillman Academic Press, New York, 1973.

9. Shafizadeh, F., "Basic principles of direct combustion," *Biomass conversion processes for energy and fuels* : Plenum Publishing Corp., New York, 1981, pp. 103-124.

10. Antal, M. J., "Biomass pyrolysis: A review of the literature. Part 1 - Carbohydrate pyrolysis," *Advances in Solar Energy*, 1983, pp. 61-111.

11. Rothermel, R. C., "Forest fires and the chemistry of forest fuels," *Thermal uses and properties of carbohydrates and lignins*, edited by F. Shafizadeh, K. V. Sarkanen, and D. A. Tillman Academic Press, New York, 1973.

12. Radlein, D., Piskorz, J., and Scott, D. S., "Fast pyrolysis of natural polysaccharides as a potential industrial process," *Analytical and Applied Pyrolysis*, Vol. 19, 1991, pp. 41-63.

13. Klemm, D., Schmauder, H.-P., and Heinze, T., "Cellulose," *Polysaccharides II: Polysaccharides from eukaryotes*, edited by E. J. Vandamme, S. De Baets, and A. Steinbüchel Biopolymers, Wiley-VCH, Weinheim, 2002, pp. 275-319.

14. *Concise encyclopedia of wood and wood-based materials*,.Concise encyclopedias Cahn, R. W. and Bever, M. B., Pergamon Press, Oxford, 1989.

15. Kandola, B. K., Horrocks, A. R., Price, D., and Coleman, G. V., "Flame-retardant treatments of cellulose and their influence on the mechanism of cellulose pyrolysis," *Rev.Macromol.Chem.Phys.*, Vol. 36, No. 4, 1996, pp. 721-794.

16. French, A. D. and Johnson, G. P., "What crystals of small analogs are trying to tell us about cellulose structure," *Cellulose*, Vol. 11, No. 1, 2004, pp. 5-22.

17. Zugenmaier, P., "Conformation and packing of various crystalline cellulose fibres," *Progress in Polymer Science*, Vol. 26, 2001, pp. 1341-1417.

18. Ball, R., McIntosh, A. C., and Brindley, J., "The role of char-forming processes in the thermal decomposition of cellulose," *Phys.Chem.Chem.Phys.*, Vol. 1, 1999, pp. 5035-5043.

19. Tillman, D. A., "Review of mechanisms associated with wood combustion," *Wood Science*, Vol. 13, No. 4, 1981, pp. 177-184.

20. Kirk and Othmer, *Encyclopedia of science and technology*, 3rd ed., Vol. 5, John Wiley & sons, New York, 1978, pp. 70-77.

21. Moldoveanu, S. C., *Analytical pyrolysis of natural organic polymers*, Vol. 20,.Techniques and Instrumentation in Analytical Chemistry, Elsevier 1998.

22. Hurd, C. D., *The pyrolysis of carbon compounds*, Vol. 50,.Monograph Series, American Chemical Society, Chemical Catalogue Company, New York, 1929.

23. Heda, P. K., Dollimore, D., Alexander, K. S., Chen, D., Law, E., and Bicknell, P., "A method of assessing solid state reactivity illustrated by thermal decomposition experiments on sodium bicarbonate," *Thermochimica Acta*, Vol. 255, 1995, pp. 255-272.

24. Turns, S. R., *An introduction to combustion*,.McGraw-Hill Series in Mechanical Engineering Holman, J. P. and Lloyd, J. R., McGraw-Hill Inc. 1996.

25. Akalin, M., Horrocks, A. R., and Price, D., "Smoke and CO evolution from cotton and flame retarded cotton. Part 1: Behaviour of single layer fabrics under LOI conditions," *J.Fire Science*, Vol. 6, 1988, pp. 333-347.

26. Sekiguchi, Y. and Shafizadeh, F., "The effect of inorganic additives on the formation, composition and combustion of cellulosic char.," *Applied Polymer Science*, Vol. 29, 1984, pp. 1267-1286.

27. Antal, M. J. and Varhegyi, G., "Cellulose pyrolysis kinetics: The current state of knowledge," *Ind.Eng.Chem.Res.*, Vol. 34, 1995, pp. 703-717.

28. Antal, M. J., Varhegyi, G., and Jakab, E., "Cellulose pyrolysis kinetics: Revisited," *Ind.Eng.Chem.Res.*, Vol. 37, 1998, pp. 1267-1275.

29. Hirata, T., "Pyrolysis of cellulose. An introduction to the literature," National Bureau of Standards, NBSIR 85-3218, Gaithersburg, MD, 1985.

30. Antal, M. J., "Biomass pyrolysis: A review of the literature. Part 2 - Lignocellulose pyrolysis," *Advances in Solar Energy*, 1985, pp. 175-255.

31. Madorsky, S. L., Hart, V. E., and Straus, S., "Thermal degradation of cellulosic materials," *Journal of the National Bureau of Standards*, Vol. 60, No. 4, 1958, pp. 343-349.

32. Cullis, C. F., "The role of pyrolysis in polymer combustion and flame retardance," *Analytical and Applied Pyrolysis*, Vol. 11, 1987, pp. 451-463.

33. Gann, R. G., Earl, W. L., Manka, M. J., and Miles, L. B., Mechanism of cellulose smouldering retardance by sulphur. Eighteenth Symposium (International) on Combustion , 571-578. 1981. The Combustion Institute.

34. Pouwels, A. D., Eijkel, G. B., and Boon, J. J., "Curie-point pyrolysis-capillary gas chromatography-high-resolution mass spectrometry of microcrystalline cellulose," *Analytical and Applied Pyrolysis*, Vol. 14, 1989, pp. 237-280.

35. Shafizadeh, F., "Thermal degradation of cellulose," *Cellulose chemistry and its applications*, edited by T. P. Nevell and S. H. Zeronian Ellis Horwood Ltd, Chichester, 1985, pp. 266-289.

36. Pastorova, I., Arisz, P. W., and Boon, J. J., "Preservation of D-glucose-oligosaccharides in cellulose chars," *Carbohydrate Research*, No. 248, 1993, pp. 151-165.

37. Basch, A. and Lewin, M., "The influence of fine structure on the pyrolysis of cellulose. II. Pyrolysis in air," *Polymer Science*, Vol. 11, 1973, pp. 3095-3101.

38. Zhu, P., Sui, S., Wang, B., Sun, K., and Sun, G., "A study of pyrolysis and pyrolysis products of flame-retardant cotton fabrics by DSC, TGA, and Py-GC-MS," *Analytical and Applied Pyrolysis*, Vol. 71, 2004, pp. 645-655.

39. Weinstein, M. and Broido, A., "Pyrolysis-crystallinity relationships in cellulose," *Combustion Science and Technology*, Vol. 1, 1970, pp. 287-292.

40. Back, E. L., Htun, M. T., Jackson, M., and Johanson, F., "The effect of auto cross-linking reactions on the thermal softening of cellulose," *Textile Research Journal*, Vol. 37, 1967, pp. 432-433.

41. Scheirs, J., Camino, G., and Tumiatti, W., "Overview of water evolution during the thermal degradation of cellulose," *European Polymer Journal*, Vol. 37, 2001, pp. 933-942.

42. Golova, O. P., "Chemical effects of heat on cellulose," *Russian Chemical Reviews*, Vol. 44, No. 8, 1975, pp. 687-697.

43. Kilzer, F. J. and Broido, A., "Speculations on the nature of cellulose pyrolysis," *Pyrodynamics*, Vol. 2, 1965, pp. 151-163.

44. Shafizadeh, F., "Introduction to pyrolysis of biomass," *Analytical and Applied Pyrolysis*, Vol. 3, 1982, pp. 283-305.

45. Rubtsov, Y. I., Kazakov, A. I., Andrienko, L. P., and Manelis, G. B., "Kinetics of heat release during decomposition of cellulose," *Combustion Explosion and Shock Waves*, Vol. 29, No. 6, 1993, pp. 710-713.

46. Piskorz, J., Radlein, D., and Scott, D. S., "On the mechanism of the rapid pyrolysis of cellulose," *Analytical and Applied Pyrolysis*, Vol. 9, 1986, pp. 121-137.

47. Shafizadeh, F. and Sekiguchi, Y., "Oxidation of chars during smouldering combustion of cellulosic materials," *Combustion and Flame*, Vol. 55, 1984, pp. 171-179.

48. Várhegyi, G., Jakab, E., and Antal, M. J., "Is the Broido-Shafizadeh model for cellulose pyrolysis true?," *Energy & Fuels*, Vol. 8, 1994, pp. 1345-1352.

49. Várhegyi, G., Szabó, P., Mok, W. S., and Antal, M. J., "Kinetics of the thermal decomposition of cellulose in sealed vessels at elevated pressures. Effects of the presence of water on the reaction mechanism," *Analytical and Applied Pyrolysis*, Vol. 26, 1993, pp. 159-174.

50. Milosavljevic, I., Oja, V., and Suuberg, E. M., "Thermal effects in cellulose pyrolysis: Relationship to char formation processes," *Ind.Eng.Chem.Res.*, No. 35, 1996, pp. 653-662.

51. Shafizadeh, F. and Bradbury, A. G. W., "Smouldering combustion of cellulosic materials," *Thermal Insulation*, Vol. 2, 1979, pp. 141-152.

52. Völker, S. and Rieckmann, Th., "Thermokinetic investigation of cellulose pyrolysis - impact of initial and final mass on kinetic results," *Analytical and Applied Pyrolysis*, Vol. 62, 2002, pp. 165-0177.

53. Mok, W. S. and Antal, M. J., "Effects of pressure on biomass pyrolysis. II. Heats of reaction of cellulose pyrolysis," *Thermochimica Acta*, Vol. 68, 1983, pp. 165-186.

54. Dollimore, D. and Hoath, J. M., "The application of thermal analysis to the combustion of cellulose," *Thermochimica Acta*, Vol. 45, 1981, pp. 87-102.

55. Whiteley, R., "Hydrated, halogenated and nanocomposite flame retardants," Flame retardancy and flammability of polymers and textiles, University of Leeds, 2004.

56. Shafizadeh, F. and DeGroot, W. F., "Combustion characteristics of cellulosic fuels," *Thermal uses and properties of carbohydrates and lignins*, edited by F. Shafizadeh, K. V. Sarkanen, and D. A. Tillman Academic press, New York, 1976.

57. Faroq, A. A., Price, D., Milnes, G. J., and Horrocks, A. R., "Use of gas chromatographic analysis of volatile products to investigate the mechanisms underlying the influence of flame retardants of the pyrolysis of cellulose in air," *Polymer Degradation and Stability*, No. 33, 1991, pp. 155-170.

58. Arseneau, D. F., "Competitive reactions in the thermal decomposition of cellulose," *Canadian Journal of Chemistry*, Vol. 49, 1970, pp. 632-638.

59. Liao, Y., Wang, S., Ma, X., Luo, Z., and Cen, K., "Numerical approach to the mechanism of cellulose pyrolysis," *Chinese J.Chemical Engineering*, Vol. 13, No. 2, 2005, pp. 197-203.

60. Nimlos, M. R., Shin, E.-J., Brown, A. L., Evans, R. J., and Daily, J. W., "Molecular and kinetic modelling of levoglucosan pyrolysis," *Fuel Chemistry Division Preprints*, Vol. 46, No. 1, 2001, pp. 185-187.

61. Shafizadeh, F. and Sekiguchi, Y., "Development of aromaticity in cellulosic chars," *Carbon*, Vol. 21, No. 5, 1983, pp. 511-516.

62. Sekiguchi, Y., Frye, J. S., and Shafizadeh, F., "Structure and formation of cellulosic chars," *Applied Polymer Science*, Vol. 28, 1983, pp. 3513-3525.

63. Mok, W. S., Antal, M. J., Szabó, P., Várhegyi, G., and Zelei, B., "Formation of charcoal from biomass in a sealed reactor," *Ind.Eng.Chem.Res.*, Vol. 31, 1992, pp. 1162-1166.

64. Antal, M. J., Mok, W. S., Várhegyi, G., and Szekely, T., "Review of methods for improving the yield of charcoal from biomass," *Energy & Fuels*, Vol. 4, No. 3, 1990, pp. 221-225.

65. Bradbury, A. G. W. and Shafizadeh, F., "Role of oxygen chemisorption in low-temperature ignition of cellulose," *Combustion and Flame*, Vol. 37, 1980, pp. 85-89.

66. DeGroot, W. F. and Shafizadeh, F., "The influence of exchangeable cations on the carbonisation of biomass," *Analytical and Applied Pyrolysis*, Vol. 6, 1984, pp. 217-232.

67. Narayan, R. and Antal, M. J., "Thermal lag, fusion and the compensation effect during biomass pyrolysis," *Ind.Eng.Chem.Res.*, Vol. 35, 1996, pp. 1711-1721.

68. Magnaterra, M. R., Cukierman, A. L., and Lemcoff, N. O., "Kinetic study of combustion of cellulose and a hardwood species chars," *Latin American Applied Research*, Vol. 19, 1989, pp. 61-65.

69. Bradbury, A. G. W. and Shafizadeh, F., "Chemisorption of oxygen on cellulose char," *Carbon*, Vol. 18, No. 2, 1980, pp. 109-116.

70. DeGroot, W. F. and Shafizadeh, F., "Influence of inorganic additives on oxygen chemisorption on cellulosic chars," *Carbon*, Vol. 21, No. 1, 1983, pp. 61-67.

71. Milosavljevic, I. and Suuberg, E. M., "Cellulose thermal decomposition kinetics: Global mass loss kinetics," *Ind.Eng.Chem.Res.*, Vol. 34, 1995, pp. 1081-1091.

72. Baker, R. R., "Thermal decomposition of cellulose," *Thermal Analysis*, Vol. 8, 1975, pp. 163-173.

73. Antal, M. J., Mok, W. S., Roy, J. C., T-Raissi, A., and Anderson, D. G. M., "Pyrolytic sources of hydrocarbons from biomass," *Analytical and Applied Pyrolysis*, Vol. 8, 1985, pp. 291-303.

74. Banyasz, J., Li, S., Lyons-Hart, J., and Shafer, K. H., "Cellulose pyrolysis: the kinetics of hydroxyacetaldehyde evolution," *Analytical and Applied Pyrolysis*, Vol. 57, 2001, pp. 223-248.

75. Tang, W. K., "Effects of inorganic salts on pyrolysis of wood, alpha-cellulose, and lignin," *US Forest Serv.Res.Pap.*, Vol. FPL 71, 1967.

76. Visanuvimol, V., Studies of the pyrolysis and combustion of cellulose. PhD Thesis. 1978. City University, London.

77. Antal, M. J., Friedman, H. L., and Rogers, F. E., "Kinetics of cellulose pyrolysis in nitrogen and steam," *Combustion Science and Technology*, Vol. 21, 1980, pp. 141-152.

78. Capart, R., Khezami, L., and Burnham, A. K., "Assessment of various kinetic models for the pyrolysis of a microgranular cellulose," *Thermochimica Acta*, Vol. 417, No. 1, 2004, pp. 79-89.

79. Nada, A. M. A. and Hassan, M. L., "Thermal behaviour of cellulose and some cellulose derivatives," *Polymer Degradation and Stability*, No. 67, 2000, pp. 111-115.

80. Bradbury, A. G. W., Sakai, Y., and Shafizadeh, F., "A kinetic model for pyrolysis of cellulose," *Applied Polymer Science*, Vol. 23, 1979, pp. 3271-3280.

81. Braun, R. L. and Burnham, A. K., "Analysis of chemical reaction kinetics using a distribution of activation energies and simpler models," *Energy & Fuels*, Vol. 1, 1987, pp. 153-161.

82. Ozawa, T., "A new method for analysing thermogravimetric data," *Bull.Chem.Soc.Japan*, Vol. 38, No. 11, 1965, pp. 1881-1886.

83. Suuberg, E. M., "Approximate solution technique for nonisothermal, Gaussian distributed activation energy models," *Combustion and Flame*, Vol. 50, 1983, pp. 243-245.

84. Flynn, J. H. and Wall, L. A., "General treatment of the thermogravimetry of polymers," *Journal of Research of the National Bureau of Standards*, Vol. 70A, No. 6, 1966, pp. 487-523.

85. Friedman, H. L., "Kinetics of thermal degradation of char-forming plastics from thermogravimetry. Application to a phenolic plastic," *Polymer Science*, Vol. Part C, No. 6, 1965, pp. 183-195.

86. Zuru, A. A., Whitehead, R., and Griffiths, D. L., "A new technique for determination of the possible reaction mechanism from non-isothermal thermogravimetric data," *Thermochimica Acta*, Vol. 164, 1990, pp. 285-305.

87. Faroq, A. A., Price, D., Milnes, G. J., and Horrocks, A. R., "Thermogravimetric analysis study of the mechanism of pyrolysis of untreated and flame retardant treated cotton fabrics under a continuous flow of nitrogen," *Polymer Degradation and Stability*, No. 44, 1994, pp. 323-333.

88. Diebold, J. P., "A unified, global model for the pyrolysis of cellulose," *J.Biomass and Bioenergy*, Vol. 7, No. 1-6, 1994, pp. 75-85.

89. Brown, A. L., Dayton, D. C., and Daily, J. W., "A study of cellulose pyrolysis chemistry and global kinetics at high heating rates," *Energy & Fuels*, Vol. 15, 2001, pp. 1286-1294.

90. Flynn, J. H. and Wall, L. A., "A quick, direct method for the determination of activation energy from thermogravimetric data," *Polymer Letters*, Vol. 4, 1966, pp. 323-328.

91. Flynn, J. H., "The effect of heating rate upon the coupling of complex reactions. I. Independent and competitive reactions," *Thermochimica Acta*, Vol. 37, 1980, pp. 225-238.

92. Shafizadeh, F., "Pyrolysis and combustion of cellulosic materials," *Advances in Carbohydrate Chemistry*, Vol. 23, 1968, pp. 419-474.

93. Shafizadeh, F. and Fu, Y. L., "Pyrolysis of cellulose," *Carbohydrate Research*, Vol. 29, No. 1, 1973, pp. 113-122.

94. Banyasz, J., Li, S., Lyons-Hart, J., and Shafer, K. H., "Gas evolution and the mechanism of cellulose pyrolysis," *Fuel*, No. 80, 2001, pp. 1757-1763.

95. Drews, M. J. and Barker, R. H., "Pyrolysis and combustion of cellulose: Part VI. The chemical nature of the char," *Fire & Flammability*, Vol. 5, 1974, pp. 116-124.

96. Shafizadeh, F. and Bradbury, A. G. W., "Thermal degradation of cellulose in air and nitrogen at low temperatures," *Applied Polymer Science*, Vol. 23, 1979, pp. 1431-1442.

97. Shafizadeh, F., Furneaux, R. H., Cochran, T. G., Scholl, J. P., and Sakai, Y., "Production of levoglucosan and glucose from pyrolysis of cellulosic materials," *Applied Polymer Science*, Vol. 23, 1979, pp. 3525-3539.

98. Lomax, J. A., Commandeur, J. M., Arisz, P. W., and Boon, J. J., "Characterisation of oligomers and sugar ring-cleavage products in the pyrolysate of cellulose," *Analytical and Applied Pyrolysis*, Vol. 19, 1991, pp. 65-79.

99. Horrocks, A. R., Price, D., and Akalin, M., "FTIR analysis of gases evolved from cotton and flame retarded cotton fabrics pyrolysed in air," *Polymer Degradation and Stability*, No. 52, 1996, pp. 205-213.

100. Horrocks, A. R., Akalin, M., and Price, D., "Smoke, carbon dioxide and carbon monoxide evolution from cotton and flame retarded cotton: Part 2. Behaviour of single layer fabrics in air at elevated temperatures," *J.Fire Science*, Vol. 8, 1990, pp. 135-151.

101. Price, D., Horrocks, A. R., Akalin, M., and Faroq, A. A., "Influence of flame retardants on the mechanism of pyrolysis of cotton (cellulose) fabrics in air," *Analytical and Applied Pyrolysis*, No. 40-41, 1997, pp. 511-524.

102. Price, D., Coleman, G. V., and Horrocks, A. R., "Use of cyclic differential scanning calorimetry. Experiments to investigate the formation of an 'activated cellulose' species during cotton (cellulose) fabric pyrolysis in air and the influence on flame retarded treatments thereon," *Thermal Analysis*, Vol. 40, 1993, pp. 649-656.

103. Price, D., Horrocks, A. R., and Akalin, M., "Use of DTA with infrared analysis of evolved gas to investigate the effect of flame retardants on gas evolution from pyrolysed cellulose (cotton)," *British Polymer Journal*, No. 20, 1988, pp. 61-67.

104. Hajaligol, M., Howard, J. B., Longwell, J. P., and Peters, W. A., "Product compositions and kinetics for rapid pyrolysis of cellulose," *Ind.Eng.Chem.Process Des.Dev.*, Vol. 21, 1982, pp. 457-465.

105. Essig, M., Richards, G. N., and Schenck, E., "Mechanisms of formation of the major volatile products from the pyrolysis of cellulose," John Wiley & Sons, 1988, pp. 841-862.

106. Pan, W. P. and Richards, G. N., "Influence of metal ions on volatile products of pyrolysis of wood," *Analytical and Applied Pyrolysis*, No. 16, 1989, pp. 117-126.

107. Sanders, E. B., Goldsmith, A. I., and Seeman, J. I., "A model that distinguishes the pyrolysis of D-glucose, D-fructose and sucrose from that of cellulose. Application to the understanding of cigarette smoke formation.," *Analytical and Applied Pyrolysis*, Vol. 66, 2003, pp. 29-50.

108. *Training manual on Gracilaria culture and seaweed processing in China*, Zhanjiang Fisheries College 1990.

109. Gacesa, P., "Alginates," *Carbohydrate Polymers*, Vol. 8, 1988, pp. 161-182.

110. McHugh, D. J., *A guide to the seaweed industry*, FAO Fisheries Technical Paper 441 2003.

111. Rehm, B. H. A., "Alginates from bacteria," *Polysaccharides I. Polysaccharides from prokaryotes*, edited by E. J. Vandamme, S. De Baets, and A. Steinbüchel, Vol. 5, Biopolymers, Wiley-VCH, Weinheim, 2002, pp. 179-212.

112. Draget, K. I., Smidsrød, O., and Skjåk-Bræk, G., "Alginates from algae," *Polysaccharides II: Polysaccharides from eukaryotes*, edited by E. J. Vandamme, S. De Baets, and A. Steinbüchel, Vol. 6, Biopolymers, Wiley-VCH, Weinheim, 2002, pp. 215-244.

113. Kienzle, E., Schrag, I., Butterwick, R., and Opitz, B., "Calculation of gross energy in pet foods: new data on heat combustion and fibre analysis in a selection of foods for dogs and cats.," *Animal Physiology and Animal Nutrition*, Vol. 85, 2001, pp. 148-157.

114. DeGroot, W. F., Pan, W. P., Rahman, M. D., and Richards, G. N., "First chemical events in pyrolysis of wood," *Analytical and Applied Pyrolysis*, Vol. 13, 1988, pp. 221-231.

115. Garn, P. D., *Thermoanalytical methods of investigation*, Academic Press, New York, 1965.

116. Haines, P. J., *Thermal methods of analysis: Principles, applications and problems*, Blackie academic and professional, London, 1995.

117. McNaughton, J. L. and Mortimer, C. T., *Differential scanning calorimetry*, Perkin Elmer Corp., Connecticut, 1975.

118. Aggarwal, P. and Dollimore, D., "The combustion of starch, cellulose and cationically modified products of these compounds investigated using thermal analysis," *Thermochimica Acta*, Vol. 291, 1997, pp. 65-72.

119. Colbert, J. C., Xiheng, H., and Kirklin, D. R., "Enthalpy of combustion of microcrystalline cellulose," *Journal of Research of the National Bureau of Standards*, Vol. 86, No. 6, 1981, pp. 655-660.

120. Hajaligol, M., Wojtowicz, M. A., Carangelo, R. M., Bassilakis, R., Chen, Y., and Serio, M. A., "Quantitative characterisation of tobacco pyrolysis products using TG-FTIR," Coresta Conference, Innsbruck, 1999.

121. Hilton, M. and Black, J. D., Detection of soot particles in gas turbine engine combustion gases using non intrusive FTIR spectroscopy. SPIE International.European symposium of remote sensing, Barcelona, Sep.1998 3493. 1998.

122. Hilton, M., Arrigone, G. M., and Miller, M. N., Non intrusive spectroscopic investigations of soot and unburnt hydrocarbons in combustion gases. SPIE International.Part of the EUROPTO conference on Environmental Sensing and Applications, Munich, Germany, June 1999 3821, 198-208. 1999.

123. Koller, K. B., Thomas, C. E., Parrish, M. E., and Leydee, D. E., Puff-by-puff determination of gas phase acetaldehyde, HCN, NO and CO using FTIR spectrometry. Website - www.pmdocs.com . 11-12-2001.

124. Li, S., Lyons-Hart, J., Banyasz, J., and Shafer, K. H., "Real-time evolved gas analysis by FTIR method: an experimental study of cellulose pyrolysis," *Fuel*, Vol. 80, 2001, pp. 1809-1817.

125. Pitts, J. N., Biermann, H. W., Tuazon, E. C., Green, M., Long, W. D., and Winer, A. M., "Time-resolved identification and measurement of indoor air pollutants by spectroscopic techniques: gaseous nitrous acid, methanol, formaldehyde and formic acid," *JAPCA Notebook*, Vol. 39, No. 10, 1989, pp. 1344-1347.

126. Lephardt, J. O. and Fenner, R. A., "Characterization of pyrolysis and combustion of complex systems using Fourier transform infrared spectroscopy," *Applied Spectroscopy*, Vol. 34, No. 2, 1980, pp. 174-185.

127. Visser, T., Sarobe, M., Jenneskens, L. W., and Wesseling, J. W., "Identification of isomeric polycyclic aromatic hydrocarbons (PAH) in pyrolysates from ethynylated PAH by gas chromatography-Fourier infrared spectroscopy. Their relevance for the understanding of PAH rearrangement and interconversion processes during combustion," *Fuel*, Vol. 77, No. 9/10, 1998, pp. 913-920.

128. Lucena, M. d. C. C., de Alenca, A. E. V., Mazzeto, S. E., and Soares, S. d. A., "The effect of additives on the thermal degradation of cellulose acetate," *Polymer Degradation and Stability*, Vol. 80, No. 1, 2003, pp. 149-155.

129. Ouajai, S. and Shanks, R. A., "Composition, structure and thermal degradation of hemp cellulose after chemical treatments," *Polymer Degradation and Stability*, Vol. 89, No. 2, 2005, pp. 327-335.

130. Pastorova, I., Botto, R. E., Arisz, P. W., and Boon, J. J., "Cellulose char structure: a combined analytical Py-GC-MS, FTIR and NMR study," *Carbohydrate Research*, No. 262, 1994, pp. 27-47.

131. Shafizadeh, F., "Thermal behaviour of carbohydrates," *Polymer Science*, No. 36, 1971, pp. 21-51.

132. Bryce, D. J. and Greenwood, C. T., "The thermal degradation of starch. Part II. The identification by gas chromatography of the minor volatile products," *Die Stärke*, Vol. 15, No. 8, 1963, pp. 285-290.

133. Daniels, T., *Thermal analysis*, Kogan Page, London, 1973.

134. Smith, A. L., *Applied infrared spectroscopy*, Vol. 54,.Chemical analysis series Elving P J and Winefordner J D, J Wiley & Sons, New York, 1979.

135. Banwell C.N., *Fundamentals of molecular spectroscopy*, 3rd ed., McGraw-Hill, London, 1983.

136. Smith, B. C., *Fundamentals of Fourier Transform infrared spectroscopy*, CRC Press, New York, 1996.

137. Liebman, S. A., Ahlstrom, D. H., and Griffiths, P. R., "On-line Fourier transform infrared analysis of pyrolysis and combustion products," *Applied Spectroscopy*, Vol. 30, No. 3, 1976, pp. 355-357.

138. Lavine, B. and Workman, J. J., "Chemometrics," *Analytical Chemistry*, Vol. 76, 2004, pp. 3365-3372.

139. Meloun, M., Militký, J., and Forina, M., *Chemometrics for analytical chemistry. Volume 1: PC-aided statistical data analysis*,.Ellis Horwood Series in Analytical Chemistry Masson, M., Tyson, J. F., and Stockwell, P., Ellis Horwood Ltd, Chichester, 1992.

140. Malinowski, E. R. and Howery, D. G., *Factor analysis in chemistry*, Wiley-Interscience, New York, 1980.

141. Malinowski, E. R., *Factor analysis in chemistry*, 3rd ed., Wiley-Interscience, New York, 2002.

142. *InSight user manual*, DiKnow Ltd, 84 Rushdean Road, Rochester, Kent ME2 2QB, U.K., 2003.

143. *Matlab user manual*, The Mathworks Inc. USA 1999.

144. Dias, M., Hadgraft, J., Raghavan, S. L., and Tetteh, J., "The effect of solvent on permeant diffusion through membranes studies using ATR-FTIR and chemometric data analysis," *Journal of Pharmaceutical Sciences*, Vol. 92, 2003, pp. 1-11.

145. Benzeval, I. and Coburn, S., "TGA-FTIR, Ability to distinguish between functional groups," British American Tobacco, R&D, Southampton (Internal memorandum), Aug. 2004.

146. Baker, R. R., Coburn, S., Liu, C., and Tetteh, J., "Pyrolysis of saccharide tobacco ingredients: a TGA-FTIR investigation," *Analytical and Applied Pyrolysis*, Vol. 74, 2005, pp. 171-180.

147. Coburn, S. and Benzeval, I., "Evaluation of 2.5m path length gas cell," British American Tobacco, R&D, Southampton (Internal memorandum), May 2004.

148. Williams, D. H. and Fleming, I., *Spectroscopic methods in organic chemistry*, 4th ed., McGraw-Hill Book Company (UK) Ltd, Maidenhead, 1989.

149. Baker, R. R., "Smoke chemistry," *Tobacco: production, chemistry and technology*, edited by D. L. Davis and M. T. Nielsen Blackwell Science, 1999.

150. Davies, B. G. and Fairbanks, A. j., *Carbohydrate Chemistry*,.Oxford Chemistry Primers Davies, S. G., Compton, R. G., Evans, J., and Gladden, L. F., Oxford University Press, Oxford, 2004.

151. Glassman, I., *Combustion*, 3rd ed., Academic Press Ltd, London, 1996.

Appendix A. Ash and Metal Analysis of the Cellulose and Alginic Acid used in this Study

Table A-1. Percentage inorganic ash (wet weight basis) measurement of sample materials

	Cellulose	Alginic Acid
	%	%
Replicate 1	0.01	1.49
Replicate 2	0.01	1.45
Mean	**0.01**	**1.47**

Table A-2. Semi-quantitative analysis of trace metals in the cellulose and alginic acid samples (mean of two replicates)

Metal	Cellulose	Alginic Acid
	µg/g	µg/g
Cr 52	0.422	0.377
Ni 62	0.185	0.000
As 75	0.022	0.203
Se 78	0.013	0.001
Cd 111	0.003	0.000
Hg 200	0.000	0.000
Pb 208	0.058	0.006
Al 27	0.022	0.041
K 39	0.115	0.149
Ca 43	1.293	1.535
Mn 55	0.009	0.005
Fe 57	0.285	0.421
Co 59	0.000	0.000
Cu 63	0.008	0.004
Zn 66	0.318	0.176
Br 79	0.022	0.137
Sn 118	0.003	0.007

Appendix B. Calibration Range for Factors used with InSight™

Reference. No.	Compound Name	Calibration Range (µg/mg)	
		Lower Limit	Upper Limit
1	Acetylene	0.29	14.52
2	Ammonia	0.05	4.70
3	CO	0.47	25.01
4	CO2	0.8	12.69
5	Ethane	0.10	7.62
6	Ethylene	0.09	20.31
7	Formaldehyde	0.11	6.74
8	Methane	0.03	3.98
9	Nitrous Oxide	0.04	16.87
10	NO	0.73	13.86
11	Propylene Oxide	0.35	10.39
12	Ethylene Oxide	0.15	16.77
13	Water Vapour	1.03	15.17
14	Acrolein (2-Propenal)	0.28	8.52
15	Acetaldehyde	0.75	14.75
16	1,3-butadiene	1.15	15.45
17	Acetic Acid	0.21	3.95
18	Formic Acid	0.15	1.24
19	Propionic Acid	0.12	3.97
20	Methanol	0.34	4.70
21	Ethanol	0.51	9.29
22	n-Propanol	0.23	9.74
23	Acetone	0.94	7.34
24	3 Methyl-2-Cyclopenten-1-one	0.35	3.71
25	2,5-Dimethylfuran	0.40	9.01
26	Furfural	0.29	2.29
27	2-Furanmethanol	0.30	7.61
28	2-Butanone	0.51	5.08
29	2,3-Dihydrofuran	0.49	15.10
30	Furan	Single calibration point extrapolated to form an artificial linear calibration	
31	Levoglucosan		
32	Glyceraldehyde Dimer		